Effect of *Faecalibacterium prausnitzii* on intestinal barrier function and immune homeostasis

A dissertation presented in partial fulfilment of the requirements for the degree of

Doctor of Philosophy in Nutritional Science

Massey University
Manawatū, New Zealand

Eva Maier

2017

Abstract

Various gastrointestinal (GI) diseases, for example inflammatory bowel disease, are linked to impaired barrier function, chronic inflammation and dysbiosis of the resident microbiota. *Faecalibacterium prausnitzii*, an abundant obligate anaerobe of the healthy human microbiota, has reduced abundance in the GI tract of people with these diseases, and has been suggested to exert beneficial effects. Only a few studies have investigated its mechanisms of action, partly due to the difficulty of co-culturing live obligate anaerobes with oxygen-requiring human cells. The novel apical anaerobic co-culture model used in this study allows this co-culture through the separation of anaerobic and aerobic compartments. This model was used to investigate the effects of live *F. prausnitzii* (strains A2-165, ATCC 27768 and HTF-F) on intestinal barrier integrity, measured by trans-epithelial electrical resistance (TEER) of the intestinal epithelial cell line Caco-2, and on immune homeostasis, specifically on Toll-like receptor (TLR) activation. Method development was required to adapt these assays to the novel model and to optimise the growth of *F. prausnitzii* co-cultured with Caco-2 cells and TLR-expressing cell lines while maintaining their viabilities. Firstly, the optimised co-culture conditions were used to determine the effect of the three *F. prausnitzii* strains on barrier integrity of healthy and tumour necrosis factor alpha (TNF-α) treated Caco-2 cells. Live and growing *F. prausnitzii* did not alter the TEER across healthy Caco-2 cells. However, under TNF-α mediated inflammatory conditions, dead *F. prausnitzii* decreased TEER, whereas live bacteria maintained TEER. Secondly, the TLR activation assay was adapted to be carried out in the novel model. Using the adapted assay conditions it was determined that live *F. prausnitzii* induced greater TLR2 and TLR2/6 activation than dead *F. prausnitzii*. Collectively, these results indicate greater immuno-stimulatory effects of live *F. prausnitzii*, via TLR2

activation, and this effect is potentially linked to its barrier maintaining properties, because previous research showed enhancement of barrier integrity induced by TLR2 signalling. This new knowledge contributes to the understanding of how *F. prausnitzii* may maintain immune homeostasis in the GI tract. Unravelling the biological mechanisms used by prevalent species of the human microbiota, such as *F. prausnitzii*, will ultimately allow better comprehension of microbial regulation of GI function.

Acknowledgements

Firstly, I would like to express my sincere gratitude to my supervisors associate Prof Nicole Roy and Dr Rachel Anderson for their continuous support during my PhD. Thanks a lot for your time and effort and the many helpful advice and discussions that kept me positive and motivated throughout my research. Besides my supervisors at AgResearch, I would like to thank my supervisor Prof Paul Moughan at the Riddet Institute. Furthermore, I acknowledge AgResearch and the Riddet Institute for funding this research and my PhD fellowship.

For their technical assistance, I would like to thank Kelly Armstrong, Leigh Ryan and Stacey Burton, for always taking the time to answer my questions and helping out with the cell culture in busy times. Also, thanks to Dr Mark McCann and Kelly Armstrong for their advice on stable transfections and to Dr Eric Altermann for helping me with the bioinformatics analyses. For developing the prototype II co-culture chamber and the adapter for the oxygen probe I would like to acknowledge the AgResearch engineering team, specifically Steve Gebbie and Scott Sevier. My thanks also go to associate Prof Hermie Harmsen and Dr Muhammad Tanweer Khan for providing the *F. prausnitzii* strains used in these studies. For the help with the statistical analysis I am grateful to Dr Carlos Montoya who was an immense help during the very busy times in the final stage of my PhD. In addition, I would like to thank Denise Martin for helping with the many administrative tasks along the road to completing this thesis. Furthermore, my special thanks go to Natascha Stroebinger for the help with the formatting of this thesis.

A special thanks also goes to my fellow students, it was amazing to share an office with such great people, and meeting so many people from all over the world. I never wanted to

miss our lunch breaks which were always fun and contributed a lot to keep up the positive energies and motivation.

In the end I would like to thank my parents and my brother and sister for their constant support, despite being on the other side of the world. Finally, for the constant motivation and moral support I want to thank Carlos. Your positive energies definitely helped me a lot to complete this work.

Table of contents

List of figures

List of tables

Abbreviations

ANOVA	Analysis of variance
ATCC	American Type Culture Collection
BHI	Brain-heart infusion
CD	Cluster of differentiation
CFU	Colony-forming unit
DAMP	Damage-associated molecular pattern
DC	Dendritic cell
DMEM	Dulbecco's Modified Eagle Medium
DMSO	Dimethyl sulphoxide
DNA	Deoxyribonucleic acid
DO	Dissolved oxygen
DSM	Deutsche Sammlung von Mikroorganismen (German Collection of Microorganisms)
DSS	Dextran sodium sulphate
FBS	Foetal bovine serum
GALT	Gut-associated lymphoid tissue
GI	Gastrointestinal
HEK	Human embryonic kidney

Abbreviations

HKLM	Heat-killed *Listeria monocytogenes*
IBD	Inflammatory bowel disease
IBS	Irritable bowel syndrome
IEC	Intestinal epithelial cell
IFN-γ	Interferon gamma
IKK	Inhibitor of kappa B kinase
IL	Interleukin
IRAK	Interleukin-1 receptor-associated kinase
IκB	Inhibitor of kappa B
LPS	Lipopolysaccharide
LSD	Least Significant Difference
M199 Std	M199 Standard medium
MAPK	Mitogen-activated protein kinase
MOI	Multiplicity of infection
MyD88	Myeloid differentiation primary response protein 88
NCBI	National Center for Biotechnology Information
NEAA	Non-Essential Amino Acid
NF-κB	Nuclear factor-kappa B
NOD	Nucleotide-binding and oligomerisation domain

OD	Optical density
ODS	Output delivery system
PAMP	Pathogen-associated molecular pattern
PBMC	Peripheral blood mononuclear cell
PBS	Phosphate-buffered saline
PCR	Polymerase chain reaction
PPAR-γ	Peroxisome proliferator-activated receptor gamma
PRR	Pattern recognition receptor
rRNA	Ribosomal ribonucleic acid
SCFA	Short-chain fatty acid
SEM	Standard error of the mean
SFB	Segmented filamentous bacteria
sIgA	Secretory immunoglobulin A
TEER	Trans-epithelial electrical resistance
TJ	Tight junction
TLR	Toll-like receptor
TNBS	2,4,6-Trinitrobenzenesulfonic acid
TNF-α	Tumour necrosis factor alpha
TOLLIP	Toll-interacting protein

TRAF	TNF receptor associated factor
TRIF	TIR-domain-containing adapter-inducing interferon beta
YCFAG	Yeast extract, casitone, fatty acid, glucose
ZO	Zona occludens

Introduction

The human gastrointestinal (GI) tract is colonised by trillions of commensal bacteria which are generally known to be critical for human health [1]. It also harbours the largest number of immune cells within the human body [2]. Maintaining a homeostatic balance between tolerance towards commensal bacteria and food antigens and immunity against pathogens is the major challenge for the gut-associated lymphoid tissue (GALT), which is achieved through tightly regulated host-microbe cross-talk [3]. In addition, the barrier between the lumen and underlying tissues formed by the intestinal epithelium is vital to maintain homeostasis in the GI tract as it prevents the entry of unwanted luminal contents into the body [4]. Various GI inflammatory disorders, such as inflammatory bowel disease (IBD), irritable bowel syndrome (IBS) or celiac disease, are linked to an increased permeability of the intestinal barrier and disturbed immune homeostasis resulting in chronic inflammation [5]. Moreover, inflammatory disorders are associated with changes in the human GI microbiota composition, referred to as dysbiosis [6].

The incidence of inflammatory disorders is increasing in industrialised countries [7]. Due to the clear link between dysbiosis and disease, approaches to positively modulate the composition of the GI microbiota to prevent or treat diseases are gaining increasing interest [8]. The concept of probiotics is well established, with current probiotic species mainly belonging to the lactic acid bacteria, such as lactobacilli [9]. In addition, recent evidence points towards species from the human GI microbiota that may exert beneficial effects on human health since their abundance is decreased in people with inflammatory diseases. For example, *Faecalibacterium prausnitzii,* an abundant member of the healthy human GI microbiota, is reduced in people with IBD [10-14], IBS [15] and celiac disease [16] and has therefore been suggested as a marker for a healthy GI tract. Beneficial commensal species

could be potential candidates for a next generation of probiotics [17]. However, the mechanisms underlying the beneficial effects of these functional commensals are yet to be explored. A major limitation in this investigation is the technical difficulty of co-culturing obligate anaerobic commensal bacteria, which represent over 99% of the bacterial species in the human GI tract [18], with oxygen-requiring human cells to study their interaction.

Novel dual-environment co-culture models have been recently developed which overcome this technical difficulty since they allow the co-culture and study of the direct interactions between live obligate anaerobes with human cells [19-21]. In this PhD dissertation one such model was used to study the mechanisms by which *F. prausnitzii* interacts with host cells. The gained knowledge will open opportunities to improve both intestinal and overall health.

CHAPTER ONE:
Review of literature[†]

[†] Selected material from this section was published as a critical review in the journal *Nutrients*: Maier, E., Anderson, R. C. & Roy, N. C. Understanding How Commensal Obligate Anaerobic Bacteria Regulate Immune Functions in the Large Intestine. *Nutrients* 7, 45-73, (2014).

1.1. HUMAN GASTROINTESTINAL MICROBIOTA

The human GI tract is colonised by an estimated 10^{14} microorganisms. It was long postulated that microbial cells outnumber human cells by a factor of ten [22], however, recent calculations suggested roughly equal numbers of bacterial and human cells in the human body [23]. Some consider the GI microbiota to be a human microbial "organ" [18]. It is well established that microbial colonisation of the GI tract is critical for human health.

1.1.1. Composition

The human GI microbiota consists of a diverse community, which is dominated by bacteria, but also contains archaea, eukaryotes (e.g., fungi, protozoa) and viruses [24]. Most bacterial species colonising the human GI tract belong to the phyla *Firmicutes* and *Bacteroidetes*, while species of the phyla *Actinobacteria*, *Proteobacteria* and *Verrucomicrobia* exist in lower numbers [18]. The number of bacterial species within the human GI microbiota has often been estimated to be in the range of 500 to over 1000 species [18,25]. With an increasing number of metagenomic sequencing studies undertaken over recent years, the GI microbiota is often defined based on its genetic content. Results of the Metagenomics of the Human Intestinal Tract (MetaHIT) project revealed an approximate total of 3.3 million non-redundant microbial genes in the human microbiota derived from faecal samples of 124 European individuals; approximately 150 times more genes than the human genome [24]. From this result it was estimated that the GI microbiota of the entire cohort comprised 1000 to 1150 prevalent (more frequent) bacterial species, with at least 160 prevalent bacterial species per person. In addition, a common bacterial core was identified, with 18 species shared among all individuals, 57 species shared among 90% and 75 species detected in 50% of all individuals [24]. Furthermore, this study demonstrated the predominance of bacteria within the human microbiota

because 99% of the genes were of bacterial origin. The rest were mostly archaeal and only 0.1% of the genes were of eukaryotic and viral origins [24].

Due to their anaerobic nature, the majority of the bacterial strains in the GI tract is difficult to culture using standard laboratory techniques. Therefore, progress in molecular biology techniques including 16S ribosomal ribonucleic acid (rRNA) gene and metagenomic sequencing has been crucial in unravelling the diversity of the GI microbiota [18,24].

The composition and density of bacteria changes along the GI tract. Bacterial numbers increase from 10^3 to 10^5 bacteria per mL of luminal contents in the stomach and duodenum to approximately 10^9 to 10^{12} per mL in the ileum and colon, respectively [26,27]. Additionally, bacterial diversity increases from proximal to distal locations of the GI tract. The stomach is often colonised by species of *Helicobacter* and to a lesser extent *Prevotella*, *Streptococcus*, *Veillonella*, and *Rothia*. The genera *Streptococcus*, *Lactobacillus*, *Enterococcus* and members of the *Enterobacteriaceae* family are major constituents of the microbiota in the small intestine [28].

The microbiota composition in the colon is more diverse and shows considerable variation between individuals. However, several studies proposed that the microbial communities can be divided into distinct clusters. For example, three predominant variants were suggested to exist, which were designated as enterotypes [29]. These three enterotypes are either enriched in *Bacteroides* (enterotype 1), *Prevotella* (enterotype 2) or *Ruminococcus* (enterotype 3). Enterotypes were shown to be influenced by long-term diet [30]. Another study identified four distinct community types within bacteria from stool samples [31]. Community type A was characterised by the highest levels of *Bacteroides* but a lack of *Prevotella* and *Ruminococcaceae*. Community type B had the lowest proportion of *Bacteroides* and was dominated by genera within the *Firmicutes*. Compared to community

type A, community type C had lower levels of *Bacteroides* but a higher abundance of *Alistipes*, *Faecalibacterium* and *Ruminococcaceae*, and also lacked *Prevotella*. The relative abundance profile of community type D showed lower levels of *Bacteroides* compared to community types A and C but a higher proportion of *Prevotella* [31]. However, in contrast to the concept of dividing the human GI microbiota into distinct clusters, several authors also suggested the concept of a continuum or gradient of genera within GI microbial communities [32-35]. For example, a recent analysis summarising the combined microbiome data from five studies, which included samples from five continents, suggested the two taxa *Bacteroides* and *Prevotella* as biomarkers, rather than enterotypes, which are influenced by diet, lifestyle and disease state [35].

In addition to differences in the microbiota composition between proximal and distal parts of the GI tract, distinct microbial compositions exist in the lumen and the mucosa [18,36]. However, knowledge regarding the mucosa-associated microbiota remains limited, as invasive methods are required for sampling [37]. The analysis of microbial communities of different colonic mucosal sites (caecum, ascending colon, transverse colon, descending colon, sigmoid colon, and rectum) suggested a pattern of patchiness and heterogeneity in the distribution of mucosal bacteria along the course of the colon, which may indicate the existence of microanatomic niches [18].

Generally, the mucosa-associated microbiota comprises a higher abundance of *Firmicutes* compared to *Bacteroidetes* [38]. The intestinal mucosa represents a glycan-rich environment, which is formed by the cell surface glycocalyx and the extracellular secreted mucus. Bacterial species colonising this milieu are specialised through the production of mucin-degrading enzymes and mucin-binding extracellular proteins. Although several mucin-degrading bacteria are increased in number during inflammation, which suggests

they contribute to the disease pathogenesis, they are also part of the mucosa-associated microbiota in healthy humans [39]. Species described as mucin-degrading specialists include prominent commensals such as *Bacteroides thetaiotaomicron* [40] and *Akkermansia muciniphila* [41], both of which have been associated with protective effects *in vitro* and *in vivo* [42-45].

A simplified model of the human GI microbiota has demonstrated the specialisation of *B. thetaiotaomicron* to utilise host-derived mucin glycans [46]. Germ-free mice were colonised with *B. thetaiotaomicron* and *Eubacterium rectale* and microbial-microbial and microbial-host interactions were characterised. *B. thetaiotaomicron* adapts to the presence of *E. rectale* by increasing the expression of various genes involved in the harvest of host-derived mucin glycans that *E. rectale* is unable to utilise as a substrate. Furthermore, the bacterial signals produced by *B. thetaiotaomicron* induce the production of intestinal mucosal glycans. Adaptations of *E. rectale* in response to *B. thetaiotaomicron* include decreased production of its glycan-degrading enzymes and increased expression of selected amino acid and sugar transporters, and generation of butyrate, which is used by intestinal epithelial cells (IECs). These results demonstrate the niche specialisation of the two bacterial species as the reciprocal effects on their metabolism enables them to utilise different nutrients.

The composition of the human GI microbiota is shaped by the influence of various factors, e.g., host genetics [47]. In addition, it is recognised that diet modulates the microbial composition in the intestine [48]. For instance, the influence of diet on microbiota composition is exploited in the use of prebiotics, currently defined as "selectively fermented ingredients that allow specific changes, both in the composition and/or activity in the GI microbiota that confers benefits upon host wellbeing and health" [49]. For

example, the prebiotic inulin increased the proportion of *Bifidobacterium adolescentis* and *Faecalibacterium prausnitzii* in the human GI microbiota [50].

1.1.2. Establishment and compositional changes associated with ageing

Whereas earlier research suggested the human foetus to be microbiologically sterile with bacterial colonisation of the GI tract starting after birth, evidence is now accumulating that bacterial exposure may start *in utero* [51-53]. Bacteria have been isolated from the meconium of full-term, healthy neonates and shown to belong mainly to the genera *Enterococcus* and *Staphylococcus* [54]. The further colonisation of the GI tract of the neonate has been shown to depend on the mode of birth. Whereas the GI microbiota of vaginally delivered infants are characterised by a high abundance of lactobacilli, the delivery by Caesarean section has been associated with an initial microbiota composition containing *Staphylococcus*, *Corynebacterium*, and *Propionibacterium*, reflecting the microbiota composition of the mothers' vaginal tract or skin, respectively [55]. Additionally, the type of feeding (breast-feeding vs formula) has been reported to influence the microbial composition of the infants' GI tract, with a dominance of bifidobacteria within the GI microbiota of breast-fed babies compared to a more diverse microbiota in formula-fed babies [56]. The simple microbial composition of the neonate changes rapidly during the first year of life, with an increase in diversity as a consequence of the increasing complexity of the diet and environmental exposure. It has been reported that after around three years the microbial composition of the infant's GI tract is similar to that of an adult [57].

The microbial composition of the GI tract changes with ageing [58]. Analysis of the faecal microbiota of elderly subjects (> 65 years) and younger adults revealed differences in the core microbiota in the different age groups [58]. These differences include an increased

abundance of *Bacteroides* spp. and characteristic prevalence of *Clostridium* groups in the elderly. Furthermore, the microbiota composition of the elderly is highly variable [58]. Interestingly, the microbiota composition in elderly correlates with the diet, health status and living conditions [48]. For example, a decreased bacterial diversity was observed in the microbiota of people in long-stay care compared to community dwellers [48]. In addition, ageing has been associated with the development of chronic, low-level inflammation often described as inflamm-aging [59]. The increased systemic pro-inflammatory status in the elderly has been associated with the age-related changes in the composition of the GI microbiota [60].

1.1.3. The role of commensal bacteria in human health

Human health depends largely on the symbiotic benefits of the host-microbe relationship. The GI microbiota has a protective function through the prevention of the colonisation of the mucosa by pathogens. This effect is often referred to as colonisation resistance and is achieved through various mechanisms [61]. Adherent bacteria of the GI microbiota occupy binding sites on the epithelium and thereby prevent the attachment and invasion of pathogenic bacteria into epithelial cells [62,63]. In addition, commensal bacteria can inhibit pathogenic microorganisms directly through production of antimicrobial substances such as bacteriocins [64], or indirectly by competing for available nutrients [65].

The GI microbiota provides energy and nutrients to the host through the breakdown of nondigestible products in the large intestine and thereby producing short-chain fatty acids (SCFAs) such as acetate, butyrate and propionate [66,67]. Butyrate, in particular, has a central function as the main energy source for colonocytes. Moreover, butyrate exerts anti-inflammatory properties. For example, butyrate decreased pro-inflammatory cytokine expression in colonic biopsy specimens and lamina propria mononuclear cells isolated

from patients with Crohn's disease [68]. Additionally, the GI microbiota plays an important metabolic role through synthesising vitamins K and B_{12} and folic acid [66].

In addition, bacterial colonisation is necessary for the normal postnatal development of the GI tract. Germ-free animals that are raised in isolators to prevent colonisation of the GI tract and other body surfaces by environmental microorganisms [69,70] have impaired development of the GI tract [71-74]. In particular, the immune system of the GI tract is underdeveloped in these animals [69]. Furthermore, the indigenous microbiota regulates intestinal angiogenesis, with adult germ-free mice displaying arrested capillary network formation [75]. The development of the vascular network could be initiated through inoculation with a complete microbiota harvested from conventional mice, but also by colonisation with one of the major members of the GI microbiota, *B. thetaiotaomicron* [75]. Recent findings have also demonstrated that commensal *Lactobacillus* spp. promote the proliferation of IECs, highlighting the importance of microbial stimuli [76]. This process is the result of the stimulation of NADPH oxidase 1-dependent reactive oxygen species generation by the bacteria, which in turn increases cellular proliferation [76].

1.2. INTESTINAL BARRIER FUNCTION

In addition to the absorption of nutrients, the intestinal epithelium also plays an important role by forming a barrier between the lumen and underlying tissues [4]. Appropriate intestinal barrier function is crucial in preserving health by preventing pathogens and harmful substances entering the human body [77]. It is well established that an increased intestinal permeability, often called a "leaky barrier", plays a role in the pathophysiology of several GI disorders like IBD [78], IBS [79] and celiac disease [80]. Additionally, extra-intestinal disorders like diabetes [81], asthma [82] and multiple sclerosis [83] have been linked to barrier dysfunction. Ageing is also associated with a decrease in barrier integrity

[84]. The concept of the brain-gut-microbiota axis, a link between the GI microbiota, the enteric and the central nervous system, indicates possible connections between intestinal barrier integrity, the GI microbiota and stress related psychiatric disorders as recently reviewed by Kelly *et al.* [85].

1.2.1. Components

The barrier between the intestinal lumen containing bacteria, food antigens and toxins and the internal milieu consists of four components, the physical, chemical, immunological and microbiological barriers [86] as shown in Figure 1.1. The physical component is formed by a single layer of IECs that are connected by the junctional complex to prevent translocation of luminal antigens. This complex is composed of different protein complexes with tight junctions (TJs) and adherens junctions together forming the apical junctional complex, gap junctions serving for intracellular communication and desmosomes which are involved in cell-cell adhesion [87]. IECs are covered by a mucus layer, which together with antimicrobial peptides (mainly belonging to the family of defensins and cathelicidins) forms the chemical component of the intestinal barrier [88-90]. The immunological barrier is formed by the GALT with its cellular and humoral defence systems [91]. As the commensal bacteria can block binding sites on the GI epithelium and thereby limiting pathogen colonisation, they form the microbiological component of the intestinal barrier [61].

The structure and regulation of TJs representing the physical barrier and the regulation of intestinal barrier integrity with a specific focus on the regulation of TJ integrity by commensal and probiotic bacteria are described in more detail in the sections below.

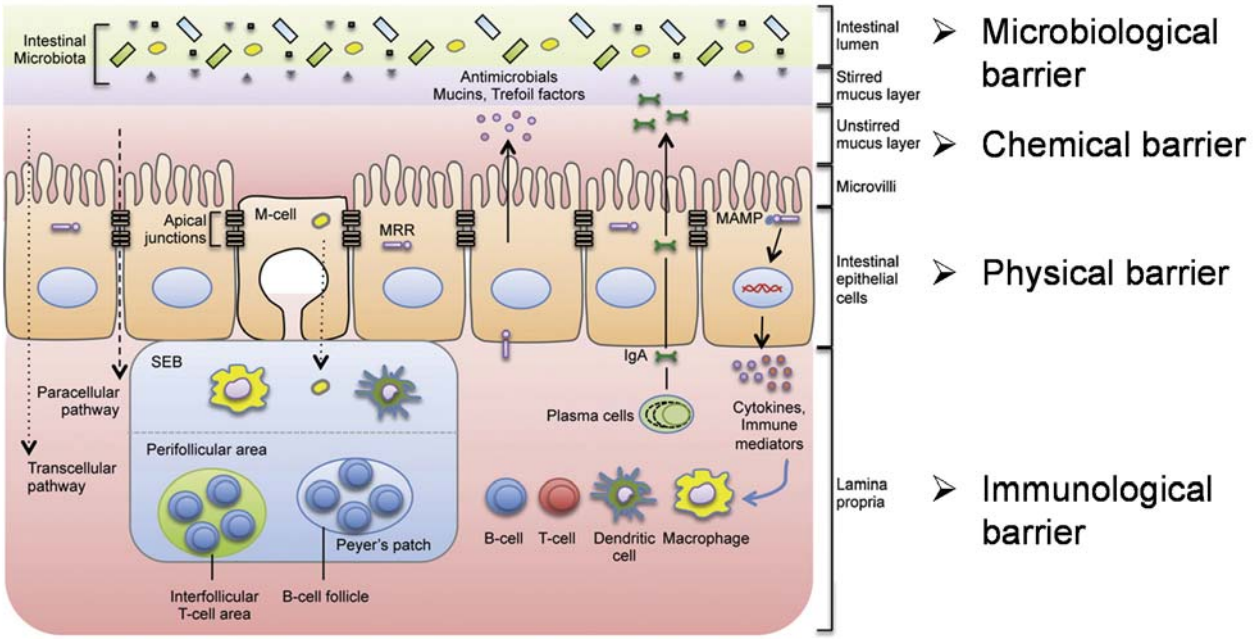

Figure 1.1 Components of the intestinal barrier.

The intestinal barrier can be divided into four components. IECs connected by the junctional complex represent the physical component. The chemical component is formed by the mucus layer and antimicrobial peptides. Immune cells of the lamina propria are part of the immunological barrier. Finally, commensal bacteria are occupying binding sites on the GI epithelium and are therefore forming the microbiological component of the intestinal barrier. Together the four components of the intestinal barrier prevent the entry of harmful pathogens and toxins into the body. Figure adapted from Natividad and Verdu (2013) [92]**. (**Permission obtained**)**

1.2.1.1. Structure and regulation of tight junctions

TJs play an important role in the function of the intestinal barrier, as they connect neighbouring IECs thereby sealing the paracellular space between the cells and prevent the entry of pathogens and toxins [93]. However, TJs are not static structures, they are continuously undergoing processes of disassembly and assembly, which depends on the influence of various factors, such as exposure to pathogenic and commensal bacteria or food components as reviewed by Ulluwishewa *et al.* [87].

TJs are complex structures which consist of at least 50 proteins. These proteins can be divided into transmembrane proteins, which connect neighbouring IECs, and plaque proteins, which anchor the transmembrane proteins within the cytoplasma. The transmembrane proteins can be further divided into tetra-span and single-span proteins. The tetra-span proteins include occludin, the claudin family of proteins and tricellulin [94-96]. Tricellulin is a component of TJs in locations where three IECs are joined together [96].

Junctional adhesion molecules (JAMs) are single-span proteins which belong to the immunoglobulin (Ig) superfamily [97]. The family of zona occludens (ZO) proteins (ZO-1, ZO-2, and ZO-3) are plaque proteins which connect the transmembrane proteins occludin and claudin to the actin cytoskeleton [98-103]. A schematic overview of the structure of TJs is shown in Figure 1.2.

The constant remodelling of TJs in response to external stimuli is regulated through various signalling molecules. For example, TJ assembly depends on the activity of protein kinase C [104]. Furthermore, myosin regulatory light-chain (MLC) phosphorylation by MLC kinase contributes to the physiological regulation of epithelial TJs [105]. Increased

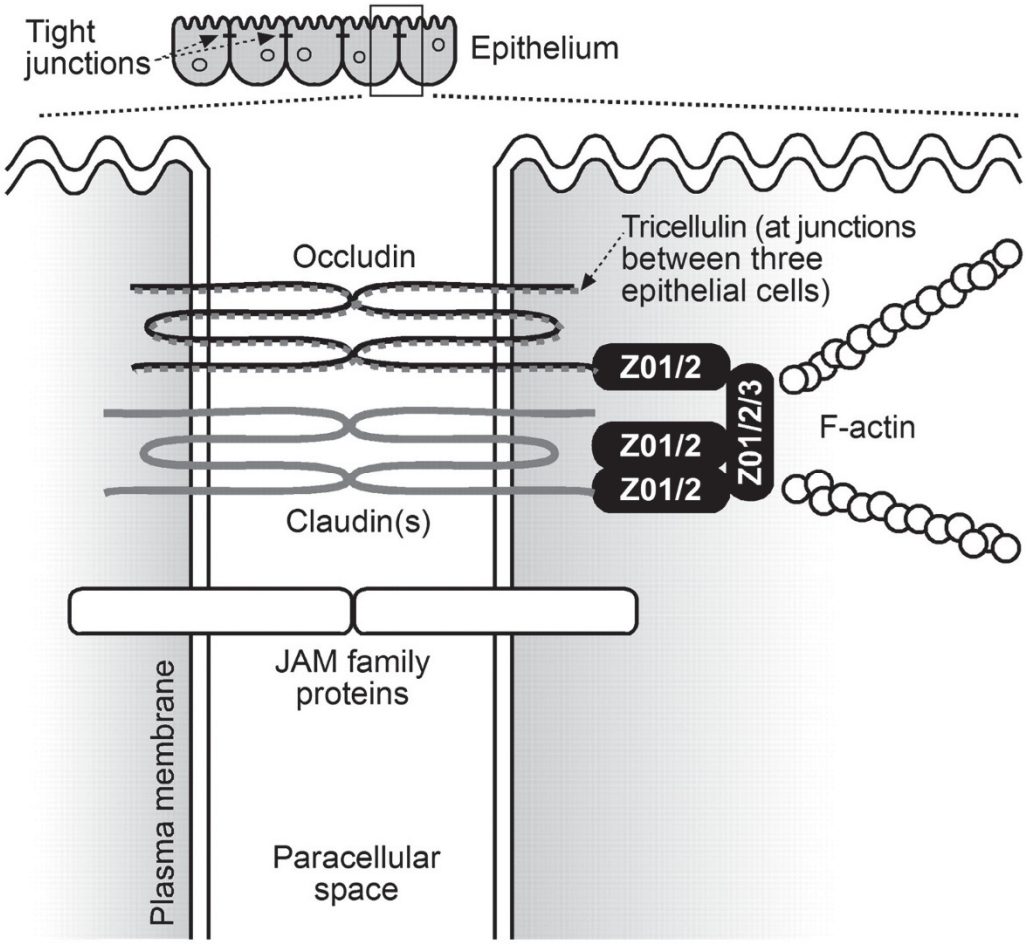

Figure 1.2 Tight junction structure.

TJs connect neighbouring IECs. They are composed of transmembrane proteins, with occludin, claudin and tricellulin belonging to the tetra-span proteins and the JAM family of proteins belonging to the single-span proteins. Additionally, plaque proteins including ZO-1, ZO-2 and ZO-3 contribute to the formation of TJs and connect the transmembrane proteins with the actin cytoskeleton. Figure from Ulluwishewa *et al.* (2011) [87]. **(**Permission obtained**)**

MLC phosphorylation has been shown to be associated with an increased TJ permeability [105]. Another group of signalling molecules involved in TJ regulation are the Rho family of small GTPases. For instance, RhoA and Rac1 small GTPases regulate the structure and function of TJs [106]. Phosphorylation of TJ proteins is another mechanism contributing to TJ regulation. One example is the phosphorylation of occludin, which is implicated as a critical factor during TJ assembly [107].

1.2.2. Regulation by commensal and probiotic bacteria

Numerous studies have investigated the effect of commensal and probiotic bacteria on intestinal barrier function and have shown that all components (physical, chemical and immunological) of the barrier can be influenced by bacteria. For instance, specific probiotic strains are able to improve barrier function by promoting mucus secretion [108] or by altering expression levels of host cell-derived antimicrobial peptides [109]. Other strains augment secretory immunoglobulin A (sIgA) production and thus promote immune exclusion of microbes [110].

In addition, specific commensal and probiotic bacteria increase the integrity of TJs both *in vitro* and *in vivo* as reviewed by Ulluwishewa *et al.* [87]. For example, the exposure of Caco-2 cells, a continuous cell line originating from human epithelial colon adenocarcinoma cells [111], to strains of *Lactobacillus plantarum* (MB452 and DSM 2648) increased the trans-epithelial electrical resistance (TEER), a measurement for barrier integrity [112,113]. In case of *L. plantarum* MB452 the barrier enhancing effect was linked to an increased expression of genes involved in TJ formation [112]. The probiotic mixture VSL#3 (*Streptococcus thermophilus*, *B. longum*, *B. breve*, *B. infantis*, *L. acidophilus*, *L. plantarum*, *L. casei* and *L. bulgaricus*) also exerts barrier protecting properties [114,115]. For instance, in mice with dextran sodium sulphate (DSS)-induced colitis a decreased

expression and redistribution of the TJ proteins occludin, ZO-1, and claudin-1, -3, -4, and -5 was determined. These detrimental effects of DSS on TJ integrity were prevented through administration of VSL#3 [115]. Supporting these findings of *in vitro* and animal studies, Karczewski *et al.* have shown an increase in the TJ proteins ZO-1 and occludin in healthy human subjects administered *L. plantarum* WCFS1 [116].

Specific probiotic and commensal bacterial strains reduce the negative effects of pathogens on intestinal barrier function [113,117,118]. For example, pre-treatment of IEC monolayers with the probiotic *L. rhamnosus* GG prevented enterohemorrhagic *Escherichia coli* (EHEC) O157:H7-induced increase in barrier permeability [117]. Furthermore, the EHEC-induced redistribution of the TJ proteins claudin-1 and ZO-1 between epithelial cells was reduced by the probiotic strain. Similarly, the probiotics *Streptococcus thermophilus* ATCC 19258 and *L. acidophilus* ATCC 4356 protected IECs from barrier dysfunction induced by enteroinvasive *E. coli* O29:NM [118] and the potential probiotic *L. plantarum* DSM 2648 prevented the barrier disrupting effect of enteropathogenic *E. coli* O127:H6 [113].

Furthermore, some probiotic and commensal bacteria can reduce the barrier dysfunction induced by the pro-inflammatory cytokines tumour necrosis factor alpha (TNF-α) and interferon gamma (IFN-γ) [119-121]. The probiotics *S. thermophilus* ATCC 19258 and *L. acidophilus* ATCC 4356 and the commensal *B. thetaiotaomicron* ATCC 29184 prevented the TNF-α- or IFN-γ-induced decrease in TEER and increase in permeability in IEC monolayers [119]. The deleterious effects of TNF-α and/or IFN-γ on the barrier integrity of IEC monolayers was also attenuated through treatment with the probiotic *L. rhamnosus* GG [121] and secreted bioactive factors from *Bifidobacterium infantis* (a component of the probiotic mixture VSL#3) [120]. The probiotics protected against TNF-α- or IFN-γ-

induced barrier dysfunction by preventing the rearrangement of TJ proteins and inhibiting the pro-inflammatory signalling in response to these cytokines [120,121].

1.3. MICROBIAL REGULATION OF IMMUNE FUNCTIONS IN THE GASTROINTESTINAL TRACT

Various regulatory adaptations exist to maintain the symbiotic relationship between humans and their GI microbiota [3]. In a healthy intestine, these adaptations prevent a constant activation of the immune system by commensal bacteria and food antigens but at the same time enable defence against pathogens. Commensal bacteria are critical for the development and function of the immune system and contribute to maintaining homeostasis in the GI tract.

Immune cell populations and their respective functions vary greatly between the upper and the lower part of the GI tract, as recently reviewed [2]. Immune responses within the small intestine focus on the defence against pathogens and tolerance towards food antigens. With the vast increase of the microbial density towards the distal locations of the GI tract, the focus of the immune responses within the colon is the prevention of inflammatory responses against the commensal microbiota. First, the thicker mucus layer in the colon compared to the small intestine provides a physical barrier to prevent the entry of bacteria into the epithelium. In addition, the large numbers of mucosal immunoglobulin A producing plasma cells, interleukin-10 (IL-10) producing macrophages and regulatory T cells in the colon demonstrate the importance of regulatory immune functions within this part of the GI tract [2].

1.3.1. Microbial influence on development and function of the immune system

The importance of the GI microbiota in the development and function of the immune system is widely recognised [122]. Studies using germ-free animals have provided a valuable tool to investigate how commensal bacteria shape immune function. The absence of microorganisms in germ-free animals has been associated with an impaired development of the immune system compared to conventionally housed animals. For example, germ-free mice have poorly developed Peyer's patches, lymphoid aggregates of the GALT [69]. Furthermore, germ-free mice have a reduced number of $CD4^+$ T cells and immunoglobulin A producing B cells in the lamina propria compared to colonised animals [123,124]. Differences between germ-free and conventionally housed animals are not limited to the intestinal immune system. Germ-free animals also display an impaired development of systemic lymphoid structures with a reduction in B and T cells in the spleen and peripheral lymph nodes [69,125]. Numerous effects on non-immune systems of the GI tract have also been reported. These include changes in morphology, absorptive function, electrolyte handling, bile metabolism, motility, and enteroendocrine and exocrine function as previously reviewed [70]. It has been shown that germ-free animals exposed to commensal bacteria develop an immune system similar to conventional animals within several weeks of inoculation [69].

In addition to the central role of the GI microbiota in the development of the immune system, an association between alterations in the composition of the microbiota, so-called dysbiosis, and inflammatory diseases has been reported [12,16,126,127]. For example, IBD is associated with a reduction in bacterial diversity, an increase in the abundance of *Bacteroidetes* and a reduction in the abundance of *Firmicutes* [128]. However, conflicting findings have also shown a decrease in the abundance of *Bacteroidetes* and *Firmicutes* in

patients with IBD compared to healthy controls [129]. One explanation for these inconsistent findings may be differences in the samples analysed. For example, results obtained from compositional analysis of faecal samples were compared to that of mucosal tissue samples, which are known to harbour distinct microbial compositions [128,129]. In addition to the described phylum level changes, specific bacterial species were decreased in the GI microbiota of patients with inflammatory diseases, e.g., *F. prausnitzii* was reduced in IBD [10-14], IBS [15] and coeliac disease [16]. However, it remains unclear if GI dysbiosis is the cause or the consequence of disease pathogenesis [130].

Induction of inflammation by changes in the composition of the GI microbiota has been demonstrated using a colitis mouse model. Mice deficient in T-bet, a transcription factor involved in the regulation of mucosal immune responses to commensal bacteria, developed spontaneous ulcerative colitis in the absence of adaptive immunity [131]. Remarkably, this colitis was both vertically and horizontally transmissible to genetically intact hosts as shown in cross-fostering and co-housing experiments, respectively. The authors suggested that the loss of T-bet supports the development of a colitogenic microbial community in this colitis mouse model. The finding that colitis was communicable to wild-type mice highlights the significance of commensal bacteria in controlling immune function.

1.3.2. The role of innate signalling in maintaining immune homeostasis

Bacteria in the intestinal lumen are recognised by IECs and immune cells via the expression of pattern recognition receptors (PRRs) [132,133]. These receptors recognise common structures on microbial surfaces, so-called pathogen-associated molecular patterns (PAMPs) [133]. PRRs are also activated by endogenous products derived from damaged tissue, known as damage-associated molecular pattern (DAMPs) [134]. PRRs comprise several families of receptors, namely the nucleotide oligomerisation domain-like

receptors, retinoic acid inducible gene I-like receptors and Toll-like receptors (TLRs) [133]. The best characterised PRRs are the TLRs. Some of the 10 TLRs identified in humans to date are localised in the cell membrane (TLRs 1, 2, 4, 5 and 6) and recognise extracellular PAMPs like lipids, lipoproteins and proteins. The others (TLRs 3, 7, 8 and 9) are found in endosomal membranes to recognise endocytosed PAMPs, primarily nucleic acids [135].

TLR stimulation triggers downstream signalling cascades leading to the activation of transcription factors, which induce the release of pro-inflammatory cytokines and chemokines resulting in the induction of inflammatory immune responses against pathogens [136]. Activation of TLRs can induce different intracellular signalling pathways as shown in Figure 1.3 [137]. The first step in signal transduction upon TLR activation is the recruitment of adapter proteins of which myeloid differentiation primary response protein 88 (MyD88) and TIR-domain-containing adapter-inducing interferon-β (TRIF) are the most commonly used. The pathways initiated by the two adaptor proteins are referred to as MyD88 signalling pathway and TRIF signalling pathway [137].

In the MyD88 signalling pathway, MyD88 mediates the binding of interleukin-1 receptor-associated kinase (IRAK) 1, 2, and 4 to TLRs which leads to their phosphorylation and association with TNF receptor associated factor (TRAF) 6. This in turn activates the transforming growth factor beta-activated kinase 1 kinase complex which subsequently activates the inhibitor of kappa B (IκB) kinase (IKK) complex. The IKK complex catalyses the phosphorylation of IκB proteins which results in the proteasomal degradation of IκB. Upon the degradation of its inhibitor IκB, the transcription factor nuclear factor-kappa B (NF-κB) is translocated into the nucleus. Finally, this signal transduction pathway leads to the induction of inflammatory cytokines and chemokines upon TLR stimulation. An

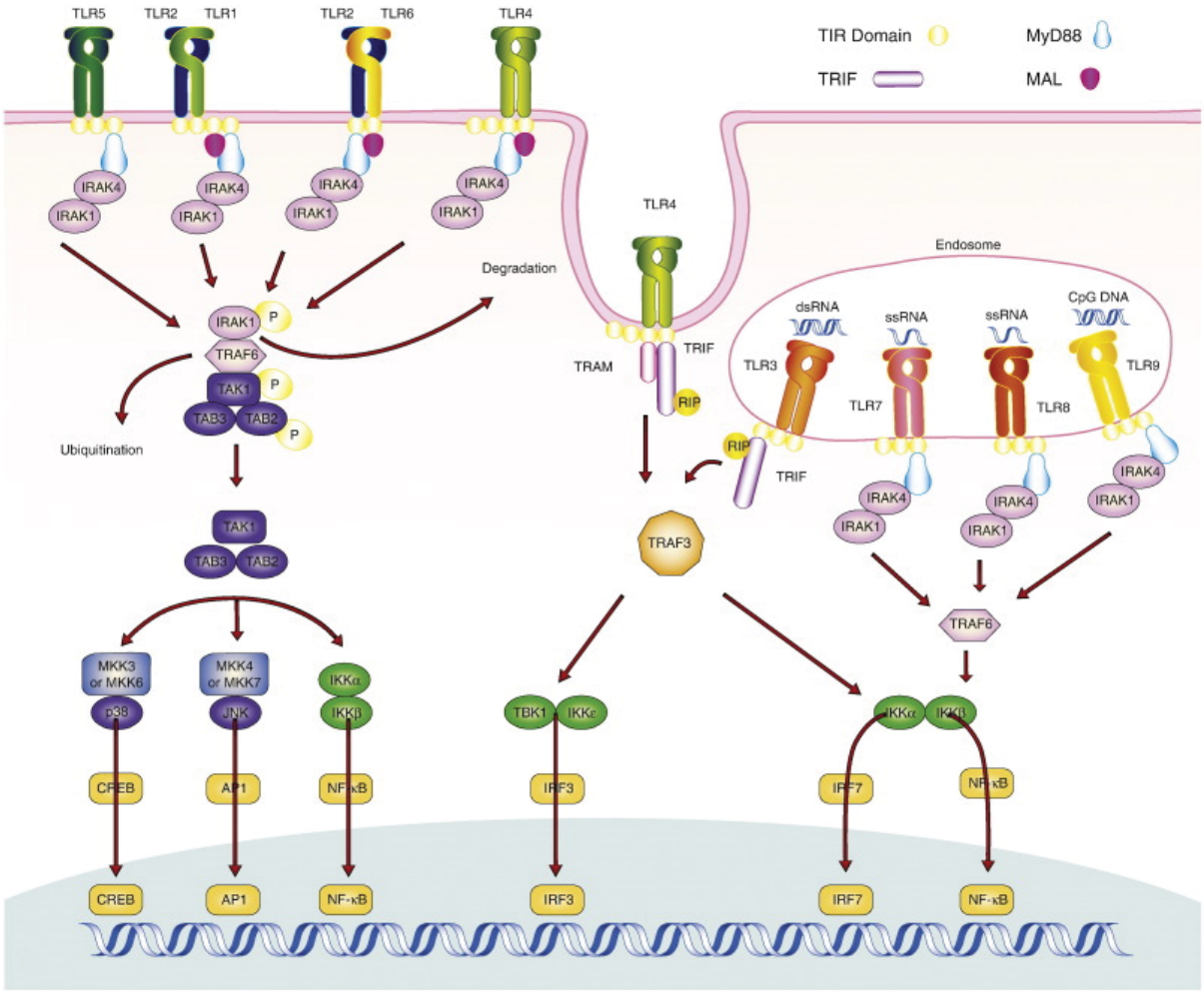

Figure 1.3 Schematic diagram of TLR distribution and signalling.

TLRs are localised in the cell membrane or in endosomal membranes and recognise common bacterial and viral structures. TLR stimulation triggers downstream signalling cascades leading to the activation of specific transcription factors. This induces the release of pro-inflammatory cytokines and chemokines resulting in the induction of inflammatory immune responses against pathogens. Figure from Jiménez-Dalmaroni *et al.* (2016) [137]. **(**Permission obtained**)**

alternative pathway is the activation of the mitogen-activated protein kinases (MAPKs) p38 and JUN N-terminal kinase, which leads to the activation of the transcription factors cyclic AMP-responsive element-binding protein and activator protein 1, respectively, and the subsequent induction of inflammatory cytokines and chemokines [137].

In the TRIF signalling pathway, the adaptor protein TRIF is recruited after TLR3 and TLR4 activation. This leads to the recruitment of IKKε and TRAF family member-associated NF kappa-B activator-binding kinase 1 (TBK1) and TRAF3 to the receptor complexes. TBK1 phosphorylates the transcription factors interferon regulatory factor 3 and interferon regulatory factor 7 which then activate the expression of interferon inducible genes [137].

It is becoming increasingly evident that innate immune responses are not only induced by the signalling of single TLRs but rather are a consequence of a complex crosstalk between different TLRs and other PRRs as recently reviewed [133,135,138]. Cross-activation contributes to signal amplification in the defence against pathogens whereas cross-inhibition prevents chronic inflammation. TLR crosstalk is therefore crucial in maintaining immune homeostasis.

TLR signalling is critical in the innate defence against pathogens. Constant activation of the immune system of the GI tract through the recognition of the resident microbiota would be pathological. Therefore, the host needs to be able to distinguish between commensals and pathogens, and balance tolerance and immunity. This is partly achieved through the regulated expression and distribution of PRRs in the GI tract [27,139]. For example, IECs express low levels of TLR2 and TLR4 under healthy conditions, reflecting one of the mechanisms for the immunological hyporesponsiveness to commensal bacteria [140,141]. Differences in the expression of PRRs between apical and basolateral surfaces of IECs are

another way to distinguish between pathogenic and commensal bacteria. TLR5, which recognises bacterial flagellin, is only expressed on the basolateral side of IECs. It has been shown that pathogenic *Salmonella*, but not commensal *E. coli*, translocate flagellin across the epithelia. Thus, only pathogenic *Salmonella* activates TLR5 and induces epithelial pro-inflammatory gene expression [142]. Moreover, stimulation of TLRs expressed on the apical or basolateral surface of IECs induces distinct immune responses. For instance, the stimulation of apical TLR9 triggers anti-inflammatory responses, whereas stimulation of basolateral TLR9 elicits a pro-inflammatory response [143]. Therefore, pathogens that are able to breach the epithelial barrier, induce inflammation, whereas the recognition of the commensal microbiota is restricted to the apical surface and induces regulatory responses.

Another mechanism to limit uncontrolled TLR activation by commensal bacteria in the intestine is the expression of negative regulators of TLR signalling by IECs. One example is the Toll-interacting protein (TOLLIP), an intracellular adaptor protein which inhibits the activity of IRAK upon TLR stimulation and consequently limits the production of pro-inflammatory mediators [141,144,145]. In addition, single immunoglobulin IL-1R-related molecule (SIGIRR), a member of the IL-1 receptor (IL-1R) superfamily, is implicated in the negative regulation of TLR signalling and maintenance of colonic epithelial homeostasis [146,147].

Despite these mechanisms to reduce TLR signalling in the healthy intestine, it is becoming increasingly evident that a basal level of TLR signalling induced by luminal microbiota contributes to homeostasis [148]. Evidence for this homeostatic influence of TLR signalling on the GI epithelium mainly originated from work in TLR knockout mice. For instance, mouse models with the genes for TLR2, 4, 9 or the adaptor protein MyD88 knocked out have increased susceptibility to colitis induced by DSS [143,148].

The beneficial effects of TLR signalling in the GI epithelium is an area of intense research as reviewed by Abreu [149]. TLR signalling promotes epithelial cell proliferation, IgA production and the expression of antimicrobial peptides [149]. Moreover, the recognition of the commensal microbiota contributes to maintaining intestinal barrier function through the regulation of TJ integrity and expression. For instance, TLR2 signalling regulates TJ integrity in IECs and influences susceptibility to intestinal injury and inflammation as shown in studies with TLR2 knockout mice [150]. TLR2-ligand induced signalling activates specific isoforms of protein kinase C in IECs which results in the enhancement of barrier integrity through translocation of the TJ protein ZO-1 [151].

In addition, TLR2 activation can result in pro- and anti-inflammatory responses, which is dependent upon the interaction of TLR2 with multiple co-receptors [152]. TLR2 recognises surface structures of Gram-negative and Gram-positive bacteria and yeast, such as lipoproteins, lipoteichoic acid and zymosan, respectively. TLR2 occurs in the form of heterodimers with different co-receptors; TLR1 and TLR6. It has been reported both *in vitro* and *in vivo*, that stimulation of the TLR2/6 heterodimer results in the differentiation of dendritic cells (DCs) towards a tolerogenic phenotype and an increase of IL-10 producing regulatory T cells [153]. However, the activation of the TLR2/1 heterodimer results in increased production of IL-12p40 and less IL-10 by DCs and promotes the differentiation of inflammatory T cells. The pro- and anti-inflammatory responses upon activation of TLR2/1 and TLR2/6, respectively, is a consequence of different cell signalling pathways activated by the different heterodimers. The pro-inflammatory response upon TLR2/1 activation is induced by p38 MAPK activation. In contrast, the regulatory response upon TLR2/6 activation is dependent on c-Jun N-terminal kinase activation [153].

In the case of the example above, the differentiation of tolerogenic DCs that promote regulatory IL-10 immune responses was induced through TLR2/6 activation by a virulence factor of the pathogen *Yersinia pestis* [153]. This mechanism allows the pathogen to escape immune defence mechanisms through blocking inflammation. Similarly, *Staphylococcus aureus*, a commensal bacterium which can also cause infections, causes independent pro- and anti-inflammatory responses through different signalling pathways induced by TLR2 activation [154]. Whereas the anti-inflammatory response is mediated through phosphoinositol 3-kinase-Akt-mTOR and extracellular signal-regulated kinase signalling, the pro-inflammatory response is mediated through p38 MAPK [154]. Furthermore, the pathogen *Mycobacterium tuberculosis* heat shock protein 60 causes anti-inflammatory responses through IL-10 production in macrophages which is mediated through TLR2 signalling [155]. The anti-inflammatory effect is induced by p38 MAPK activation and requires endocytosis of *M. tuberculosis* heat shock protein 60 [155]. Similar anti-inflammatory mechanisms may also be used by commensal bacteria to maintain immune homeostasis in the GI tract.

Results of several studies provide further evidence for anti-inflammatory TLR2 signalling. For example, TLR2 signalling contributes to the anti-inflammatory effects of *Lactobacillus amylovorus* which inhibits TLR4 mediated pro-inflammatory signalling caused by enterotoxigenic *E. coli* in Caco-2 cells and pig explants [156]. Similarly, the TLR2 activation and up-regulation of the TLR negative regulator A20 by several bifidobacteria strains reduces TLR4-induced pro-inflammatory responses to enterotoxigenic *E. coli* in porcine IECs [157]. The authors suggested the potential of bifidobacteria strains to activate TLR2 and to induce the production of A20 as a selection criteria in the screening for immunoregulatory strains [157]. Furthermore, the TLR2/MyD88 pathway activated by a single strain of *Clostridium butyricum* induces anti-inflammatory responses through IL-10

production by macrophages in the GI tract which protects mice from acute experimental colitis [158]. The anti-inflammatory effects of polysaccharide A (PSA) produced by the commensal *Bacteroides fragilis*, which protects mice from experimental colitis, are also mediated through TLR2 activation [159,160].

The signalling in response to TLR4 and TLR9 activation can also contribute to immune homeostasis in the GI tract. For example, Assas *et al.* propose a mechanism for TLR4 activation to indirectly maintain mucosal homeostasis by inducing intracellular signalling that leads to the release of the anti-inflammatory neuropeptide calcitonin gene-related peptide [161]. In addition, deoxyribonucleic acid (DNA) derived from *L. rhamnosus* GG and *B. longum* and from five different *Lactobacillus* species induces anti-inflammatory effects mediated through TLR9 signalling in human IECs (HT-29, T84 and Caco-2 cells) when apically applied [162,163].

1.3.3. Microbial modulation of the function of epithelial cells and immune cells

IECs play a more complex role than simply forming a physical barrier between the lumen and underlying tissues. They also maintain immune homeostasis through sensing the microbial environment via the expression of PRRs and subsequently regulating the function of antigen-presenting cells and lymphocytes [26,139]. IEC function is influenced by commensal bacteria which are able to actively modulate signalling in IECs [26]. These modulations provide a mechanism for commensal bacteria to be recognised by IECs without activating a pro-inflammatory immune response, and therefore allowing the co-existence of humans and their GI microbiota [27].

Some commensal bacteria are able to inhibit PRR-mediated NF-κB activation [42,164]. Under steady-state conditions, this transcription factor is bound by its inhibitor IκB, which

prevents its nuclear translocation. The classical NF-κB activation following receptor stimulation is obtained through tightly regulated phosphorylation, ubiquitination and proteasomal degradation of IκB, resulting in the translocation of NF-κB into the nucleus where it activates the transcription of inflammatory cytokines and chemokines [165]. Experiments with nonvirulent *Salmonella* strains have shown that these commensal bacteria inhibit this pathway by blocking IκB ubiquitination and subsequent degradation, therefore preventing NF-κB activation and maintaining epithelial hyporesponsiveness towards the luminal microbiota [164].

Commensal-derived metabolites are also known to modulate innate immune responses providing another mechanism for maintaining immune homeostasis and tolerance in the GI tract. Butyrate, a SCFA and one of the main end products of fermentation of dietary fibre by bacteria in the GI tract, is a major source of energy for IECs. Moreover, butyrate can exert direct immunomodulatory and anti-inflammatory effects [166]. For instance, butyrate inhibits histone deacetylase activity and thereby suppresses proteasome activity by reducing the expression levels of selected proteasome subunits. This results in the inhibition of the proteasomal degradation of IκB and consequently limits NF-κB activation [167].

Furthermore, IEC recognition of commensal bacteria triggers the production of several immunoregulatory molecules, for example thymic stromal lymphopoietin (TSLP) and transforming growth factor β (TGFβ) [168,169]. These signals, in turn, promote the development of mucosal immune cells with tolerogenic properties. This cross-talk between commensal bacteria, IECs and immune cells is important for maintaining homeostasis and limiting uncontrolled inflammation in the GI tract [132].

1.4. APPROACHES TO MANIPULATE THE GASTROINTESTINAL MICROBIOTA TO PROMOTE HEALTH

With the fast progress in understanding the role of the human microbiota in physiology, the interest in seeking approaches to manipulate their composition and function to obtain health benefits and prevent or treat diseases increased. The concept to modify the microbiota in the GI tract using probiotics and prebiotics is well established. Furthermore, several bacterial species within the human microbiota that have been associated with beneficial effects *in vitro* and *in vivo* have been suggested as a next generation of probiotics for future approaches to manipulate the microbiota and optimising health.

1.4.1. Classical probiotic concept

The health promoting effect of fermented foods was discovered more than a century ago by Elie Metchnikoff [170], a finding that established the origin of the probiotic concept. Probiotics, currently defined as 'live microorganisms that, when administered in adequate amounts, confer a health benefit on the host' [171,172] mainly belong to the lactic acid bacteria such as *Lactobacillus* spp., *Bifidobacterium* spp. and *Enterococcus* spp., but also *Escherichia* spp. and *Saccharomyces* spp. are used in probiotic products. Classical probiotic microorganisms are regarded as "Generally recognised as safe" (GRAS), which is either supported by results of scientific studies or by experiences made throughout their long history of use in foods [173]. Commercially used probiotic strains often originate from the human GI microbiota, e.g. the well characterised *Lactobacillus rhamnosus* GG [174]. Applications for probiotics include the prevention or treatment of various disorders like infectious and antibiotic-associated diarrhoea, IBD and IBS [175].

The beneficial effects of probiotics are ascribed to different mechanisms, although the exact mechanism of action at the molecular level often remains unknown. Generally, the effects of probiotics can be divided into three levels of action as shown in Figure 1.4 [176]. The first level includes effects of probiotic bacteria inside the GI tract, for example inhibiting the adhesion and growth of pathogens or direct metabolic contributions through the production of enzymes. The interactions between probiotic bacteria with the mucus layer and IECs can be described as the second level of action of probiotics. This includes enhancing barrier function, modulating mucosal immune responses and effects on the enteric nervous system. With effects reaching beyond the GI tract, the third level of action of probiotics includes for example effects on the systemic immune system, the nervous system and the liver [176].

1.4.2. Commensal obligate anaerobes as next-generation probiotics

Classical probiotics mainly belong to the lactic acid bacteria, including lactobacilli, as discussed above. Lactobacilli are common members of the infant GI microbiota, whereas their abundance in adults is low, with most Lactobacillus spp. colonising the upper GI tract [177]. However, the colon, the lower part of the GI tract with the highest bacterial density, is dominated by obligate anaerobic species [18]. Due to the economic success of probiotics, research on lactobacilli has greatly accelerated over the last few decades to the detriment of study on other bacteria. In addition, oxygen-tolerant bacteria such a lactobacilli provide the technological advantage of an easier incorporation into probiotic products. Technical difficulties have also been a limiting factor in the investigation of host-microbe interactions. Oxygen-tolerant bacteria such as lactobacilli can be readily co-cultured with human cells to enable study of the mechanism of action behind the effects of these bacteria. However, obligate anaerobic bacteria cannot survive in the presence of

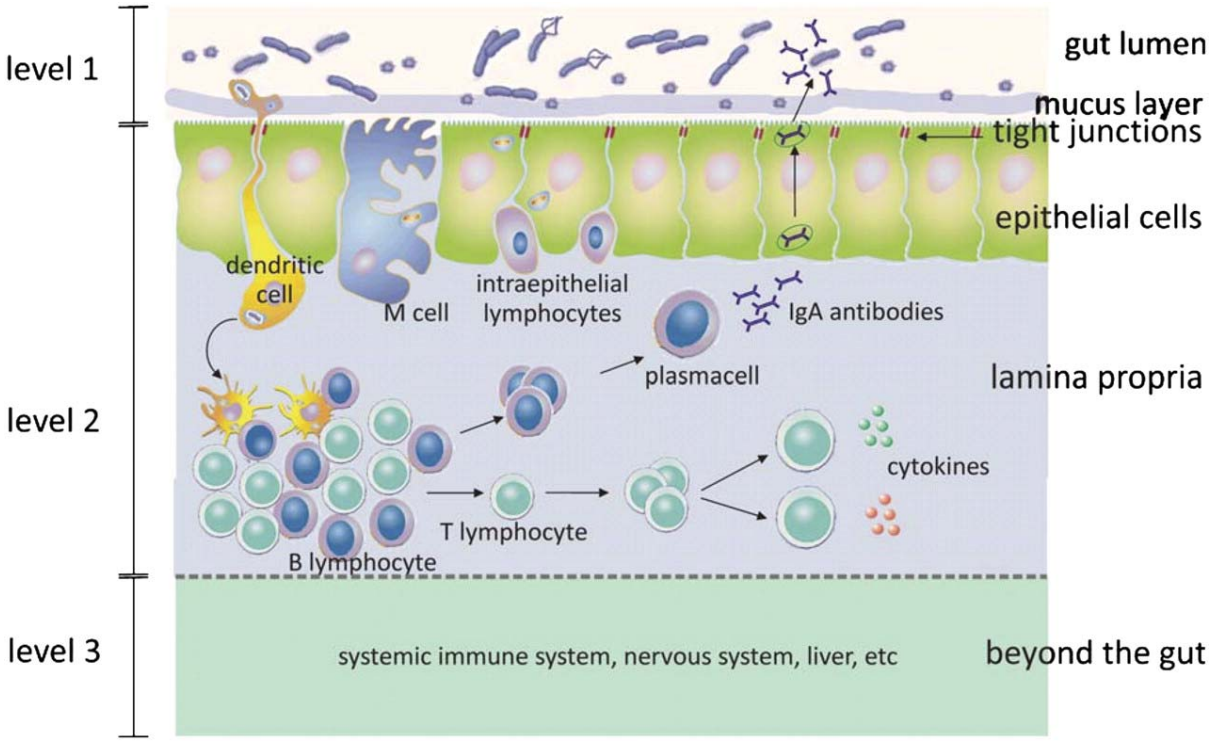

Figure 1.4 Effects of probiotic bacteria divided into three levels of action.

Probiotic bacteria exert their effects in the intestinal lumen, e.g. by influencing the GI microbiota (level 1). Additionally, probiotics modulate the function of IECs and immune cells in the underlying lamina propria, thereby improving intestinal barrier integrity or modulating mucosal immune responses (level 2). Finally, probiotics affect extra-intestinal locations, for example the systemic immune system or the nervous system (level 3). Figure from Rijkers *et al.* (2010) [176]. **(**Permission obtained**)**

oxygen and it is therefore impossible to co-culture these bacteria with oxygen-requiring IECs in conventional systems. Consequently, little is known about the exact mechanisms behind the effects of commensal obligate anaerobes, which means that the effects of the majority of the GI microbiota remain unknown.

The use of high-throughput and next-generation sequencing techniques has rapidly increased our knowledge of the GI microbiota and its significance in human health and disease [17]. In addition, various studies have shown that dysbiosis is associated with diseases involving chronic inflammation in the GI tract (e.g., IBD) and that a decrease in the abundance of certain bacterial species occur in these diseases [12,16,126,127]. It has therefore been hypothesised that these species have a positive effect on human health. Taken together, this information could lead to a broadening of the classical probiotic concept, where currently most of the bacterial strains belong to the lactic acid bacteria, to include a selection of strains from a potential next generation of probiotics originating from indigenous bacteria [17]. Examples of obligate anaerobic commensal bacteria that may exert beneficial effects on human health, as indicated by the results of *in vitro* and animal studies, are described below, with a particular focus on *F. prausnitzii,* the species studied in this dissertation. Most of the beneficial effects of obligate anaerobes are associated with their role in maintaining immune homeostasis in the GI tract. Therefore, some of the known immunoregulatory effects of four representative obligate anaerobic species are summarised in Figure 1.5.

1.4.2.1. *Faecalibacterium prausnitzii*

The obligate anaerobe *F. prausnitzii*, a major member of the clostridial cluster IV within the phylum Firmicutes, is regarded as one of the most prevalent bacteria within the human GI tract [178,179] and accounts for 1.4% to 5.9% of the total faecal microbiota of healthy

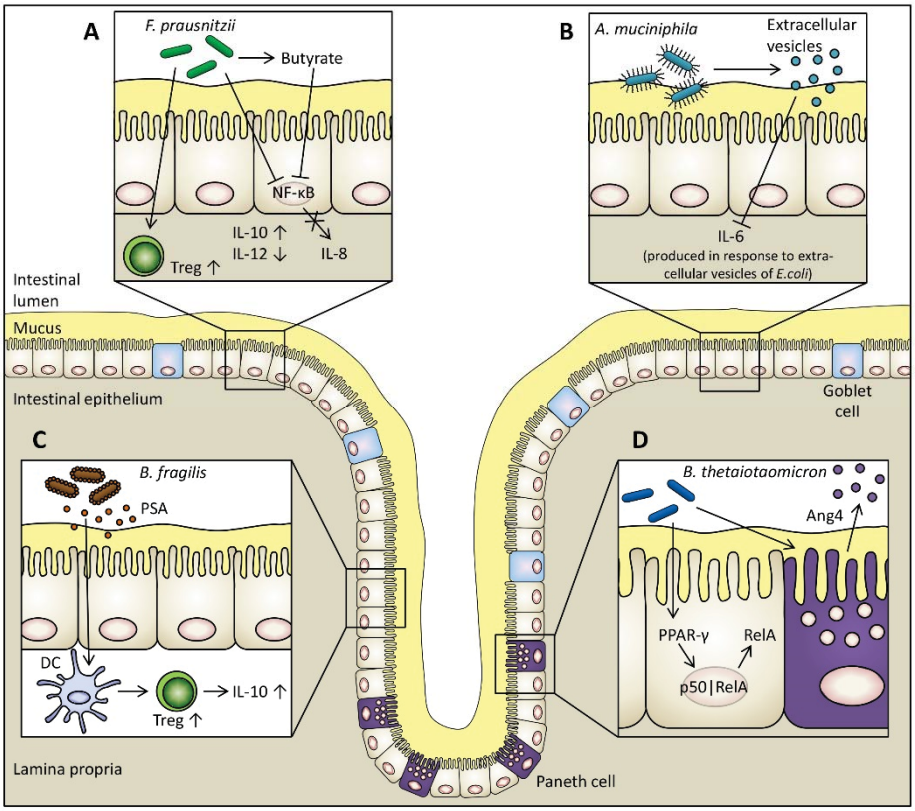

Figure 1.5 Proposed immunomodulatory mechanisms of four examples of obligate anaerobic commensals.

(A) The supernatant of *F. prausnitzii* blocks the activation of transcription factor NF-κB which inhibits the production of pro-inflammatory IL-8 by IECs [179]. *F. prausnitzii* is one of the major butyrate producers in the large intestine. Butyrate also blocks NF-κB activation [167]. Furthermore, *F. prausnitzii* increases the differentiation of regulatory T cells (Treg) [182] and the production of anti-inflammatory IL-10 by peripheral blood mononuclear cells (PBMCs) and decreases the production of pro-inflammatory IL-12 [179,182]. (B) Extracellular vesicles produced by *A. muciniphila* block the production of pro-inflammatory IL-6 from colon epithelial cells in response to extracellular vesicles of *E. coli* [44]. (C) A surface molecule of *B. fragilis*, PSA, exerts immunomodulatory functions within the GI tract. PSA is recognised by DCs which induces increased production of Treg and anti-inflammatory IL-10 [160,183]. (D) *B. thetaiotaomicron* causes the PPAR-γ dependent nuclear export of the NF-κB transcriptionally active subunit RelA in IECs which attenuates pro-inflammatory cytokine expression [42]. *B. thetaiotaomicron* also stimulates the release of the antimicrobial peptide Ang4 by Paneth cells thereby maintaining mucosal barrier function [43].

adults [180]. Originally isolated in 1922 by C. Prausnitz and named *Bacillus mucosus anaerobius*, the bacterium has been reclassified several times. After being named *Fusobacterium prausnitzii* in 1973 [181], the bacterium was further reclassified to its current name *Faecalibacterium prausnitzii* in 2002 [178]. The complete genome sequences of two strains, *F. prausnitzii* L2-6 (PRJNA197183, PRJNA45961) and *F. prausnitzii* SL3/3 (PRJNA197157, PRJNA39151), are available. *F. prausnitzii* is a Gram-negative bacterium, even though phylogenetic analysis based on 16S rRNA sequencing indicates that *F. prausnitzii* is related to the Gram-positive bacteria of the clostridial cluster IV [178]. Furthermore, *F. prausnitzii* is non-spore forming, non-motile and rod-shaped [178]. This commensal bacterium produces butyrate, d-lactate and formate as fermentation products and utilises acetate. A study determining the influence of GI environmental factors on the growth of several *F. prausnitzii* strains showed that the growth of all strains tested was inhibited in the presence of bile salts. Additionally, some of the strains showed growth inhibition at mildly acidic pH [184]. It has been proposed that these attributes help to explain the abundance of *F. prausnitzii* in the colonic community. The sensitivity to bile salts was suggested as a factor that might limit the abundance of *F. prausnitzii* in regions with high bile concentration like the small intestine [184].

The abundance of *F. prausnitzii* in the colon can be influenced by diet. For example, the prebiotics inulin and arabinoxylan increase *F. prausnitzii* in faecal samples of healthy humans [50] and pigs [185], respectively. *F. prausnitzii* is also able to grow on the prebiotics apple pectin [184] and fructooligosaccharides [186] *in vitro*. Moreover, *F. prausnitzii* strains are able to compete with two other known pectin-utilising species, *B. thetaiotaomicron* and *Eubacterium eligens* for apple pectin as a substrate, suggesting an important role for *F. prausnitzii* in pectin fermentation in the colon. It has therefore been concluded that pectin rich substrates could be used to develop prebiotic approaches for

stimulating *F. prausnitzii* [184]. It was also suggested that a diet rich in flavin and antioxidants might have an influence on the abundance of *F. prausnitzii* in the intestine. *F. prausnitzii* uses these compounds to shuttle electrons extracellularly to oxygen which stimulates its growth [187,188]. In addition, vegetarian diet induces a higher ratio (% of group-specific DNA in relation to all bacterial DNA) of *F. prausnitzii* compared to an omnivorous diet as revealed by human faecal microbiota analysis [189]. In contrast, a high-protein diet causes a decrease in beneficial bacterial species in the rat colon, including a decreased abundance of *F. prausnitzii* [190,191]. This effect is associated with an increased risk of colonic disease as demonstrated in epithelial transcriptome analysis showing an upregulation of genes associated with disease pathogenesis and a downregulation of genes associated with protective immune functions [190].

Numerous studies have shown a reduced abundance of *F. prausnitzii* in patients with IBD compared to healthy controls [10-14]. Furthermore, a reduction of this bacterium is associated with a higher risk of postoperative recurrence of ileal Crohn's disease [179]. Interestingly, healthy siblings of patients with Crohn's disease, who have an increased risk to develop this condition, have less *F. prausnitzii* in their intestine, allowing insights into early Crohn's disease pathogenesis [192,193]. *F. prausnitzii* is also reduced in patients with IBS [15], colorectal cancer [194] and coeliac disease [16]. More recent studies associated a decreased abundance of *F. prausnitzii* with cystic fibrosis [195,196], early frailty [197] and depression [198]. In addition, a link has been established between metabolic diseases including obesity, type 2 diabetes and metabolic syndrome and low concentrations of *F. prausnitzii* within the GI microbiota, which can be increased through fasting [199-202].

Based on these findings, it has been hypothesised that the presence of *F. prausnitzii* acts as a protective factor for the mucosa and promotes health of the GI tract. Nevertheless, the mechanisms of the effects of *F. prausnitzii* are only partially understood and require further exploration. *F. prausnitzii* has also been suggested as a promising candidate for treating IBD [179,182,203]. This is supported by the finding that administering *F. prausnitzii* protects against experimental colitis in animal models [179,182,204-208], but has not yet been tested in human clinical studies. The finding that the antioxidants cysteine and riboflavin in combination with the cryoprotectant inulin maintain the viability of *F. prausnitzii* at ambient air over 24 h could open possibilities for the clinical application of this extreme oxygen-sensitive bacterium [209].

Only few studies challenge the model of a protective role for *F. prausnitzii*. In contrast to adult Crohn's disease, where a reduced abundance of *F. prausnitzii* was observed, this species was increased in the colonic mucosa of children with newly diagnosed Crohn's disease [210,211]. Moreover, treatment of paediatric Crohn's disease with enteral nutrition resulted in a decrease in *F. prausnitzii* and concomitant disease improvement [212]. The authors suggested a more dynamic function of *F. prausnitzii* than described in previous studies [210]. However, it could be possible that paediatric IBD is associated with different changes in microbial composition compared to adult disease.

F. prausnitzii may contribute to the maintenance of intestinal health through several mechanisms. It may exhibit its beneficial effects indirectly by providing colonocytes with their most important energy source, butyrate, and therefore strengthen the epithelium [178]. However, direct anti-inflammatory effects of *F. prausnitzii* have also been demonstrated both *in vitro* and *in vivo*. In an *in vitro* model, secreted metabolites from *F. prausnitzii* A2-165 (DSM 17677) were able to block NF-κB activation and IL-8 production [179], which

was not due to bacterial butyrate production. Additionally, the stimulation PBMCs by *F. prausnitzii* has been shown to increase production of anti-inflammatory IL-10 and decrease production of pro-inflammatory IL-12. The same group demonstrated a reduction in 2,4,6-trinitrobenzenesulfonic acid (TNBS) induced colitis activity in mice orally administered *F. prausnitzii* or its culture supernatant [179].

Following the initial characterisation of *F. prausnitzii* as anti-inflammatory bacterium by Sokol *et al.* described above, several *in vitro* and *in vivo* studies provided additional insights into the immunomodulatory mechanisms of this beneficial bacterium. For instance, both *F. prausnitzii* (ATCC 27766) and its culture supernatant induced anti-inflammatory cytokine production in human PBMCs and a rat model of TNBS-induced colitis [182]. Cytokine concentrations were quantified in PBMC culture supernatants and rat blood serum. The *F. prausnitzii* supernatant exhibited the strongest anti-inflammatory effect and showed improved protection against experimental colitis compared to the other treatment groups, which also included a probiotic *Bifidobacterium longum* (strain provided by Shanghai Sine Pharmaceutical Company, China). Furthermore, *F. prausnitzii* and its culture supernatant increased the production of regulatory T cells [182]. In addition, *F. prausnitzii* A2-165 induced the highest secretion of anti-inflammatory IL-10 by human and murine DCs compared to four other *F. prausnitzii* strains and eight abundant commensals [207]. This was associated with relative high TLR2 and TLR2/6 activation by *F. prausnitzii* A2-165. Another anti-inflammatory mechanism employed by *F. prausnitzii* (ATCC 27766) is the inhibition of the pro-inflammatory cytokine IL-17 as demonstrated *in vitro* and *in vivo* which was associated with disease improvement in colorectal colitis in rats [208].

A recent study investigated the effect of viable and dead *F. prausnitzii* A2-165 (DSM 17677) on global gene expression of Caco-2 cells [19]. Viable *F. prausnitzii* exerted differential effects on Caco-2 cells compared to dead bacteria with most of the differences observed in genes involved in immune pathways. Functional analysis using Ingenuity® Pathway Analysis, a bioinformatic tool used to analyse and interpret the biological meaning of gene expression data, predicted a decrease in functions belonging to the "inflammatory response" and "immune cell trafficking" categories in Caco-2 cells treated with live *F. prausnitzii* compared to untreated Caco-2 cells [19].

Several studies demonstrated that the anti-inflammatory effects of *F. prausnitzii* are also achieved using the bacterial supernatant, indicating that secreted metabolites cause the protective effects [179,182,208]. However, only recently a protein with anti-inflammatory properties was isolated from *F. prausnitzii* supernatant [213]. This 15 kDa protein inhibited NF-κB activation in IECs and protected mice from DNBS-induced colitis. In contrast, *F. prausnitzii* cell surface structures also exert protective effects. For example, the extracellular polymeric matrix isolated from strain *F. prausnitzii* HTF-F caused anti-inflammatory effects *in vitro* and attenuated disease parameters in DSS-induced colitis in mice [204]

F. prausnitzii improves intestinal barrier integrity *in vivo*. For instance, in mice with DSS-induced colitis, the *F. prausnitzii* culture supernatant improved intestinal barrier integrity by affecting paracellular permeability, as measured by ^{51}chromium (Cr)-EDTA transport [214]. The paracellular passage of ^{51}Cr-EDTA was increased in the ileal mucosa of mice treated with DSS compared to control animals. Treatment with *F. prausnitzii* culture supernatant resulted in decreased passage of ^{51}Cr-EDTA, indicating improved intestinal

barrier integrity. This effect was suggested to contribute to the reduction of the severity of DSS-induced colitis in mice [214].

Taken together, the results of the above-described studies indicate a role of *F. prausnitzii* in maintaining homeostasis in the GI tract. The decreased abundance of *F. prausnitzii* in diseases including IBD and coeliac disease may contribute to the reduction in commensal bacteria-mediated, anti-inflammatory activities in the intestinal mucosa [14].

1.4.2.2. *Bacteroides thetaiotaomicron*

B. thetaiotaomicron, a Gram-negative obligate anaerobic organism belonging to the phylum *Bacteroidetes*, is a prevalent member of the human GI microbiota [215]. A study investigating the diversity of the human GI microbiota showed that within this phylum, which comprises 48% of all bacterial 16S rDNA sequences analysed, *B. thetaiotaomicron* accounted for 13% [18]. The complete genome sequence of two strains, *B. thetaiotaomicron* VPI-5482 (PRJNA399) [216] and *B. thetaiotaomicron* 7330 (PRJNA289334), are available. This revealed that *B. thetaiotaomicron* may be able to utilise a large variety of complex polysaccharides as substrates [215,216]. Furthermore, the organism is able to adapt to the changing colonic environment through regulation of the expression of genes involved in its polysaccharide utilisation machinery [46]. These characteristics confer an advantage for survival in the changing host intestinal lumen and may explain the high abundance of *B. thetaiotaomicron* in the human GI microbiota [215,216]. The prevalence of *B. thetaiotaomicron* is reduced in adult and paediatric patients with IBD [126,217,218], indicating a role for this commensal bacterium in maintaining intestinal health. However, compared to *F. prausnitzii*, evidence for this association is weak with only a few studies reporting this observation. The reduced

abundance of *B. thetaiotaomicron* observed in patients with IBD could also indicate an increased susceptibility of this bacterium to inflammatory conditions.

A number of studies indicate that, in addition to providing nutrients to the host through the digestion of complex carbohydrates, *B. thetaiotaomicron* also influences the host directly via interaction with IECs. For example, the colonisation of germ-free mice with *B. thetaiotaomicron* VPI-5482 (ATCC 29148) increased the expression of several host genes important for functions including nutrient absorption, mucosal barrier function, production of angiogenic factors and motility [219]. Additionally, *B. thetaiotaomicron* influences host immune responses. For example, *B. thetaiotaomicron* attenuates pro-inflammatory cytokine expression by inducing the expression of peroxisome proliferator-activated receptor-γ (PPAR-γ) in Caco-2 cells, which promotes nuclear export of the NF-κB transcriptionally active subunit; v-rel avian reticuloendotheliosis viral oncogene homolog A (RelA) [42]. Furthermore, *B. thetaiotaomicron* stimulates the production of antimicrobial peptides or proteins by Paneth cells [43]. Antimicrobial peptide angiogenin 4 (Ang4) released by Paneth cells in germ-free mice can be induced by colonisation with *B. thetaiotaomicron* VPI-5482 (ATCC 29148). This antimicrobial protein kills Gram-positive pathogens such as *Listeria monocytogenes*; however, the Gram-negative commensal *B. thetaiotaomicron* is less sensitive with only a 30% reduction of viable cells upon exposure to Ang4. Stimulation of the production of antimicrobial proteins, e.g., Ang4, represents a mechanism of how commensal bacteria such as *B. thetaiotaomicron* can contribute to maintaining mucosal barrier function [43].

There is preliminary evidence to suggest that *B. thetaiotaomicron* may be effective in the treatment of infectious diarrhoea. For example, *B. thetaiotaomicron* VPI-5482 (ATCC 29148) contributed to the prevention of rotavirus infection *in vitro* [220]. However, clinical

evidence for this potentially protective effect of *B. thetaiotaomicron* on rotavirus infection is not yet available.

In addition to the effects of a single species, the interplay between two major commensal bacteria, *F. prausnitzii* and *B. thetaiotaomicron*, promotes colonic mucosal homeostasis [221]. Germ-free rats mono-associated with *B. thetaiotaomicron* VPI-5482 (ATCC 29148) had increased goblet cell differentiation and expression of mucus-related genes. This stimulation of the secretory lineage and increase in mucus production was reduced in germ-free rats di-associated with *B. thetaiotaomicron* and *F. prausnitzii* A2-165 (DSM 17677). The authors suggested that the balance between these species could contribute to colonic mucosal homeostasis [221].

1.4.2.3. *Bacteroides fragilis*

B. fragilis is an obligate anaerobic bacterium within the phylum *Bacteroidetes* and a common member of the human GI microbiota [222,223]. Compared to the other members of the *Bacteroidetes*, *B. fragilis* is the least abundant species in the faecal microbiota, accounting for only 0.6% of the bacteria present in stool [223]. It is generally a commensal bacterium, however when translocated into the bloodstream or extra-intestinal tissue after surgery, disease or trauma it can cause serious infections [224].

B. fragilis exerts immunomodulatory functions within the GI tract. Mice with experimental colitis induced by colonisation with the pathobiont *Helicobacter hepaticus* were protected from disease when co-colonised with *B. fragilis* [183]. This protection was shown to depend on a surface molecule of *B. fragilis*, PSA, as the purified molecule alone prevented intestinal inflammation *in vivo*. PSA induced the production of anti-inflammatory IL-10 *in vitro* which was suggested to be required for the inhibition of inflammation [183]. PSA is packaged into outer membrane vesicles (OMVs) when released by the bacterium [160].

These OMVs containing PSA protected mice with TNBS-induced colitis. The OMV-associated PSA is recognised by DCs through TLR2 which induces increased production of regulatory T cells and anti-inflammatory cytokines [160]. Results of a recent study revealed that a specific DC subset namely plasmacytoid DCs (PDCs) are the mediators behind the PSA-induced protection against experimental colitis in mice [225]. This protection was dependent on both innate and adaptive immune mechanisms and TLR2-mediated. The exposure of PDCs to PSA increased the production of anti-inflammatory IL-10 by $CD4^+$ T cells.

Interestingly, PSA released by *B. fragilis* also conferred protection from inflammation in extra-intestinal tissue [226]. This immunomodulatory molecule protected against central nervous system demyelination and inflammation during experimental autoimmune encephalomyelitis, which is used as an animal model for multiple sclerosis. The protective effect was mediated through TLR2 signalling. These results indicate that the GI microbiota may influence the susceptibility of the host towards extra-intestinal autoimmune disorders.

1.4.2.4. *Akkermansia muciniphila*

The obligate anaerobe *A. muciniphila* belongs to the phylum *Verrucomicrobia* and is part of the mucosa-associated microbiota because of its ability to produce mucus-degrading enzymes [41]. *A. muciniphila* is a common member of the human GI microbiota; its abundance in the colon ranges between 1% to 3% of the bacterial population [227].

Several studies have shown a reduced abundance of *A. muciniphila* in humans with various conditions or diseases. For example, *A. muciniphila* is less abundant in obese children [228] and its abundance decreases with increasing body weight gain in pregnant women [229]. *Akkermansia* spp. are also reduced in children with atopic diseases [230]. The reduction of *A. muciniphila* in patients with ulcerative colitis and Crohn's disease

compared to its high abundance in the mucosa-associated microbiota of healthy controls led to the suggestion that this species might play a protective or anti-inflammatory role in the intestinal mucosa [39]. Furthermore, *A. muciniphila* has been proposed as a marker for a healthy intestine due to its reduction in disease states but high abundance in the healthy mucosa [231].

A potential protective role for *A. muciniphila* in IBD was investigated in a recent *in vivo* study. Extracellular vesicles derived from *A. muciniphila* conferred protective effects in mice with DSS-induced colitis such as amelioration of body weight loss, colon length (decreased in mice treated with DSS), and inflammatory cell infiltration of the colon wall [44]. Furthermore, pre-treatment of a colonic epithelial cell line (CT26) with *A. muciniphila*-derived extracellular vesicles resulted in an anti-inflammatory effect as shown by decreased production of the pro-inflammatory cytokine IL-6 induced by extracellular vesicles of a pathogenic strain of *E. coli* [44].

The influence of *A. muciniphila* on metabolic functions of the host and the association of this bacterium with obesity has also been investigated in a recent *in vivo* study. *A. muciniphila* was reduced in genetically obese mice (ob/ob mice) and mice fed a high-fat diet [45]. Mice fed a high-fat diet supplemented with oligofructose, a prebiotic, had a normal abundance of *A. muciniphila* and an improvement in metabolic disorders, endotoxemia and adipose tissue inflammation. In addition, when mice fed a high-fat diet were given viable *A. muciniphila* Muc^T (ATTC BAA-835), this resulted in normalisation of the metabolic endotoxemia, fat-mass gain, insulin resistance and adipose tissue inflammation; all of which were symptoms induced by the high-fat diet [45]. Based on the results of this study, the authors suggested a potential application of *A. muciniphila* in the prevention and/or treatment of obesity and associated metabolic disorders [45].

Furthermore, in a mouse model of genetic-induced hyperlipidaemia *A. muciniphila* protected from acute and chronic hyperlipidaemia by upregulating the expression of low-density lipoprotein receptors [232]. In mice fed a high-fat diet and treated with metformin, a common medication for the treatment of type 2 diabetes, an increase in the *Akkermansia* spp. population was determined which correlated with improved glucose homeostasis [233]. The change in microbiota composition induced by metformin was suggested as a mechanism of the antidiabetic effect of this medication [233].

A. muciniphila increases barrier integrity of IECs [234]. The bacterium adhered to Caco-2 and HT29 cells and increased TEER across Caco-2 monolayers [234]. The barrier enhancing properties of *A. muciniphila* may contribute to its potential protective role in IBD. Furthermore, the reduction of high-fat-diet-induced endotoxemia by the bacterium observed in mice may be a result of the enhancement in intestinal barrier integrity.

Recently, the link between the abundance of *A. muciniphila* and metabolic health was also demonstrated in humans [235]. At baseline of a caloric restriction intervention in overweight and obese adults, higher faecal *A. muciniphila* levels were associated with the healthiest metabolic status, specifically with regard to fasting plasma glucose, plasma triglycerides and body fat distribution. Individuals with a higher baseline *A. muciniphila* abundance showed a better response to the caloric restriction intervention as demonstrated in an increased improvement in glucose homoeostasis, blood lipids and body composition compared to individuals with lower baseline *A. muciniphila* [235]. Although these findings demonstrate the beneficial effects of *A. muciniphila* on metabolic health in humans, clinical studies investigating *A. muciniphila* in the treatment of obesity and type 2 diabetes do not yet exist.

Despite the increasing interest in *A. muciniphila* over the last few years, knowledge regarding the precise mechanisms of the host-microbial interaction causing these beneficial effects is still limited and will require further exploration. Furthermore, recent studies have mainly focused on the protective role of *A. muciniphila* in obesity and type-2 diabetes but only a few studies have thus far addressed the link between this species and inflammatory disorders such as IBD. In addition, it is not clear if *A. muciniphila* only exerts beneficial effects or if this bacterium may also be associated with potentially harmful effects under certain conditions. *A. muciniphila* releases sulphate during fermentation of mucin [41] which could be utilised either by this species or other sulphate-reducing bacteria to produce hydrogen sulphide. The increased availability of sulphate may lead to an increased abundance of sulphate-reducing bacteria which have been associated with inflammation in genetically susceptible hosts [236]. However, if *A. muciniphila* exerts any potential inflammatory effects these may be dependent on competition with other bacteria specialised in mucin-degradation [46], the composition of the GI microbial ecosystem [237] and/or host susceptibility [236].

1.4.2.5. *Bacteroides uniformis*

Similar to the example of *A. muciniphila* above, a connection between the abundance of *Bacteroidetes* or *Bacteroides* subgroups and obesity has been shown in various studies, with lower numbers of these bacterial groups in overweight individuals [238]. These observations have led to the hypothesis that interventions aiming to increase the proportion of specific *Bacteroides* spp. could be effective in the treatment of obesity and its related metabolic disorders [239].

To further analyse this potential beneficial effect of *Bacteroides* spp., mice with high-fat-diet-induced obesity were inoculated with *Bacteroides uniformis* CECT 7771 [239]. This

strain was chosen from a selection of human *Bacteroides* spp. because it exhibits low inflammatory activity *in vitro*. The study demonstrated numerous positive effects induced by the administration of this bacterial strain that were connected with an improvement of metabolic and immune dysfunctions caused by the high-fat diet. It was shown for example, that administration of *B. uniformis* CECT 7771 resulted in reduced body weight gain, liver steatosis and liver cholesterol and triglyceride concentrations. In addition, the concentrations of cholesterol, triglyceride, glucose, insulin and leptin in the serum of obese mice fed with *B. uniformis* CECT 7771 were reduced. Furthermore, administration of this strain increased the TNF-a production by macrophages and DCs in response to LPS stimulation as determined by enzyme-linked immunosorbent assay (ELISA) and also the induction of a T-cell proliferation response by DCs as determined using a cell proliferation ELISA. Both of these immune defence mechanisms were impaired in high-fat-diet-induced obesity. The dysbiosis observed in obese mice could be partially restored by the administration of *B. uniformis* CECT 7771 [239].

1.4.2.6. Segmented filamentous bacteria

Segmented filamentous bacteria (SFB), first observed in the ilea of mice and rats [240], are obligate anaerobic bacteria that have been observed to populate various vertebrates including humans [241]. Metagenomic comparisons indicated that SFB are closely related to *Clostridium* spp. [242]. Recently, methods to successfully culture SFB have been developed [243,244]. SFB have been shown to firmly attach to IECs by one end of the filament [240].

The ability to mono-colonise germ-free mice with SFB [245] set the starting point for numerous studies investigating the interactions between this commensal organism and its host. These studies have revealed a critical role for SFB in the maturation of the immune

system. Mono-colonisation of germ-free mice with SFB increased the number of lymphoid and IgA-secreting cells in the intestinal mucosa and elevated IgA titres in serum and secretions in comparison to germ-free mice [246]. Furthermore, SFB were reported to influence the development and activation of T helper cells. In particular, they induce the development of intestinal Th17 cells [247]. This activation of a Th17 response conferred protective effects to mice through increased colonisation resistance to the intestinal pathogen *Citrobacter rodentium* [247]. SFB have also been shown to simultaneously induce Th1, Th2, Th17, and regulatory T cell responses in mono-colonised mice [248]. Remarkably, colonisation of germ-free mice with this single species induced a similar coordinated maturation of intestinal T cell responses as induced by the colonisation with the whole mouse microbiota [248]. This effect was not observed when different bacteria (e.g. *B. thetaiotaomicron*, *B. vulgatus* or *E. coli*) were used, which points out the key role of SFB in shaping immune function in the intestine.

1.5. DUAL-ENVIRONMENT CO-CULTURE MODELS TO STUDY HOST-MICROBE INTERACTIONS

Knowledge concerning the exact mechanism(s) behind the effects of GI bacteria on the human epithelia remains limited due to the technical difficulties of co-culturing obligate anaerobic bacteria with oxygen-requiring human cells. Using conventional co-culture models, it is only possible to test the effects of non-viable obligate anaerobes in co-culture with IEC lines. Although some biological effects can be elicited by non-viable bacteria through interactions with surface structures, other effects require live bacteria to generate responses which are indicated to be caused by secreted bacterial metabolites [249]. For example, a study investigating the effect of oxygen-tolerant *Lactobacillus reuteri* on the human IEC lines T84 and HT29 showed these bacteria had an anti-inflammatory effect, as

demonstrated by the inhibition of TNF-α induced IL-8 expression [250]. This effect was only observed with live *L. reuteri*; neither heat-killed nor γ-irradiated bacteria induced a response in IECs. To test the effect of live and metabolically active obligate anaerobic bacteria, including the species described above, *in vitro* systems that enable the co-culture of live obligate anaerobes with oxygen-requiring human cells are needed. Several models have recently been established that allow this dual-environment co-culture with the aim of studying the mechanisms of action of obligate anaerobic bacteria. A comparison of four examples of recently developed models is shown in Figure 1.6. These models can be used to study the effect of obligate anaerobes on host responses. The advantages and disadvantages of the four dual-environment co-culture models are summarised in Table 1.1.

Marzorati *et al.* [20] developed the Host-Microbiota Interaction (HMI) module, a device that enables the co-culture of a complex microbial community, including obligate anaerobic bacteria, with enterocyte-like cells (Figure 1.6A). The HMI module can be used in combination with dynamic simulation of the GI tract, where digestion processes in the stomach, small intestine and colon are simulated in several reactors. Furthermore, the last compartment of this dynamic *in vitro* simulator, which mimics the ascending colon, is inoculated with faecal microbiota. In combination with this continuous culture system, the HMI module can be utilised to study bacterial adhesion to the mucus layer under relevant shear forces. It also allows the exchange of signals and metabolites between the two compartments, and through the diffusion of oxygen from the lower compartment, it creates microaerophilic conditions on the bottom of the microbial biofilm. Consequently, it is able to mimic the physiological conditions of the GI tract. Moreover, due to the separation of the two compartments by the mucus layer, this model is more representative of the GI tract compared to co-culture models that allow direct contact between bacteria and host cells.

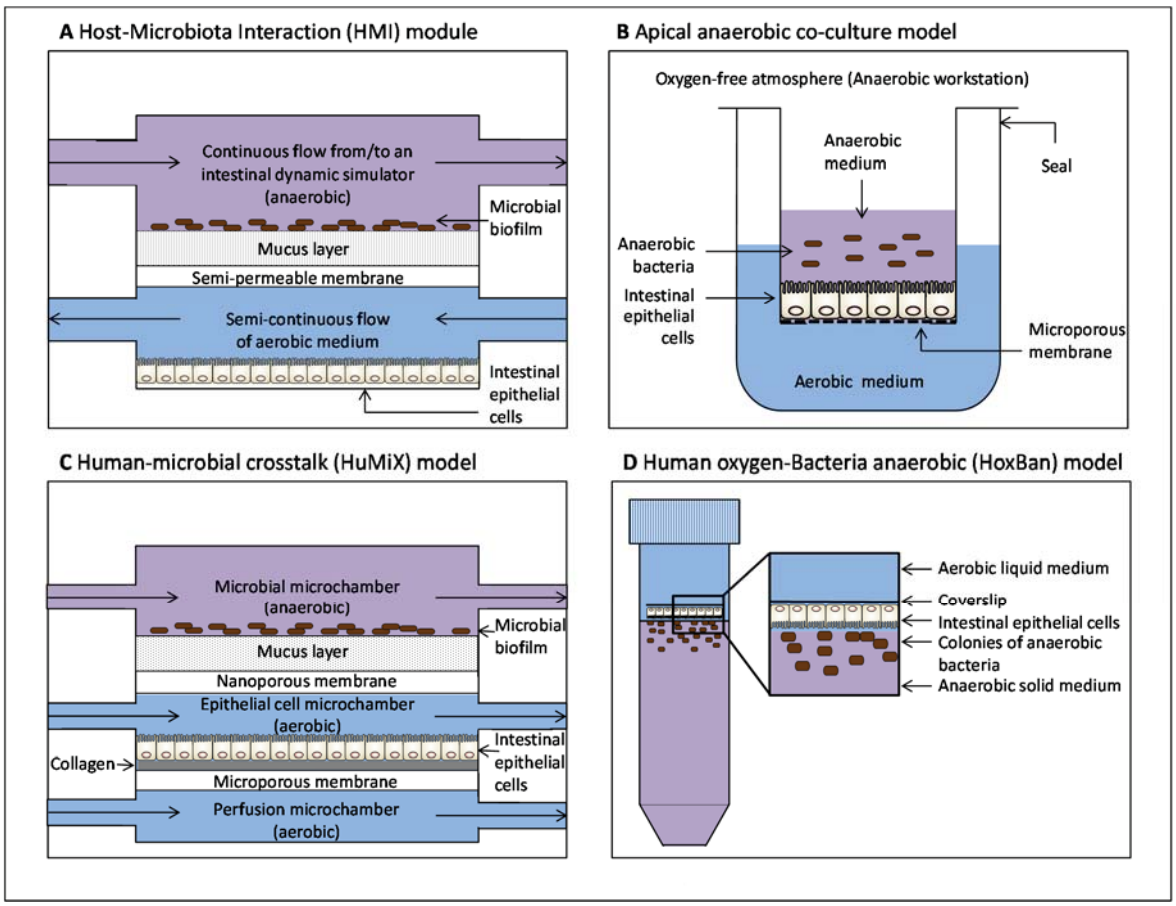

Figure 1.6 Comparison of four examples of dual-environment co-culture models.

Through the separation of aerobic and anaerobic compartments these four dual-environment co-culture models enable the co-culture of anaerobic bacteria and oxygen-requiring human cells. (A) Host-Microbiota Interaction (HMI) module [20,251]; (B) apical anaerobic co-culture model [19]; (C) Human-microbial crosstalk (HuMiX) model [21]; (D) Human oxygen-Bacteria anaerobic (HoxBan) model [252].

Table 1.1 Summary of advantages and disadvantages of four examples of dual-environment co-culture models

Co-culture model	Advantages	Disadvantages
Host-Microbiota Interaction (HMI) module (Figure 1.6A) [20]	– Combination with a dynamic simulation of the GI tract possible. – Allows the study of bacterial adhesion to the mucus layer under relevant shear forces. – Separation of the two compartments by a mucus layer, therefore more representative of the GI tract. – Co-culture of IECs with a complex microbiota.	– No inclusion of immune cells. – Not possible to study effects of bacteria on barrier integrity of IECs. – No measurements of independent biological replicates possible in one experiment.
Apical anaerobic co-culture model (Figure 1.6B) [19]	– Separation of 48 independent wells to test effects of bacteria on host cells in several biological replicates in one experiment. – Can be used to determine the effect of bacteria on barrier integrity of IECs through automated TEER measurements and determination of paracellular permeability through sampling of the basal compartment.	– Only validated for co-culture studies up to 12 h. – No separation of IECs and obligate anaerobic bacteria by a mucus layer, therefore less representative for the GI tract. – No inclusion of immune cells.
Human-microbial crosstalk (HuMiX) model (Figure 1.6C) [21]	– Separation of the two compartments by a mucus layer, therefore representative of the GI tract. – Oxygen sensors for the real-time monitoring of the dissolved oxygen concentrations within the different compartments. – Allows TEER measurements. – Co-culture of IECs, immune cells and obligate anaerobes.	– No measurements of independent biological replicates possible in one experiment.
Human oxygen-Bacteria anaerobic (HoxBan) model (Figure 1.6D) [252]	– No requirement of specialised equipment, therefore implementation in any research laboratory with access to anaerobic and cell culture facilities possible.	– No inclusion of immune cells. – No measurements of independent biological replicates possible in one experiment. – Caco-2 cells grown on coverslip, therefore no formation of a differentiated monolayer.

Direct contact between live obligate anaerobic bacteria and human cell lines occurs in a novel dual-environment co-culture model which has been developed and validated in our laboratory [19] and was used for the studies of this dissertation. This *in vitro* model, referred to as the apical anaerobic co-culture model, utilises a co-culture chamber, which is used inside an anaerobic workstation that has an oxygen-free atmosphere (Figure 1.6B). The apical anaerobic co-culture model can be used to determine the effect of bacteria on intestinal barrier function as the co-culture chamber contains built-in electrodes to monitor TEER across cell monolayers, a well-established measurement for barrier integrity [253]. Furthermore, each well of the co-culture chamber is equipped with septa to allow sampling of the basal media without altering the environment. Using paracellular tracers, e.g., [^{3}H]-mannitol, the effect of anaerobic bacteria on the small molecule paracellular permeability of cell monolayers can also be determined, which represent another indicator of TJ integrity [254].

Recently, a novel microfluidics-based dual-environment co-culture model was developed, named HuMiX (referring to human–microbial crosstalk) (Figure 1.6C) [21]. This model contains three microchambers separated through nano- and microporous membranes: a microchamber with aerobic conditions for the culture of IECs, a microchamber with anaerobic conditions for the culture of GI bacteria and a medium perfusion microchamber. Following the co-culture, HuMiX enables downstream molecular analyses of the human and bacterial cells. HuMiX allowed the co-culture of differentiated Caco-2 cells with the facultative anaerobe, *Lactobacillus rhamnosus* GG alone under aerobic or anaerobic conditions or with the combination of *L. rhamnosus* GG and the obligate anaerobe *Bacteroides caccae* under anaerobic conditions. Similar to the apical anaerobic co-culture model described above [19], HuMiX allows TEER measurements in order to assess the differentiation of the Caco-2 cells when grown in this model. The model also enables the

real-time monitoring of dissolved oxygen (DO) levels. Moreover, immune cells (CD4+ T cells) can be cultured in the perfusion microchamber of HuMiX in order to investigate interactions between IECs, immune cells and bacteria. HuMiX mimicked the *in vivo* transcriptional, metabolic and immunological responses in human IECs co-cultured with *L. rhamnosus* GG grown under anaerobic conditions, demonstrating its representation of the human-microbial interface in the GI tract [21].

Compared to the three dual-environment co-culture models described above, the design of another recently developed system, the 'Human oxygen - Bacteria anaerobic' (HoxBan) system is much simpler (Figure 1.6D) [252]. It utilises 50 mL tubes filled with 40 mL of anaerobic bacterial agar in which obligate anaerobic bacteria are grown. Glass-adhered Caco-2 cells in 10 mL of human cell culture medium are placed on top of the agar. Using this model enabled the co-culture of live *F. prausnitzii* with Caco-2 cells for over 24 h which demonstrated mutualism between the human and bacterial cells. The presence of Caco-2 cells stimulated growth and metabolism of *F. prausnitzii* and the bacteria induced anti-inflammatory and anti-oxidant responses in Caco-2 cells [252]. Compared to the other dual-environment co-culture models the HoxBan system has the advantage that it does not require specialised equipment and can therefore be readily implemented in research laboratories with access to anaerobic and cell culture facilities.

Another recently developed *in vitro* model that closely mimics the physiology of the intestine are the three-dimensional "mini-intestines" derived from isolated human intestinal epithelial stem cells from the small intestine or colon [255,256]. The so-called enteroids contain all four types of normal epithelial cells. Currently, intestinal enteroids are grown in three-dimensional cultures to be used in functional studies; however, murine enteroids were also successfully grown as polarised monolayers [257]. Moreover, preliminary tests

were performed with human enteroids seeded on porous Transwell membranes coated with a fibronectin-based peptide [258]. This resulted in the formation of confluent polarised monolayers with a high TEER (600–1000 $\Omega.cm^2$). Intestinal enteroids grown on Transwell inserts could potentially be adapted to be used under dual-environment conditions. For example, in combination with the technology of the apical anaerobic co-culture model (Figure 1.6B) these "mini-intestines" could be co-cultured with obligate anaerobic bacteria. Compared to Caco-2 cells, which are currently used in the apical anaerobic co-culture model, intestinal enteroids would be more representative for the physiology in the intestine.

1.6. AIMS AND STRUCTURE OF THE DISSERTATION

The health of humans is impacted by the symbiotic relationship with their microbiota, while a dysbiosis of the resident microbiota is associated with various disorders, such as IBD [12,126,127], colorectal cancer [259,260], coeliac disease [16] and obesity [261]. The commensal bacterium *F. prausnitzii* has been associated with this dysbiosis because numerous studies demonstrated its decreased abundance within the GI microbiota under these conditions. Therefore, it has been suggested that *F. prausnitzii* plays an important role in maintaining intestinal health and that its use as a probiotic could be a promising approach in the treatment of IBD [14,182].

Even though the beneficial role of *F. prausnitzii* is widely recognised, mechanistic studies explaining how this bacterium exerts its effects remain limited. This is partially a consequence of the difficulty of culturing obligate anaerobic commensal bacteria, such as *F. prausnitzii,* that cannot survive in the presence of oxygen together with human epithelial cells that require oxygen for survival. This limitation has been addressed in the development and validation of a novel *in vitro* model by AgResearch scientists and

engineers, the apical anaerobic co-culture model [19]. As described in the above section, this model contains both aerobic and anaerobic compartments, and therefore enables the co-culture of obligate anaerobic bacteria like *F. prausnitzii* with mammalian cells.

The overall aim of this study was to investigate the effect of *F. prausnitzii* on intestinal function using the novel apical anaerobic co-culture model. *F. prausnitzii* has been chosen as an example of a commensal obligate anaerobe because based on the current literature this species provides the strongest evidence to exert protective effects compared to other commensals. In particular, the effect of *F. prausnitzii* on intestinal barrier function and immune homeostasis was determined. It has been shown that *F. prausnitzii* improved intestinal barrier integrity and protected from inflammation *in vivo* [179,214]. Moreover, few *in vitro* studies provided insights into the mechanisms by which *F. prausnitzii* exerts its effects [179,182,207,208]. However, most of these studies were restricted to test the effects of non-viable bacteria, because the co-culture with human cells under conventional cell culture conditions (5% CO_2 in air atmosphere) quickly killed obligate anaerobic *F. prausnitzii*. Therefore, this study was one of the first testing the effects of live *F. prausnitzii* on intestinal function.

The main hypotheses of this study were: (i) live and growing *F. prausnitzii* (strains A2-165, ATCC 27768 and HTF-F) exerts barrier enhancing properties by increasing TEER across healthy Caco-2 monolayers, (ii) live *F. prausnitzii* mitigates the TNF-α-induced decrease in TEER across Caco-2 monolayers and (iii) live *F. prausnitzii* activates innate immune receptors (TLRs) to a greater extent compared to dead bacteria. In order to address these hypotheses method development was required. Firstly, an existing protocol of co-culturing *F. prausnitzii* with Caco-2 cells required improvement to enable growth of the bacteria and secondly the TLR activation assay, a method performed for the first time in

the apical anaerobic co-culture model, needed to be adapted to the new assay conditions. The dissertation was therefore divided into four experimental chapters comprising the two method development chapters and the respective results chapters describing the effects of *F. prausnitzii* on intestinal barrier function and immune homeostasis.

In Chapter 2 the method development to improve the growth of *F. prausnitzii* in co-culture with Caco-2 cells is described. Firstly, two approaches to supplement the apical anaerobic cell culture medium were used to enable growth of the three *F. prausnitzii* strains alone. Secondly, it was investigated if the viability and barrier integrity of Caco-2 cell monolayers were maintained when using the adapted apical medium. Finally, the growth of *F. prausnitzii* in co-culture with Caco-2 cells in the apical anaerobic co-culture model using the adapted apical medium was determined. Using the optimised co-culture conditions developed in Chapter 2, the work described in Chapter 3 investigates the effect of the three *F. prausnitzii* strains on TJ integrity of healthy and TNF-α-treated Caco-2 monolayers.

Chapter 4 describes the adaptation of the TLR activation assay to the apical anaerobic co-culture model. TLR expressing HEK293 cell lines and a control cell line were stably transfected with a NF-κB inducible luciferase reporter plasmid. The transfected cell lines were then used to perform the TLR activation assay under apical anaerobic conditions which required the optimisation of the cell attachment to the membranes of Transwell inserts. The DO content of the apical and basal compartment was determined to ensure the maintenance of the dual-environment. Throughout the method development the viability of the transfected cell lines was determined and different apical media were tested to improve the viability of *F. prausnitzii*. The assay conditions developed in Chapter 4 were applied in

Chapter 5 to determine the TLR activation by live and dead *F. prausnitzii* under conventional and apical anaerobic conditions.

Finally, a summary of the main findings of the study, a general discussion and future perspectives are presented in Chapter 6. An overview of the structure of the dissertation including its experimental chapters is shown in Figure 1.7.

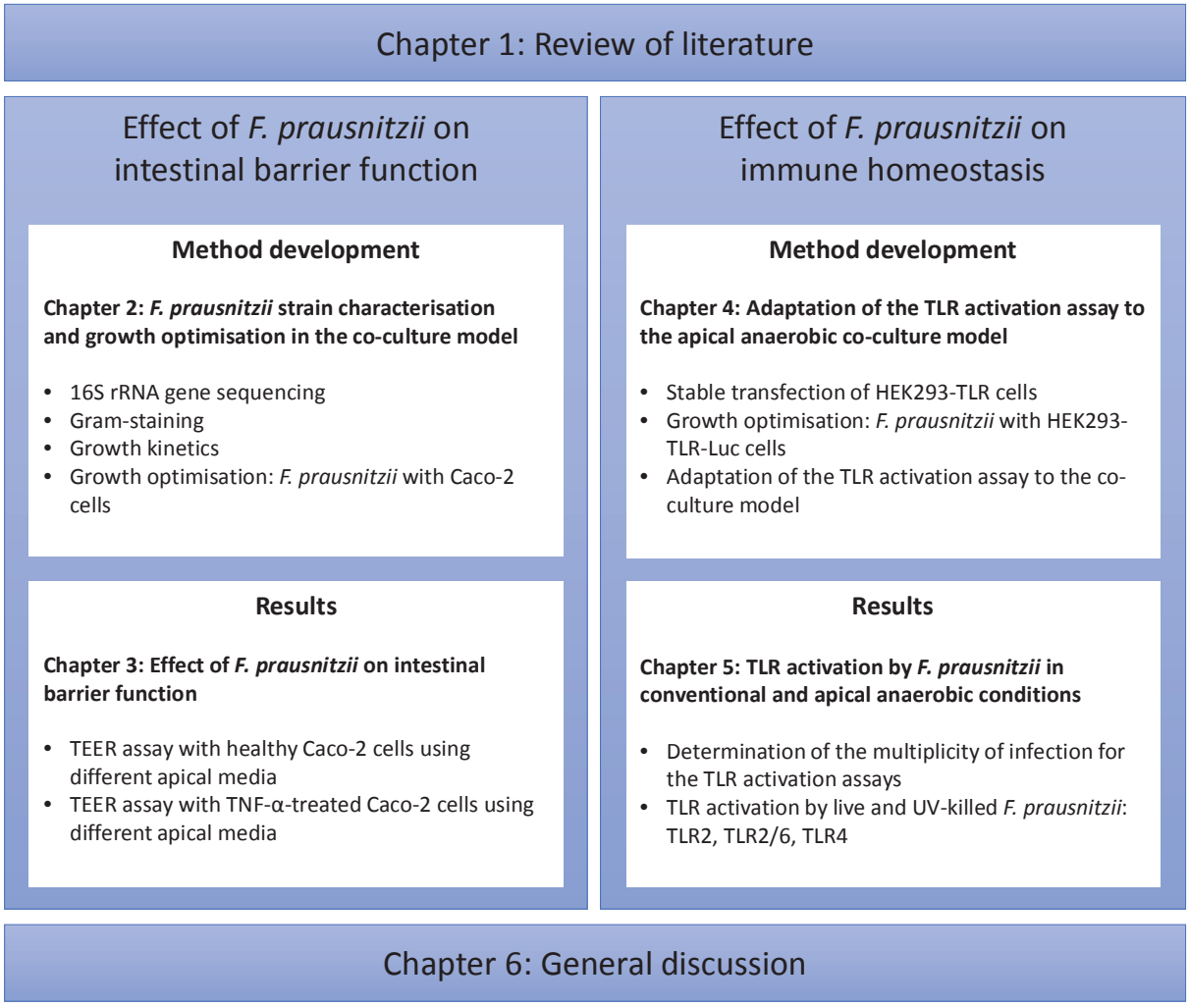

Figure 1.7 Structure of the dissertation.

The diagram provides an overview of the structure of the dissertation and its experimental chapters.

CHAPTER TWO:

Faecalibacterium prausnitzii strain characterisation and growth optimisation in the co-culture model[†]

[†] Selected material from this section combined with sections from Chapter 3 will be submitted for publication to the journal *Nutrients*.

2.1. INTRODUCTION

Bacterial colonisation of the GI tract is critical for human health [262]. Numerous studies have investigated the mechanisms of action behind the beneficial effects of bacterial species residing in the GI tract. Most of these studies focus on oxygen-tolerant bacteria, as they can be readily co-cultured with oxygen-requiring human cell lines for mechanistic studies. However, the majority of the bacterial species in the large intestine, the part of the GI tract with the highest bacterial density, are obligate anaerobes, which cannot survive in the presence of oxygen [18]. It is therefore impossible to co-culture these bacteria together with human cell lines using conventional co-culture models, which means that the majority of the bacterial effects in the GI tract remain unknown.

This limitation has been addressed in the development and validation of a new *in vitro* model in a previous PhD project at AgResearch [19]. The novel model, referred to as the apical anaerobic co-culture model, contains anaerobic and aerobic compartments separated by a semipermeable membrane on which human cell lines are grown. Due to the two environments it allows the survival of both obligate anaerobic bacteria and human cell lines. This model was used to co-culture *F. prausnitzii* (strain A2-165), an abundant obligate anaerobic bacterium in the human GI tract [178,180], with the human IEC line Caco-2 [19]. Compared to culturing *F. prausnitzii* at 37°C under standard atmospheric conditions, where the *F. prausnitzii* colony-forming units (CFU) reduced by over 4 logs within 30 min, the viability of the bacterium was increased when co-cultured with Caco-2 cells in the apical anaerobic co-culture model. However, there was still a decrease in bacterial cell numbers using the new model, the total *F. prausnitzii* CFU reduced by less than 1 log after the co-culture with Caco-2 cells for 8 h. The reason for this may have been that the cell culture medium used for these experiments was lacking substrates required for

the growth of *F. prausnitzii*, e.g. acetate [178]. Due to the loss of viability of *F. prausnitzii* determined using the apical anaerobic co-culture model, method development was required to further improve the model following its initial development.

2.2. HYPOTHESIS AND AIMS

The hypothesis of the research described in this thesis chapter was that *F. prausnitzii* is able to grow in the apical anaerobic co-culture model if the apical medium is supplemented with substrates required for its growth. To test this hypothesis two approaches to supplement the apical anaerobic cell culture medium were used, supplementation with acetate or bacterial culture medium.

The first aim was to characterise the three *F. prausnitzii* strains used for these studies by 16S rRNA gene sequencing and Gram-staining in order to confirm their identity and determine their growth kinetics in bacterial culture medium. The strains chosen for these studies were *F. prausnitzii* ATCC 27768, *F. prausnitzii* A2-165 (DSM 17677) and *F. prausnitzii* HTF-F (DSM 26943). *F. prausnitzii* ATCC 27768 was selected because this is the type strain of the genus *Faecalibacterium* [178,181]. *F. prausnitzii* A2-165 (DSM 17677) was chosen because this strain is well characterised and was used in several studies including the first application of the apical anaerobic co-culture model [19,178,184,188,221,263], and *F. prausnitzii* HTF-F (DSM 26943) was chosen because it was recently patented for its anti-inflammatory properties [264]. The second aim was to determine if the first approach to supplement the apical anaerobic cell culture medium, with acetate, enabled growth of the three *F. prausnitzii* strains. The third aim was to test if the second approach to supplement the apical cell culture medium with bacterial culture medium, affected the viability and barrier integrity of Caco-2 cell monolayers. The fourth

aim was to determine whether the three *F. prausnitzii* strains were able to grow in this mixture of cell and bacterial culture medium when grown alone and in co-culture with Caco-2 cells in the apical anaerobic co-culture chamber.

2.3. METHODS

2.3.1. *F. prausnitzii* cell culture

The three *F. prausnitzii* strains were kindly provided by Hermie J. M. Harmsen (Department of Medical Microbiology, University of Groningen, The Netherlands) and are listed in Table 2.1. The bacteria were cultured at 37°C in Hungate culture tubes sealed with butyl rubber stoppers. The bacterial culture media used were anaerobic brain-heart infusion (BHI) broth or anaerobic yeast extract, casitone, fatty acid, glucose (YCFAG) broth which were prepared as described in section 2.3.2.2 and 2.3.2.1, respectively. All bacterial inoculations were performed inside an anaerobic workstation (Concept Plus, Ruskinn Technology Ltd) which maintained an atmosphere of 10% CO_2, 10% H_2 in N_2 at 37°C.

2.3.2. Bacterial culture medium

For the initial characterisation of the three *F. prausnitzii* strains the bacteria were cultured in anaerobic YCFAG medium, a bacterial culture medium that has been used previously to culture *F. prausnitzii* [178,184]. For the optimisation of the growth conditions of the three *F. prausnitzii* strains in the co-culture model anaerobic BHI medium was used to culture the bacteria. The reason for the change in the culture medium was that *F. prausnitzii* was being used as a representative for the human GI microbiota with the intention that the apical anaerobic co-culture model was used for the co-culture of

Table 2.1 Details of the three *F. prausnitzii* strains used in this PhD project.

Species	Strain code	Culture collection	Reference for original isolation	Functional information
F. prausnitzii	A2-165	DSM 17677	[178]	Anti-inflammatory effects *in vitro* and *in vivo* [19,179,204,205,207, 213,252,265]
F. prausnitzii	ATCC 27768	ATCC 27768	[181]	None
F. prausnitzii	HTF-F	DSM 26943	[184]	Anti-inflammatory effects *in vitro* and *in vivo* [204,264]

different anaerobic bacteria with human cell lines. BHI medium is a generic broad-spectrum bacterial growth medium [19,220], whereas YCFAG medium is a specific medium, mostly used to grow *F. prausnitzii* [178,184]. Therefore, using BHI medium would make it easier to apply the optimised growth conditions in the co-culture model achieved for *F. prausnitzii* to the co-culture of human cell lines with a range of obligate anaerobic bacteria.

2.3.2.1. Anaerobic yeast extract, casitone, fatty acid, glucose broth

The components used to prepare anaerobic YCFAG broth are listed in Table 2.2. First, casitone, yeast extract, sodium acetate, glucose and all the salts listed in Table 2.2 were weighed into a flask. Distilled water was added and the solution was mixed using a magnetic stirrer until dissolved. The resazurin and haemin stock solutions were added while the solution was continuously stirred. The broth was boiled in a microwave in several short bursts, then immediately transferred into an ice-water box and cooled down under the stream of CO_2 for at least 20 min. The solution changed colour from dark green to a light yellow because resazurin was added as a redox indicator. L-cysteine and the vitamin stock 1 were added and distributed by swirling the flask. The pH of the solution was determined and if required adjusted to 6.5 ± 0.2 using HCl or NaOH and the anaerobic YCFAG broth was transferred into Hungate tubes. The pipette used to transfer the broth into the Hungate tubes was flushed several times with CO_2 before inserting into the liquid to remove remaining oxygen. While distributing the YCFAG broth, the Hungate tubes were continuously flushed with CO_2. The gassing cannula was removed and the tubes were sealed immediately with rubber septa and lids. The broth was autoclaved at 121°C for 20 min on the same day. After autoclaving and cooling down the Hungate tubes, filter

Table 2.2 Components used to prepare anaerobic yeast extract, casitone, fatty acid, glucose (YCFAG) broth.

	Media component	Company	Volume/weight
	Casitone	Becton Dickinson	10 g
	Yeast extract	Becton Dickinson	2.5 g
Short chain fatty acid	Sodium acetate	Scharlau	1.95 g (=33 mM)
Sugar	Glucose	LabServ	4.5 g (=25 mM)
Salts	$NaHCO_3$	Fisher Scientific	4 g
	K_2HPO_4	BDH Chemicals	0.45 g
	KH_2PO_4	Ajax Finechem	0.45 g
	NaCl	LabServ	0.9 g
	$MgSO_4 \cdot 7H_2O$	BDH Chemicals	0.09 g
	$CaCl_2$	Fisher Scientific	0.09 g
Redox indicator	Resazurin (0.02% stock)	Sigma-Aldrich	5 mL (= 0.1 mg)
Iron source	Haemin (0.05% stock)	Sigma-Aldrich	20 mL (= 1 mg)
Vitamins	Biotin	Sigma-Aldrich	10 µg
	Cobalamin	Sigma-Aldrich	10 µg
	p-aminobenzoic acid	Sigma-Aldrich	30 µg
	Folic acid	Sigma-Aldrich	50 µg
	Pyridoxamine	Sigma-Aldrich	150 µg
Reducing agent	L-cysteine	Sigma-Aldrich	1 g
Heat labile vitamins	Riboflavin	Sigma-Aldrich	0.5 µg/mL
	Thiamine	Sigma-Aldrich	0.5 µg/mL
	Distilled H_2O		1 L

sterilised anaerobic vitamin stock 2 was added to the broth inside the anaerobic workstation.

2.3.2.2. Anaerobic brain-heart infusion broth

For the preparation of anaerobic BHI broth all components were used according to the recipe listed in Table 2.3. BHI powder and yeast extract were weighed out into a flask. After adding the haemin solution and distilled water the solution was swirled to help dissolving and subsequently boiled in a microwave in several short bursts. The solution was placed immediately into an ice-water bath and a stream of CO_2 was passed through the broth. Once the solution was cooled, L-cystein was added and dissolved through swirling the flask. Using NaOH the pH was adjusted to 7.0 ± 0.2. During pH adjustment the solution was mixed using a magnetic stirrer to ensure an even distribution of the NaOH. The vitamin K solution was added and the anaerobic BHI broth was transferred anaerobically into Hungate tubes as described in 2.3.2.1 for the YCFAG broth. The broth was autoclaved at 121°C for 20 min on the same day.

2.3.2.3. Anaerobic brain-heart infusion agar

Anaerobic BHI broth was prepared in a high-pressure bottle as described in 2.3.2.2. For the preparation of anaerobic BHI agar plates, 15 g/L of agar were added to the BHI broth before autoclaving at 121°C for 20 min. Following autoclaving the BHI agar was cooled down to 55°C and the bottle was transferred into the anaerobic workstation. The agar was poured into Petri dishes that have been transferred inside the anaerobic workstation at least an hour before. The agar plates were left uncovered for at least an hour to set and dry, and once set they were stored upside down in a plastic bag inside the anaerobic workstation until use.

Table 2.3 Components used for the preparation of anaerobic brain-heart infusion broth.

Media component	Company	Volume/weight
BHI powder	Becton Dickinson	37 g
Yeast extract	Becton Dickinson	5 g
0.05 % (w/v) haemin, prepared in 1N NaOH	Sigma-Aldrich	10 mL
0.05 % (v/v) vitamin K solution, prepared in 95% EtOH	Sigma-Aldrich	1 mL
L-cystein	Sigma-Aldrich	2 g
Distilled H_2O		1 L

Agar plates were prepared fresh for each experiment. Before using the agar plates to culture bacteria, they were removed from the plastic bag and left uncovered inside the anaerobic workstation to dry.

2.3.3. Long term storage of bacterial cultures

The three *F. prausnitzii* strains were stored at -80°C for long term storage using glycerol as cryoprotectant. Bacterial cultures were grown in anaerobic YCFAG broth. These pre-cultured YCFAG broths were mixed with anaerobic glycerol at a ratio of 4:1 and transferred into cryogenic vials which were stored at -80°C. Repeated freeze-thawing was avoided as it affected the viability of the bacteria.

2.3.4. 16S rRNA gene sequencing

The identity of the three *F. prausnitzii* strains was confirmed by 16S rRNA gene sequencing. The bacterial DNA was extracted (2.3.4.1) and the 16S rRNA gene amplified using polymerase chain reaction (PCR; 2.3.4.2). The sequences obtained through Sanger sequencing were compared to sequences in the National Center for Biotechnology Information (NCBI) nucleotide collection database to confirm the strain identity (2.3.4.3).

2.3.4.1. Bacterial DNA extraction

The original glycerol stocks of the three *F. prausnitzii* strains obtained from Hermie J. M. Harmsen (Department of Medical Microbiology, University of Groningen, The Netherlands) were used to inoculate 10 mL of YCFAG broth with 50 µL of frozen bacterial culture inside the anaerobic workstation. *F. prausnitzii* A2-165 and *F. prausnitzii* ATCC 27768 were incubated for 24 h and *F. prausnitzii* HTF-F for 48 h in order to attain sufficient bacterial cells for DNA extraction. The bacterial DNA was extracted using the

DNeasy Blood & Tissue Kit (Quiagen, USA) according to the manufacturer's instructions. The DNA quantity and purity were determined using a NanoDrop (ND-1000 UV-Vis Spectrophotometer, Thermo Fisher Scientific, Australia). An absorbance ratio of 260/280 nm between 1.8 and 2 was considered to be an adequate purity.

2.3.4.2. Polymerase chain reaction of the 16S rRNA genes

The bacterial 16S rRNA gene was amplified by PCR using the forward and reverse primers 27f and 1492r (Table 2.4) and the Fast Start PCR Mastermix (Roche, Germany). PCR reactions were prepared by mixing 25 µL Fast Start PCR Mastermix, 1 µL of the template DNA, 1 µL each of the primers 27f and 1492r (Table 2.4, both diluted to 10pmol/µL) and 22 µL of distilled water in 0.2 mL thin wall PCR tubes. The PCR tubes were inserted into a thermal cycler (Mastercycler pro S, Eppendorf, Germany). The PCR programme listed in Table 2.5 was used. After the amplification the quality and size of the PCR products were determined using agarose gel electrophoresis. The PCR products were purified using the High Pure PCR Product Purification Kit (Roche, Germany) according to the manufacturer's instructions, and the DNA concentration of the PCR products was quantified using a Qubit Fluorometer (Life technologies, New Zealand).

2.3.4.3. Sanger sequencing and database comparison

The reactions for the Sanger sequencing were prepared by mixing approximately 30 ng of DNA obtained through 16S rDNA PCR (2.3.4.2) with 3.2 pmol of the primers 27f and 1492r (Table 2.4) and adding distilled water to a final volume of 15 µL. The samples were sequenced at the Massey Genome Service (Massey University, New Zealand) using the BigDye® Terminator v3.1 Cycle Sequencing Kit.

Table 2.4 Oligonucleotide sequences of the forward and reverse primers used for the amplification of the bacterial 16S rRNA gene.

Primer	Name	Sequence	Reference
Forward	27F	GAG TTT GAT CMT GGC TCA G	Modified from Lane (1991)
Reverse	1492R	GGY TAC CTT GTT ACG ACT T	Lane (1991)

Table 2.5 PCR program used for the amplification of the bacterial 16S rRNA gene.

Program	Temperature (°C)	Time	
Initialisation step	94	4 min	
Denaturation	94	30 sec	35 cycles
Annealing	50	30 sec	
Elongation	72	1 min	
Final elongation	72	10 min	
Final hold	12	∞	

The obtained forward and reverse sequences were edited using the programme ContigExpress (Vector NTI, Life technologies, New Zealand). Low quality sequences at the start and the end of the chromatograms were trimmed off and ambiguous bases were determined for both forward and reverse sequences. Then the forward and reverse sequence reads were assembled into a contig. The contig was aligned with known bacterial sequences in the NCBI nucleotide collection database and the percentage of similarity was reported.

2.3.5. Enumeration of bacteria

2.3.5.1. Petroff-Hausser counting chamber

Bacterial densities of broth cultures were determined using a Petroff-Hausser counting chamber which is comparable to a haemocytometer for quantifying mammalian cell populations. First, the bacterial broth cultures were mixed by inverting the tubes several times. The cultures were diluted with anaerobic phosphate-buffered saline (PBS) (1:20, 1:50 or 1:100, depending on the turbidity of the broth culture) to achieve a number of bacteria within a countable range. The bacterial dilutions were thoroughly mixed using a vortexer to avoid bacterial aggregations. The Petroff-Hausser counting chamber and the coverslip were cleaned with 70% ethanol using a soft tissue and dried. The coverslip was placed on the counting chamber and pressed down carefully. The Petroff-Hausser chamber was loaded with a small volume (25-50 µL) of the mixed and diluted bacterial cultures using a micropipette. If the counting chamber was prepared correctly the applied liquid filled the void by capillary action. The chamber was placed under the 40 x objective of a phase-contrast microscope (Leica, Wetzlar, Germany). The bacteria in at least four large squares of the counting grid were counted and only bacterial numbers in the range of 10 to 100 were used for the calculation of the bacterial densities to avoid inaccurate numbers. If

the number of bacteria counted was below or above this range, then a different dilution of the bacterial suspension was prepared and the counting was repeated. The bacterial density in cells per millilitre was calculated using Equation 1:

$$\text{Bacteria conc. (cells/mL)} = \text{average bacterial number counted in large squares} \times \text{dilution factor} \times \text{factor for large squares } (1.25 \times 10^6/\text{mL}) \quad \text{(Eq. 1)}$$

2.3.5.2. Titration of *F. prausnitzii* viable cells

In order to determine the CFU of the *F. prausnitzii* strains tenfold serial dilutions of the bacterial suspensions were prepared in 96-well plates using anaerobic PBS inside the anaerobic workstation. Anaerobic BHI agar plates were divided into quadrants, each quadrant corresponding to one dilution. From each dilution three aliquots of 20 µL were pipetted on one quadrant of the anaerobic BHI agar plate. The plates were left uncovered inside the anaerobic workstation to dry and then incubated upside down inside a plastic bag in the anaerobic workstation for around 48 h, or until bacterial colonies were visible. The bacterial colonies per spot were counted and numbers in a range of 10 to 100 colonies were considered for the calculation of the viable CFU per millilitre using Equation 2:

$$\text{Bacteria concentration (CFU)/mL)} = \text{average of bacterial colonies counted in a quadrant} \times \text{dilution factor} \times 50 \quad \text{(Eq. 2)}$$

2.3.6. Gram staining

The original frozen stocks of the three *F. prausnitzii* strains were used to inoculate 10 mL of YCFAG broth. The bacterial cultures were grown for 24 h (*F. prausnitzii* A2-165 and ATCC 27768) or 48 h (*F. prausnitzii* HTF-F). One drop of the mixed bacterial broth culture was placed on one end of a microscope slide and distributed as a smear over the complete slide using a coverslip. The slide was left to dry for 30 min and then heat fixed

over the flame of a Bunsen burner while constantly moving the slide in a circular motion to avoid burning or overheating the sample. For the staining the slide was placed on a wire rack over the sink with the smear side up. First, drops of crystal violet were added over the entire slide and left for one minute. Gram-positive bacteria retain this purple dye due to their thick cell wall made of peptidoglycan. The cell wall of Gram-negative bacteria only contains a thin layer of peptidoglycan and are therefore not stained by crystal violet. The slide was then rinsed under a gentle stream of tap water. Subsequently, drops of iodine solution were added over the entire slide, left for one minute and again rinsed under a gentle stream of tap water. Iodine binds to crystal violet causing the purple dye to be retained in the bacterial cell wall. Next, drops of the decolouriser were added over the entire slide, left for 10 s and rinsed. As the last step of the staining process, drops of safranin were added to the entire slide and left for 30 s. Safranin is used as a counterstain which gives all Gram-negative bacteria a red or pink colouring. The slides were left to air dry for 20 to 30 min before examining under a phase-contrast microscope (Leica, Wetzlar, Germany) using the 100 x objective with the oil immersion lens.

2.3.7. Growth curves

The growth kinetics of the *F. prausnitzii* strains were analysed to determine the incubation time required to reach the stationary phase of growth. The strains were used in stationary phase for co-culture experiments for consistency because metabolic activity differs between growth phases [266]. The bacteria were cultured in anaerobic BHI medium in Hungate culture tubes sealed with rubber septa at 37°C. For the primary bacterial cultures, 50 µL of frozen bacterial stocks were inoculated into 10 mL of anaerobic BHI medium inside the anaerobic workstation and were incubated at 37°C for 24 h (*F. prausnitzii* A2-165 and *F. prausnitzii* ATCC 27768) or 48 h (*F. prausnitzii* HTF-F). Two hundred µL each

of 24-hour-old primary broth cultures of *F. prausnitzii* A2-165 and *F. prausnitzii* ATCC 27768 and 200 µL of a 48-hour-old primary broth culture of *F. prausnitzii* HTF-F were used to inoculate 10 mL of anaerobic BHI medium in triplicate. The Hungate tubes were incubated at 37°C and the optical density (OD) at a wavelength of 600 nm (OD_{600nm}) was measured at 2 h intervals over 36 h. The contents of the Hungate tubes were mixed by inversion before each measurement to prevent any settling of the bacterial cells on the bottom of the tubes.

2.3.8. Culture of intestinal epithelial cells (Caco-2)

The Caco-2 cell model was used to assess the effect of *F. prausnitzii* on intestinal barrier function. This continuous cell line originates from human epithelial colon adenocarcinoma cells [111] and is a commonly used model for the intestinal epithelium [267]. Although derived from the colon, Caco-2 cells show morphological and functional similarities to small intestine enterocytes [268]. In culture the cells form a confluent monolayer and undergo spontaneous differentiation which is characterised by polarised cells with apical microvilli and the formation of TJs between neighbouring cells [269].

The formation of TJs is vital for experiments assessing intestinal barrier integrity. For that reason Caco-2 cells are the most appropriate cell line for this research since other IEC lines do not differentiate spontaneously (e.g. HT-29 [270]) or only form weak TJs (e.g. T84 [271]). The Caco-2 cells were grown on microporous membranes of Transwell inserts until differentiated and then inserted into the co-culture chamber for the use in the apical anaerobic co-culture model. The formation of a monolayer is of particular importance in this model as it allows the separation of the apical from the basal compartment of the co-culture chamber.

2.3.8.1. Maintenance of Caco-2 cells

Caco-2 cells were maintained in cell culture flasks (Corning, Australia) filled with Medium 199 (M199) cell culture medium (Life technologies, New Zealand) with the supplements added as shown in Table 2.6. This supplemented medium was referred to as M199 Standard medium (M199 Std). M199 Std was heated to 37°C in an oven before using it for culturing Caco-2 cells. Small cell culture flasks (25 cm^2 surface area) were filled with 10 mL of M199 Std, medium and large flasks (75 and 175 cm^2 surface area, respectively) with 25 mL of M199 Std. The cells were passaged once a week and the medium was changed twice a week. All cell cultures were incubated in air with 5% CO_2 at a temperature of 37°C.

2.3.8.2. Passaging of Caco-2 cells

Caco-2 cells were passaged once a week or when a confluence of around 80% was reached. First, the cell culture medium was removed from the cell culture flask containing the cell monolayer. The dissociation reagent TrypLE express (Life Technologies, New Zealand) was added to the flask (5, 10 or 15 mL for a small, medium or large flask, respectively) and incubated for 15 min at 37°C. The flask was checked regularly for detachment of the cells and after a maximum of 15 min removed from the incubator. Warm M199 Std equal to the volume of TrypLE was added to the flask and by pipetting the cell suspension up and down remaining attached cells were removed from the flask. The cell suspension was transferred to a sterile tube and centrifuged for 3 min at 240 x g (Jouan C3i Multifunction Centrifuge, Thermo Scientific, USA). After discarding the supernatant, the cell pellet was resuspended in 4 mL of warm M199 Std. When passaging cells from a small into a medium or from a medium into a large flask, the complete cell suspension was

Table 2.6 Composition of the Medium 199 standard medium (M199 Std) used for culturing Caco-2 cells.

Media component	Volume
Medium 199 (M199; Life technologies)	500 mL
Foetal bovine serum (FBS; Life technologies)	50 mL (10%)
MEM Non-Essential Amino Acids (NEAA; 100 x solution; Life technologies)	5 mL (1%)
Penicillin-Streptomycin (10 000 units/mL penicillin and 10 mg/mL streptomycin; Life technologies)	5 mL (1%)

reseeded into the next larger flask size in order to bulk up the cell population. After passaging a large flask either 1 or 2 mL of the 4 mL cell suspension were reseeded into a new large flask depending on when the next passaging was required. Fresh M199 Std was added to the flask containing the cell suspension.

2.3.8.3. Long term storage of Caco-2 cells

Caco-2 cells were stored in the vapour phase of liquid nitrogen for long term storage. For generating frozen stocks the cells were harvested using TrypLE as described in 2.3.8.2. After centrifugation and resuspension of the cell pellet in M199 Std, 10% dimethyl sulphoxide (DMSO, Sigma-Aldrich, USA) were added to the cell suspension as cryoprotectant and thoroughly mixed. From this cell suspension 1 mL aliquots were added per cryogenic vial (Corning, Australia) and transferred into a Mr. Frosty™ Freezing Container (Thermo Fisher Scientific, Australia) which was stored overnight at -80°C. The Mr. Frosty™ Freezing Container contained 100% isopropanol which ensured a slow freezing with a cooling rate of approximately 1°C per minute. The next day the frozen stocks were transferred into a liquid nitrogen dewar.

2.3.8.4. Recovering Caco-2 cells from liquid nitrogen

Caco-2 cells were revived from cryopreservation by placing the cryogenic vial containing the cells into an oven at 37°C and when completely thawed adding 1 mL of warm M199 Std to the vial. The cell suspension was mixed gently using a micropipette and subsequently transferred into a 15 mL centrifuge tube. After centrifuging the cell suspension at 240 x g for 3 min, the supernatant was discarded and the cell pellet was resuspended in 1 mL of warm M199 Std. This cell suspension was transferred into a small cell culture flask (T25, Corning, Australia), 9 mL of warm M199 Std were added and the flask was placed into an incubator with 37°C and 5% CO_2. After 48 h the flask was

checked microscopically for attachment, which was around 20% at that time. The growth of the cell population was observed over the next seven days, the medium was changed twice a week and after approximately one week the cells reached confluence and were split into a medium flask (T75). After reaching confluence in a medium flask, the Caco-2 cells were split into a large flask and from then used to seed the cells for co-culture experiments.

2.3.8.5. Counting Caco-2 cells

Caco-2 cells within a cell suspension were counted using an automated cell counter (Countess, Life technologies, Auckland, New Zealand) in order to seed Caco-2 cells at a specific seeding density. Caco-2 cells were harvested as described in 2.3.8.2. After resuspension of the cell pellet, 50 µL of the cell suspension was removed and mixed with 50 µL trypan blue (0.4% solution, Life technologies, Auckland, New Zealand). Dead cells take up trypan blue due to damages in the cell membranes, therefore, when staining cells with this viability dye, dead cells appear in a blue colour under the microscope whereas viable cells remain white. The cell suspension was applied to a counting slide for the automated cell counter (Countess, Life technologies, Auckland, New Zealand). The cell counter determined the total number of cells, the number of live and dead cells and calculated from these numbers the percentage of viable cells within a cell population.

2.3.8.6. Growing Caco-2 cells on Transwell inserts

For co-culture experiments Caco-2 cells were seeded on semipermeable polyester membranes of Transwell cell culture inserts (6.5 mm diameter, 0.4 µm pore size, Corning, New York, USA). The cells were harvested and counted as described in 2.3.8.2 and 2.3.8.5. The determined number of live cells was used to calculate the dilution required to achieve a seeding density of 4×10^5 cells/mL. The cell suspension was diluted with M199 Std and 200 µL of this diluted cell suspension were seeded onto the membrane of each

Transwell insert. The inserts were kept in 24-well cell culture plates and each well was filled with 810 µL of M199 Std. The cell culture plates containing the Transwell inserts were incubated at 37°C in 5% CO_2. Twice a week the medium was changed by carefully removing the medium from the apical and basal compartment of the Transwell inserts, drop wise adding fresh M199 Std to the apical compartment and filling the basal well with 810 µL of M199 Std. The Caco-2 cells were grown on Transwell inserts for 16-18 days to attain a differentiated cell monolayer. These differentiated cell monolayers were used for the co-culture experiments.

2.3.8.7. Measuring TEER to assess differentiation of Caco-2 monolayers

TEER across Caco-2 cell monolayers was determined prior to every co-culture experiment to assess if the Caco-2 cells seeded on the Transwell inserts formed a differentiated monolayer. TEER was measured using an EndOhm TEER cup (World Precision Instruments, USA) connected to an EVOM voltohmmeter (World Precision Instruments). The TEER cup was filled with 810 µL of warm M199 Std. Using sterile forceps the Transwell inserts containing the Caco-2 monolayers were transferred from the cell culture plate to the TEER cup and the lid containing the top electrode was placed on top of the TEER cup. The resistance (Ω) measured using the voltohmmeter was converted to TEER ($\Omega.cm^2$) using Equation 3:

$$\text{TEER } (\Omega.cm^2) = \text{Resistance } (\Omega) \times \text{surface area of membrane } (0.33\ cm^2) \quad \text{(Eq. 3)}$$

Only Caco-2 cell monolayers with a raw resistance over 1200 Ω (TEER over 400 $\Omega.cm^2$) were chosen for the experiments to ensure that only fully differentiated cell monolayers were used. When Caco-2 cell monolayers were used for a TEER assay the effect of the treatments was expressed as the change in TEER at each time point after the treatments were added using Equation 4:

$$\text{Change in TEER (\%)} = \frac{(\text{TEER}_{\text{current}} - \text{TEER}_{\text{initial}})}{\text{TEER}_{\text{initial}}} \times 100 \quad \text{(Eq. 4)}$$

2.3.9. Apical anaerobic co-culture model

The apical anaerobic co-culture model utilised a proprietary co-culture chamber which was used inside an anaerobic workstation (Concept Plus, Ruskinn Technology Ltd, Bridgend, UK) that had an atmosphere of 10% CO_2, 10% H_2 and 80% N_2, the anaerobic gas mixture commonly used to grow obligate anaerobes [272], and a temperature of 37°C. The co-culture chamber contained two compartments, the basal compartment containing aerobic cell culture medium and the apical compartment which contained anaerobic cell culture medium, and was exposed to the oxygen-free atmosphere of the anaerobic workstation. These two compartments were separated by a microporous membrane on which human cell lines were grown. By diffusion through this membrane the cell monolayer received oxygen from the basal aerobic compartment of the chamber, thereby enabling survival of the cells. In this model obligate anaerobic bacteria could be co-cultured with human cell lines as the apical anaerobic environment allowed them to survive (Figure 2.1).

The validation and first application of the apical anaerobic co-culture model were conducted using prototype I of the co-culture chamber. The design of this model has been further developed and improved by AgResearch engineers and the prototype II co-culture chamber was used in this PhD project. The main difference between the two prototypes is the decrease in size of the membrane inserts and wells in the prototype II co-culture chamber, thereby reducing the amount of cells and reagents required. The number of inserts and wells is increased in the prototype II (24) in comparison to prototype I (6), therefore increasing the throughput. Furthermore, each well of the prototype II co-culture

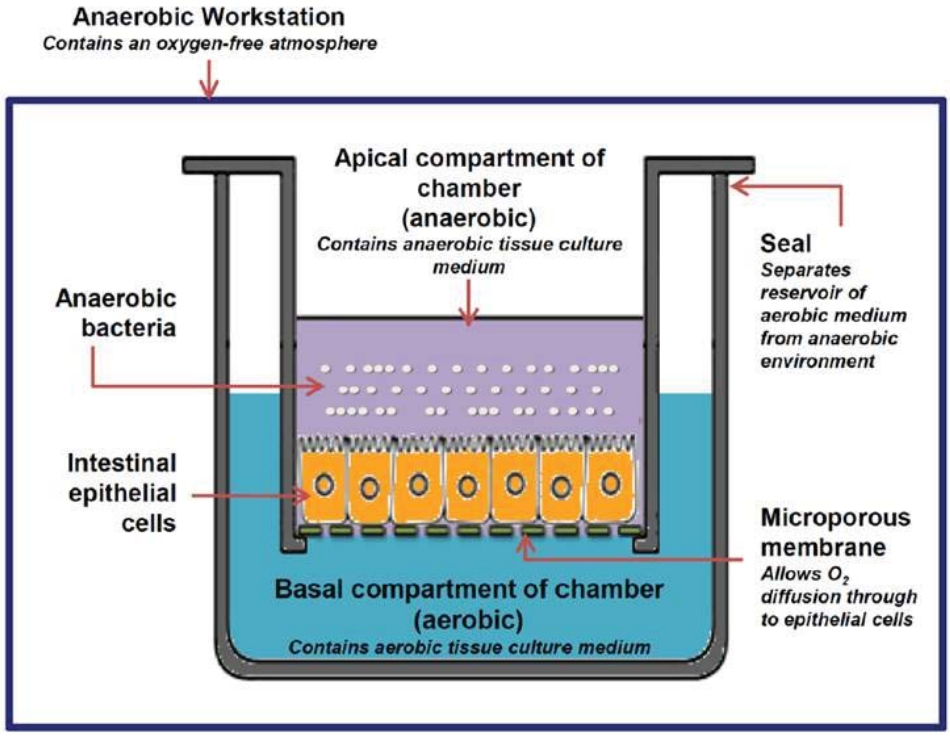

Figure 2.1 Schematic diagram of a single well of the apical anaerobic co-culture model.

The model utilises a co-culture chamber which is used inside an anaerobic workstation that has an oxygen-free atmosphere. Human cell lines are grown on a microporous membrane that separates each well of the co-culture chamber into two compartments. The basal compartment contains aerobic cell culture medium and the apical compartment contains anaerobic cell culture medium and is exposed to the oxygen-free atmosphere of the anaerobic workstation. Oxygen from the basal aerobic compartment of the chamber diffuses through the microporous membrane to the cell monolayer thereby enabling survival of the cells. In this model obligate anaerobic bacteria can be co-cultured with human cell lines, as they survive in the apical anaerobic cell culture medium [263].

chamber was equipped with a septum for basal media sampling and a one-way pressure relief valve whereas the prototype I could only be used with either a septum or a one-way pressure relief valve. Photographs of the prototype II co-culture chamber and details of its components are shown in Figure 2.2.

2.3.9.1. Setting up the apical anaerobic co-culture model

Most of the parts of the co-culture chamber were autoclaved before each experiment. The parts which were not autoclavable (chamber base, chamber lids, pressure relief valves and septa) were sterilised with 70% ethanol before use. Following autoclaving or sterilisation with 70% ethanol, the co-culture chamber was assembled in a sterile biosafety cabinet. On the day prior to an experiment all reagents and consumables required for the work in anaerobic conditions were transferred into the anaerobic workstation. All media or other solutions were left uncovered overnight inside the anaerobic workstation in order to obtain anaerobic solutions.

The day before the experiments, the M199 Std was removed from the Caco-2 cell monolayers grown on Transwell inserts and the plate wells, 260 µL of M199 supplemented only with NEAAs (1%) and FBS (10%) (referred to as M199 TEER) were added to the inserts and 810 µL into the plate wells. The culture plates containing the Caco-2 cells were kept at 37°C and 5% CO_2 until used for the experiment.

On the day of the experiment, the basal wells of the co-culture chamber were filled with 3 mL of warm M199 TEER. The Transwell inserts containing the cell monolayers were carefully inserted into the co-culture chamber using a twisting motion. The co-culture chamber was transferred into the interlock chamber of the anaerobic workstation. This interlock chamber was purged with nitrogen and after finishing the interlock cycle the co-

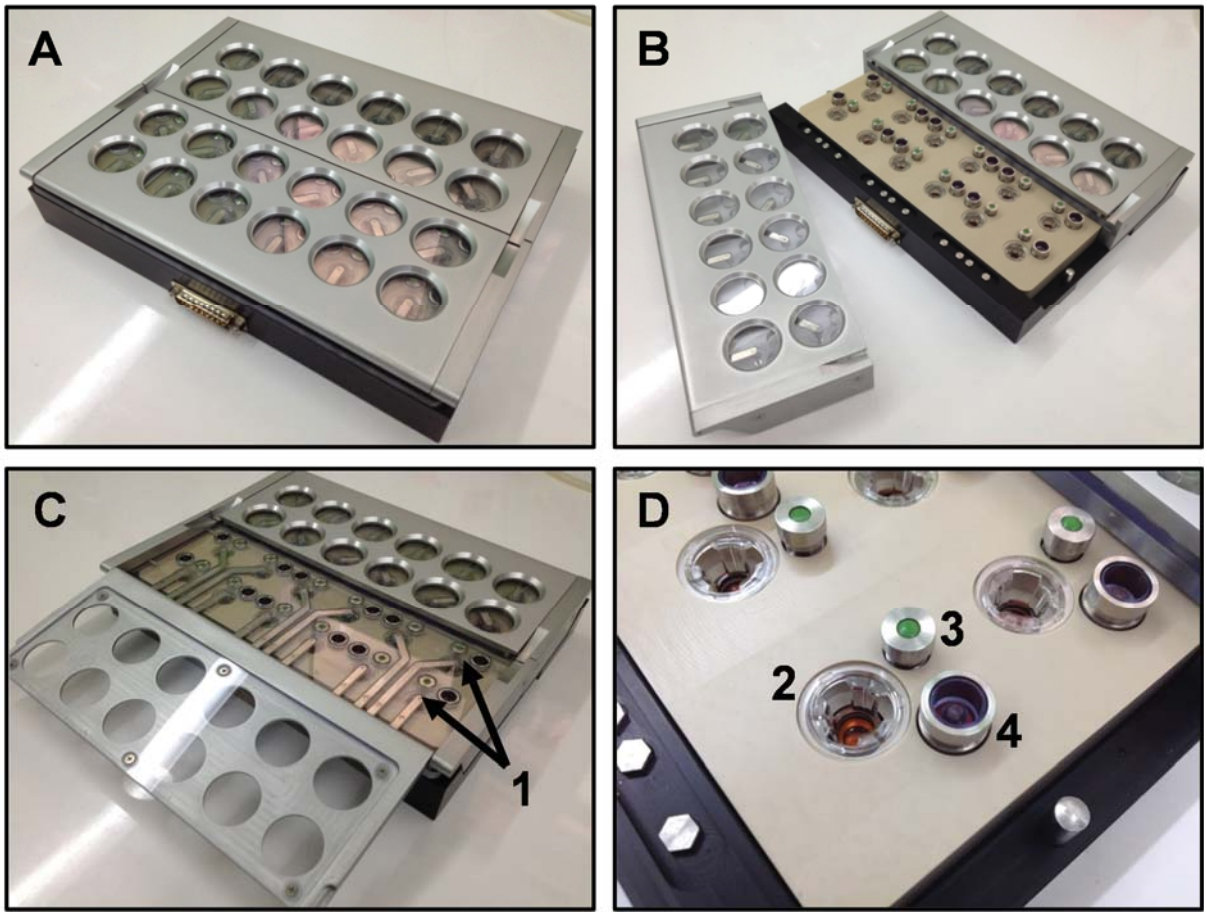

Figure 2.2 Prototype II co-culture chamber used for the apical anaerobic co-culture model. Images show (A) the prototype II co-culture chamber with closed lids, (B) with one lid removed, (C) with opened hinged window and (D) details of the components. 1: Top electrodes; 2: Transwell insert containing the Caco-2 cell monolayer; 3: Septum for basal media sampling. 4: One-way pressure relief valve.

culture chamber was moved into the anaerobic workstation. The co-culture chamber was connected to a laptop via a CellZscope controller (nanoAnalytics, Münster, Germany), which is a commercially available automated TEER monitoring system. The TEER assay could be controlled through the CellZscope software (version 2.2.3; nanoAnalytics, Münster, Germany). First, the TEER across each Caco-2 cell monolayer inserted into the 24 wells of the co-culture chamber was measured by starting the CellZscope software. After finishing one round of measurements of each well, which was used as a baseline reading, the CellZscope software was stopped. The apical aerobic medium was removed and 260 µL of anaerobic medium or treatments prepared in anaerobic medium were added. The TEER measurements were resumed by restarting the CellZscope software and taking hourly measurements over 12 h.

2.3.10. Viability of *F. prausnitzii* in different culture media

The three *F. prausnitzii* strains were incubated in cell culture medium alone and in cell culture medium supplemented with additional supplements (acetate and the bacterial culture medium BHI). Bacterial growth was monitored in order to determine whether these supplements can improve the growth of the bacteria.

The bacterial strains were grown in 10 mL of anaerobic YCFAG broth for 24 h (*F. prausnitzii* A2-165 and *F. prausnitzii* ATCC 27768) or 48 h (*F. prausnitzii* HTF-F). From each of the primary broth cultures 200 µL were used to inoculate 10 mL of anaerobic YCFAG broth and these secondary broth cultures were incubated until the three *F. prausnitzii* strains reached stationary phase which was determined as described in 2.3.7. These cultures were pelleted by centrifugation at 2492 x g for 6 min (11180/13190 rotor, Sigma 3-18K centrifuge, Osterode am Harz, Germany) and resuspended in the different anaerobic media inside an anaerobic workstation. Bacterial numbers in the solutions were

estimated using a Petroff-Hauser counting chamber as described in 2.3.5.1. Based on this estimate, bacterial solutions were diluted in Hungate culture tubes with the different anaerobic media to a concentration of 2.4 x 10^7 cells/mL, the bacterial density used in the co-culture experiment described in 2.3.13. It was estimated previously that a Transwell insert (0.33 cm^2) contained 6.38 x 10^4 Caco-2 cells at confluence. For co-culture experiments a MOI of 100 was used, which means that 6.38 x 10^6 bacterial cells were added per insert (in 260 µL of medium) resulting in a bacterial density of 2.4 x 10^7 cells/mL to be prepared. Triplicates of the bacterial solutions were incubated at 37°C and the OD_{600nm} was measured at 2 h intervals over 24 h. Before each measurement the contents of the Hungate tubes were mixed by inversion to prevent any settling of the bacterial cells on the bottom of the tubes. In addition, when supplementing cell culture medium with bacterial culture medium, the viable CFU at the beginning of the experiment and after 12 h of incubation were determined as described in 2.3.5.2.

2.3.11. TEER and viability of Caco-2 cells using aerobic media

In an initial experiment, differentiated Caco-2 cell monolayers grown on Transwell inserts in 24-well plates as described in 2.3.8.6 were apically exposed to mixtures of M199 supplemented with 1% NEAAs (M199+NEAA) and the bacterial culture medium BHI in different ratios. The effect of these treatments on TEER and the viability of the cells was determined. Immediately prior to the experiment TEER of the differentiated Caco-2 cell monolayers was measured using an EndOhm TEER cup connected to an EVOM voltohmmeter as described in 2.3.8.7. The apical medium was then replaced with 260 µL of the treatment solutions consisting of M199+NEAA mixed with increasing percentages of anaerobic BHI (0, 20, 40, 60, 80 and 100% BHI). The basal medium was replaced with 810 µL of fresh M199+NEAA. Three repetitions were used per treatment. TEER was

measured immediately after the treatments were added and then every two hours over 12 h. In between the TEER measurements the cell culture plates containing the Transwell inserts were placed in the incubator (37°C, 5% CO_2). In addition, the cell culture inserts treated with 0% BHI (i.e. 100% M199+NEAA) and 100% BHI were used to determine the viability of the Caco-2 cells after 12 h of incubation with the trypan blue viability test as described in 2.3.14.

2.3.12. TEER and viability of Caco-2 cells using anaerobic media

The above described experiment was repeated using the apical anaerobic co-culture model. The co-culture chamber was prepared as described in 2.3.9.1. The basal wells were filled with 3 mL of M199 TEER. Differentiated Caco-2 cell monolayers on Transwell inserts were inserted into the co-culture chamber which was then transferred into an anaerobic workstation as described in 2.3.9.1. The initial resistance was recorded after 1 h inside the anaerobic workstation. The apical medium was removed and replaced with 260 µL of the anaerobic treatment solutions consisting of anaerobic M199 TEER mixed with increasing percentages of anaerobic BHI (0, 25, 50, 75 and 100% BHI). After an incubation for 12 h with automated hourly TEER measurements, the inserts were removed from the co-culture chamber and the viability of the Caco-2 cells was determined using the neutral red uptake assay as described in 2.3.15. This experiment was performed in five replications using four repetitions per treatment. Only Caco-2 monolayers with an initial TEER over 400 $\Omega.cm^2$ were included for the TEER data analysis and monolayers that did not reach this threshold were also excluded from the viability data analysis.

2.3.13. Viability of the *F. prausnitzii* strains in the apical anaerobic co-culture model using mixtures of cell and bacterial culture media

Mixtures of anaerobic cell and bacterial culture media were used for co-culturing Caco-2 cells and the three *F. prausnitzii* strains in the apical anaerobic co-culture model and it was determined if the bacteria were growing in these adapted conditions. The media compositions chosen were anaerobic M199 TEER supplemented with 25 or 50% of anaerobic BHI (referred to as 25 and 50% BHI). This adapted medium was only used for the apical compartment of the co-culture chamber; the basal wells were filled with aerobic M199 TEER.

Primary and secondary broth cultures of the three *F. prausnitzii* strains listed in Table 2.1 were prepared as described in 2.3.7. The secondary cultures were prepared in duplicate and incubated for 20 h for *F. prausnitzii* A2-165 and *F. prausnitzii* ATCC 27768 and for 26 h for *F. prausnitzii* HTF-F in order to use the bacteria in the stationary phase of growth for the co-culture experiments. These cultures were pelleted by centrifugation at 2492 x g for 6 min (11180/13190 rotor, Sigma 3-18K centrifuge, Osterode am Harz, Germany) and resuspended in anaerobic M199 TEER inside the anaerobic workstation. The bacteria were counted using a Petroff-Hauser counting chamber as described in 2.3.5.1. Based on this determined bacterial density, the bacterial solutions were diluted with 25 and 50% BHI to a concentration of 2.4 x 10^7 cells/mL in order to use a MOI of 100 as described in 2.3.10. The duplicate bacterial cultures of the three *F. prausnitzii* strains were used to prepare 5 mL each of bacterial solutions with a bacterial concentration of 2.4 x 10^7 cells/mL using the two different M199 TEER-BHI mixtures.

The co-culture chamber was prepared as described in 2.3.9.1. The apical medium was removed from the Caco-2 cell monolayers and 260 µL of dilutions of the three *F.*

prausnitzii strains (A2-165, ATCC 27768, HTF-F) in each of the two different media compositions (25 and 50% BHI), were added. The viability of the *F. prausnitzii* strains in the co-culture model was assessed by determining the viable CFU of the bacteria before and after the co-culture with the Caco-2 cells as described in 2.3.5.2. Three repetitions were used per treatment and the assay was performed in five replications.

2.3.14. Trypan blue viability test of Caco-2 cells grown on Transwell inserts

For the fast determination of the viability of Caco-2 cells grown on Transwell inserts the trypan blue viability test was used. First, the apical medium was removed from the inserts and 100 µL of the dissociation reagent TrypLE were added. The cell culture plate containing the Transwell inserts was placed in a 5% CO_2 incubator at 37°C for around 10 min or until the cells detached from the membrane. After this incubation 100 µL of M199 Std were added to the inserts, the cell suspension was mixed using a micropipette and transferred into an Eppendorf tube. The cell suspension was centrifuged for 3 min at 240 x g using a microcentrifuge (Hettich Mikro 120, Germany). After discarding the supernatant, the cell pellet was resuspended in 100 µL of M199 Std. The viability of the Caco-2 cells within this cell suspension was determined using trypan blue and an automated cell counter as described in 2.3.8.5.

2.3.15. Neutral red uptake assay

The neutral red uptake assay was used as another method to determine the viability of Caco-2 cells grown on Transwell inserts. Viable cells are able to incorporate and bind neutral red whereas dead cells cannot retain the dye. Therefore, the more viable cells are present, the more dye is retained. Following an incubation time with the dye, an acidified ethanol solution is used to extract the dye from the viable cells and the amount of the

solubilised dye is quantified by measuring its absorbance using a spectrophotometer. Compared to the trypan blue viability assay this assay is longer as it contains several incubation steps. Therefore both methods were used for the method development experiments, the trypan blue method for the initial quick determination of the viability of Caco-2 cells and the neutral red uptake assay to confirm the results gained by staining with trypan blue. However, the results gained using the neutral red viability assay were considered more reliable as the trypan blue method stains the non-viable cells that often start to detach from the inserts before staining which results in an underestimation of the amount of non-viable cells. The results of the neutral red assay would not be influenced by the detachment of non-viable cells because only viable cells can incorporate and bind the dye.

Neutral red (3-amino-7-dimethylamino-2-methyl-phenazine hydrochloride, Sigma) was dissolved in PBS at 5 mg/mL and filter sterilised. This stock solution was further diluted with M199 Std (Table 2.6) to a concentration of 50 µg/mL on the day prior to the experiment and incubated overnight at 37°C. On the day of the experiment, this solution, from here on referred to as neutral red medium, was centrifuged for 10 min at 2000 x g (11180/13190 rotor, Sigma 3-18K centrifuge, Germany) in order to remove any precipitated dye crystals. The cell culture medium or the relevant treatments were aspirated off the Caco-2 cell monolayers on Transwell inserts and 200 µL neutral red medium were added to each insert. The Caco-2 cells were incubated with the neutral red medium for two h at 37°C in a CO_2 incubator. Following this incubation time the neutral red medium was removed and the cell monolayers were washed twice by adding 200 µL of PBS to the Transwell insert and 810 µL PBS to the plate well and gently swirled using a rocking motion. This step ensured that adhering but unincorporated dye was removed. The dye was

extracted from viable cells by adding 200 µL solubilisation solution (1% acetic acid – 50% ethanol) and incubating at room temperature shaking on a plate shaker at 200 rpm for 7 min. This extract was then transferred in 150 µL aliquots to a 96-well titre plate and the absorbance of neutral red was determined on a microplate reader at 540 nm. The background absorbance of the 96-well titre plate was measured at 690 nm and subtracted from the 540 nm measurement.

2.3.16. Statistical analysis

The statistical analyses were performed using SAS (SAS/STAT version 9.3; SAS Institute Inc., Cary, NC, USA). An analysis of repeated measures was conducted to test the effect of the factors (acetate supplementation or BHI concentration), the factor time and their interaction, on the response variables (TEER or OD_{600nm}). The most appropriate covariance structure of the mixed model for each response variable was selected after fitting the models by Restricted Maximum Likelihood method and comparing them using the log-likelihood ratio test. When an interaction was not significant it was removed from the model. An analysis of variance (ANOVA) was also conducted to test the effect of the BHI concentration on the viability of Caco-2 cells in apical anaerobic conditions. When the F-value of the analyses were significant ($P < 0.05$), the means were compared using adjusted Tukey tests. A two independent samples t-test procedure was performed to test the effect of the BHI concentration on the viability of Caco-2 cells in conventional conditions and to compare the viability of the three *F. prausnitzii* strains before and after the co-culture with Caco-2 cells in the apical anaerobic co-culture model. Additionally, a paired t-test was conducted to compare the viability of the three *F. prausnitzii* strains before and after the incubation in 50% BHI. For all the analyses the model assumptions (e.g. normal distribution and the homogeneity of variance) was evaluated using the Output Delivery

System (ODS) graphics in SAS. When the response variable did not fulfil these assumptions a $\log_{10}$ transformation was performed to reach these assumptions. Using cell lines such as Caco-2 has the limitation that there is no biological independence between the replicates because all cells have the same origin. However, applying the different treatments to the cells induces changes on the cell populations and therefore variation. For this reason, each cell monolayer seeded into one Transwell insert was used as a replicate which was independent for this experimental purpose but not biologically independent. For the method development described in this chapter the number of independent replicates was three (n = 3) if not otherwise stated. For experiments that were performed in several runs a complete randomised block design was firstly performed with the run (or experimental day) as a random effect. There was no effect of the run for any of the tested variables, consequently the random effect was removed from the model.

2.4. RESULTS

2.4.1. 16S rRNA gene sequencing

The identities of the three *F. prausnitzii* strains were confirmed using 16S rRNA gene sequencing. The 16S rRNA gene sequences were compared with known bacterial sequences in the NCBI nucleotide collection database. The trace of *F. prausnitzii* A2-165 showed the highest sequence identity with the sequence of 'Butyrate-producing bacterium A2-165 16S rRNA gene' (99%). The trace of *F. prausnitzii* ATCC 27768 produced an alignment with the sequence of '*F. prausnitzii* strain ATCC 27768 16S rRNA, partial sequence' with a sequence identity of 99%. An alignment for the sequence of *F. prausnitzii* HTF-F was produced with the sequence of '*F. prausnitzii* strain HTF-F 16S rRNA gene, partial sequence' with a sequence identity of 99%. Therefore the identities of the strains

were confirmed. When comparing the 16S rRNA gene sequences of the three strains with each other, a sequence identity of 98% was determined. The 16S rRNA gene sequences of *F. prausnitzii* A2-165 and *F. prausnitzii* HTF-F showed 97% similarity to the 16S rRNA gene sequences of the type strain *F. prausnitzii* ATCC 27768 (AJ413954).

2.4.2. Gram staining

The cellular morphology of the three *F. prausnitzii* strains was determined by Gram staining. Figure 2.3 shows the light micrographs (100-fold magnification) of the *F. prausnitzii* strains. These micrographs demonstrate the morphological differences between the three Gram-negative bacterial strains. The cells of *F. prausnitzii* A2-165 (Figure 2.3A) were straight and occurred singly, in pairs or in long chains. In contrast, the cells of *F. prausnitzii* ATCC 27768 (Figure 2.3B) and *F. prausnitzii* HTF-F (Figure 2.3C) were curved. *F. prausnitzii* ATCC 27768 occurred mainly singly or in pairs, whereas *F. prausnitzii* HTF-F formed longer chains.

2.4.3. Growth curves

Growth curves of the three *F. prausnitzii* strains in anaerobic BHI broth in sealed Hungate culture tubes at 37°C for 38 h were completed (Figure 2.4). *F. prausnitzii* A2-165 and *F. prausnitzii* ATCC 27768 reached stationary phase after 14 h of incubation and *F. prausnitzii* HTF-F after 26 h. However, for logistic reasons during setting up the experiments (i.e. subculture bacteria at night), *F. prausnitzii* A2-165 and *F. prausnitzii* ATCC 27768 were used at 20 h of incubation when the bacteria were still in the stationary phase of growth. Therefore, for the experiments described in the following sections secondary cultures of the three *F. prausnitzii* strains at stationary phase were used after

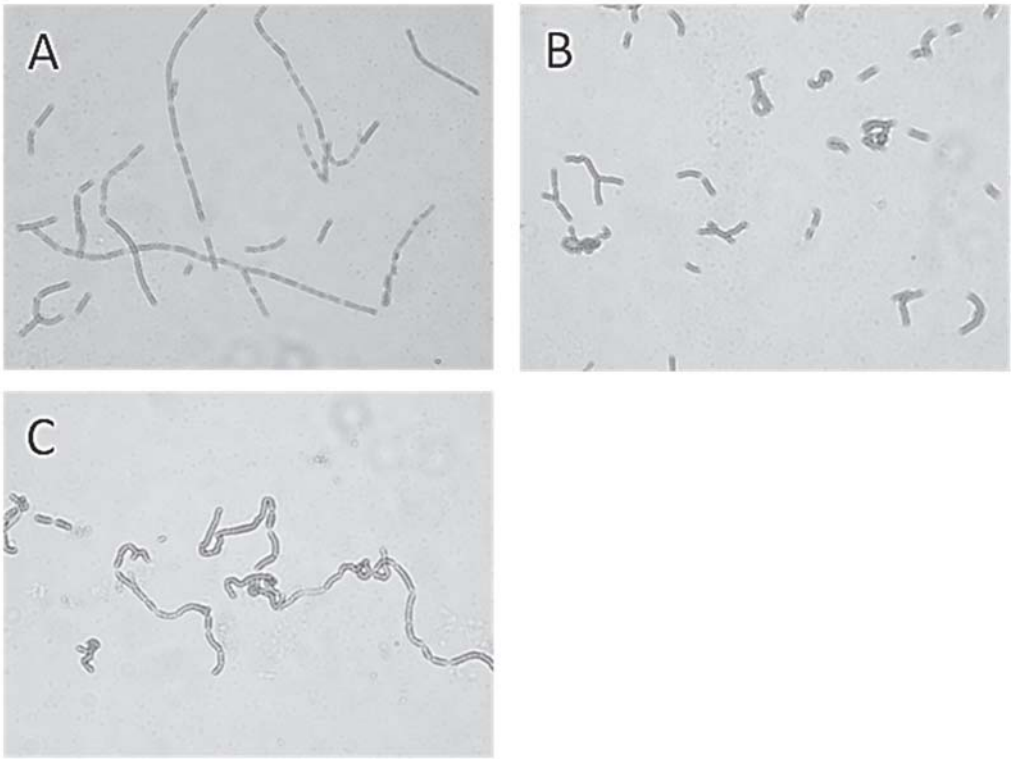

Figure 2.3 Gram staining of the three *F. prausnitzii* strains.

The light micrographs (100-fold magnification) show the three *F. prausnitzii* strains after Gram staining to illustrate the differences in their morphology. A: *F. prausnitzii* A2-165 (DSM 17677); B: *F. prausnitzii* ATCC 27768; C: *F. prausnitzii* HTF-F (DSM 26943).

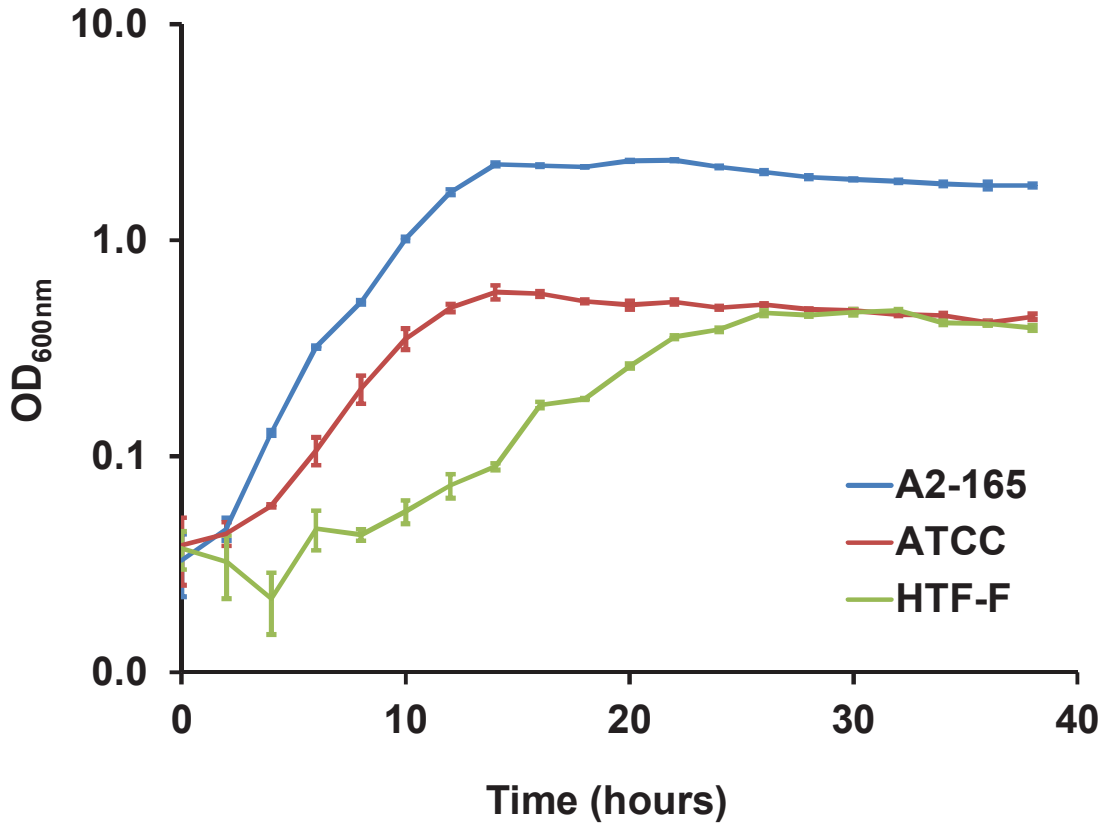

Figure 2.4 Growth curves for the three *F. prausnitzii* strains in BHI broth.

The graph shows for each of the three *F. prausnitzii* strains (A2-165, ATCC 27768 and HTF-F) the mean (± standard error of the mean (SEM); n = 3) OD_{600nm} over time. The bacterial strains were cultured in anaerobic BHI broth in Hungate culture tubes sealed with butyl rubber stoppers at 37°C.

growing for 20 h (*F. prausnitzii* A2-165 and *F. prausnitzii* ATCC 27768) and 26 h (*F. prausnitzii* HTF-F).

2.4.4. Viability of the *F. prausnitzii* strains in cell culture medium

The growth of the three *F. prausnitzii* strains in the anaerobic cell culture medium M199+NEAA at 37°C was determined. FBS was not added to M199 as it was previously shown that supplementation of cell culture medium with FBS led to bacterial overgrowth causing M199 to become too acidic for the Caco-2 cells. Furthermore, no antibiotics were added to M199 to allow bacterial growth when co-cultured with Caco-2 cells. The absolute OD_{600nm} values are shown in Figure 2.5A. However, due to the different starting OD_{600nm} values for the three *F. prausnitzii* strains, the statistical analysis was performed after normalising by the OD_{600nm} at time 0 h. None of the strains showed the ability to grow in this medium over the period of 24 h of incubation as shown by the change in the OD_{600nm} graph (Figure 2.5B). There were no significant differences in the change of the OD_{600nm} until 8 h of incubation for each of the three strains. However, after 24 h of incubation, all three strains showed a decrease in the OD_{600nm} compared to the previous time points (0 to 8 h; $P < 0.05$).

2.4.5. Viability of the *F. prausnitzii* strains in cell culture medium supplemented with acetate

The first approach to optimise the growth conditions of the *F. prausnitzii* strains in the co-culture model was to supplement anaerobic cell culture medium with acetate, a compound known to stimulate the growth of *F. prausnitzii* [178,187]. The bacteria were either resuspended in filter sterilised anaerobic M199+NEAA supplemented with 33 mM acetate (referred to as acetate) or in anaerobic M199+NEAA (referred to as control). The

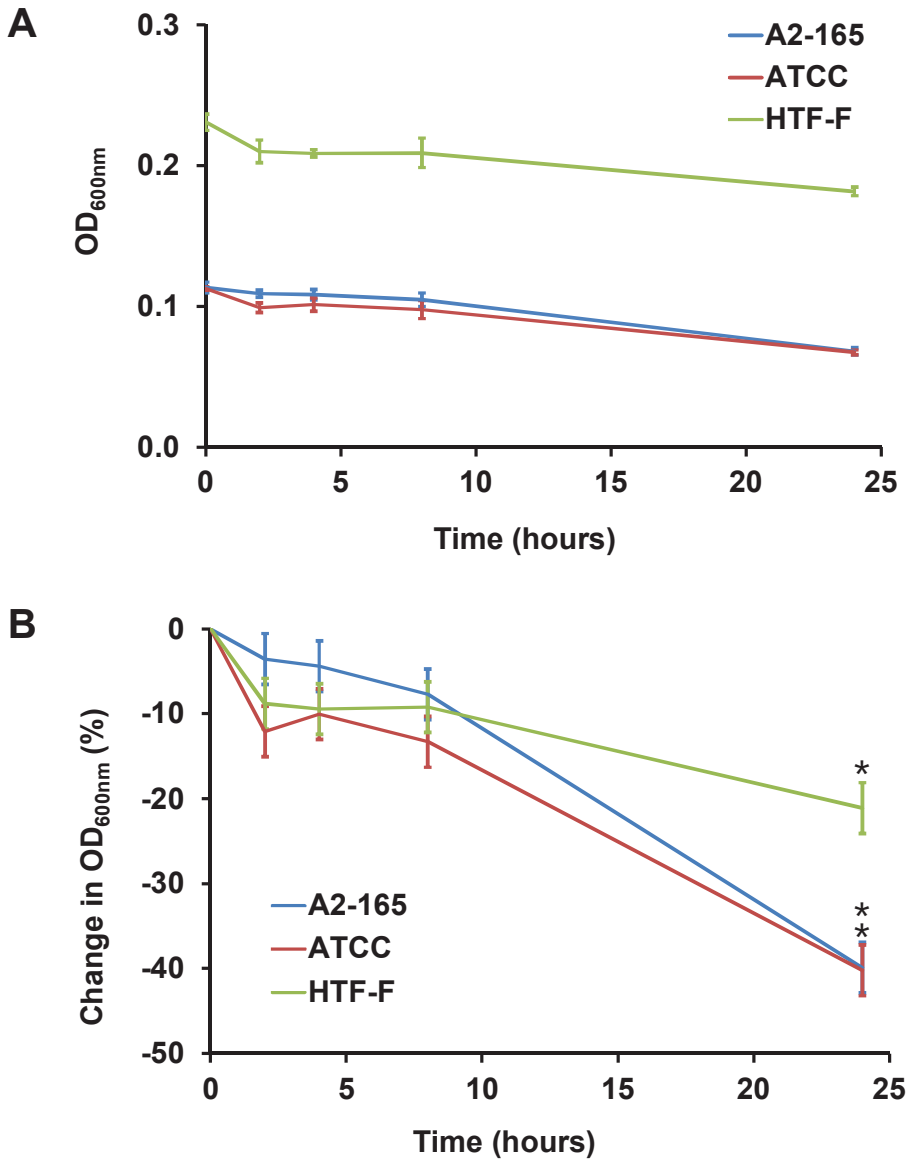

Figure 2.5 OD_{600nm} (A) and normalised change in OD_{600nm} (%) (B) of the three *F. prausnitzii* strains in anaerobic cell culture medium.

The three *F. prausnitzii* strains (A2-165, ATCC 27768 and HTF-F) in stationary phase were resuspended in anaerobic M199+NEAA, incubated at 37°C and the OD_{600nm} was measured over 24 h. Graphs show (A) the mean (± SEM; n = 3) OD_{600nm} for each of the three *F. prausnitzii* strains over 24 h and (B) the mean values (± SEM; n = 3) after normalising by the OD_{600nm} at time 0 h. The normalised change in OD_{600nm} was used for the statistical analysis because of the different starting OD_{600nm}. The time point with the sign * for each curve differs significantly to previous time points at $P < 0.05$.

concentration of acetate was chosen as it represents the concentration used to prepare the YCFAG medium. The growth of the bacterial strains was determined by measuring the OD_{600nm} at 2 h intervals over 8 h and in addition after 24 h.

Figure 2.6 shows the OD_{600nm} values of the three *F. prausnitzii* strains in acetate and control media over 24 h. However, due to the different starting OD_{600nm} values the statistical analysis was performed after normalising by the OD_{600nm} at 0 h for each strain in each medium as shown in Figure 2.7. There was a significant interaction between the strain, time and medium ($P < 0.001$). For *F. prausnitzii* ATCC 27768, there was a higher drop in the OD_{600nm} after 8 h for acetate compared to the control media ($P < 0.05$). However, there was no difference in the change in OD_{600nm} between the control and acetate media for *F. prausnitzii* A2-165 and HTF-F at any time point ($P > 0.05$). Overall, the supplementation did not improve the viability of the *F. prausnitzii* strains, all three strains showed a decrease in the OD_{600nm} over the incubation time in both acetate and control media.

2.4.6. Supplementation of cell culture medium with bacterial culture medium

The supplementation of the cell culture medium with acetate did not improve the viability of the *F. prausnitzii* strains, as shown in the previous section (2.4.5). Therefore, the next approach for the growth optimisation was to supplement cell culture medium (M199) with bacterial culture medium (BHI). Studies were conducted to test the effect of different M199-BHI ratios on the viability of the bacteria, and the TEER and viability of the Caco-2 cell monolayers.

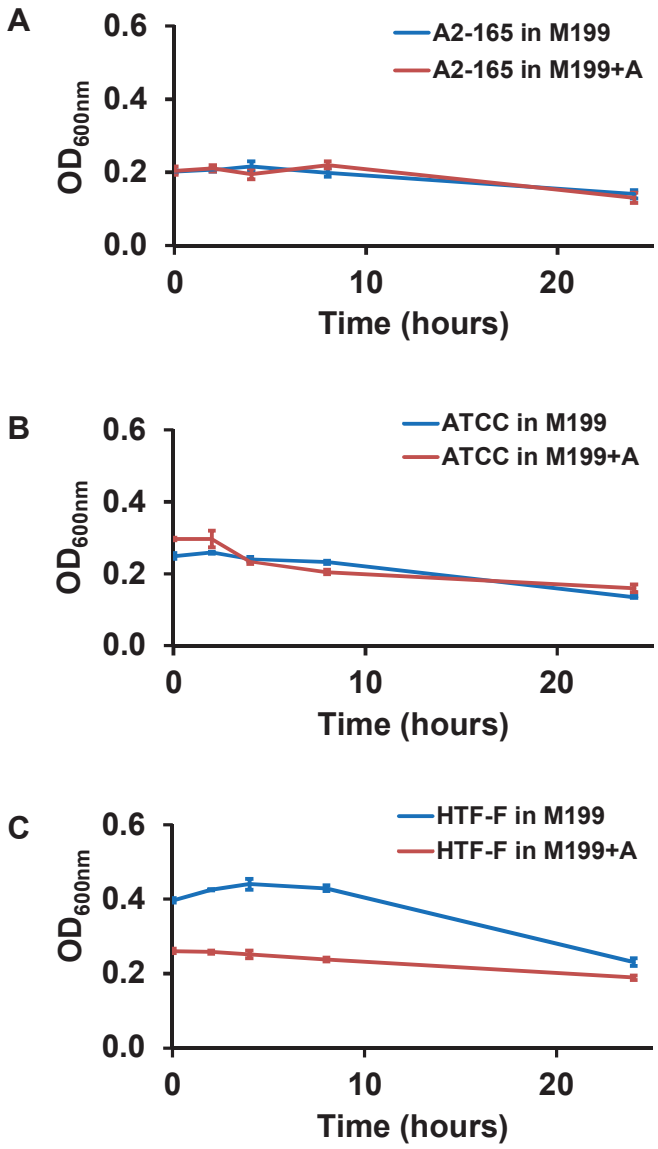

Figure 2.6 OD_{600nm} of the three *F. prausnitzii* strains in anaerobic M199+NEAA with or without acetate supplementation.

Secondary cultures of the three *F. prausnitzii* strains ((A) A2-165, (B) ATCC 27768 and (C) HTF-F) in stationary phase were resuspended in anaerobic M199+NEAA or anaerobic M199+NEAA supplemented with 33 mM acetate (M199+A), incubated at 37°C and the OD_{600nm} was measured over 24 h. The graph shows for each of the three *F. prausnitzii* strains the mean (± SEM; n = 3) OD_{600nm} over time. Due to the different starting OD_{600nm} values the statistical analysis was performed after normalising by the OD_{600nm} at 0 h for each strain in each medium (Figure 2.7).

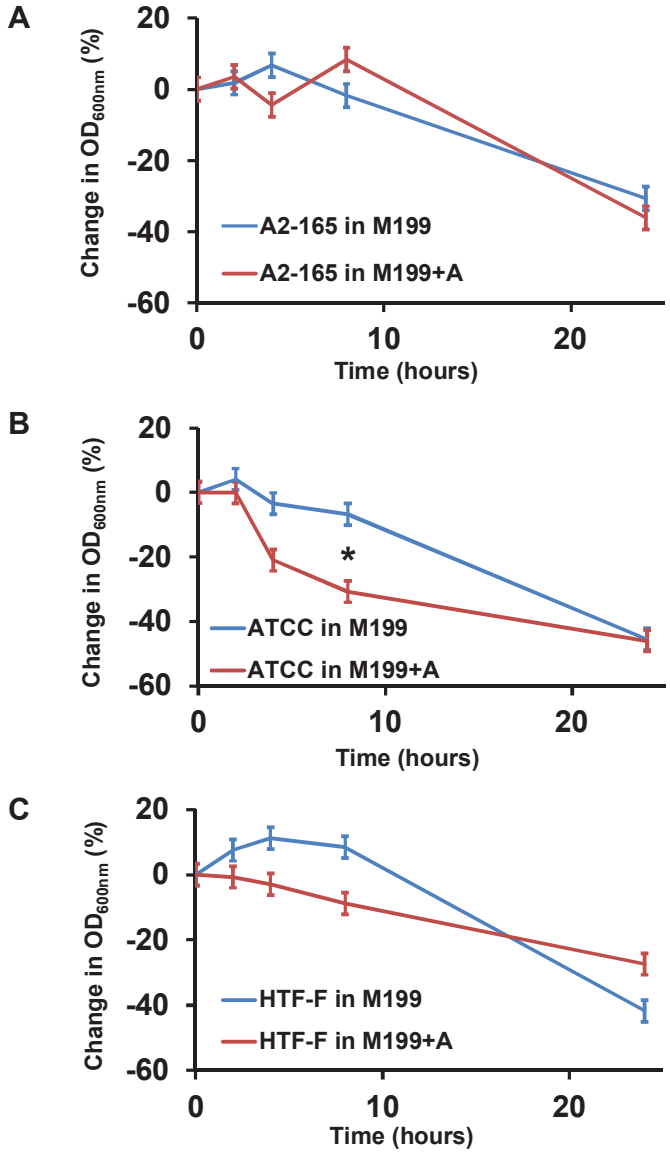

Figure 2.7 Normalised change in OD_{600nm} (%) of the three *F. prausnitzii* strains in anaerobic M199+NEAA with or without acetate supplementation.

The three *F. prausnitzii* strains ((A) A2-165, (B) ATCC 27768 and (C) HTF-F) in stationary phase were resuspended in anaerobic M199+NEAA or anaerobic M199+NEAA supplemented with 33 mM acetate (M199+A), incubated at 37°C and the OD_{600nm} was measured over 24 h. The mean values (± SEM; n = 3) were obtained after normalising by the OD_{600nm} at 0 h for each strain in each medium. There was a significant interaction between the strain, time and medium ($P < 0.001$). * Mean OD_{600nm} values for each *F. prausnitzii* strain differ between acetate and control media for this time point at $P < 0.05$.

2.4.6.1. Effect of ratios of cell and bacterial culture medium on TEER and viability of Caco-2 cells in conventional conditions

It was previously shown that de Man, Rogosa and Sharpe broth, a bacterial culture medium used for the cultivation of lactobacilli [273], had detrimental effects on TEER across Caco-2 monolayers (Dr Rachel Anderson, personal communication). Therefore, it was important to first test the effect of mixtures of cell culture medium and BHI on TEER and the viability of Caco-2 cell monolayers. As a first step the viability of the Caco-2 cells exposed to M199+NEAA (i.e. 0% BHI) and 100% BHI in conventional conditions (5% CO_2 in air atmosphere) was determined after 12 h of incubation using the trypan blue viability test. There was no significant difference between the viability of Caco-2 cell monolayers treated with 0 and 100% BHI ($P = 0.22$) as shown in Figure 2.8.

In addition, the effect of mixtures of M199+NEAA and BHI in different ratios on TEER across Caco-2 cell monolayers was tested in conventional conditions over 12 h. Figure 2.9A shows the absolute TEER values. The initial TEER values were in the range from approximately 1200 to 2100 $\Omega.cm^2$. Following the initial drop in TEER after adding the treatments, with values ranging from 650 to 1100 $\Omega.cm^2$, the TEER values recovered and plateaued with values between approximately 1100 and 1600 $\Omega.cm^2$ after 13 h of incubation. Because of the different starting TEER values the statistical analysis was performed after normalising by the values at 0 h for each medium as shown in Figure 2.9B. There was a significant interaction between the time and the BHI concentration on the change in TEER ($P < 0.001$). The Caco-2 monolayers treated with the 100% M199+NEAA or 100% BHI media had the lowest normalised TEER values across all time points ($P < 0.05$). In contrast, cells treated with 20 or 60% BHI had the highest normalised TEER values across all time points.

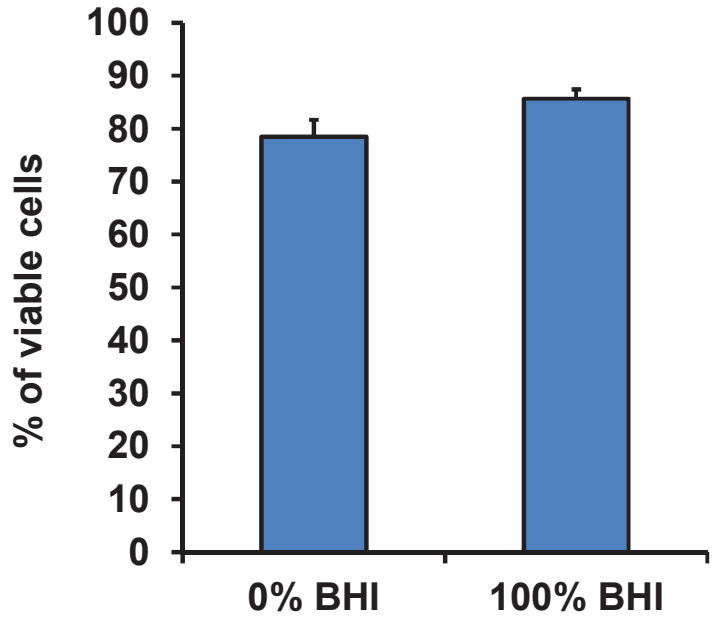

Figure 2.8 Viability of Caco-2 cells exposed to cell and bacterial culture medium in conventional conditions (5% CO_2 in air atmosphere).

Graph shows the viability of Caco-2 cells after 12 h of incubation with 0 and 100% BHI (mean ± SEM; n = 3) determined with the trypan blue viability test. There was no difference between the viability of Caco-2 cells treated with 0 and 100% BHI (P = 0.22).

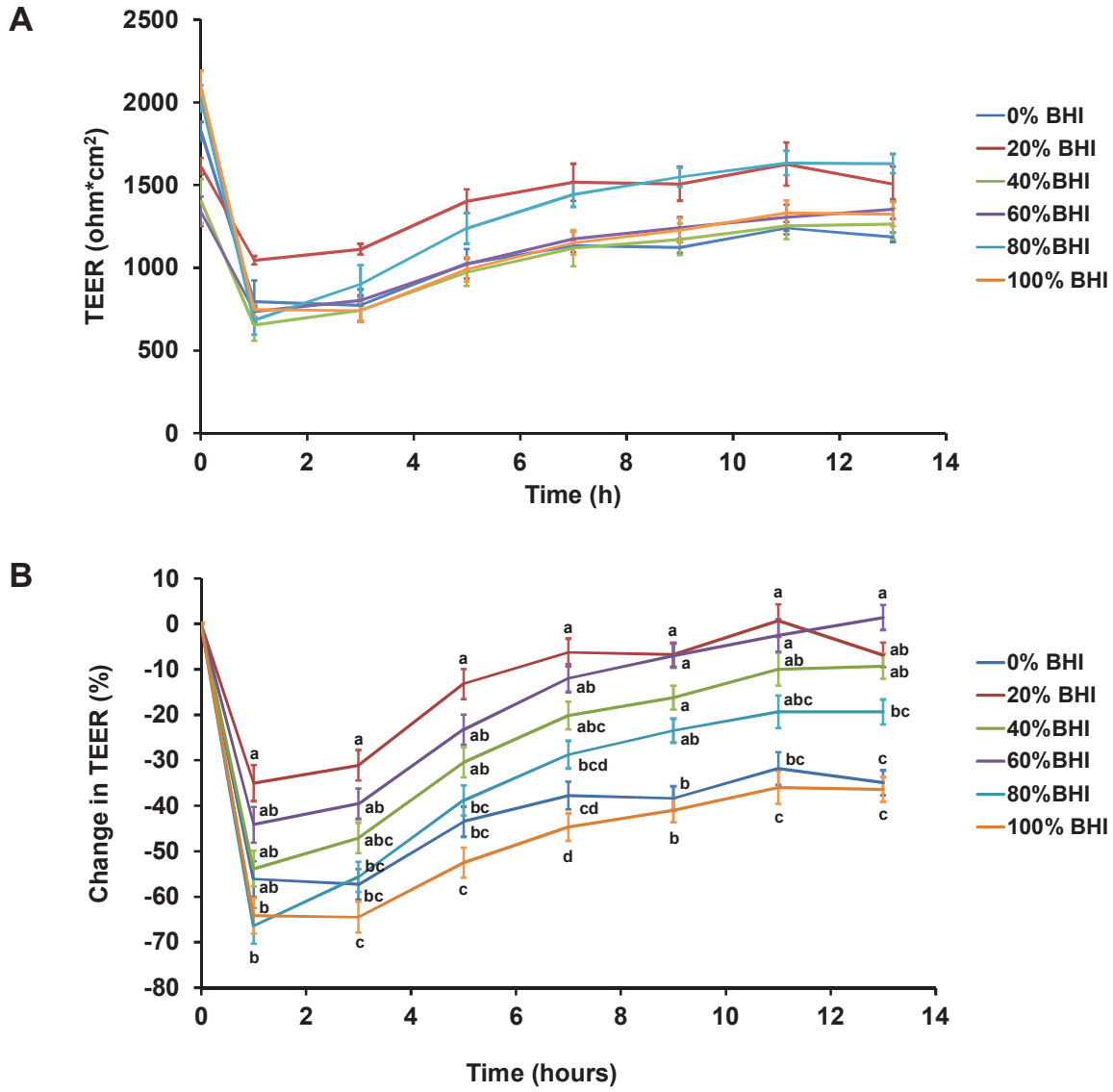

Figure 2.9 TEER across Caco-2 cell monolayers exposed to mixtures of cell and bacterial culture medium in conventional conditions (5% CO_2 in air atmosphere).

Caco-2 cell monolayers were exposed on the apical side to M199+NEAA supplemented with 0, 20, 40, 60, 80 and 100% BHI. Graphs show (A) the mean (± SEM; n = 3) TEER across Caco-2 cell monolayers over 13 h and (B) the mean (± SEM; n = 3) change in TEER over 13 h after normalising by the TEER at 0 h for each medium. Due to the different starting TEER values the statistical analysis was performed using the normalised data. There was a significant interaction between the time and the BHI concentration on the change in TEER ($P < 0.001$). Treatments that do not share the same letters are significantly different ($P < 0.05$).

2.4.6.2. Effect of ratios of cell and bacterial culture medium on TEER and viability of Caco-2 cells in the apical anaerobic co-culture model

The above described experiment was repeated in apical anaerobic conditions (co-culture chamber inside the anaerobic workstation). For this experiment anaerobic M199 TEER (M199 plus NEAAs and FBS) was used instead of anaerobic M199+NEAA. Previous experiments co-culturing bacteria with Caco-2 cells showed that the addition of FBS led to bacterial overgrowth causing the cell culture medium to become too acidic for Caco-2 cells. The experiments were therefore performed without the addition of FBS to the cell culture medium [112,113,274]. However, the bacteria used in those studies were fast growing, lactic acid producing facultative anaerobic lactobacilli [112,113,274]. *F. prausnitzii* is a slow growing bacteria, thus it was decided to supplement M199 in addition to NEAAs further with FBS (M199 TEER). Anaerobic M199 TEER was then mixed with anaerobic BHI in different ratios (0, 25, 50, 75 and 100% BHI).

The viability of the Caco-2 cell monolayers treated with the different mixtures of cell and bacterial culture medium over 12 h was determined using the neutral red viability assay. As shown in Figure 2.10, there was no significant difference ($P = 0.07$) between the viability of Caco-2 cell monolayers treated with 0, 25, 50, 75 and 100% BHI in the apical anaerobic co-culture model. Therefore, the BHI concentration had no effect on the viability of the Caco-2 cells.

Additionally, the effect of the different M199 TEER-BHI mixtures on TEER of Caco-2 monolayers in apical anaerobic conditions was tested over 12 h. The absolute TEER values are shown in Figure 2.11A. The starting TEER values were in the approximate range of 1300 to 1500 $\Omega.cm^2$ for all treatments. After adding the treatments, the TEER values dropped to 630 $\Omega.cm^2$ for cells treated with M199 TEER (i.e. 0% BHI) and to values

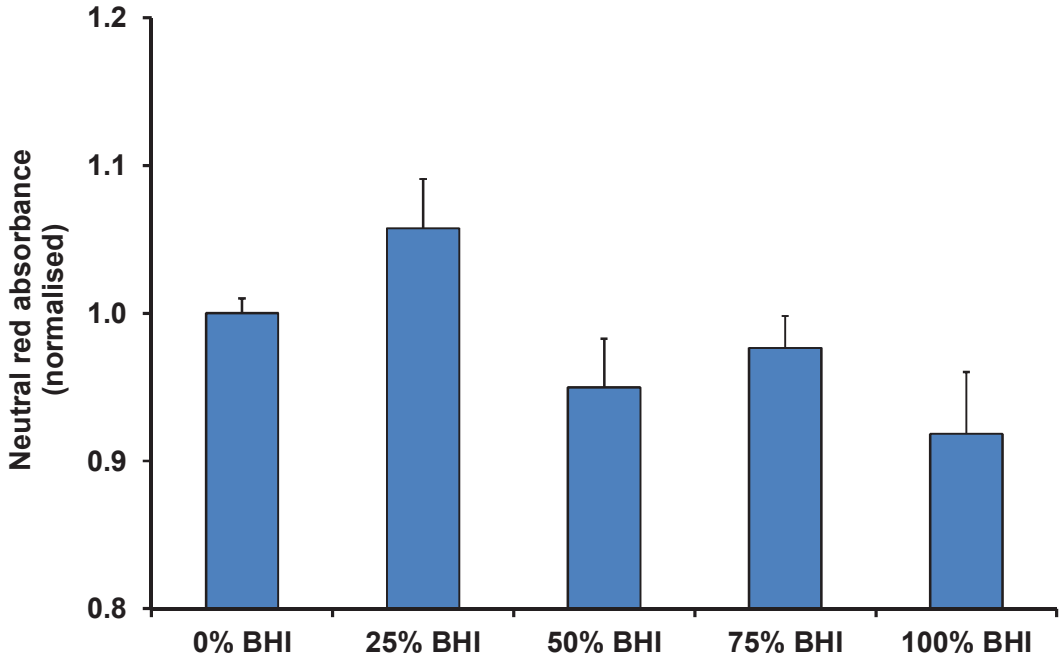

Figure 2.10 Viability of Caco-2 cells exposed to mixtures of cell and bacterial culture medium in the apical anaerobic co-culture model.

Caco-2 cell monolayers were exposed on the apical side to anaerobic M199 TEER supplemented with 0, 25, 50, 75 and 100% of anaerobic BHI. This graph shows the viability (mean ± SEM; n = 20) of Caco-2 cells after 12 h of incubation with the treatments. Neutral red absorbance was normalised by adjusting the control cells (treated with 0% BHI, i.e. M199 TEER) to 1. No differences between treatments were determined for the viability of the Caco-2 cells exposed to the different ratios of M199 TEER and BHI ($P = 0.07$).

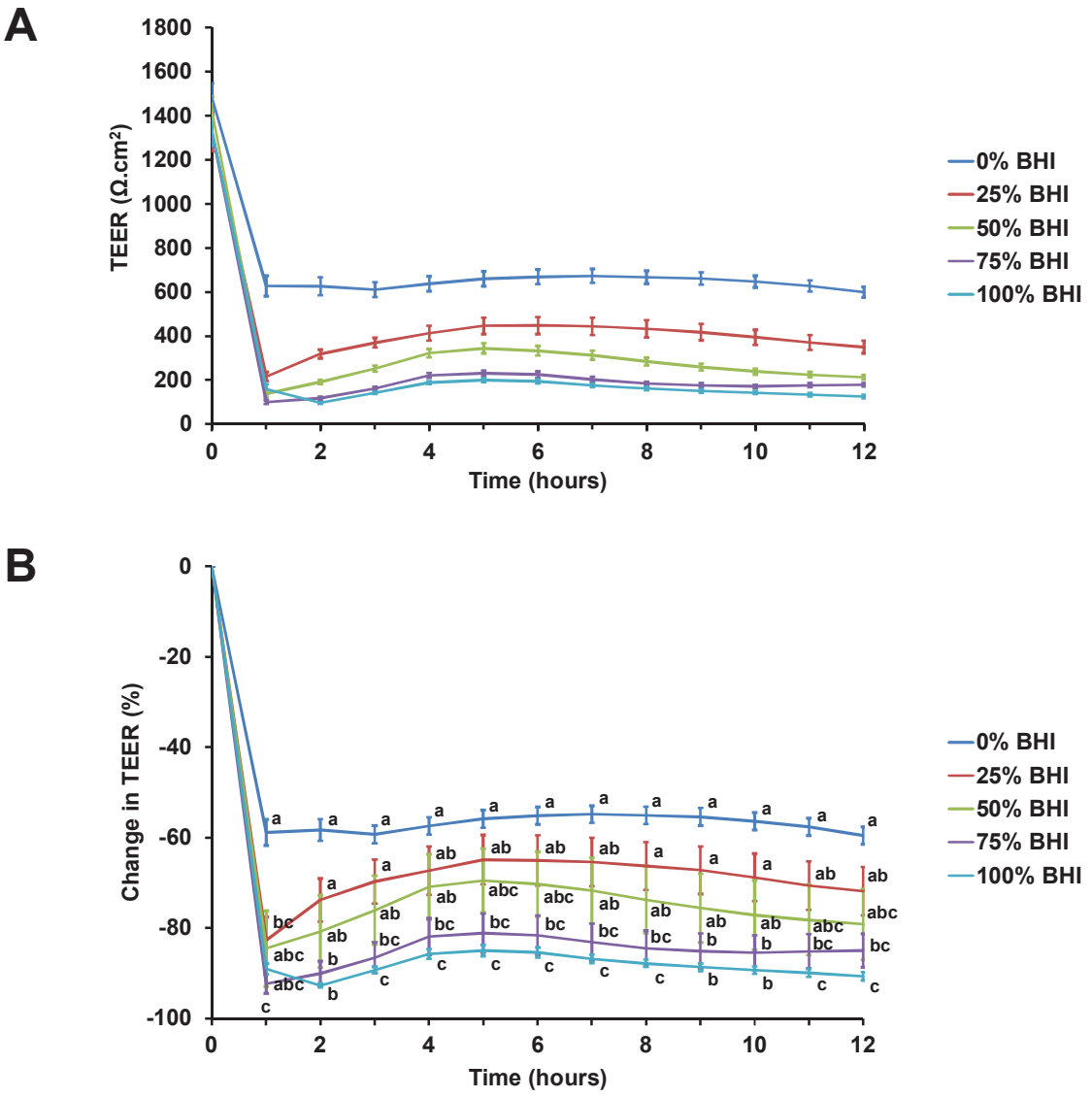

Figure 2.11 TEER across Caco-2 cell monolayers exposed to mixtures of cell and bacterial culture medium in the apical anaerobic co-culture model.

Caco-2 cell monolayers were exposed on the apical side to anaerobic M199 TEER supplemented with 0, 25, 50, 75 and 100% of anaerobic BHI. Graphs show (A) the mean (± SEM; n = 20) TEER across Caco-2 cell monolayers over 12 h and (B) the mean (± SEM; n = 20) change in TEER across Caco-2 cell monolayers over 12 h after normalising by the TEER at 0 h for each medium. The statistical analysis was performed using the normalised data because of the different starting TEER values. There was a significant interaction between the time and the BHI concentration on the change in TEER ($P < 0.01$). Treatments that do not share the same letters are significantly different ($P < 0.05$).

between 100 and 220 $\Omega.cm^2$ for the cells treated with 25, 50, 75 and 100% BHI. Following the initial drop in TEER, the cells recovered and TEER values plateaued at approximately 600, 400, 300, 200 and 200 $\Omega.cm^2$ for 0, 25, 50, 75 and 100% BHI, respectively.

Due to the different starting TEER values the statistical analysis was performed after normalising by the TEER at 0 h for each medium as shown in Figure 2.11B. There was a significant interaction between the time and the BHI concentration on the change in TEER ($P < 0.01$). When treated with 25% BHI, the normalised TEER across Caco-2 cell monolayers was significantly lower at one hour after adding the treatments compared to 0% BHI, however after that time point onwards there was no difference between 0 and 25% BHI. Caco-2 cell monolayers treated with 50% BHI showed no difference to Caco-2 cells treated with 0% BHI across all time points. In contrast, when 75 or 100% BHI were added to the apical side of Caco-2 cell monolayers, the normalised TEER values were significantly lower compared to cells treated with 0% BHI across all time points ($P < 0.05$).

2.4.6.3. Viability of the *F. prausnitzii* strains in a mixture of cell and bacterial culture medium

Based on the results of the previous section, the viability of the *F. prausnitzii* strains was tested using the anaerobic M199 TEER: BHI ratio (1:1), which was referred to as 50% BHI. The results of the OD_{600nm} measurements (Figure 2.12A) showed that all of the three bacterial strains had increased in numbers after 2 h of incubation compared to time 0 and from then continued to grow ($P < 0.001$). In addition to the OD_{600nm} measurements, the CFUs of the three *F. prausnitzii* strains were determined before and after the incubation in 50% BHI over 12 h (Figure 2.12B). The number of CFUs of *F. prausnitzii* A2-165 increased by 1.7 logs after the 12 h of incubation ($P < 0.001$), while the other two strains

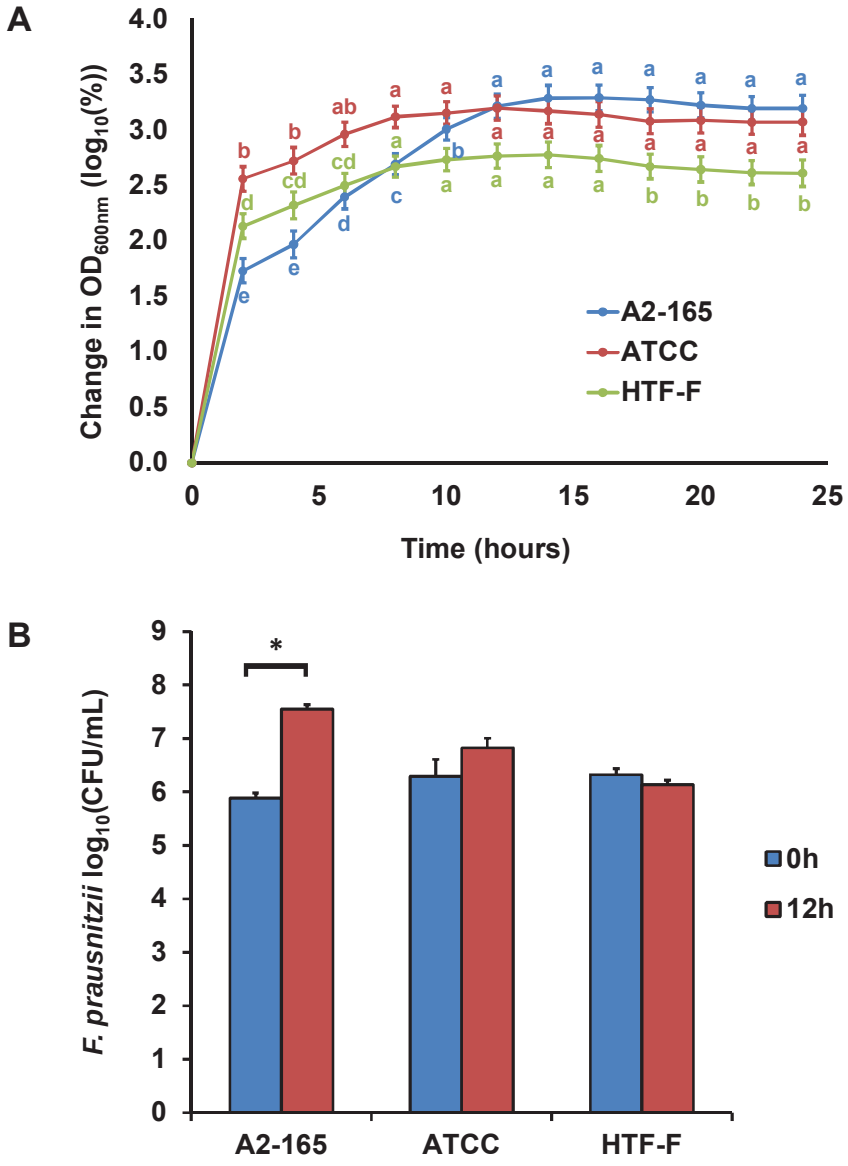

Figure 2.12 Viability of the three *F. prausnitzii* strains in cell culture medium supplemented with bacterial culture medium.

The three *F. prausnitzii* strains (A2-165, ATCC 27768 and HTF-F) in stationary phase were resuspended in anaerobic M199 TEER: BHI (1:1) (referred to as 50% BHI) and incubated anaerobically at 37°C. (A) Normalised and $\log_{10}$ transformed mean (± SEM, n = 3) OD_{600nm} over 24 h of the three *F. prausnitzii* strains grown in 50% BHI. The statistical analysis was performed after normalising by the OD_{600nm} at time 0 h due to the different starting OD_{600nm} values for the three *F. prausnitzii* strains. Treatments that do not share the same letters are significantly different ($P < 0.05$). (B) Mean (± SEM; n = 3) $\log_{10}$(CFU/mL) of the three *F. prausnitzii* strains before and after 12 h of incubation in 50% BHI. * Mean $\log_{10}$(CFU/mL) differ between 0 and 12 h at $P < 0.05$. A $\log_{10}$ transformation was required to fulfil the model assumptions.

showed no significant differences between the CFUs before and after 12 h of incubation in 50% BHI.

2.4.6.4. Viability of the *F. prausnitzii* strains in the apical anaerobic co-culture model using mixtures of cell and bacterial culture media

The three *F. prausnitzii* strains were co-cultured with differentiated Caco-2 cell monolayers in the apical anaerobic co-culture model using M199 TEER supplemented with 25 or 50% BHI medium on the apical side of the cell monolayers. These medium compositions were chosen as they did not compromise the TEER and viability of the Caco-2 cell monolayers. The viability of the bacterial strains was determined by comparing the CFU before and after 12 h of co-culture with Caco-2 cells. No bacteria were able to be cultured from the Caco-2 cell lysate, therefore indicating that none of the three strains adhered to the Caco-2 cells. When 25% BHI was used at the apical side of the Caco-2 cell monolayer none of the three *F. prausnitzii* strains had an increase in CFUs (Figure 2.13). The number of CFUs of both *F. prausnitzii* A2-165 and *F. prausnitzii* ATCC 27768 increased by 0.8 log after the 12 h of incubation ($P < 0.05$) when 50% BHI was used as the apical culture medium. However, there was no significant difference in CFUs of *F. prausnitzii* HTF-F at 0 and 12 h of co-culture with Caco-2 cells when 50% BHI was used as the apical culture medium.

2.5. DISCUSSION

The results reported in this thesis chapter demonstrate that *F. prausnitzii* A2-165 and *F. prausnitzii* ATCC 27768 were able to grow in the apical anaerobic co-culture model when the apical anaerobic cell culture medium was supplemented with 50% bacterial culture medium (BHI). This is in accordance with the hypothesis of the research described in this

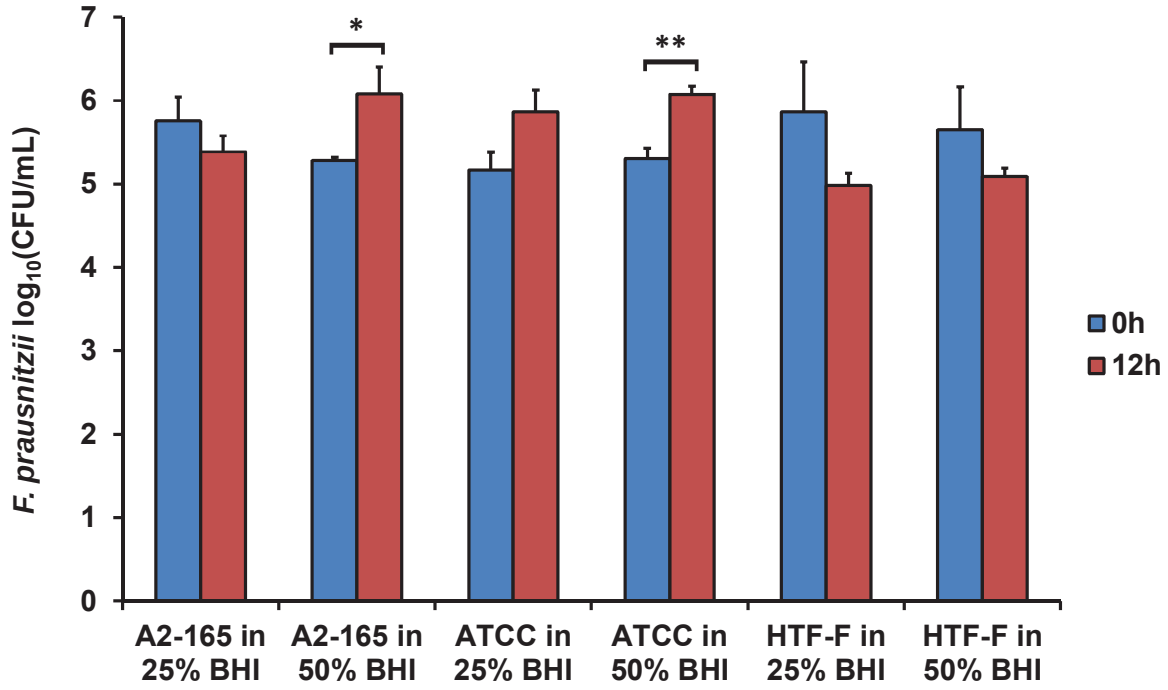

Figure 2.13 Viability of the three *F. prausnitzii* strains in the apical anaerobic co-culture model with Caco-2 cells.

The three *F. prausnitzii* strains (A2-165, ATCC 27768 and HTF-F) were co-cultured with Caco-2 cells using two different media on the apical side of the Caco-2 cell monolayer (25 and 50% BHI). The graph shows the mean (± SEM; n = 4 and 8 for time 0 and 12 h, respectively) $\log_{10}$(CFU/mL) of the bacteria at 0 and 12 h of incubation with Caco-2 cells in the co-culture model. Mean $\log_{10}$(CFU/mL) differ between 0 and 12 h at * $P < 0.05$ and ** $P < 0.01$. A $\log_{10}$ transformation was required to fulfil the model assumptions. The bacterial treatments were added to three inserts with Caco-2 cells, however, several cell monolayers were disrupted after the 12 h of incubation. For these reasons the number of observations differed between time 0 and 12 h.

thesis chapter. The first approach of supplementing the apical medium using acetate did not enable growth of the three *F. prausnitzii* strains. However, the second approach, supplementation of the apical medium with 50% of bacterial culture medium, resulted in an increase in CFU for *F. prausnitzii* A2-165 and *F. prausnitzii* ATCC 27768 after 12 h of incubation when co-cultured with Caco-2 cells in the apical anaerobic co-culture model. The supplementation of the apical cell culture medium with 50% bacterial culture medium did not compromise the viability and barrier integrity of the Caco-2 cell monolayers.

It is a well-established method for bacterial-mammalian cell co-culture experiments to harvest bacterial cells by centrifugation and then resuspend the bacteria in mammalian cell culture media [19,274,275]. Studies have shown that there was no difference in the viability for strains of *E. coli*, *S. typhimurium* and *Lactobacillus fructosus* in mammalian and bacterial culture medium [275]. However, in this study none of the three *F. prausnitzii* strains (A2-165, ATCC 27768 and HTF-F) showed growth in the anaerobic mammalian cell culture medium M199+NEAA over 24 h. Hence, it was necessary to supplement the apical mammalian cell culture medium with compounds known to stimulate the growth of *F. prausnitzii* in order to enable growth of the three *F. prausnitzii* strains in the apical anaerobic co-culture model.

Acetate, a SCFA produced by many bacteria of the GI microbiota, is known to be a substrate required for the growth of *F. prausnitzii* [178,187]. However, in this study, the supplementation of M199+NEAA with acetate did not result in an improved growth of *F. prausnitzii*. One of the three *F. prausnitzii* strains (ATCC 27768) even showed a lower OD_{600nm} value after 8 h of incubation. In this study, the mammalian cell culture medium M199+NEAA was supplemented with acetate. However, the studies showing growth stimulation of *F. prausnitzii* by acetate were conducted by supplementing bacterial culture

medium with acetate [178]. Acetate may therefore improve growth but may not be sufficient to induce growth.

The nutrient concentration of the M199 medium may be too low for *F. prausnitzii* and it may also lack important substrates required for its growth. For example, *F. prausnitzii* A2-165 did not grow without the addition of yeast extract to the bacterial culture medium YCFAG [178]. Furthermore, iron is essential for bacterial growth [276]. Bacterial culture media often contain haemin as iron source [19,178,277]. Most likely this is a more suitable iron source for *F. prausnitzii* compared to the ferric nitrate, the only iron source of the cell culture medium M199. Bacteria have developed haem acquisition systems to obtain iron from host haem-sequestering proteins [278]. In addition, bacterial culture media often contain vitamin K_1 [277,279] which bacteria convert into vitamin K_2 required for electron transport processes during anaerobic respiration [280]. M199 only contains vitamin K_3 (menadione), a synthetic type of vitamin K, which is a provitamin that requires conversion to menaquinone-4 in order to be active [281]. The bioavailability of vitamin K_3 may therefore be lower for *F. prausnitzii* compared to other vitamin K sources.

F. prausnitzii may require complex media to grow. A recent study used a combined approach of computational modelling, *in vitro* experiments, metabolomic analysis and genomic analysis to identify the metabolic capabilities of *F. prausnitzii* A2-165 and to develop a chemically defined medium for this bacterium [282]. Interestingly, this study reports that this medium did not enable growth of *F. prausnitzii* A2-165 [282]. When using an improved version of the medium, enriched with additional vitamins, amino acids, and bases, *F. prausnitzii* A2-165 growth was still poorer than on YCFAG [282]. Together with the results obtained here, it was hypothesised that *F. prausnitzii* has a requirement for complex media containing for example yeast extract. Consequently, for the second

approach to enable growth of the *F. prausnitzii* strains in the co-culture model it was decided to supplement cell culture medium with a complex bacterial culture medium (BHI).

In apical anaerobic conditions (co-culture chamber inside the anaerobic workstation) TEER of the Caco-2 cells treated with 50% BHI reached a plateau of approximately 300 $\Omega.cm^2$ following the initial drop in TEER. The TEER of human colon tissues has been reported to be in the range of approximately 100 to 300 $\Omega.cm^2$ [283,284]. Therefore, the Caco-2 cell monolayers treated with this mixture of bacterial and cell culture medium had TEER values that resembled more those reported *in vivo* than TEER of Caco-2 cells treated with pure cell culture medium. These Caco-2 cell monolayers had TEER values which plateaued at approximately 600 $\Omega.cm^2$.

The drop in TEER after the first measurement in anaerobic conditions is caused by replacing the apical medium with the treatments, which is normal for all TEER assays. However, when performing TEER assays using the apical anaerobic co-culture model, the Caco-2 cell monolayers are further influenced when the inserts are transferred into the co-culture chamber. Furthermore, the cells are exposed to an apical anaerobic environment. These factors may contribute to the higher initial drop in TEER in apical anaerobic compared to aerobic conditions. Future experiments should therefore be performed using two baseline TEER measurements instead of one, to allow the adaptation of the Caco-2 cell monolayers to the apical anaerobic environment before adding the treatments.

The lower TEER values of Caco-2 cells exposed to 75 and 100% BHI in anaerobic conditions, but not in aerobic conditions, may be due to structural changes of molecules of the components of BHI. Previous studies determined an altered functionality of the antimicrobial peptide human β-defensin 1 (hBD-1) in a reducing environment compared to

aerobic conditions [285]. The reduction of disulphide bonds of hBD-1 increased the antibiotic killing activity which was suggested to depend on the free cysteins in the reduced hBD-1. Also, milk ingredients had different effects on TEER when added to Caco-2 cells in conventional or apical anaerobic conditions [286]. BHI is produced by boiling cow or porcine hearts and brains which releases soluble factors into the broth resulting in a very complex and undefined culture medium. It is therefore possible that some of its components undergo structural changes in the absence of oxygen which in turn may cause the disruption of the TJs connecting the Caco-2 cells only in an anaerobic environment. For example, proteins which are denatured due to the boiling of the brains and hearts and autoclaving of the BHI media, may contain reduced disulphide bonds due to the absence of oxygen and may therefore have altered functionality in apical anaerobic conditions compared to conventional conditions. Remarkably, both in conventional and apical anaerobic conditions the viability of the Caco-2 cells was not affected by the BHI concentrations.

The presence of the Caco-2 cells may have stimulated the growth of the *F. prausnitzii* strains since two of the strains (A2-165 and ATCC 27768) were growing when co-cultured with Caco-2 cells using 50% BHI but only one strain (A2-165) increased in CFU when grown alone in the same medium. Caco-2 secreted mucins may be part of the mechanism causing the enhanced growth of *F. prausnitzii* A2-165 and ATCC 27768 in co-culture with Caco-2 cells. Though Caco-2 cells do not express mucin-2, the predominant mucin in the GI tract, they have been shown to express MUC3 and MUC5A/C [287,288]. Similar to the currently described work, Caco-2 cells were shown to promote growth and metabolism of *F. prausnitzii* A2-165 in studies using a simple dual-environment co-culture model [252].

The authors hypothesised that Caco-2 secreted mucin may contribute to this effect because exogenously added porcine mucin also stimulated *F. prausnitzii* growth.

Furthermore, *F. prausnitzii* may benefit from the oxygen gradient close to the Caco-2 cell monolayer. *F. prausnitzii* uses an extracellular electron shuttle of flavins and thiols to transfer electrons to oxygen [188]. Small amounts of oxygen may diffuse from the aerobic basal compartment of the apical anaerobic co-culture model through the Caco-2 cell monolayer to the apical side. The *F. prausnitzii* strains may be able to use riboflavin, one component of M199, for its extracellular electron transfer which may benefit growth at this oxic-anoxic interphase [187].

In future experiments a longer incubation time could be tested for the co-culture of *F. prausnitzii* HTF-F with Caco-2 cells. Whereas *F. prausnitzii* A2-165 and ATCC 27768 were growing in co-culture with Caco-2 cells when 50% BHI was used as apical medium, *F. prausnitzii* HTF-F did not increase in CFU. In general, this strain was slower growing compared to the other strains. The 12 h incubation with the Caco-2 cells in the apical anaerobic co-culture model may have been too short to enable growth of *F. prausnitzii* HTF-F. Before performing experiments with more than 12 h of incubation, further validation studies would be necessary to ensure survival and barrier integrity of the Caco-2 cells as the validation studies for the co-culture model were performed for 12 h. When M199 TEER was supplemented with 25% BHI none of the three *F. prausnitzii* strains grew within the 12 h of incubation. This medium composition may not have a sufficient concentration of nutrients required for the growth of these strains.

Based on the results of this thesis chapter, cell culture medium (M199 TEER) supplemented with 50% BHI was chosen for the co-culture experiments presented in the next chapter to test the effects of the three *F. prausnitzii* strains on intestinal barrier

integrity. This media composition was chosen because it did not compromise Caco-2 cell viability and barrier integrity, and enabled growth of two of the *F. prausnitzii* strains (A2-165 and ATCC 27768).

CHAPTER THREE:

Effect of *F. prausnitzii* on intestinal barrier function[†]

[†] Selected material from this section combined with sections from Chapter 2 will be submitted for publication to the journal *Nutrients*.

3.1. INTRODUCTION

In addition to the absorption of nutrients, the intestinal epithelium acts as a barrier between the lumen and underlying tissues [4]. Appropriate intestinal barrier function is crucial to prevent the entry of bacteria and food antigens from the lumen into underlying tissues [77]. Various inflammatory GI diseases, for example IBD or celiac disease, have been linked to an impaired epithelial barrier [77]. In addition, these diseases have been associated with a dysbiosis of the resident microbiota [289]. For example, *F. prausnitzii*, an abundant obligate anaerobe within the human microbiota [178,180], is reduced in people with GI diseases [10-16,194]. It has therefore been hypothesised that *F. prausnitzii* plays an important role in maintaining homeostasis in the GI tract [11,14]. Nevertheless, the mechanisms behind the beneficial effects of *F. prausnitzii* are only partially understood. This is, at least in part, due to the difficulty of performing *in vitro* studies to investigate the effects of obligate anaerobes on human oxygen requiring cells using conventional co-culture models.

Previous studies at AgResearch used the novel apical anaerobic co-culture model which overcomes the above mentioned limitation, to determine the effect of *F. prausnitzii* A2-165 (DSM 17677) on intestinal barrier function [19]. Under the test conditions neither live nor UV-killed *F. prausnitzii* A2-165 altered the barrier integrity of the Caco-2 monolayers. In addition, live but not UV-killed *F. prausnitzii* A2-165 increased small molecule permeability of Caco-2 cells and could in this respect be considered detrimental [19]. In contrast, *F. prausnitzii* improved barrier integrity in mice with DSS-induced colitis; culture supernatant alleviated the increase in paracellular permeability caused by DSS [214]. This discrepancy may be due to the limitations of the co-culture model used by Ulluwishewa *et al*. [19]. Even though the viability of *F. prausnitzii* A2-165 was improved compared to

when grown in conventional conditions (5% CO_2 in air atmosphere), the bacterial cell numbers were still reduced after 8 h of co-culture with Caco-2 cells in the new model. Growing and metabolically active bacteria may exert differential and more profound effects on the barrier integrity of Caco-2 cells compared to dead bacteria as differing responses of mammalian host cells to the same bacterium in different growth phases were shown [290].

3.2. HYPOTHESIS AND AIMS

The main hypothesis of this research chapter was that strains of live and growing *F. prausnitzii* (A2-165, ATCC 27768 and HTF-F) co-cultured with IEC monolayers increase the barrier integrity of these cells. A secondary hypothesis was that live *F. prausnitzii* mitigates the TNF-α-induced decrease in barrier integrity of the IEC monolayers.

The first aim was to determine whether the effects of the three *F. prausnitzii* strains on TEER, a measure of barrier integrity, across healthy Caco-2 monolayers, a model of IECs, were altered when using an apical medium that enabled growth (50% BHI) or not (25% BHI). The second aim was to assess whether live *F. prausnitzii* were able to lessen the TNF-α-induced decrease in TEER across Caco-2 monolayers in the apical anaerobic co-culture model.

3.3. METHODS

3.3.1. Culture of *F. prausnitzii*

Primary broth cultures of the three *F. prausnitzii* strains (Table 2.1) were prepared by inoculating 10 mL of anaerobic BHI broth (section 2.3.2.2) in Hungate culture tubes with 50 µL (*F. prausnitzii* A2-165 and ATCC 27768) or 100 µL (*F. prausnitzii* HTF-F) of

frozen cultures inside the anaerobic workstation (Concept Plus, Ruskinn Technology Ltd, Bridgend, UK). The primary cultures were incubated for 24 h (*F. prausnitzii* A2-165 and ATCC 27768) or 48 h (*F. prausnitzii* HTF-F). After this incubation, secondary cultures were prepared by subculturing 200 µL of primary cultures into 10 mL of anaerobic BHI broth. The secondary cultures were incubated for 20 h (*F. prausnitzii* A2-165 and ATCC 27768) and 26 h (*F. prausnitzii* HTF-F) in order to obtain bacteria in the stationary phase of growth. For the co-culture with Caco-2 cells secondary cultures in stationary phase were used.

3.3.2. Caco-2 cell culture

Caco-2 cells were maintained and subcultured as described in sections 2.3.8.1 and 2.3.8.2. For the co-culture experiments the Caco-2 cells were seeded on semipermeable membranes of Transwell inserts as described in 2.3.8.6 and cultured for 16 to 18 days prior to each experiment in order to attain a differentiated monolayer. The day before the co-culture experiments the TEER across Caco-2 monolayers was determined using an EndOhm TEER cup (World Precision Instruments, USA) connected to an EVOM voltohmmeter (World Precision Instruments) as described in 2.3.8.7 to assess if the Caco-2 cells formed a differentiated monolayer. Only Caco-2 monolayers with a TEER over 400 $\Omega.cm^2$ were chosen for the co-culture experiments in order to use only fully differentiated monolayers. The average TEER across Caco-2 monolayers used for the co-culture experiments was approximately 1200 $\Omega.cm^2$. One day before the experiments the apical and basal M199 Std (Table 2.6) was replaced with M199 TEER in order to remove the antibiotics before co-culturing the cells with bacteria.

3.3.3. Trans-epithelial electrical resistance assay using different apical media

Differentiated Caco-2 monolayers were co-cultured with *F. prausnitzii* (strains A2-165, ATCC 27768 and HTF-F) in the apical anaerobic co-culture model using 25 and 50% BHI as apical medium and the effect of the bacteria on TEER was assessed. These apical media were chosen as one of them enabled growth of *F. prausnitzii* A2-165 and ATCC 27768 in co-culture with Caco-2 cells (50% BHI) whereas the other medium did not enable growth of any of the three strains (25% BHI) as shown in Chapter 2. It could therefore be determined if TEER across Caco-2 monolayers differed when co-cultured with growing or non-growing bacteria.

The co-culture chamber was assembled inside a biosafety cabinet. All solutions used for the preparation of the anaerobic treatments were placed inside the anaerobic workstation with opened lids overnight in order to remove the oxygen. For the TEER assay the co-culture chamber was prepared as described in section 2.3.9.1. After inserting the Transwell inserts containing the differentiated Caco-2 monolayers into the co-culture chamber, the chamber was transferred into the anaerobic workstation and connected to a laptop using the Nanoanalytics controller as described in 2.3.9.1. The TEER across the Caco-2 monolayers in all wells of the co-culture chamber was measured once to attain a baseline TEER reading before stopping the software and adding the treatments.

Secondary cultures of the three *F. prausnitzii* strains in stationary phase prepared as described in 3.3.1 were harvested and diluted with 25 and 50% BHI as described in 2.3.13. After completing one round of baseline TEER measurements the apical medium was replaced with 260 µL of the anaerobic treatment solutions. The eight anaerobic treatment solutions were the two control media (25 and 50% BHI) and the three *F. prausnitzii* strains diluted with the two different media. The TEER measurements were resumed and TEER

was recorded hourly over 12 h. The treatments were added in triplicate and the experiment was repeated 5 times (total n = 15).

3.3.4. Trans-epithelial electrical resistance assay with TNF-α-treated Caco-2 cells

The effect of the *F. prausnitzii* strains on TEER across healthy or TNF-α-treated Caco-2 monolayers in the apical anaerobic co-culture model was determined. This pro-inflammatory cytokine is known to decrease TEER [119]. The aim was to determine if the co-culture of Caco-2 cells with *F. prausnitzii* mitigates the TEER decreasing effect of TNF-α. This experiment was performed in two sets, using 50% BHI as apical medium for the first set and M199 TEER for the second set.

The effect of both live and UV-killed *F. prausnitzii* on TEER across healthy and TNF-α-treated Caco-2 monolayers was determined. The bacterial treatment solutions of the three *F. prausnitzii* strains were prepared for the co-culture experiments as described in 2.3.13. A 2 mL aliquot was removed from each bacterial solution, added to wells of a 6-well plate and placed with open lid on ice under a UV lamp (UVP 3UV-38, Bio-Strategy LTD, Auckland, New Zealand). The bacteria were exposed for 15 min to UVC light. The UV-treated bacteria were plated on anaerobic BHI agar plates to confirm that the bacteria were dead.

The TEER assays were prepared as described in the previous section (3.3.3), however using two co-culture chambers. Furthermore, before stopping the software and adding the treatments, the TEER across the Caco-2 monolayers in all wells of the co-culture chamber was measured twice instead of once as described above, in order to allow the cells to adapt to the apical anaerobic conditions. After finishing the baseline TEER measurements, the measurements were stopped. A Hamilton syringe was disinfected by flushing several times

with 70% ethanol and then rinsing thoroughly with sterile distilled water. This syringe was used to inject 60 µL of TNF-α (5 µg/mL; Sigma-Aldrich, Auckland, New Zealand) through the septa into the basal compartment of each well of one of the co-culture chambers. This resulted in a TNF-α concentration of 100 ng/mL in the basal compartments. For the second co-culture chamber 60 µL of aerobic M199 TEER were injected into the basal compartments as a control.

The apical medium was removed from the Caco-2 monolayers and replaced with 260 µL of the anaerobic treatment solutions. The seven anaerobic treatment solutions were the control medium (50% BHI for the first set of TEER experiments and M199 TEER for the second set), and live and UV-killed *F. prausnitzii* (strains A2-165, ATCC 27768 and HTF-F, diluted with the respective medium). The apical treatments were the same for both of the co-culture chambers in order to test the effects of the treatments on healthy and TNF-α-treated Caco-2 cells. After the treatments were added, the TEER measurements were resumed and TEER was recorded over 12 h. For each set of TEER assays using the two different apical media the treatments were added in triplicate and the assays were repeated three times (total n = 9).

3.3.4.1. Viability of *F. prausnitzii* in co-culture with TNF-α-treated Caco-2 cells

In order to assess whether the viability of *F. prausnitzii* in co-culture with Caco-2 cells was influenced by the basal TNF-α treatment in the above described TEER assays (3.3.4), the CFUs of the three strains were determined before and after 12 h of co-culture. Since TNF-α decreases TEER [119] it may lead to oxygen leakage from the basal to the apical compartment of the co-culture chamber which may reduce the viability of the *F. prausnitzii* strains. The *F. prausnitzii* CFUs before and after 12 h of co-culture with TNF-α-treated Caco-2 cells were determined as described in section 2.3.5.2. The bacterial

viability was assessed for both TEER assays using the two different apical media (50% BHI and M199 TEER).

3.3.5. Statistical analysis

All of the statistical analyses were performed using SAS (SAS/STAT version 9.3; SAS Institute Inc., Cary, NC, USA). The TEER experiments were analysed using repeat measure analyses to test the effect of the treatment and time and their interaction on TEER. The most appropriate covariance structure of the mixed model was selected after fitting the models by Restricted Maximum Likelihood method and comparison of the models with the log-likelihood ratio test. If the interaction between the treatment and time was not significant it was removed from the model. When using M199 TEER as apical medium, the viability of the *F. prausnitzii* strains before and after the co-culture with Caco-2 cells in the presence or absence of TNF-α was also compared using an ANOVA. If the F-value of the analyses were significant ($P < 0.05$), adjusted Tukey tests were used for the mean comparison. When using 50% BHI as apical medium, a t-test was performed to compare the viability of the three *F. prausnitzii* strains before and after the co-culture with Caco-2 cells. The model assumptions (e.g. normal distribution and the homogeneity of variance) were evaluated using the ODS graphics in SAS for all of the analyses. In case of the response variable not fulfilling these assumptions, transformations were performed to reach these assumptions. Due to the reasons stated in section 2.3.16 each Caco-2 monolayer seeded into one Transwell insert was used as an independent replicate for the statistical analysis. A complete randomised block design was firstly performed with the run (or experimental day) as a random effect. There was no effect of the run for any of the tested variables, consequently the random effect was removed from the model.

3.4. RESULTS

3.4.1. Trans-epithelial electrical resistance assay with different apical media

Differentiated Caco-2 monolayers were co-cultured with the three *F. prausnitzii* strains (A2-165, ATCC 27768 and HTF-F) in the apical anaerobic co-culture model using 25 or 50% BHI as apical medium. The TEER across the Caco-2 monolayers was recorded over 12 h and the results of the TEER measurements are shown in Figure 3.1. The interaction between the treatment and time was significant for both data sets ($P < 0.001$). However, there were no differences between the TEER of Caco-2 cells treated with the control medium (25 and 50% BHI) or the three *F. prausnitzii* strains in the respective medium for each time point ($P > 0.05$).

3.4.2. Trans-epithelial electrical resistance assay with TNF-α-treated Caco-2 cells using 50% BHI as apical medium

Caco-2 cells in the apical anaerobic co-culture model with or without basal exposure to the pro-inflammatory cytokine TNF-α were co-cultured with live or UV-killed *F. prausnitzii* (strains A2-165, ATCC 27768 and HTF-F). The TEER across the Caco-2 monolayers was recorded over 12 h. The culture media used were M199 TEER in the basal compartment and 50% BHI in the apical compartment. The TEER across TNF-α-treated Caco-2 monolayers was not different from that of healthy cells ($P > 0.05$) as shown in Figure 3.2.

The observed TEER values of healthy Caco-2 cells treated with live or UV-killed *F. prausnitzii* or control medium (50% BHI) are shown in Figure 3.3. For healthy Caco-2 monolayers the interaction between the treatment and time was not significant and was removed from the statistical analysis. There was a significant treatment effect ($P = 0.002$). No differences were observed between the TEER across Caco-2 monolayers exposed to the

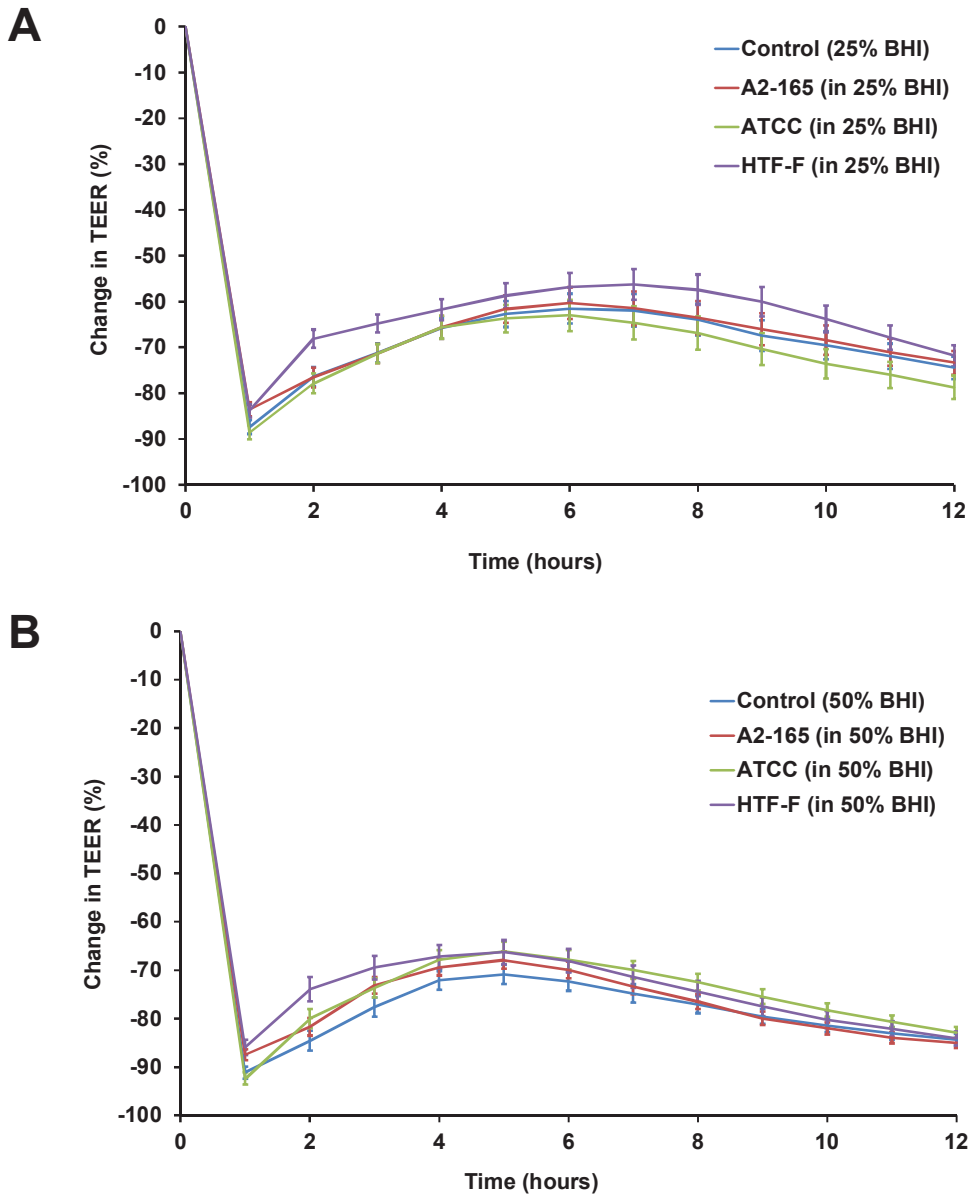

Figure 3.1 Change in TEER across healthy Caco-2 monolayers co-cultured with live *F. prausnitzii* using 25 and 50% BHI as apical medium.

Differentiated Caco-2 monolayers were co-cultured with the three *F. prausnitzii* strains (A2-165, ATCC 27768 and HTF-F) in the apical anaerobic co-culture model using 25 and 50% BHI as apical medium. The TEER across the Caco-2 monolayers was recorded over 12 h. The interaction between the treatment and time was significant for both datasets ($P < 0.001$). The graphs show the fitted mean (± SEM; n = 12) change in TEER across Caco-2 monolayers after normalising by the TEER at 0 h when using (A) 25% BHI and (B) 50% BHI as apical medium. No differences were determined between the two control media and the three *F. prausnitzii* strains in the respective medium at any time point ($P > 0.05$).

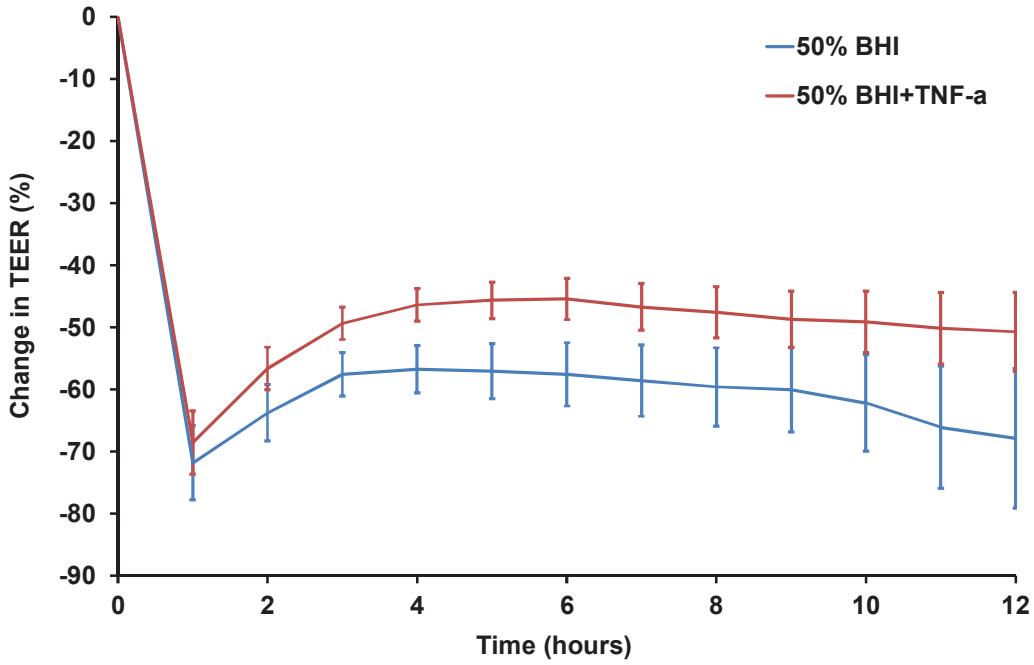

Figure 3.2 Change in TEER across Caco-2 monolayers with or without TNF-α treatment using 50% BHI as apical medium.

The TEER across Caco-2 monolayers in the apical anaerobic co-culture model with or without basal exposure to TNF-α using 50% BHI as apical medium was recorded over 12 h. The interaction between the treatment and time was significant ($P = 0.03$). The graph shows the fitted mean (± SEM; $n = 9$) change in TEER across Caco-2 monolayers with or without TNF-α treatment after normalising by the TEER at 0 h. No differences were determined between the TEER across Caco-2 monolayers treated with TNF-α and untreated healthy cells at any time point ($P > 0.05$).

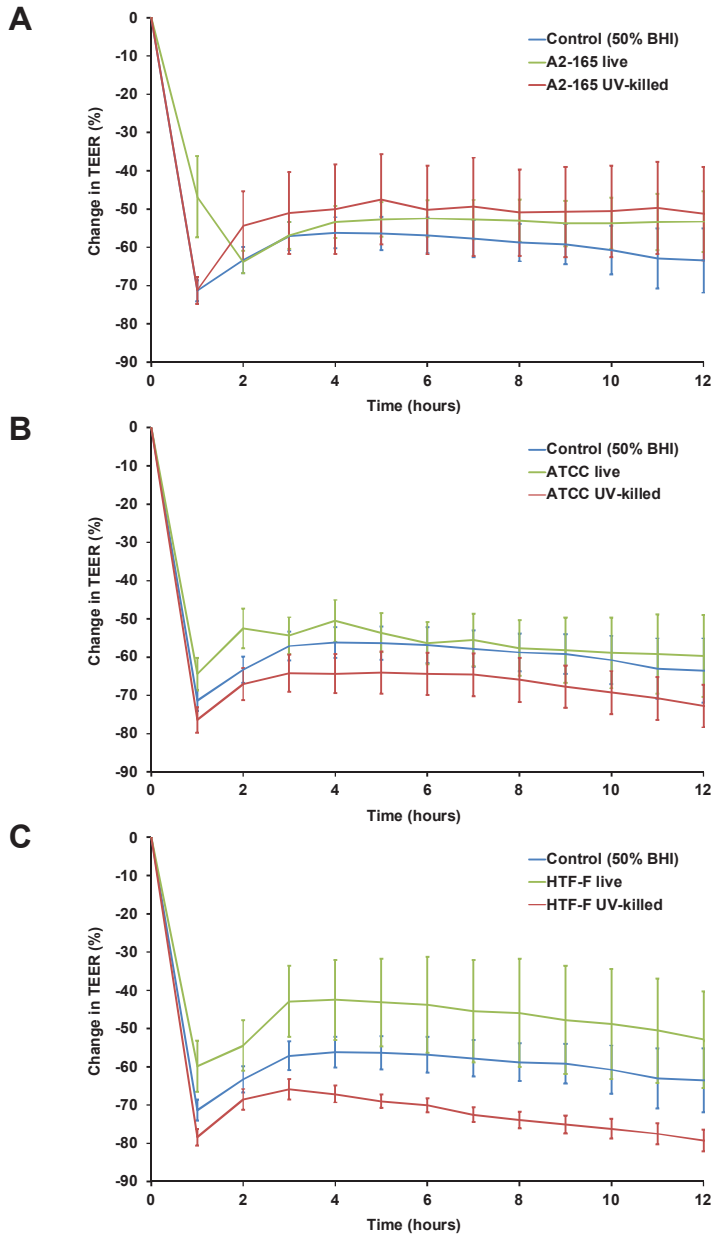

Figure 3.3 Change in TEER across healthy Caco-2 monolayers co-cultured with live or UV-killed *F. prausnitzii* using 50% BHI as apical medium.

Caco-2 monolayers were exposed to live or UV-killed *F. prausnitzii* (strains A2-165, ATCC 27768 and HTF-F) in the apical anaerobic co-culture model using 50% BHI as apical medium. The TEER across the Caco-2 monolayers was recorded hourly over 12 h. The interaction between the treatment and time was not significant and was removed from the statistical analysis. The graphs show the observed mean (± SEM; n = 9) change in TEER across Caco-2 monolayers co-cultured with live or UV-killed *F. prausnitzii* (A) A2-165, (B) ATCC 27768 and (C) HTF-F after normalising by the TEER at 0 h.

bacterial treatments and the untreated controls ($P > 0.05$) as shown in Figure 3.4. However, the TEER across Caco-2 monolayers co-cultured with live or UV-killed *F. prausnitzii* HTF-F was significant different ($P < 0.05$) with higher TEER values recorded for cells treated with live bacteria. There was also a significant effect of the time on the change in TEER ($P < 0.001$; data not shown). The TEER values increased until 3 h, then they reached a plateau until 7 h and from 8 h onwards the values gradually decreased.

For the change in TEER of TNF-α-treated Caco-2 cells exposed to live or UV-killed *F. prausnitzii* and control medium (50% BHI) the interaction between the treatment and time was significant ($P < 0.001$; Figure 3.5). After 11 and 12 h of incubation the TEER across Caco-2 monolayers treated with UV-killed *F. prausnitzii* HTF-F was lower compared to the untreated control ($P < 0.05$).

3.4.3. Trans-epithelial electrical resistance assay with TNF-α-treated Caco-2 cells using M199 TEER as apical medium

Unexpectedly, the presence of TNF-α did not decrease TEER across Caco-2 monolayers when using 50% BHI as apical medium as described in the section above (3.4.2). Using 50% BHI as apical medium caused a greater initial drop in TEER when adding the treatments compared to when using cell culture medium alone. It was therefore hypothesised that due to this effect TEER was not further decreased through TNF-α treatment. Therefore, the experiment was repeated using cell culture medium (M199 TEER) in the basal and apical compartment of the co-culture chamber.

There was also no difference between TEER across healthy or TNF-α-treated Caco-2 monolayers when using M199 TEER as apical medium as shown in Figure 3.6 ($P > 0.05$). For the change in TEER across healthy Caco-2 monolayers the interaction between the treatment and time was significant ($P = 0.02$). No difference was determined between the

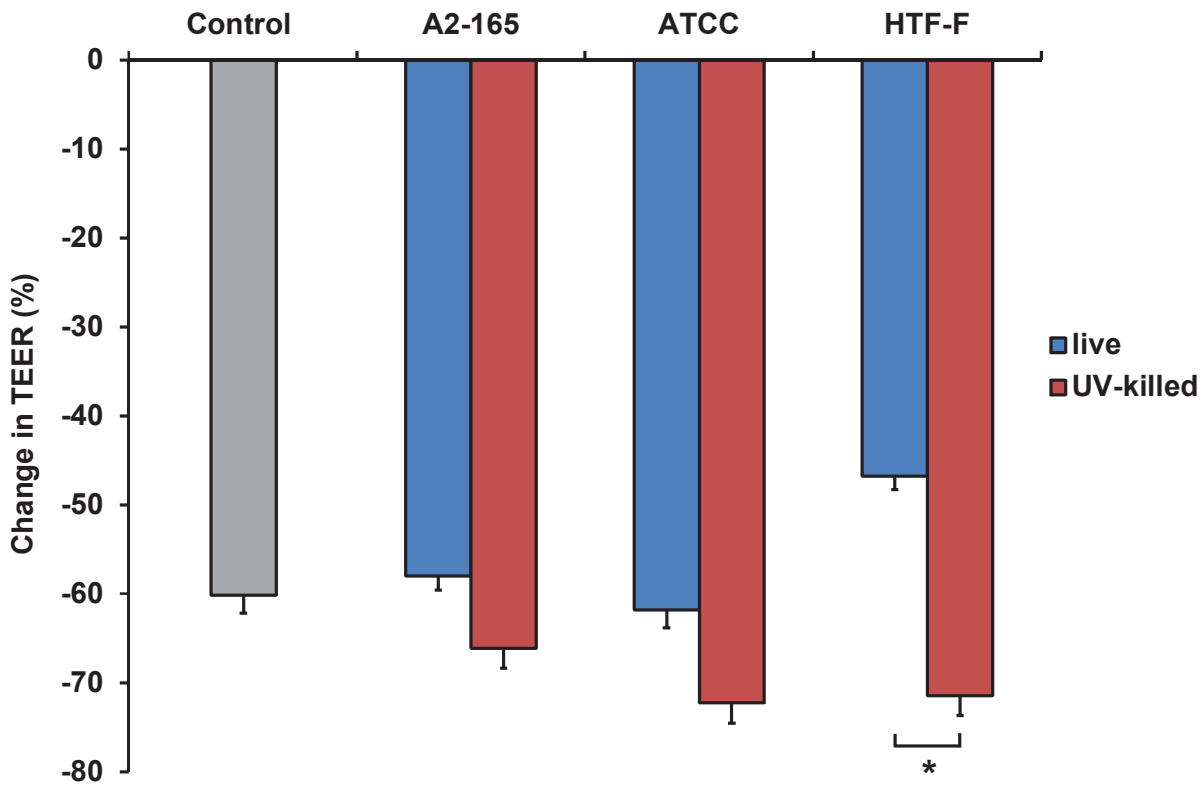

Figure 3.4 Change in TEER across healthy Caco-2 monolayers co-cultured with live or UV-killed *F. prausnitzii* using 50% BHI as apical medium.

Caco-2 monolayers were co-cultured with live or UV-killed *F. prausnitzii* (strains A2-165, ATCC 27768 and HTF-F). The TEER across the Caco-2 monolayers was recorded hourly over 12 h. The interaction between the treatment and time was not significant and removed from the statistical model. There was a significant treatment effect on the change in TEER ($P = 0.002$). The graph shows the fitted mean (± SEM; $n = 9$) change in TEER across healthy Caco-2 monolayers co-cultured with live or UV-killed *F. prausnitzii* after normalising by the TEER at 0 h. * TEER significantly different ($P < 0.05$).

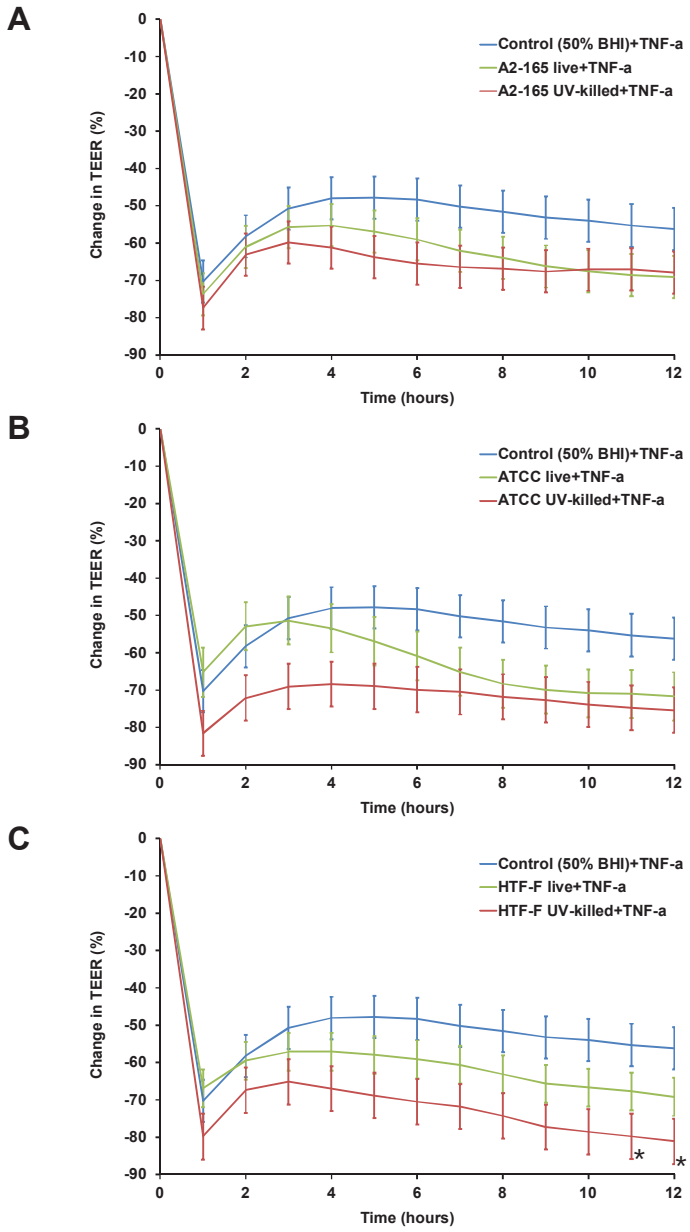

Figure 3.5 Change in TEER across TNF-α-treated Caco-2 monolayers co-cultured with live or UV-killed *F. prausnitzii* using 50% BHI as apical medium.

Caco-2 monolayers were exposed on the basal side to TNF-α and co-cultured with live or UV-killed *F. prausnitzii* (strains A2-165, ATCC 27768 and HTF-F) in the apical anaerobic co-culture model using 50% BHI as apical medium. The TEER across the Caco-2 monolayers was recorded over 12 h. The interaction between the treatment and time was significant ($P < 0.001$). The graphs show the fitted mean (± SEM; n = 9) change in TEER across Caco-2 monolayers co-cultured with live or UV-killed *F. prausnitzii* (A) A2-165, (B) ATCC 27768 and (C) HTF-F after normalising by the TEER at 0 h. * TEER significantly different to the untreated control ($P < 0.05$).

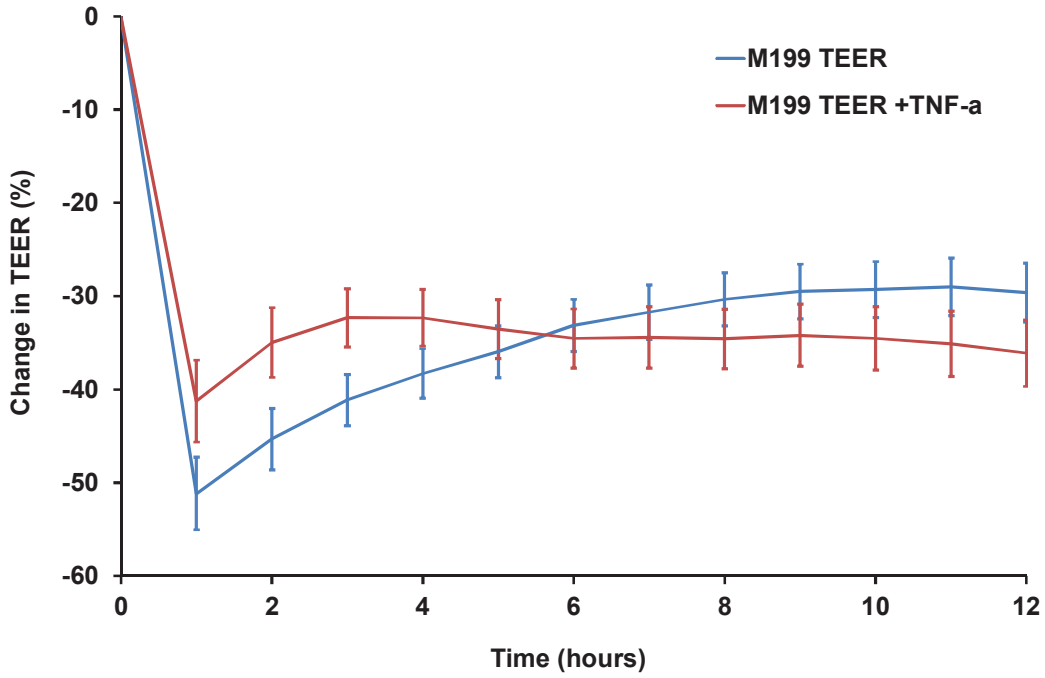

Figure 3.6 Change in TEER across Caco-2 monolayers with or without TNF-α treatment using M199 TEER as apical medium.

The TEER across Caco-2 monolayers in the apical anaerobic co-culture model with or without basal treatment with TNF-α was recorded over 12 h. M199 TEER was used in the apical and basal compartment. The interaction between the treatment and time was significant ($P < 0.001$). The graph shows the fitted mean (± SEM; $n = 9$) change in TEER across Caco-2 monolayers with or without TNF-α treatment after normalising by the TEER at 0 h. No differences were determined between the TEER across Caco-2 monolayers in the presence or absence of TNF-α at any time point ($P > 0.05$).

TEER across healthy Caco-2 monolayers exposed to the bacterial treatments and the untreated control at any time point as shown in Figure 3.7 ($P > 0.05$).

For the change in TEER across TNF-α-treated Caco-2 monolayers the interaction between the treatment and time was not significant and removed from the statistical analysis. The observed TEER values of TNF-α-treated Caco-2 monolayers co-cultured with live or UV-killed *F. prausnitzii* are shown in Figure 3.8. There was a significant treatment effect ($P < 0.001$). TEER across Caco-2 monolayers treated with UV-killed *F. prausnitzii* HTF-F were significant lower compared to the untreated control ($P < 0.05$; Figure 3.9). In addition, there was a difference between the TEER across Caco-2 monolayers treated with live or UV-killed *F. prausnitzii* ATCC 27768, with higher TEER values for cells treated with live bacteria ($P < 0.05$). There was also a significant effect of the time on the change in TEER ($P < 0.001$; data not shown), with increasing TEER values until 3 h, reaching the highest values between 3 h and 5 h and a gradual decrease after 6 h.

3.4.4. Viability of *F. prausnitzii* in co-culture with TNF-α-treated Caco-2 cells

The viability of the three *F. prausnitzii* strains (A2-165, ATCC 27768 and HTF-F) in co-culture with TNF-α-treated Caco-2 cells in the apical anaerobic co-culture model was assessed by determining the CFUs before and after 12 h of incubation. The co-culture experiments with TNF-α-treated Caco-2 cells were performed in two sets of experiments, one using 50% BHI on the apical side and one using M199 TEER. For both sets of experiments the viability of the *F. prausnitzii* strains was determined.

When 50% BHI was used as apical medium, no differences in CFUs before and after 12 h of co-culture with TNF-α-treated Caco-2 cells were determined for all of the three *F. prausnitzii* strains ($P > 0.05$) as shown in Figure 3.10. When using M199 TEER as apical

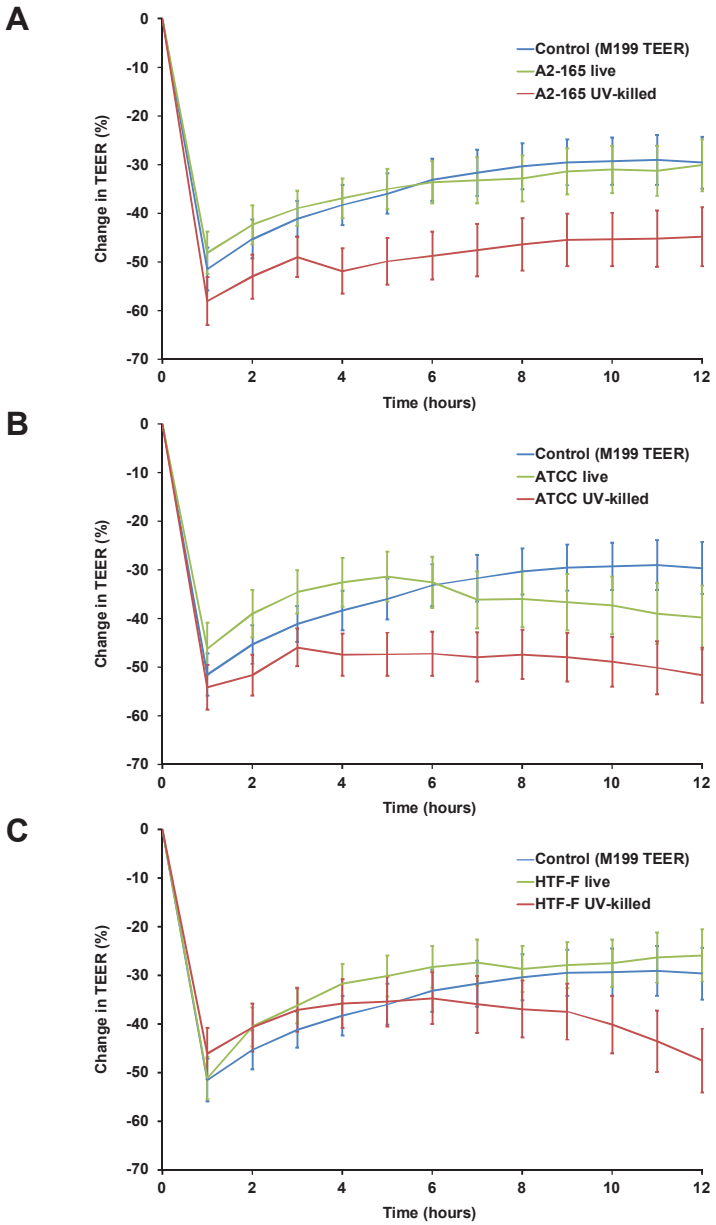

Figure 3.7 Change in TEER across healthy Caco-2 monolayers co-cultured with live or UV-killed *F. prausnitzii* using M199 TEER as apical medium.

Differentiated Caco-2 monolayers were exposed to live or UV-killed *F. prausnitzii* (strains A2-165, ATCC 27768 and HTF-F) in the apical anaerobic co-culture model using M199 TEER as apical medium and the TEER was measured over 12 h. The interaction between the treatment and time was significant ($P = 0.02$). The graphs show the fitted mean (± SEM; $n = 9$) change in TEER across Caco-2 monolayers after normalising by the TEER at 0 h when treating the cells with live or UV-killed *F. prausnitzii* (A) A2-165, (B) ATCC 27768 and (C) HTF-F. No differences were determined between the TEER of Caco-2 cells exposed to the control medium or the bacterial treatments at any time point ($P > 0.05$).

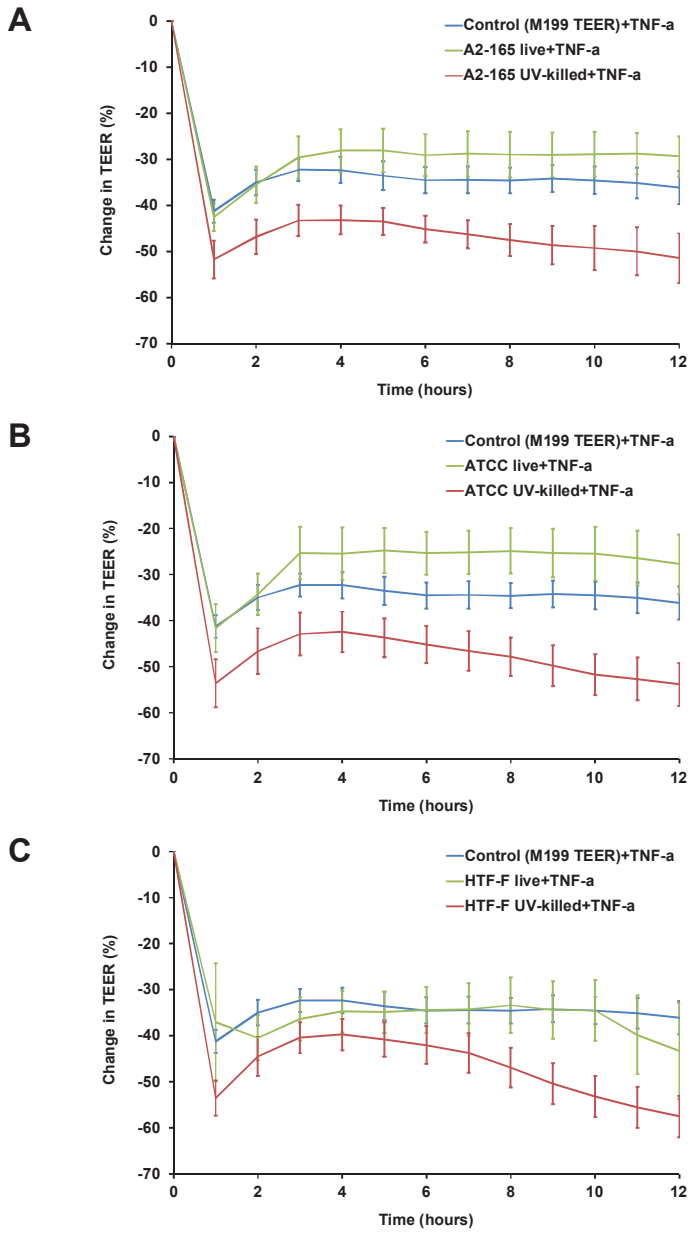

Figure 3.8 Change in TEER across TNF-α-treated Caco-2 monolayers co-cultured with live or UV-killed *F. prausnitzii* using M199 TEER as apical medium.

TNF-α-treated Caco-2 monolayers were co-cultured with live or UV-killed *F. prausnitzii* (strains A2-165, ATCC 27768 and HTF-F) in the apical anaerobic co-culture model using M199 TEER as apical medium. The TEER across the Caco-2 monolayers was recorded over 12 h. The interaction between the treatment and time was not significant and removed from the statistical analysis. The graphs show the observed mean (± SEM; n = 9) change in TEER across TNF-α-treated Caco-2 monolayers exposed to live or UV-killed *F. prausnitzii* (A) A2-165, (B) ATCC 27768 and (C) HTF-F after normalising by the TEER at 0 h.

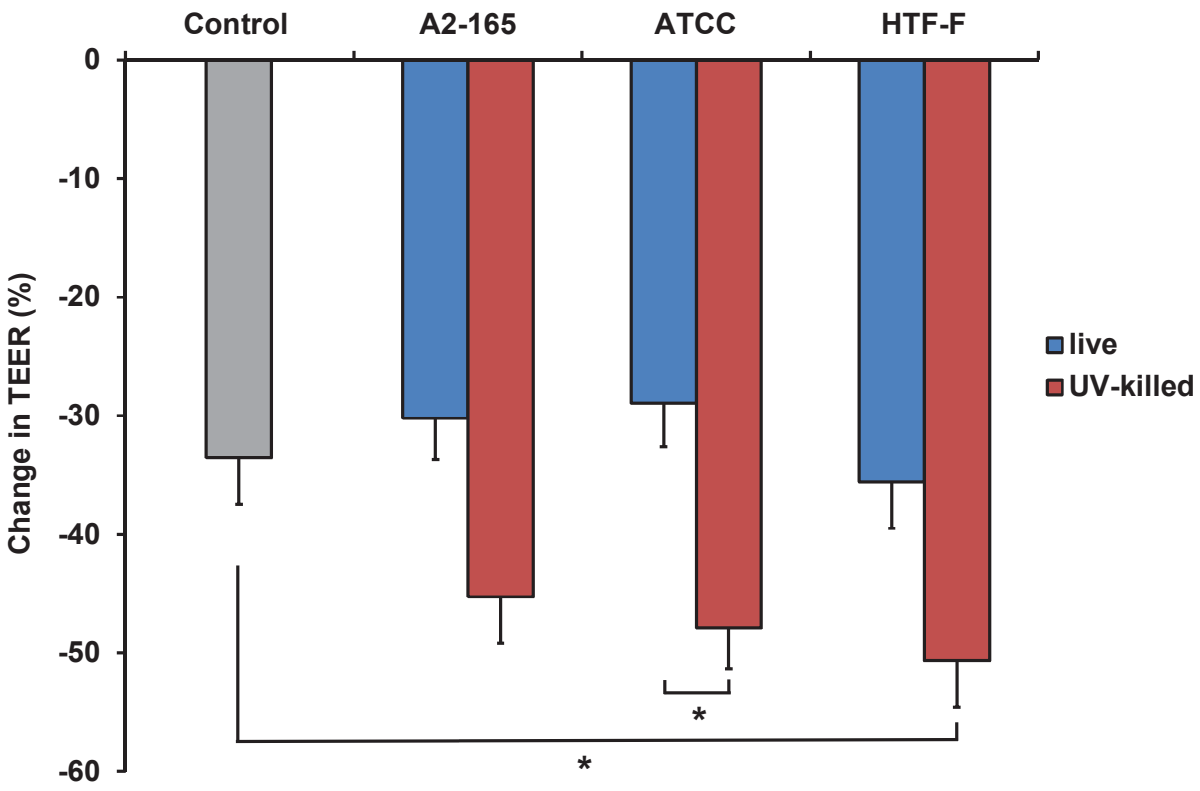

Figure 3.9 Change in TEER across TNF-α-treated Caco-2 monolayers co-cultured with live or UV-killed *F. prausnitzii* using M199 TEER as apical medium.

TNF-α-treated Caco-2 cells were exposed to live or UV-killed *F. prausnitzii* (strains A2-165, ATCC 27768 and HTF-F) and the TEER across the Caco-2 monolayers was recorded over 12 h. The interaction between the treatment and time was not significant and removed from the statistical model. There was a significant treatment effect on the change in TEER ($P < 0.001$). The graph shows the fitted mean (± SEM; $n = 9$) change in TEER across TNF-α-treated Caco-2 monolayers co-cultured with live or UV-killed *F. prausnitzii* after normalising by the TEER at 0 h. * TEER significantly different ($P < 0.05$).

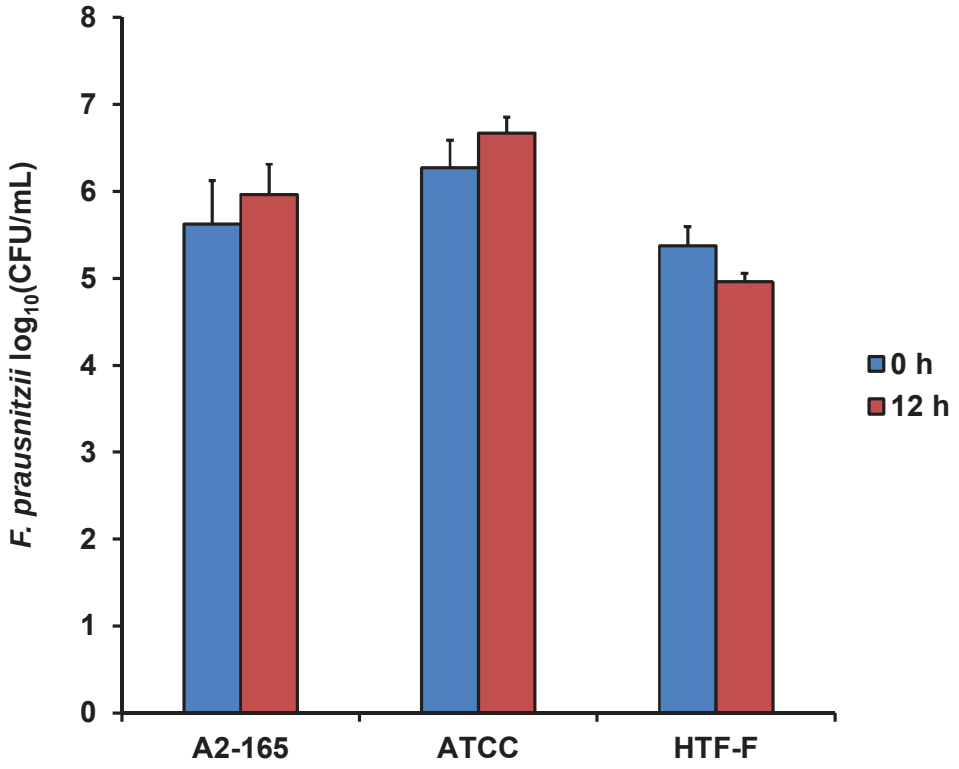

Figure 3.10 Viability of the three *F. prausnitzii* strains co-cultured with TNF-α-treated Caco-2 cells using 50% BHI as apical medium.

The three *F. prausnitzii* strains (A2-165, ATCC 27768 and HTF-F) were co-cultured with TNF-α-treated Caco-2 cells using 50% BHI as apical medium. The graph shows the mean (± SEM; n = 3 and 10 for time 0 and 12 h, respectively) $\log_{10}$(CFU/mL) of the bacteria at 0 and 12 h of incubation with Caco-2 cells in the apical anaerobic co-culture model. The bacterial treatments were added to three inserts with Caco-2 cells, however, several cell monolayers were disrupted after the 12 h of incubation. For these reasons the number of observations differed between time 0 and 12 h.

medium, a significant drop in CFUs after the 12 h of co-culture was observed for all of the three *F. prausnitzii* strains ($P < 0.05$; Figure 3.11). However, the absence or presence of TNF-α did not affect the viability of *F. prausnitzii*. After 12 h of co-culture there were no differences in CFUs of the three *F. prausnitzii* strains co-cultured either with healthy or TNF-α-treated Caco-2 cells.

3.5. DISCUSSION

The results presented in this thesis chapter disprove the hypothesis that strains of live and growing *F. prausnitzii* (A2-165, ATCC 27768 and HTF-F) co-cultured with IECs increase the barrier integrity of these cells, as measured by TEER. This was the case when using an apical medium that enabled growth of *F. prausnitzii* A2-165 and ATCC 27768 (50% BHI) and when using an apical medium that did not enable growth of these bacteria (25% BHI). Furthermore, it was not possible to prove or disprove the hypothesis that live *F. prausnitzii* mitigate the TNF-α-induced decrease in TEER because the expected TNF-α induced TEER decrease did not occur. However, contrary to the healthy Caco-2 monolayers, the TNF-α treated Caco-2 cells exposed to UV-killed *F. prausnitzii* had decreased TEER values whereas live *F. prausnitzii* maintained it. This suggests that surface structures of UV-killed *F. prausnitzii* exert detrimental effects on barrier integrity under TNF-α-mediated inflammatory conditions, whereas live bacteria maintain barrier function. It is plausible that live *F. prausnitzii* secretes metabolites which are able to compensate for the decrease in TEER induced by surface-structures.

Specific probiotic and commensal bacteria play a role in enhancing the function of the intestinal barrier [87,112-114,116,291]. Previous studies investigating the effect of *F. prausnitzii* A2-165 on intestinal barrier integrity showed that live *F. prausnitzii* A2-165 did not affect TEER across Caco-2 monolayers when using the apical anaerobic co-culture

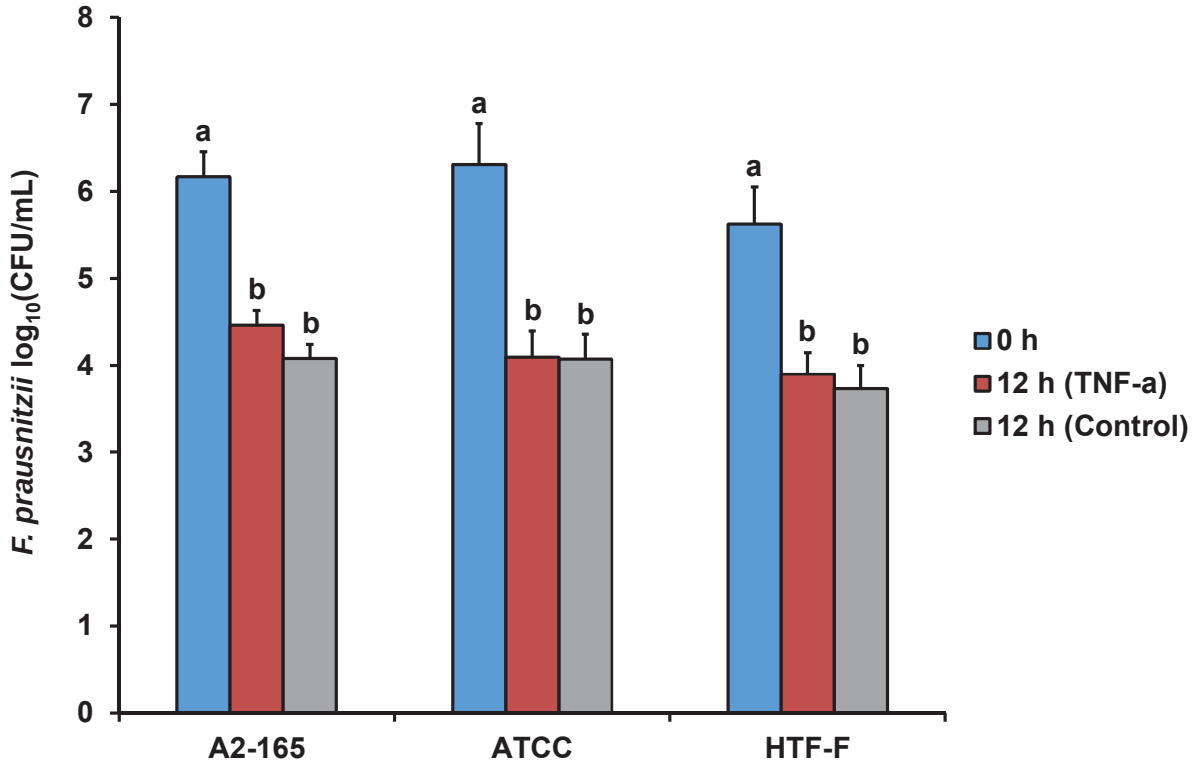

Figure 3.11 Viability of the three *F. prausnitzii* strains co-cultured with healthy or TNF-α-treated Caco2-cells using M199 TEER as apical medium.

The three *F. prausnitzii* strains (A2-165, ATCC 27768 and HTF-F) were co-cultured with Caco-2 cells with or without TNF-α treatment using M199 TEER as apical medium. The graph shows the mean (± SEM; n = 3 and 10 for time 0 and 12 h, respectively) $\log_{10}$(CFU/mL) of the three *F. prausnitzii* strains before and after 12 h of incubation with healthy or TNF-α-treated Caco2-cells in the apical anaerobic co-culture model. Treatments that do not share the same letters are significantly different ($P < 0.05$). The bacterial treatments were added to three inserts with Caco-2 cells, however, several cell monolayers were disrupted after the 12 h of incubation. For these reasons the number of observations differed between time 0 and 12 h.

model [19]. However, the bacterial growth was stagnant in the cell culture medium used for these experiments. Using the optimised growth conditions for *F. prausnitzii* in this model (Chapter 2) and testing *F. prausnitzii* A2-165, ATCC 27768 and HTF-F, the bacteria did also not change TEER across healthy Caco-2 monolayers. Even though *F. prausnitzii* A2-165 and ATCC 27768 were shown to grow in co-culture with Caco-2 cells when using 50% BHI as apical medium but not when using 25% BHI, the bacterial treatments had no effect on TEER both when using 25 and 50% BHI. These results suggest that, unlike hypothesised, the growth phase of *F. prausnitzii* and potential bacterial metabolites secreted by growing bacteria did not alter the effects on TEER across healthy Caco-2 monolayers.

It is plausible that metabolites secreted by live *F. prausnitzii* may require a longer treatment time to exert effects on intestinal barrier integrity. Specific probiotics and commensal bacteria influence intestinal barrier integrity through secreted metabolites [120,291,292]. For example, butyrate, a SCFA produced during bacterial fermentation, enhanced the intestinal epithelial barrier through the regulation of TJ assembly [293]. However, the barrier enhancing properties of butyrate occurred only after 24 h of incubation and TEER values reached maximum levels between 48 to 72 h [293]. It is therefore plausible that effects of *F. prausnitzii* secreted metabolites may occur only after an extended treatment time. The initial validation studies for the apical anaerobic co-culture model were performed using 12 h of incubation. In order to determine effects of metabolites secreted by live *F. prausnitzii* over a prolonged incubation time in this model, further studies would be required to ensure the viability of the Caco-2 cells. However, although *F. prausnitzii* is known as one of the major butyrate producers in the GI microbiota [178], it is unknown whether it produced butyrate when using 50% BHI as apical medium. Further studies could analyse the composition of the apical medium after

the co-culture of *F. prausnitzii* with Caco-2 cells. The addition of fermentable substrates like cellobiose to the apical medium could be tested in order to increase the metabolic activity of *F. prausnitzii*. In addition, in order to determine the effect of *F. prausnitzii* secreted metabolites on TEER, further experiments could be conducted testing the cell-free culture supernatant. The three *F. prausnitzii* strains could first be cultured alone using a longer incubation time (e.g. 48 h) and the resulting bacterial supernatants could then be used to stimulate the Caco-2 cells.

The pro-inflammatory cytokine TNF-α decreases TEER of IECs by disrupting the structure of TJs [294]. Unexpectedly, TNF-α did not decrease TEER of Caco-2 cells in the apical anaerobic co-culture model both when using 50% BHI and M199 TEER as apical medium. It was therefore not possible to conclude whether live *F. prausnitzii* alleviate the TNF-α-induced decrease in TEER, which has been reported for specific probiotics and the commensal *B. thetaiotaomicron* [119,120]. Future experiments could aim to determine the optimum concentration of TNF-α required to decrease TEER across Caco-2 monolayers in the apical anaerobic co-culture model.

Although TNF-α did not decrease TEER across Caco-2 monolayers in the co-culture model, the addition of this pro-inflammatory cytokine to the basal compartment increased the susceptibility of the cells to the bacterial treatments. In healthy Caco-2 cells the *F. prausnitzii* strains did not alter TEER. However, TNF-α-treated cells exposed to UV-killed *F. prausnitzii* HTF-F had lower TEER values. This effect was observed both when using 50% BHI and M199 TEER as apical medium. This is in agreement with reported findings that Caco-2 cells remain hypo-responsive to challenge by some non-pathogenic bacterial species [295]. However, in Caco-2/PBMC co-cultures stimulated with the same non-pathogenic bacteria, Caco-2 cells produced pro-inflammatory cytokines [295]. The authors

hypothesised that Caco-2 cell responses to bacteria require the interaction with immune cells and TNF-α was shown to play a key role in this cross-talk [295]. Similarly, these findings may explain the differential response to the bacterial treatments in healthy and TNF-α-treated Caco-2 cells in this research.

Live *F. prausnitzii* may maintain the structure of TJs, an indicator of barrier integrity, under inflammatory conditions. Whereas live *F. prausnitzii* did not affect TEER across TNF-α-treated Caco-2 monolayers compared to the untreated control, UV-killed bacteria decreased TEER. However, since TNF-α treatment did not decrease TEER, it could not be determined if live *F. prausnitzii* strains were are able to reduce the cytokine-mediated drop in TEER. Nevertheless, TNF-α-treated Caco-2 cells exposed to live *F. prausnitzii* had higher TEER values than cells treated with UV-killed bacteria. In case of UV-killed bacteria, the effects of *F. prausnitzii* are most likely mediated through surface interactions likely causing barrier disrupting effects in TNF-α-treated Caco-2 cells. In contrast, live *F. prausnitzii* maintained TJ integrity, possibly through secreted metabolites that compensate the detrimental effects mediated through surface interactions. Similarly, metabolites secreted by the probiotic *Bifidobacterium infantis* protected against TNF-α-induced TJ disruption in T84 human IECs [120]. However, this protection was achieved in T84 cells preincubated with *B. infantis* conditioned medium prior to TNF-α treatment. In this respect, it is plausible that preincubation with live *F. prausnitzii* may prevent TNF-α-induced reduction in barrier integrity. This would involve an extended treatment time in the apical anaerobic co-culture model and it would therefore be necessary to determine whether the viability of the Caco-2 cells could be maintained for a longer incubation time.

Live *F. prausnitzii* may also maintain barrier integrity of Caco-2 monolayers through the activation of innate signalling. For example, commensal induced TLR2 signalling was

shown to enhance intestinal barrier function and thereby limiting mucosal inflammation [116,150,296]. The stimulation of IECs with TLR2 ligands activated specific isoforms of protein kinase C which was correlated with the translocation of the TJ protein ZO-1 resulting in an increase in TEER [151]. Although UV-killed *F. prausnitzii* would also activate TLR2, it may be possible that live *F. prausnitzii* activate TLR2 to a greater extent and therefore protect the TJ integrity.

The lower TEER of Caco-2 cells treated with UV-killed *F. prausnitzii* may also be due to differences in surface structures between live and UV-killed bacteria. The UV treatment may damage bacterial surface structures leading to differential effects on innate signalling in Caco-2 cells and thereby affecting epithelial barrier integrity. In contrast, UV light did not disrupt bacterial surface structures of the food-borne pathogens *L. monocytogenes* and *E. coli* O157:H7 [297]. However, the sensitivity of bacteria to UV radiation was demonstrated to differ between bacterial species [298]. Thus, it may be possible that UV treatment caused changes in the surface structures of the three *F. prausnitzii* strains. Further studies could be conducted using bacteria inactivated through a different method, for example through exposure to oxygen, to test whether UV treatment caused the differential effects of *F. prausnitzii* on TEER.

Although TNF-α did not decrease TEER in Caco-2 cells in this study, small amounts of oxygen may have diffused from the basal to the apical side leading to a decrease in the viability of *F. prausnitzii* co-cultured with TNF-α-treated cells. When using 50% BHI as apical medium, *F. prausnitzii* A2-165 and ATCC 27768 increased in CFUs after 12 h of co-culture with healthy Caco-2 cells in the apical anaerobic co-culture model (section 2.4.6.4). However, using the same apical medium for the co-culture of the *F. prausnitzii* strains with TNF-α-treated Caco-2 cells, no differences were observed between the CFUs

before and after the 12 h of incubation for all of the three strains. The diffusion of oxygen through the Caco-2 monolayer in the presence of TNF-α may be an effect occurring independently from a decrease in TEER since TEER is a measure of paracellular ion permeability. When using M199 TEER as apical medium, a decrease in *F. prausnitzii* CFUs after 12 h of co-culture with healthy and TNF-α-treated Caco-2 cells was determined for all three strains. Contrary to the results obtained with 50% BHI as apical medium, no difference was observed between the CFUs after 12 h of co-culture with healthy or with TNF-α-treated Caco-2 cells. It is plausible that in this case the growth limiting factor was the availability of nutrients because M199 TEER did not contain enough nutrients to allow growth of the *F. prausnitzii* strains. Under these conditions the oxygen diffusion through the Caco-2 monolayer potentially caused by the TNF-α treatment may only play a minor role in affecting the viability of *F. prausnitzii*.

The method of plate counting using serial dilutions of bacterial suspensions was not a suitable method to determine the CFUs of *F. prausnitzii* HTF-F, which most likely led to an underestimation of the bacterial numbers. It was observed that the bacteria grew well on anaerobic BHI agar when using undiluted bacterial suspensions. However, when using serial dilutions of the bacterial suspensions to obtain bacterial numbers in a countable range, no or little growth was determined. The reason for this was most likely that *F. prausnitzii* HTF-F is a biofilm forming strain [204,264] which may require higher bacterial cell concentrations for growth to allow intercellular aggregation. Therefore, the results obtained for the CFUs for *F. prausnitzii* HTF-F co-cultured with Caco-2 cells here and in Chapter 2 may not accurately reflect bacterial viability. A different bacteria quantification method would be required to determine viable cell counts of *F. prausnitzii* HTF-F, for example microscopy or flow cytometry in combination with a live/dead stain.

In conclusion, live *F. prausnitzii* (strains A2-165, ATCC 27768 and HTF-F) did not exert barrier enhancing properties in healthy and TNF-α-treated Caco-2 cells in the apical anaerobic co-culture model. However, UV-killed *F. prausnitzii* decreased TEER across TNF-α-treated Caco-2 monolayers most likely mediated through surface interactions, whereas live *F. prausnitzii* maintained TEER under these inflammatory conditions. It may therefore be possible that live *F. prausnitzii* secretes metabolites that compensates for the decrease in TEER induced by bacterial surface structures. Furthermore, live *F. prausnitzii* may maintain TJ integrity through the activation of innate signalling and it could therefore be further investigated whether live *F. prausnitzii* induce greater TLR activation than UV-killed bacteria. The differential effects of live and dead bacteria determined in this research demonstrate the importance of using novel co-culture models such as the apical anaerobic co-culture model which allow the investigation of bacterial effects in physiologically relevant conditions.

CHAPTER FOUR:

Adaptation of the Toll-like receptor activation assay to the apical anaerobic co-culture model[†]

[†] Selected material from this section combined with sections from Chapter 5 will be submitted for publication to the journal *Cellular Microbiology*.

4.1. INTRODUCTION

The interactions between the GI microbiota, IECs and immune cells of the GALT have been intensively studied and it is established that well regulated cross-talk between these components is important for maintaining homeostasis [26]. Innate signalling contributes to the homeostatic balance between tolerance towards commensals and immunity against pathogens [27]. TLRs, innate immune receptors expressed on the surface of IECs and immune cells, recognise common structures on microorganisms, for example LPS [299]. Their activation triggers downstream signalling cascades leading to the activation of transcription factor NF-κB, which induces either pro- or anti-inflammatory responses [299].

Determining the activation of TLRs by bacteria (from here on referred to as the TLR activation assay) is a common method to test the immune-stimulatory potential of bacteria [207,300,301]. Human embryonic kidney cell lines (HEK293) stably transfected to express human TLRs are routinely used for TLR activation assays. Furthermore, these cells are transfected with a reporter plasmid containing the luciferase gene under the control of the human NF-κB promoter to be able to quantify the TLR activation. These assays are routinely performed in conventional conditions (5% CO_2 in air atmosphere) but not using more physiologically relevant models like the apical anaerobic co-culture model. Hence, when the effect of obligate anaerobes, which make up the majority of the bacteria in the large intestine [18], on TLR activation has been investigated [207], these bacteria were not viable due to the presence of oxygen. Therefore, the observed effects were only relevant to dead bacteria.

It was previously reported that live and dead *F. prausnitzii*, a prominent obligate anaerobe within the GI microbiota, had different effects on the gene expression of Caco-2 cells [19].

Specifically, Caco-2 cells exposed to live bacteria had lower expression of inflammatory mediators compared to Caco-2 cells exposed to UV-killed bacteria. This highlights the importance of using more physiologically relevant co-culture models, such as the apical anaerobic co-culture model, to study the interactions between live obligate anaerobes and human cells.

In order to determine the level of TLR activation caused by live *F. prausnitzii* using the apical anaerobic co-culture model (chapter 5), method development was required to adapt the TLR activation assay to be performed in the co-culture model. For example, in the altered assay conditions the transfected HEK293 cell lines only received oxygen from the basal compartment of the co-culture chamber while being exposed to the apical anaerobic environment.

4.2. HYPOTHESIS AND AIMS

The hypothesis of this thesis chapter was that the viability of both TLR expressing HEK293 cell lines and *F. prausnitzii* is maintained in the TLR activation assay carried out in the apical anaerobic co-culture model.

The first aim was to stably transfect three HEK293 cell lines expressing different TLRs (TLR2, TLR2/6 and TLR4) and a control cell line (HEK293-null) with a NF-κB inducible luciferase reporter plasmid to be able to quantify the TLR activation. These cell lines were referred to as HEK293-TLR-Luc cells.

The second aim was to optimise the growth of the three *F. prausnitzii* strains in anaerobic DMEM, the medium used to culture the HEK293-TLR-Luc cell lines, by supplementing the medium with acetate and with the bacterial culture medium BHI.

The third aim was to adapt the TLR activation assay to the apical anaerobic co-culture model. For these experiments one of the transfected cell lines, the HEK293-TLR2-Luc cell line, was selected because it had the fastest growth rate. The TLR activation assay was carried out with HEK293-TLR2-Luc cells grown on Transwell inserts and the attachment and viability of the cells in the adapted assay conditions was determined. In addition, the DO content of the apical and basal compartment was determined to ensure that the cells received sufficient oxygen from the basal compartment and that no oxygen was leaking from the basal to the apical compartment.

The fourth aim was to determine the viability of one of the three *F. prausnitzii* strains (A2-165) in co-culture with HEK293-TLR2-Luc cells when using different medium compositions on the apical side.

4.3. METHODS

4.3.1. Culture of HEK293-TLR cells

The HEK293 cell line is a stable cell line originated from primary HEK cells transformed by adenovirus type 5 DNA [302]. Three HEK293 cell lines expressing one or two TLR and a control cell line as listed in Table 4.1 were purchased from Invivogen (San Diego, USA). The cells were provided in a shipping flask and recovered and cultured as per the manufacturer's instructions. First, the four cell lines were cultured to expand the cell populations and generate frozen stocks for the following experiments.

4.3.1.1. Maintenance of HEK293-TLR cells

When recovering HEK293-TLR cells from frozen stocks, the cells were maintained in Dulbecco´s Modified Eagle Medium (DMEM, Life technologies, Auckland, New Zealand)

Table 4.1 HEK293 cell lines expressing different cell surface TLRs used in this study.

Cell line	Recognised ligands
HEK293-TLR2	Peptidoglycan and lipoteichoic acid (Gram-positive bacteria)
HEK293-TLR2/6	Diacyl lipopeptides (mycoplasma) and peptidoglycan (Gram-positive bacteria)
HEK293-TLR4	Lipopolysaccharide (LPS) (Gram-negative bacteria)
HEK293-null	Control cell line

supplemented with the components listed in Table 4.2, from here on referred to as unselective DMEM. As per manufacturer's instructions, the unselective DMEM was supplemented after the second subculture with the appropriate selective antibiotics to keep the selective pressure for the plasmid expressing the respective TLRs. For the HEK293-TLR4 cell line the unselective DMEM was supplemented with the selective antibiotics hygromycin B gold (50 µg/mL) and blasticidin (10 µg/mL), this medium was referred to as DMEM+BH. For the other HEK293-TLR cell lines (HEK293-TLR2 and HEK293-TLR2/6) and the control cell line (HEK293-null) the unselective DMEM was supplemented with blasticidin (10 µg/mL). This medium was referred to as DMEM+B. The cells were maintained in cell culture flasks (Corning, New York, USA) that were filled with 10 mL for small cell culture flasks (25 cm^2 surface area) or 25 mL for medium and large flasks (75 and 175 cm^2 surface area, respectively) of pre-warmed (37°C) unselective DMEM for the first two passages and selective DMEM supplemented with the appropriate selective antibiotics from the third passage onwards. The growth medium was renewed twice a week. The cell cultures were incubated in air with 5% CO_2 at a temperature of 37°C.

4.3.1.2. Passaging of HEK293-TLR cells

The HEK293-TLR cells were subcultured when they reached 70 to 80% confluence in the cell culture flask. First, the cell culture medium was removed from the flask. Ten millilitres of fresh unselective or selective DMEM, depending on how often the cells have been passaged before, were added to the cell culture flask and the cells were removed from the bottom of the flask by pipetting the medium up and down. The cell suspension was transferred to a sterile 50 mL centrifuge tube and centrifuged for 3 min at 240 x g (Jouan

Table 4.2 Composition of the growth media used to culture HEK293-TLR cells (without selective antibiotics).

Product	Company
500 mL DMEM (Dulbecco's Modified Eagle Medium), high glucose, GlutaMAX™	Life technologies, Auckland, New Zealand
50 mL (10%) FBS	Sigma-Aldrich, Auckland, New Zealand
2.5 mL Penicillin-Streptomycin (10,000 U/mL)	Life technologies, Auckland, New Zealand
1 mL Normocin	Invivogen, San Diego, USA

C3i Multifunction Centrifuge, Thermo Scientific, USA). After discarding the supernatant the cell pellet was resuspended in 4 mL of fresh unselective or selective DMEM and 1 mL of the cell suspension was used to reseed a new cell culture flask.

4.3.1.3. Long term storage of HEK293-TLR cells

The HEK293-TLR cell lines were stored in liquid nitrogen for long term storage. In order to prepare frozen stocks, the cells were detached from the cell culture flasks as described in 4.3.1.2 and the cell suspension was transferred into a sterile 50 mL centrifuge tube. The cell suspension was centrifuged at 240 x g for 3 min. After discarding the supernatant, the cell pellet was resuspended in 4 mL of unselective DMEM. The cell density was determined using an automated cell counter (Countess, Life Technologies, Auckland, New Zealand) and the cell suspension was diluted to a density of 5 x 10^6 cells/mL. From this cell suspension 1 mL was transferred into cryogenic vials, 110 µL of DMSO (10%) was added and thoroughly mixed with the cell suspension. The cryogenic vials were placed in a Mr. Frosty™ Freezing Container (Thermo Fisher Scientific, Australia), stored at -80°C overnight and the next day transferred into a liquid nitrogen dewar.

4.3.1.4. Recovering HEK293-TLR cells from liquid nitrogen

The cryogenic vials were removed from the liquid nitrogen dewar and rapidly thawed inside an oven at 37°C. The contents of the cryogenic vial were transferred into a sterile 50 mL centrifuge tube containing 15 mL of unselective DMEM. This cell suspension was centrifuged at 240 x g for 3 min, the supernatant was discarded and the cell pellet was resuspended in 1 mL of unselective DMEM. The cell suspension was transferred into a small cell culture flask (T25, Corning, New York, USA) and 9 mL of unselective DMEM was added. The cell culture flask was placed into an incubator with 37°C and 5% CO_2. The medium was changed twice a week. The cells were passaged twice before adding the

selective antibiotics. The HEK293-TLR cells were used for experiments once they had been cultured in selective DMEM for at least one passage.

4.3.2. Stable transfection of HEK293-TLR cells

The three HEK293-TLR cell lines and the control cell line were stably transfected with a luciferase expressing reporter plasmid under the control of the human NF-κB promoter to be able to quantify the TLR activation. These transfected cell lines were referred to as HEK293-TLR-Luc cells. The luciferase plasmid was extracted from transformed *E. coli*. The HEK293-TLR cell lines were then transfected with this plasmid and upon antibiotic selection the stable clones were picked. The cell population was expanded and frozen stocks were prepared as described in 4.3.1.3. An overview of the process of stably transfecting the HEK293-TLR cell lines with the reporter plasmid is shown in Figure 4.1.

4.3.2.1. Growth of pNiFty2-Luc-transformed bacteria

Lyophilised *E. coli* transformed with the plasmid pNiFty2-Luc was purchased from Invivogen (San Diego, USA). For the antibiotic selection of the pNiFty2-Luc transformed bacteria, Luria-Bertani (LB) agar and broth supplemented with the antibiotic zeocin were provided by the manufacturer (Invivogen). The resuspended bacteria were grown on LB agar containing zeocin as per manufacturer's instructions. A single colony was isolated from the agar plate and grown in LB broth supplemented with zeocin. This culture was used to extract the pNiFty2-Luc plasmid DNA.

4.3.2.2. Extraction of pNiFty2-Luc plasmid DNA

The pNiFty2-Luc plasmid DNA was extracted from the *E. coli* broth culture prepared as described in 4.3.2.1 using the PureLink HiPure Plasmid DNA Filter Purification Kit (Life

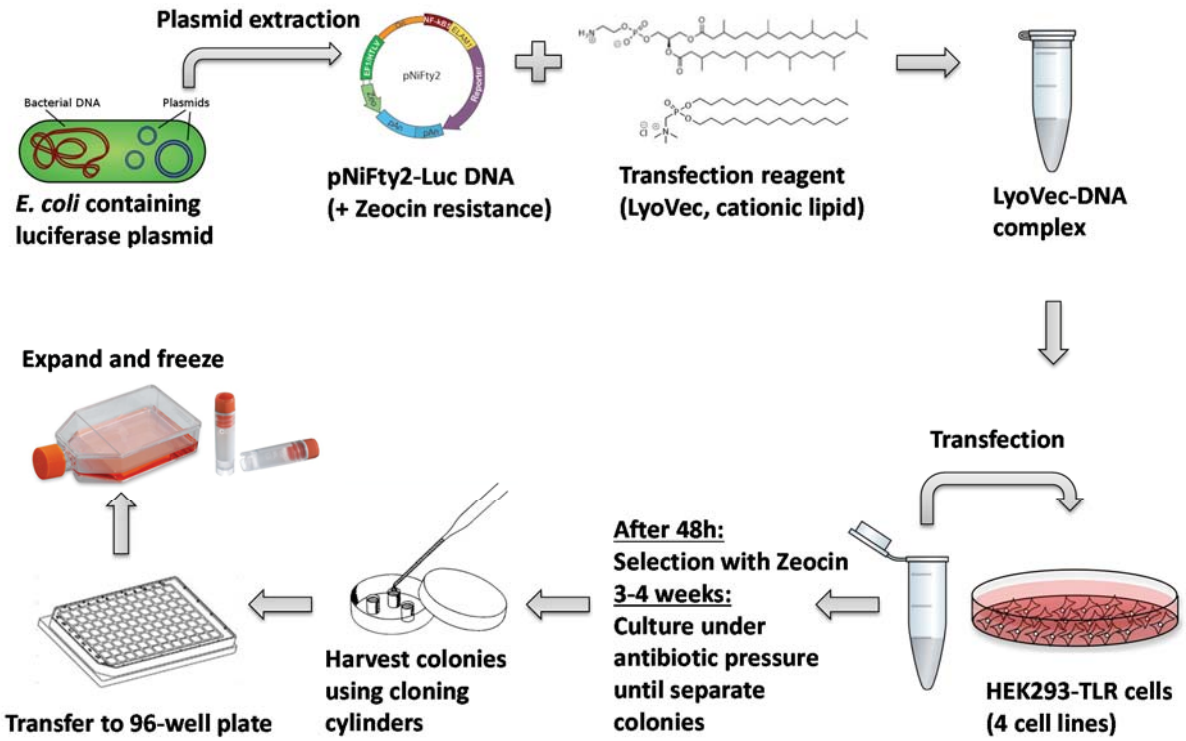

Figure 4.1 Overview of the stable transfection of HEK-TLR cell lines with a NF-κB inducible luciferase plasmid.

The flow chart shows the process of generating stably transfected HEK293-TLR-Luc cell lines. The pNiFty2-Luc plasmid was extracted from *E. coli* cells, mixed with the transfection reagent and this complex was used to transfect the four HEK293-TLR cell lines seeded into 10 cm culture dishes. The stable clones were selected using the antibiotic zeocin until individual colonies were visible. These colonies of stably transfected cells were transferred into 96-well plates and the cell population was expanded until sufficient cells were obtained to generate frozen stocks.

technologies, Auckland, New Zealand) as per manufacturer's instructions. The quality of the extracted plasmid DNA was determined by the presence of distinct bands of the different DNA forms of a plasmid on an agarose gel and the quantity using the Qubit Fluorometer (Life technologies, Auckland, New Zealand).

4.3.2.3. Determining zeocin sensitivity of the HEK293-TLR cells

In addition to the luciferase reporter gene, the pNiFty2-Luc plasmid also contained a resistance gene to the antibiotic zeocin which was used for antibiotic selection after transfection. First, the sensitivity of the HEK293-TLR cells to zeocin was determined in order to choose the minimal concentration of this antibiotic required to kill the untransfected cell line. For this experiment the HEK293-TLR2 cell line was used.

The HEK293-TLR2 cells were harvested from a large flask as described in 4.3.1.2. Upon centrifugation the cell pellet was resuspended in 4 mL of DMEM+B and the cell concentration was determined using an automated cell counter (Countess, Life technologies, Auckland, New Zealand). The cell suspension was diluted with DMEM+B to a cell density of 2 x 10^5 cells/mL. One millilitre of this cell suspension was seeded per well of two 12-well plates and 500 µL of DMEM+B were added to each well. The cell culture plates were incubated in air with 5% CO_2 at a temperature of 37°C for 24 h. After this incubation time the cell layer was approximately 25% confluent.

The zeocin stock solution (100 mg/mL) was diluted with DMEM+B to seven different concentrations (50, 100, 200, 400, 600, 800 and 1000 µg/mL). The cell culture medium was removed from the HEK293-TLR2 cells grown in the 12-well plates after the 24 h of incubation and replaced with one of the seven dilutions of zeocin and additionally with DMEM+B without zeocin as a control. Each treatment was tested in triplicate. The medium supplemented with the different zeocin concentrations or the control medium

(DMEM+B) was replenished every three to four days and the percentage of attached, i.e. viable, cells over time was observed under a light microscope. The zeocin concentration that killed the majority of the cells within 1 – 2 weeks was selected to be used for the antibiotic selection of stable clones after transfection.

4.3.2.4. Stable transfection and selection of stable clones

For the stable transfection of the three HEK293-TLR cell lines and the HEK293-null cell line (control cell line) the lipid-based transfection reagent Lyovec (Invivogen, San Diego, USA) was used. This lyophilised cationic lipid was reconstituted by adding 2 mL of deionised sterile water per vial. After homogenising the Lyovec reagent by gently vortexing for 30 sec, the vial was kept in 4°C for at least 30 min before using for the transfection of the cell lines.

The Lyovec reagent was brought to room temperature and before use vortexed to homogenise. Three micrograms of the pNiFty2-Luc plasmid DNA extracted from *E. coli* (4.3.2.2) were mixed with 100 µL of the Lyovec reagent in a sterile 1.5 mL micro-centrifuge tube at room temperature. The mixture was incubated at room temperature for at least 15 min to allow the formation of the Lyovec-DNA complexes. The complexes were used either immediately for the transfection of the cell lines or stored at 4°C for up to two months for further transfections.

The cell lines were seeded in 8 mL of DMEM+B (HEK293-TLR2, HEK293-TLR2/6 and HEK293-null) or DMEM+H+B (HEK293-TLR4) in a 10 cm cell culture dish at a seeding density of 1.5 x 10^6 cells per dish. Immediately after seeding the cells were transfected by adding 400 µL of the Lyovec-DNA complexes directly to the culture dish and swirling the culture dish to allow an even distribution of the complexes. In addition, a dish of

untransfected cells was seeded as a negative control. The cell culture dishes were incubated in air with 5% CO_2 at a temperature of 37°C for 48 h.

Following this incubation the cell culture medium was carefully removed and fresh culture medium supplemented with the antibiotic zeocin was added at the concentration determined in 4.3.2.3 (200 µg/mL) to select the stably transfected cells. Every three to four days the culture medium was carefully removed and replaced with fresh culture medium containing zeocin. The culture dishes were regularly observed under the microscope. During the first few days of antibiotic selection all cells from the negative control (untransfected cells) were killed. For the cell culture dish containing the transfected cells, very few cells survived the antibiotic pressure and after around 3 weeks isolated colonies of transfected cells could be observed under the microscope.

The isolated colonies were picked and transferred into 96-well plates using cloning cylinders (Corning, 6 mm, pyrex, New York, USA). First, the cloning cylinders, silicone grease (Dow Corning silicone high vacuum grease, Dow Corning, Midland, USA) and forceps were autoclaved. The culture medium in the cell culture dishes was removed completely. Using sterile forceps the cloning cylinders were picked up and gently pressed into the silicone grease. The greased cylinders were placed over the isolated colonies of transfected cells and gently pressed down evenly with forceps. Two hundred microliters of culture medium was added into the cylinder, the cells were removed by carefully pipetting the medium up and down, and transferred into a 96-well plate. The cells were incubated in air with 5% CO_2 at a temperature of 37°C to near confluence before expanding the cell population into the wells of 24- and 6-well plates and later into small, medium and large cell culture flasks. The culture medium was removed and replaced every three to four days

and the cell population was expanded until sufficient cells were obtained to prepare frozen stocks.

4.3.3. Culture of HEK293-TLR-Luc cells

The three HEK293-TLR-Luc cell lines and the HEK293-null-Luc cell line were maintained and passaged as described in 4.3.1.1 and 4.3.1.2. Frozen stocks of the transfected cell lines were prepared as described in 4.3.1.3 and the recovery of frozen cells from liquid nitrogen was conducted as described in 4.3.1.4. As for the original cell lines, the generated cell lines were maintained in unselective DMEM for the first two passages. In order to maintain the antibiotic pressure to keep the pNiFty2-Luc plasmid, the culture medium was supplemented with zeocin (200 µg/mL) from the third passage onwards. Hence, the culture medium for HEK293-TLR2-Luc, HEK293-TLR2/6-Luc and HEK293-null-Luc cells was supplemented with blasticidin and zeocin (referred to as DMEM+BZ) and the media for the HEK293-TLR4-Luc cells with blasticidin, hygromycin B gold and zeocin (referred to as DMEM+BHZ).

4.3.3.1. Passaging of HEK293-TLR-Luc cells using trypsin

For harvesting HEK293-TLR-Luc cells using TrypLE, the cell culture medium was first removed from the flask. For a large flask 15 mL of TrypLE were added, the flask was incubated at 37°C and after 5 min inspected for detachment of the cells. All cells detached within a maximum of 10 min incubation with TrypLE. Fifteen millilitres of culture medium (DMEM supplemented with the appropriate selective antibiotics) were added to the flask and the cell suspension was transferred into a sterile 50 mL centrifuge tube. Following centrifugation at 240 x g for 3 min (Jouan C3i Multifunction Centrifuge, Thermo Scientific, USA) and discarding of the supernatant, the cell pellet was resuspended in 12 mL of culture medium. The cell density was determined using the automated cell

counter and the cells were used for seeding on Transwell inserts or reseeding cell culture flasks as required.

4.3.3.2. Coating of Transwell inserts with collagen I

A 1% solution of rat-tail collagen I (Corning, New York, USA) was prepared using ultra-pure distilled water. The solution was filter-sterilised (0.22 µm) and further diluted with ultra-pure distilled water to a final concentration of 0.1% collagen I. Fifty microliters of this solution was pipetted directly on the membrane of the Transwell inserts. The cell culture plates containing the inserts were left partially covered inside a biosafety cabinet for one hour. Subsequently, the lids of the plates were closed, the insert plates were exposed to UV light for two hours and then left overnight inside the biosafety cabinet. The next day the excess collagen I solution was removed and each insert was washed with 100 µL of sterile PBS. The PBS was removed and the collagen-coated inserts were used on the same day to seed the HEK293-TLR-Luc cells.

4.3.4. Toll-like receptor activation assay in conventional conditions

In order to test whether the stable transfection was successful, one vial of the frozen HEK293-TLR2-Luc cell line was revived as described in 4.3.1.4. Following two passages using unselective DMEM as culture medium, the cells were maintained in DMEM+BZ. The HEK293-TLR2-Luc cell line was then used to perform a TLR activation assay using a positive control (heat-killed *L. monocytogenes* (HKLM), a known TLR2 ligand) and a negative control (sterile endotoxin-free water). A schematic diagram of the TLR activation assay is shown in Figure 4.2. When bacteria are recognised by TLR expressed on the cell surface of the HEK293-TLR-Luc cell lines, it triggers downstream signalling cascades leading to the activation of the transcription factor NF-κB. The HEK293-TLR-

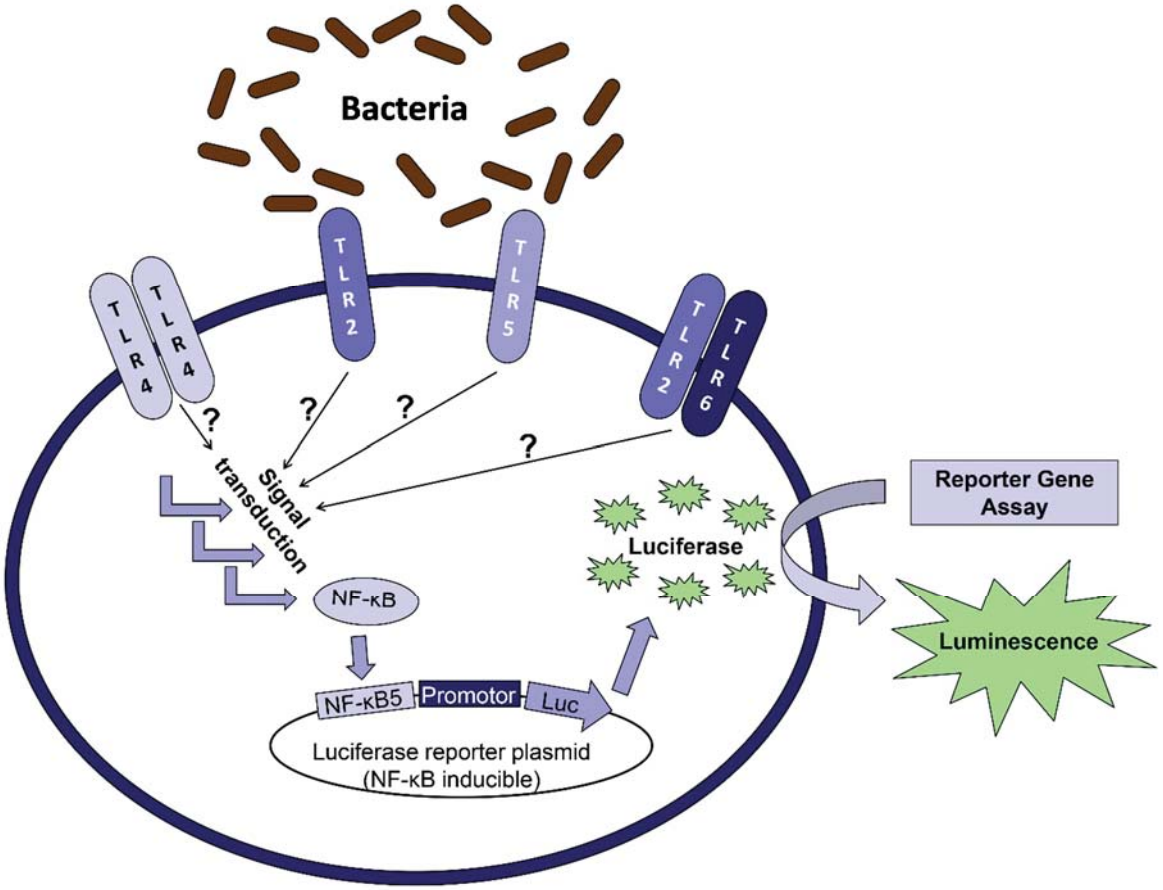

Figure 4.2 Schematic diagram of the TLR activation assay.

HEK293 cells are transfected to express TLR on the cell surface. If bacteria are recognised by TLR, it triggers downstream signalling cascades leading to the activation of transcription factor NF-κB. The HEK293 cells are also transfected with a NF-κB inducible luciferase reporter plasmid resulting in the production of luciferase following TLR activation. By using a reporter gene assay and measuring the luminescence it is therefore possible to quantify TLR activation.

Luc cells are transfected with a NF-κB inducible luciferase reporter plasmid. Therefore the activation of TLR by bacteria results in the production of luciferase and the luminescence can be quantified using a reporter gene assay.

HEK293-TLR2-Luc cells were cultured in a large cell culture flask and detached from the bottom of the flask as described in 4.3.1.2. Following the centrifugation, the supernatant was discarded and the cell pellet was resuspended in 4 mL of DMEM+BZ. The cell density was determined using an automated cell counter (Countess, Life technologies, Auckland, New Zealand) and the cell suspension was diluted to a cell density of 3 x 10^5 cells/mL with DMEM+BZ. This cell suspension was seeded into a 96-well assay plate (Corning Costar 3610, New York, USA) with 200 µL seeded per well resulting in 6 x 10^4 HEK-TLR2-Luc cells per well. The cells were incubated overnight at 5% CO_2 and 37°C.

The next day the HEK293-TLR2-Luc cells were stimulated with HKLM as a positive control and sterile endotoxin free water as a negative control. HKLM was supplied as a lyophilised powder and reconstituted as per manufacturer's instructions. The stock solution (10^{10} HKLM cells/mL) was diluted with DMEM+BZ to 10^8 HKLM cells/mL. The solution was vortexed for 10 sec and stored at 4°C for up to one month. The HEK293-TLR2-Luc cells seeded in the 96-well plate were stimulated with 20 µl of HKLM (10^8 cells/mL) and 20 µl of sterile endotoxin free water (n = 6) and incubated at 37°C in a 5% CO_2 incubator for 24 h.

The following day 120 µL of medium was removed from each well. The lyophilised Bright-Glo luciferase assay substrate was reconstituted using the Bright-Glo luciferase assay buffer according to the manufacturer's instructions. Surplus reagent was frozen at -80°C in aliquots to avoid repeated freeze-thawing and used for up to one month. The assay plate and the reconstituted Bright-Glo reagent were left at room temperature for at least 30

min to ensure that they reached the same temperature. Hundred microliters of the Bright-Glo reagent were added per well of the 96-well plate and mixed with the cell suspension. Following an incubation of at least 2 min at room temperature to allow cell lysis, the luminescence was measured using a plate reader (FlexStation 3, Molecular Devices, Sunnyvale, USA; top read, 750 ms integration time, wavelength nonspecific (between 360 nm and 630 nm)).

This experiment was performed three times using six replicates per treatment. Between the three TLR activation assays the HEK293-TLR2-Luc cells were cultured in unselective DMEM in order to test if the transfection was stable.

4.3.5. Growth optimisation of *F. prausnitzii* in cell culture medium

4.3.5.1. Culture of the *F. prausnitzii* strains

The three *F. prausnitzii* strains listed in Table 2.1 were grown in anaerobic BHI broth prepared as described in section 2.3.2.2. The bacterial cultures were prepared as described in section 2.3.7 and secondary cultures in stationary phase were used for the experiments.

4.3.5.2. Viability of the *F. prausnitzii* strains in different culture media

The viability of the three *F. prausnitzii* strains in anaerobic DMEM with additional supplements (acetate and the bacterial culture medium BHI) was determined as described in Chapter 2 for analysing the growth of the *F. prausnitzii* strains in supplemented anaerobic M199 (2.3.10).

4.3.6. Adaptation of the Toll-like receptor activation assay to the apical anaerobic co-culture model

The standard TLR activation assay was performed using HEK293-TLR-Luc cells grown in 96-well plates and incubated with the treatments in conventional conditions (5% CO_2 in air atmosphere). When conducting the TLR activation assay in the apical anaerobic co-culture model, several adaptations were required as shown in Figure 4.3 and Figure 4.4. The transfected cell lines were seeded on Transwell insert membranes which were inserted into the co-culture chamber. The co-culture chamber was transferred into an anaerobic workstation (Concept Plus, Ruskinn Technology Ltd) where the anaerobic treatments were added. The HEK293-TLR-Luc cells were exposed to the apical anaerobic treatments and only received oxygen from the basal aerobic medium. Furthermore, following receptor activation the cells were transferred from the inserts into a 96-well plate to be able to measure the luminescence signal using a plate reader.

For the above described adaptations of the TLR activation assay to the apical anaerobic co-culture model one of the four transfected cell lines, the HEK293-TLR2-Luc cell line, was chosen. The assay was performed using cells grown on Transwell inserts and experiments were conducted to improve the attachment of the HEK293-TLR2-Luc cells to the membranes of the Transwell inserts when used in the apical anaerobic co-culture model. The TLR activation assay was then performed with positive and negative controls using the adapted assay conditions and the receptor activation obtained in apical anaerobic conditions was compared to the activation obtained in conventional conditions. Furthermore, the DO content of the apical and basal compartments were determined.

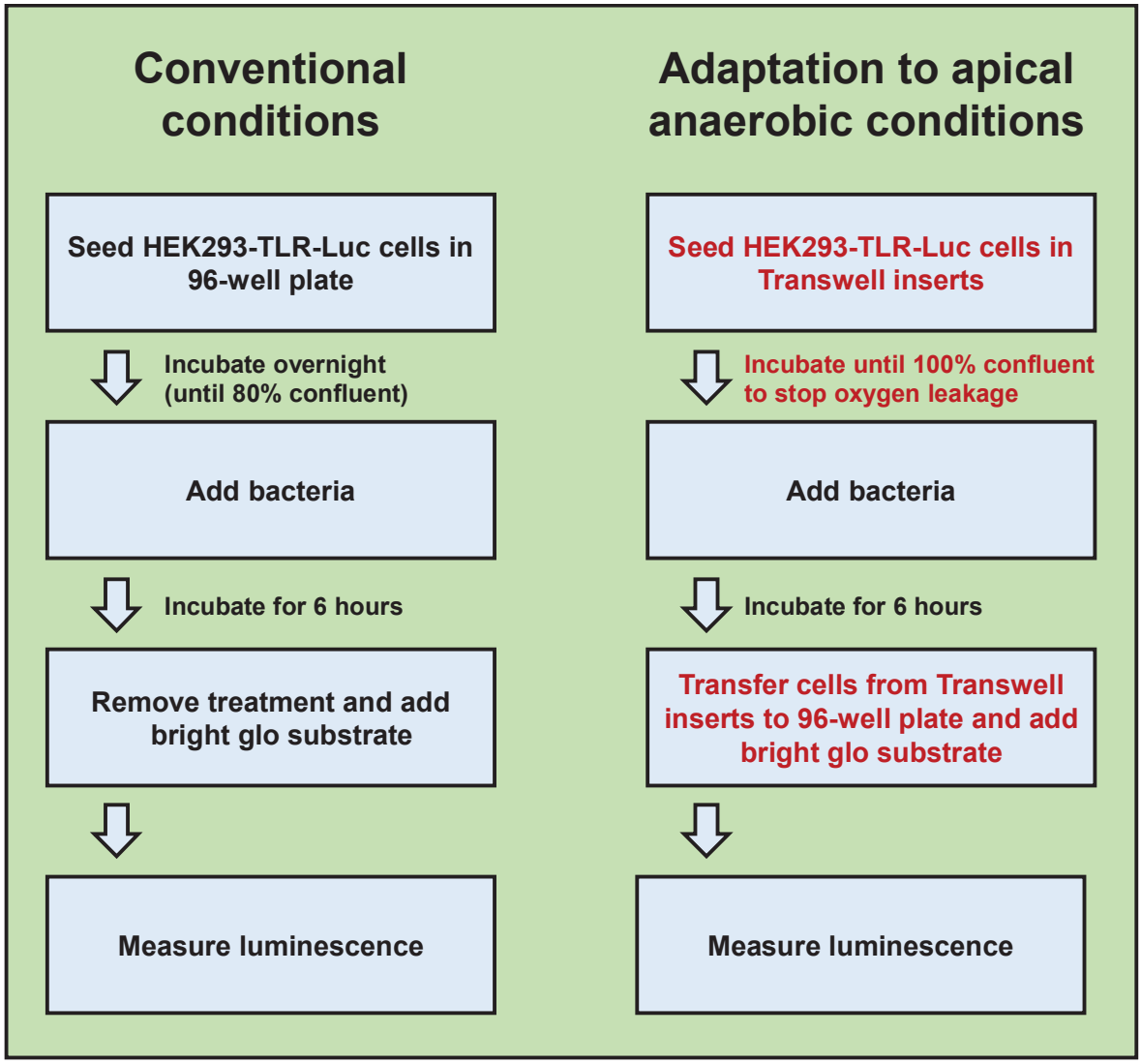

Figure 4.3 Adaptation of the TLR activation assay to the apical anaerobic co-culture model.

A flow chart describing the steps of the TLR activation assay in conventional conditions and the adaptations required to be able to perform the assay in apical anaerobic conditions highlighted in red colour.

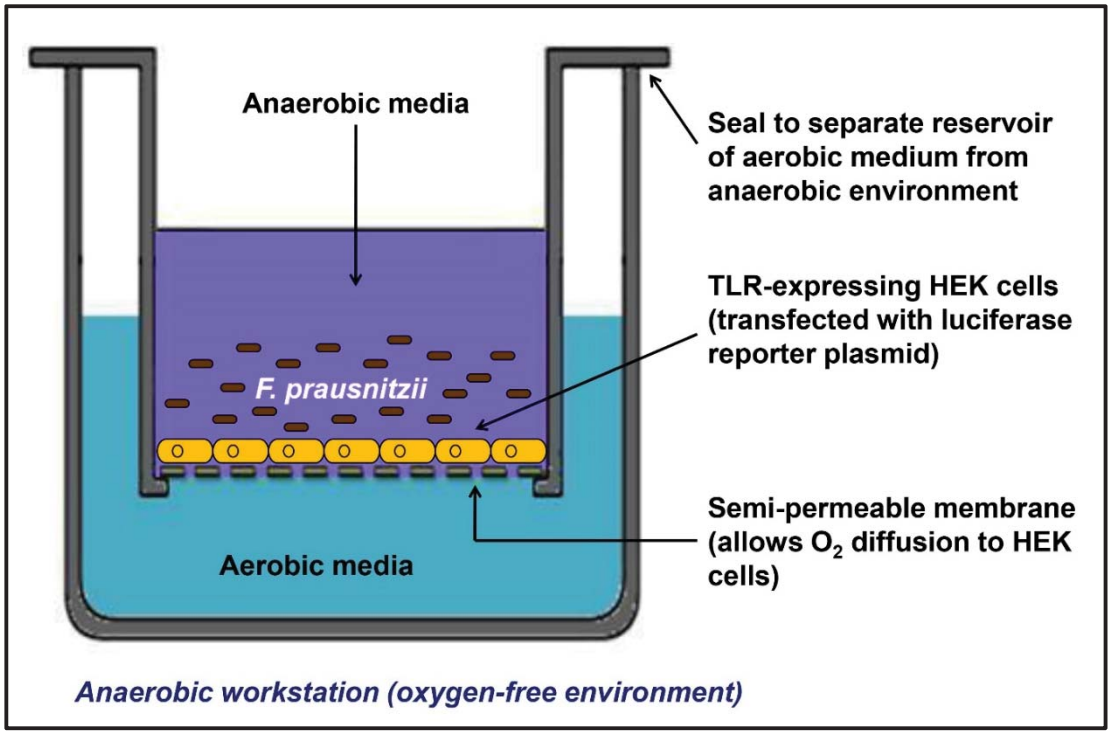

Figure 4.4 HEK293-TLR-Luc cells in the apical anaerobic co-culture model.

The TLR activation assay was adapted to be performed using the apical anaerobic co-culture model. HEK293-TLR-Luc cells were seeded onto the membrane of Transwell inserts instead of 96-well plates. The Transwell inserts containing the cell layers were inserted into the co-culture chamber which was transferred into an anaerobic workstation. The apical medium was replaced with the anaerobic treatment solutions. HEK-TLR-Luc cells received oxygen from the basal aerobic medium and anaerobic bacteria could survive in the apical anaerobic medium. Following receptor stimulation, the HEK293-TLR-Luc cells were transferred into a 96-well plate for luminescence quantification.

4.3.6.1. Toll-like receptor activation assay using Transwell inserts

The TLR activation assay described in 4.3.4 was performed using HEK293-TLR2-Luc cells seeded in a 96-well assay plate and cells seeded in Transwell inserts, and stimulated each with a positive control and a negative control (HKLM, 10^8 cells/mL and sterile endotoxin free water, respectively). The luminescence signals obtained from the two different methods were compared.

The HEK293-TLR2-Luc cells were detached from a large cell culture flask as described in 4.3.1.2. Following centrifugation, the cell pellet was resuspended in 4 mL of DMEM+BZ, the cell density was determined using an automated cell counter (Countess, Life technologies, Auckland, New Zealand) and the cell suspension was diluted to 3 x 10^5 and 5 x 10^5 cells/mL with DMEM+BZ. The two dilutions were seeded into a 96-well assay plate and into Transwell inserts using 200 µL per well and the cells were incubated overnight in a 5% CO_2 incubator at 37°C.

The next day 20 µL each of the positive control (HKLM, 10^8 cells/mL) and the negative control (sterile endotoxin free water) were added to the cells in the inserts and 96-well assay plate (n = 3 per treatment). Only the wells or inserts seeded at a density of 5 x 10^5 cells/mL were used for the receptor stimulation, as those seeded at 3 x 10^5 cells/mL did not reach confluence. The cells were incubated with the treatments for 24 h in a 5% CO_2 incubator at 37°C.

On the following day the luminescence quantification was performed using the HEK293-TLR2-Luc cells seeded in the 96-well assay plate as described in 4.3.4. For the HEK293-TLR2-Luc cells seeded into Transwell inserts the cell layers were first transferred from the Transwell inserts into a 96-well plate. The luminescence signal upon receptor activation was quantified using the Bright-Glo reagent as described in 4.3.4.

4.3.6.2. Determining the viability and attachment of HEK293-TLR2-Luc cells under different assay conditions

Various approaches were tested to improve the attachment of the HEK293-TLR2-Luc cells to the membranes of the Transwell inserts when inserted into the apical anaerobic co-culture model. In addition, different apical medium compositions were tested in order to improve the growth of *F. prausnitzii* co-cultured with HEK293-TLR2-Luc cells.

For these experiments the HEK293-TLR2-Luc cells were detached from a large cell culture flask and seeded on Transwell inserts as described in 4.3.1.2 and 4.3.6.1, respectively, or using TrypLE as described in 4.3.3.1. After 24 h of incubation at a 5% CO_2 in air atmosphere and 37°C, the cell layers were examined under a light microscope (10 x objective) to ensure that they were 100% confluent. The co-culture chamber was prepared as described in 2.3.9.1. The basal wells were filled with 3 mL of DMEM+FBS and the inserts were carefully transferred into the co-culture chamber using a twisting motion. The co-culture chamber was closed with the lids and transferred inside an anaerobic workstation (Concept Plus, Ruskinn Technology Ltd). Inside the anaerobic workstation the apical medium was carefully removed and the different anaerobic treatment solutions were added. Following an incubation period, the co-culture chamber was removed from the anaerobic workstation and the inserts were transferred to a 24-well plate filled with 810 µL of DMEM+FBS. The cell layers were inspected for detachment or disruption under a light microscope. The viability of the cells was determined using the neutral-red viability assay as described in 2.3.15.

For all of the experiments testing the different assay conditions, HEK293-TLR2-Luc cells treated with aerobic DMEM+FBS and incubated in conventional condition (5% CO_2 in air atmosphere and 37°C) were used as a control.

4.3.6.3. Toll-like receptor activation assay in apical anaerobic conditions

HEK293-TLR2-Luc cells seeded on collagen-coated Transwell inserts were stimulated for 6 h with a positive control HKLM at two concentrations (10^8 and 10^9 cells/mL) and a negative control (sterile endotoxin free water) in conventional and apical anaerobic conditions (n = 4 per treatment). After 6 h of incubation the Transwell inserts from both environments were transferred to a 24-well plate filled with 810 µL of DMEM+FBS and 120 µL of the apical medium was removed from each insert. The remaining medium in the inserts was used to remove the cell layers by pipetting the medium up and down. The cell suspensions from each insert were transferred to wells of a 96-well assay plate. The 96-well assay plate and the Bright-Glo substrate (Promega, Madison, USA) were left at room temperature for at least 30 min. Into each well 100 µL of the Bright-Glo substrate was added and mixed with the cell suspension. After incubating for 2 min with the reagent to allow for the complete cell lysis the luminescence was measured using a plate reader (FlexStation 3, Molecular Devices, Sunnyvale, USA; top read; 750 ms integration time).

4.3.6.4. Dissolved oxygen concentration in the apical and basal compartments

HEK293-TLR2-Luc cells were incubated in the apical anaerobic co-culture model for 6 h and the basal and apical DO concentrations were measured to determine if the basal compartment contained sufficient oxygen and if oxygen leaked from the basal to the apical compartment. HEK293-TLR2-Luc cells were seeded on collagen-coated Transwell inserts and inserted into the co-culture chamber as described in 4.3.6.2. The co-culture chamber was transferred into the anaerobic workstation and the apical medium was replaced with anaerobic 50% M199 TEER+50% BHI. The two different methods used to determine the apical and basal DO concentrations using the DO probe and meter (Lazar Research Laboratories, Los Angeles, USA) are shown in Figure 4.5. The DO concentrations in the

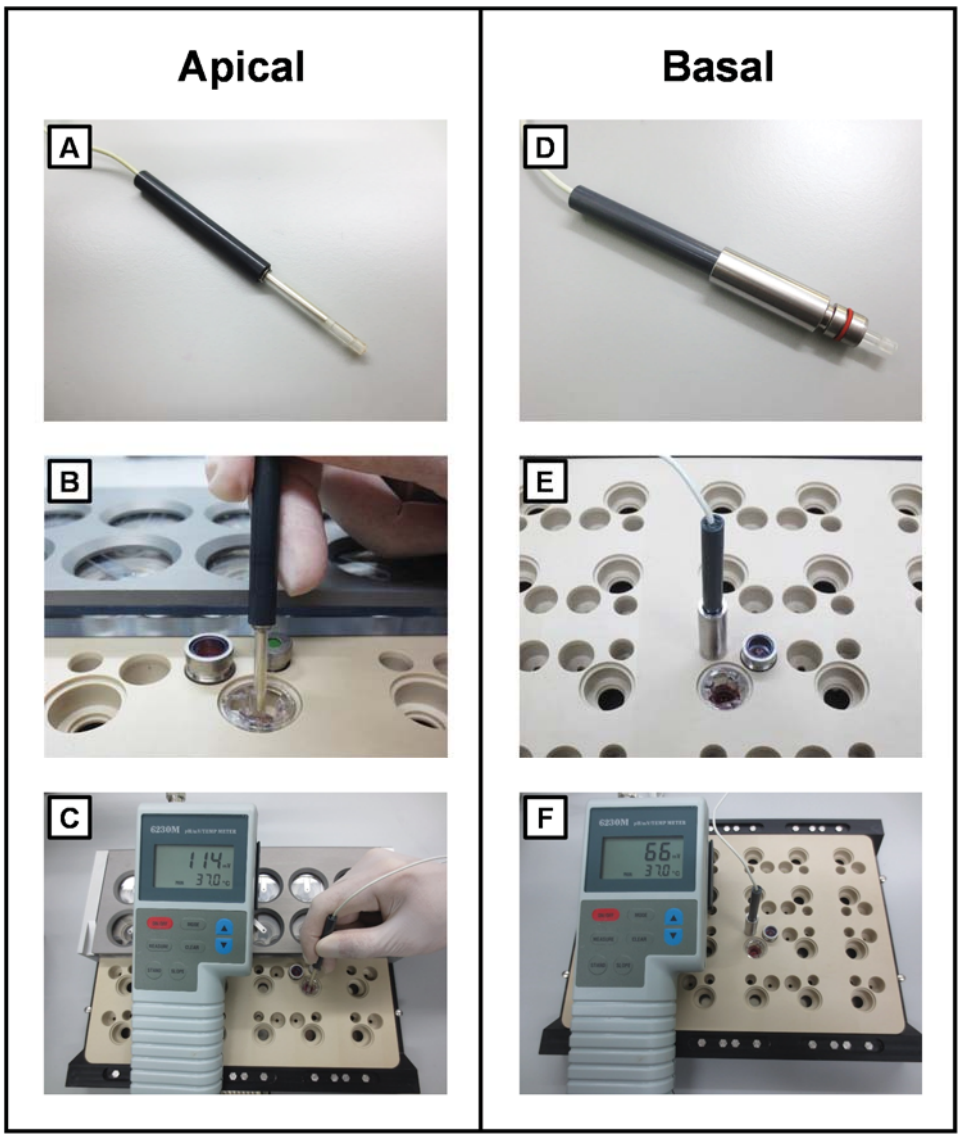

Figure 4.5 Methods to measure the DO concentrations in the apical and basal compartments of the co-culture chamber.

HEK293-TLR2-Luc cells on Transwell inserts were transferred into the apical anaerobic co-culture model and the apical medium was replaced with anaerobic 50% M199 TEER+50% BHI. The DO concentrations in the apical compartment were measured manually by submerging the tip of the DO probe in the apical medium. For the basal measurements a special adapter was designed in order to stabilise and protect the delicate glass electrode of the DO probe while sealing the chamber well off from the external environment. Images show (A) the DO probe, (B) details of the apical DO measurements, (C) apical DO measurements including the DO meter, (D) the DO probe inserted into the adapter for basal measurements, (E) details of the basal DO measurements and (F) the basal DO measurements including the DO meter.

apical compartment were measured hourly over 6 h by submerging the DO probe into the apical medium. This experiment was performed twice using 24 replicates for each experiment (total n = 48). The basal DO concentration could only be measured in one well of the co-culture chamber at a time as a special adapter was required to stabilise and protect the DO probe and to seal off the basal well from the anaerobic environment. The basal DO concentrations were measured hourly over 6 h and the measurements were repeated three times.

4.3.7. Viability of *F. prausnitzii* A2-165 in co-culture with HEK293-TLR2-Luc cells in the apical anaerobic co-culture model

In order to determine which medium is best for the growth of *F. prausnitzii*, one of the three strains (*F. prausnitzii* A2-165) was chosen to be co-cultured with HEK293-TLR2-Luc cells in the apical anaerobic co-culture model using different media on the apical side of the cell layer.

HEK293-TLR2-Luc cells cultured in a large cell culture flask were removed from the flask using TrypLE as described in 4.3.3.1 and seeded in collagen-coated inserts. After 24 h of incubation at 5% CO_2 in air atmosphere and 37°C, the cells were used for the co-culture experiment with *F. prausnitzii* A2-165 and inserted into the co-culture chamber as described in 4.3.6.2.

Two Hungate culture tubes with secondary bacterial cultures of *F. prausnitzii* A2-165 in stationary phase prepared as described in 2.3.7 were centrifuged at 2492 x g for 6 min (11180/13190 rotor, Sigma 3-18K centrifuge, Sigma, Osterode am Harz, Germany). The supernatant was discarded inside the anaerobic workstation and one pellet each was resuspended in 2.5 mL of anaerobic M199 TEER and anaerobic DMEM+FBS. The bacterial cell density was determined using a Petroff-Hauser counting chamber as

described in 2.3.5.1. Five millilitres of bacterial suspensions with a density of 1.5 x 10^7 bacterial cells/mL were prepared using six different anaerobic medium compositions (DMEM+FBS, M199 TEER, 75% M199 TEER + 25% BHI, 50% M199 TEER + 50% BHI, 25% M199 TEER + 75% BHI and BHI). Using this bacterial density resulted in a MOI of 10 as the HEK293-TLR2-Luc cells were seeded at a concentration of 1.5 x 10^6 cells/mL.

Inside the anaerobic workstation the apical medium was removed carefully from the HEK293-TLR2-Luc cell layers and 200 µL of the six treatment solutions (*F. prausnitzii* A2-165 in anaerobic DMEM+FBS, M199 TEER, 75% M199 TEER + 25% BHI, 50% M199 TEER + 50% BHI, 25% M199 TEER + 75% BHI and BHI) were added. The viability of *F. prausnitzii* A2-165 in co-culture with HEK293-TLR2-Luc cells was assessed by determining the CFU of the bacteria before and after 6 h of co-culture with the cells as described in 2.3.5.2. In addition to the bacterial supernatant, the HEK293-TLR2-Luc cell lysate was plated on BHI agar to determine if bacteria have attached to the cells. After removing the complete supernatant from the HEK293-TLR2-Luc cells, the cell layers were washed with 200 µL of anaerobic PBS. Into each insert 100 µL of 1% triton-X prepared in anaerobic PBS was added and incubated for 15 min in order to lyse the cells. Following this incubation the cell lysate was thoroughly mixed by pipetting and transferred into 96-well plates. Tenfold serial dilutions of this suspension were prepared and aliquots of the dilutions were pipetted onto BHI agar plates as described in 2.3.5.2. The agar plates were incubated inside an anaerobic workstation for 48 h. This experiment was performed three times using four replicates per treatment (total n = 12 per treatment).

4.3.8. Statistical analysis

The statistical analyses were performed using SAS (SAS/STAT version 9.3; SAS Institute Inc., Cary, NC, USA). Repeat measure analyses were performed to test the effect of time, strain, status, acetate supplementation or BHI concentration and all their interactions, on the response variable (OD_{600nm}, apical and basal DO levels). After fitting the models by Restricted Maximum Likelihood method and comparing them using the log-likelihood ratio test the most appropriate covariance structure of the mixed model for the response variable was selected. If an interaction was not significant ($P > 0.05$) it was removed from the model. In addition, ANOVA was performed to test the effect of the different apical medium compositions on the viability of HEK293-TLR2-Luc cells in apical anaerobic and conventional conditions and the viability of *F. prausnitzii* A2-165 after 6 h of co-culture with HEK293-TLR2-Luc cells. When the F-value of the analyses were significant ($P < 0.05$), the means were compared using adjusted Tukey tests. Independent T-tests were conducted to compare between TLR2 activation by positive and negative controls for testing HEK293-TLR2-Luc cells for successful stable transfection, for performing the assay with Transwell inserts and for testing the effect of TrypLE on the luminescence signals. For the experiments to improve the attachment of the HEK293-TLR2-Luc cells in the co-culture model, the viability of the cells in conventional and apical anaerobic conditions was also compared using independent T-tests. Furthermore, the viability of *F. prausnitzii* A2-165 before and after the co-culture with HEK293-TLR2-Luc cells using different apical media was compared using the independent T-Test procedure. A 3 x 2 factorial design was used to test the effect of the three treatments (negative control and two concentrations of the positive control) on TLR2 activation in two environments (conventional and apical anaerobic). For all of the statistical analyses the model assumptions (e.g. normal distribution and the homogeneity of variance) was evaluated

using the ODS graphics in SAS. If the response variable did not fulfil these assumptions a $\log_{10}$ transformation was performed in order to reach these assumptions. Due to the reasons stated in section 2.3.16 each HEK293-TLR2-Luc cell monolayer seeded into one Transwell insert was used as an independent replicate for the statistical analysis. For the method development described in this chapter the number of independent replicates was three (n = 3) if not otherwise stated. For experiments that were performed in several runs a complete randomised block design was firstly performed with the run (or experimental day) as a random effect. There was no effect of the run for any of the tested variables, consequently the random effect was removed from the model.

4.4. RESULTS

4.4.1. Zeocin sensitivity of HEK293-TLR2 cells

The sensitivity of HEK293-TLR2 cells to the antibiotic zeocin is shown in Figure 4.6. The graph shows the percentage of attached, i.e. viable, cells after exposure to different concentrations of zeocin over 16 days. The control cells (no zeocin added to the culture medium) reached 100% confluence in the 12-well plate after 6 days. The overgrown cell layers detached from the surface of the culture plate when the media was changed, therefore the graph only shows the percentage of attached cells until 6 days for the control cells. With 50 µg/mL of zeocin the cells reached 75% confluence after 5 days, however with the following medium changes the confluence was reduced to 50% between 6 to 8 days and to 30% after 9 to 12 days as the cells were killed by the antibiotic. When using 100 µg/mL of zeocin, the cells did not increase in confluence after the antibiotic was added and the percentage of attached cells decreased over time. However, after 16 days of incubation with the antibiotic 5% of attached cells remained. With a concentration of 200

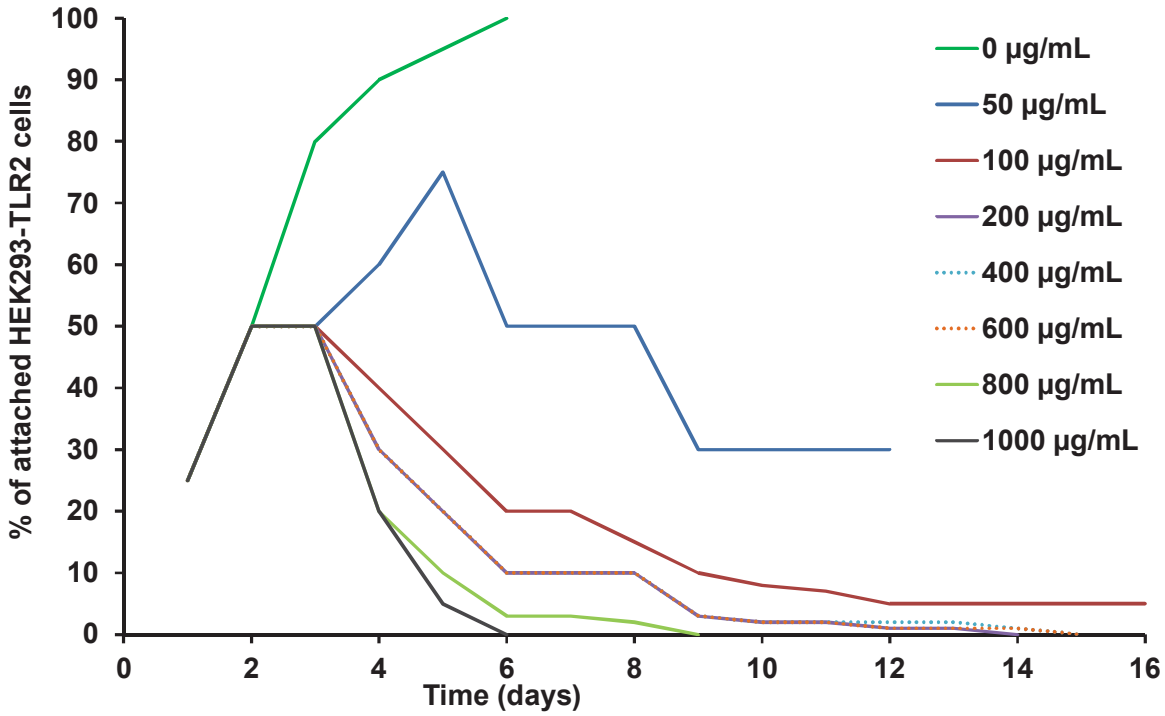

Figure 4.6 Zeocin sensitivity of HEK293-TLR2 cells.

HEK293-TLR2 cells were exposed to the antibiotic zeocin in different concentrations (50, 100, 200, 400, 600, 800 and 1000 µg/mL) to determine the concentration that killed the majority of the cells within two weeks. This was required for the antibiotic selection of the stably transfected cells. The percentage of attached cells (i.e. viable cells) was determined by inspection under a light microscope. The graph shows the mean percentage (n = 3) of remaining attached cells after exposure to the different zeocin concentrations over 16 days. As the quantification of the percentage of attached cells was only done by estimation through microscopic inspection of cells in 3 wells per treatment, no standard error is shown. The cell density in the wells with the control cells (0 µg/mL zeocin) and the cells treated with 50 µg/mL zeocin was too high 6 and 12 days after seeding, respectively, causing the media to become too acidic and the cell layers to detach from the surface of the culture plate.

μg/mL zeocin all cells were killed after 14 days of incubation. Therefore, this concentration of zeocin was chosen for the antibiotic selection after the transfection of the HEK293-TLR cells because it was the minimal concentration that killed all cells within 14 days which was required. Higher zeocin concentrations (400, 600, 800 and 1000 μg/mL) were therefore not required for antibiotic selection.

4.4.2. Toll-like receptor activation assay in conventional conditions

HEK293-TLR2-Luc cells stimulated with the TLR2 ligand HKLM (10^8 cells/mL) had a higher luminescence signal compared to the negative control (sterile endotoxin-free water) as shown in Figure 4.7 ($P < 0.001$). Figure 4.7 shows the pooled data of three assays with cells being cultured in unselective DMEM between the assays. It could therefore be concluded that the stable transfection of the HEK-TLR2 cell line with the luciferase plasmid was successful.

4.4.3. Viability of the three *F. prausnitzii* strains in cell culture medium

Secondary cultures of the three *F. prausnitzii* strains in stationary phase were resuspended in anaerobic DMEM, incubated at 37°C and the OD_{600nm} was measured over 24 h. Figure 4.8A shows the absolute OD_{600nm} values, however due to the different starting OD_{600nm} values the statistical analysis was performed after normalising by the OD_{600nm} at time 0 h (Figure 4.8B). There was no significant interaction between strain and time, therefore this interaction was removed from the statistical model and the pooled data from three strains are shown in Figure 4.8B. There was a significant decrease in the OD_{600nm} after 8 and 24 h compared to the previous time points (0 to 4 h; $P < 0.05$).

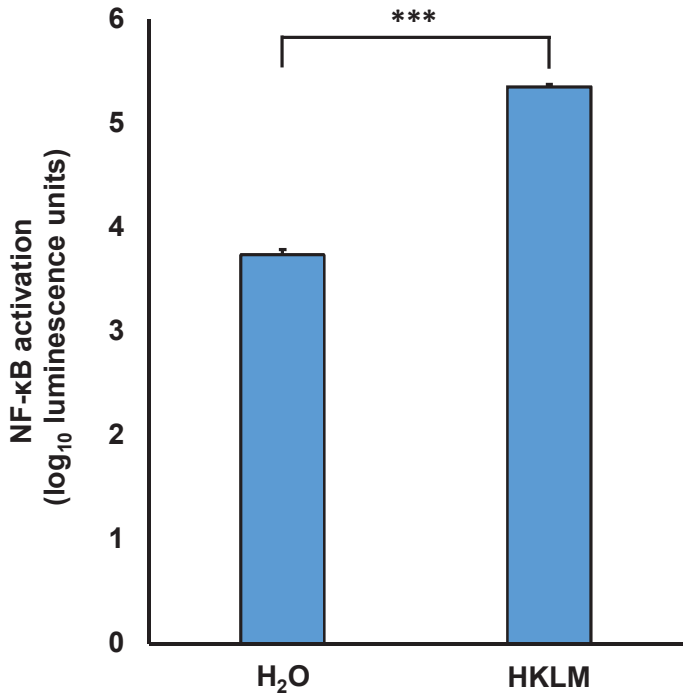

Figure 4.7 TLR activation assay in conventional conditions.

The HEK293-TLR2-Luc cells were stimulated with a positive control (HKLM, 10^8 cells/mL) and a negative control (sterile endotoxin free water) to test if the stable transfection was successful. The assay was repeated three times with cells being cultured in unselective DMEM to test if the transfection was stable. The graph shows the mean (± SEM, n = 18) $\log_{10}$ luminescence units following TLR2 activation. *** TLR2 activation significantly different ($P < 0.001$).

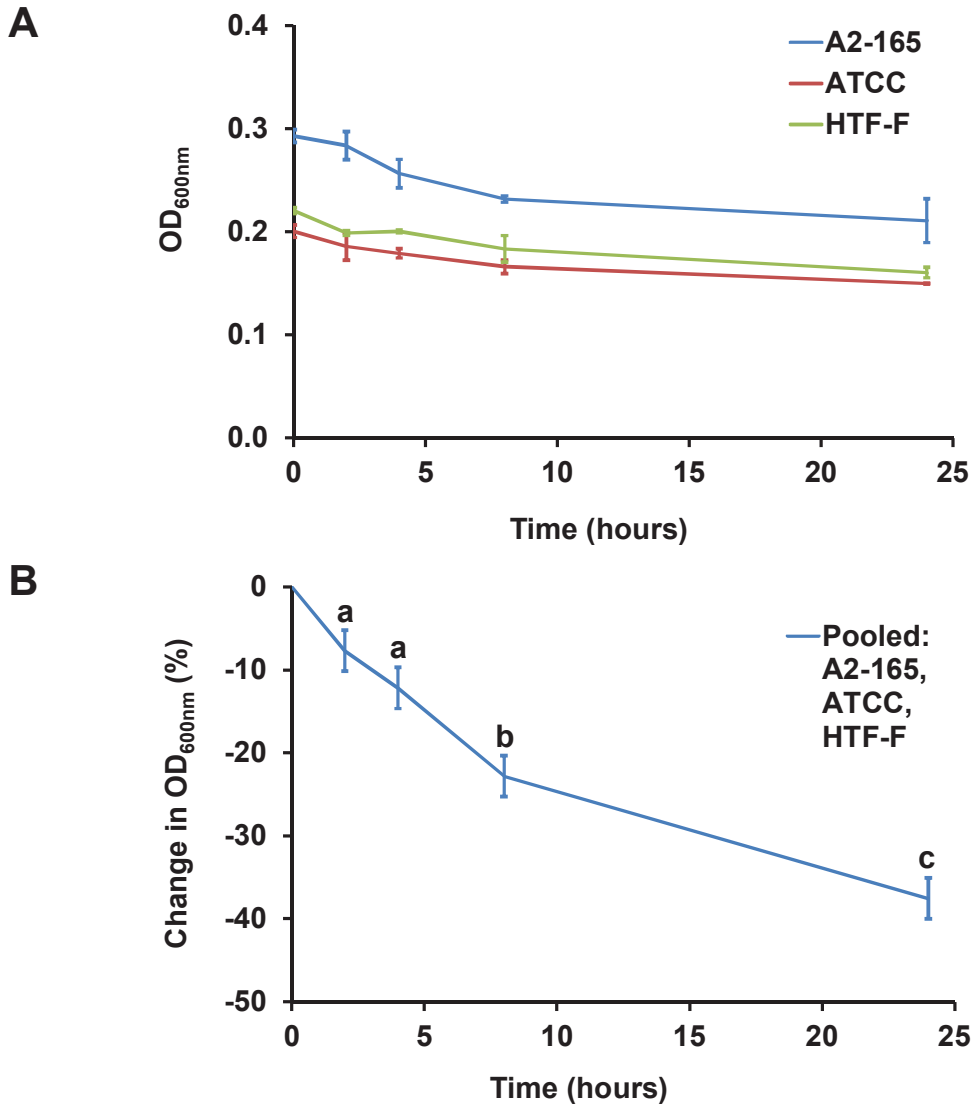

Figure 4.8 OD_{600nm} (A) and normalised change in OD_{600nm} (%) (B) of the three *F. prausnitzii* strains in anaerobic cell culture medium (DMEM).

The three *F. prausnitzii* strains (A2-165, ATCC 27768 and HTF-F) were resuspended in stationary phase in anaerobic DMEM and incubated at 37°C. The OD_{600nm} was measured over 24 h: (A) Mean (± SEM; n = 3) OD_{600nm} for each of the three *F. prausnitzii* strains over 24 h; (B) Percent change in OD_{600nm} (± SEM; n = 3) after normalising by the OD_{600nm} at time 0 h. The normalised data was used for the statistical analysis because of the different starting OD_{600nm}. There was no significant interaction between strain and time, therefore this interaction was removed from the statistical model. The pooled data from three strains are shown in this graph. Time points with different letters are significant different to previous time points ($P < 0.05$).

4.4.4. Viability of the *F. prausnitzii* strains in cell culture medium supplemented with acetate

The first approach to improve the growth of *F. prausnitzii* in anaerobic DMEM was to supplement the cell culture medium with acetate which was previously reported as an important substrate for the growth of *F. prausnitzii* [178]. The secondary cultures of the three *F. prausnitzii* strains in stationary phase were resuspended in anaerobic DMEM (referred to as control) or DMEM supplemented with 33 mM acetate (referred to as acetate). The OD_{600nm} was measured after 2, 4, 8 and 24 h of anaerobic incubation at 37°C to determine if the acetate supplementation enhanced the growth of *F. prausnitzii*. The absolute OD_{600nm} values are shown in Figure 4.9. However, due to the different starting values at 0 h, the statistical analysis was performed after normalising by the OD_{600nm} at 0 h for each strain in each medium as shown in Figure 4.10. There was a significant interaction between the strain, time and medium ($P = 0.01$). For *F. prausnitzii* ATCC 27768 there was a greater drop in the OD_{600nm} at all time points for acetate compared to the control media ($P < 0.05$). The other *F. prausnitzii* strains (A2-165 and HTF-F) did not show differences in the change in OD_{600nm} between the control and acetate media at any time point ($P > 0.05$). The supplementation with acetate therefore did not improve the viability of the *F. prausnitzii* strains in anaerobic DMEM.

4.4.5. Viability of the *F. prausnitzii* strains in cell culture medium supplemented with bacterial culture medium

The next approach to improve the growth of the three *F. prausnitzii* strains was to supplement cell culture medium with bacterial culture medium. The supplementation of anaerobic cell culture medium M199 TEER with 50% of anaerobic BHI enabled growth of *F. prausnitzii* A2-165 and *F. prausnitzii* ATCC 27768 in co-culture with Caco-2 cells in

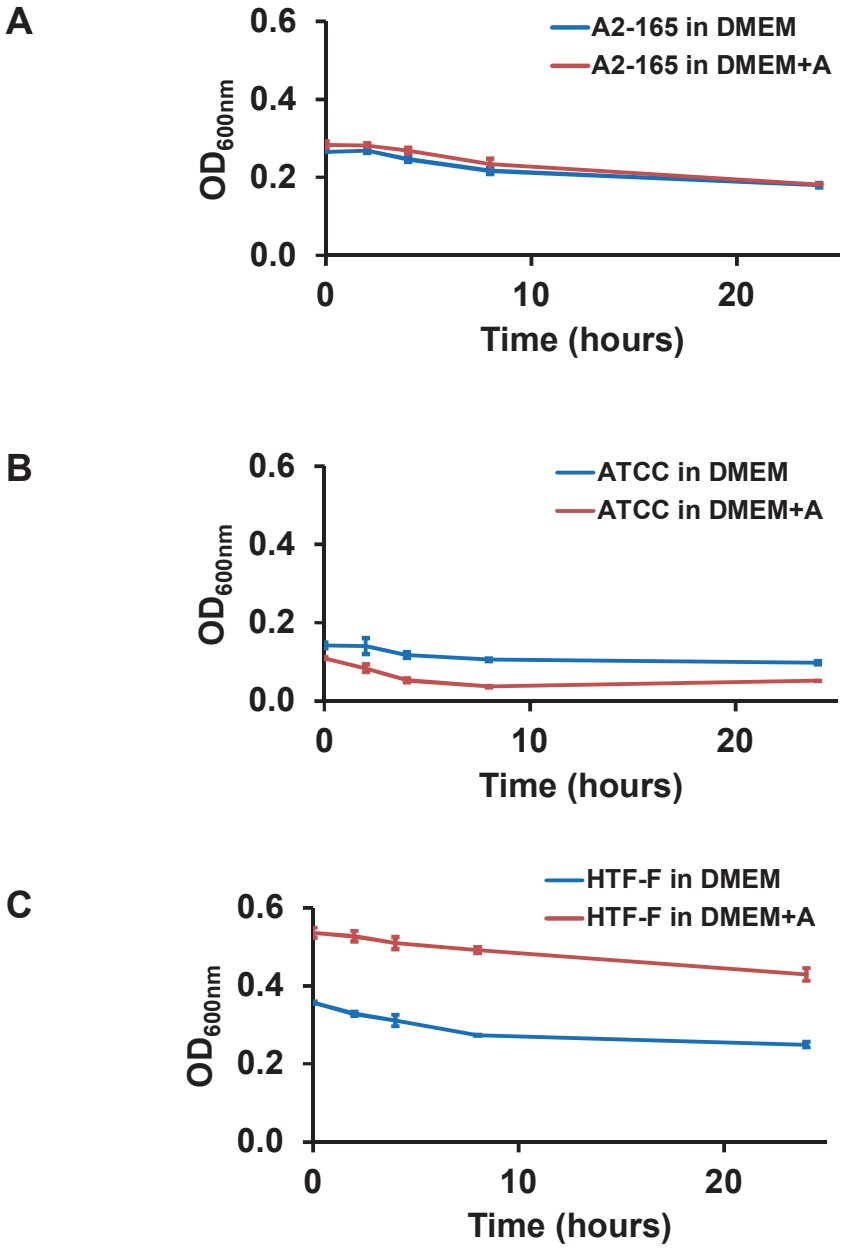

Figure 4.9 OD_{600nm} of the three *F. prausnitzii* strains in anaerobic DMEM with or without acetate supplementation.

Secondary cultures of the three *F. prausnitzii* strains ((A) A2-165, (B) ATCC 27768 and (C) HTF-F) in stationary phase were resuspended in anaerobic DMEM or anaerobic DMEM supplemented with 33 mM acetate (DMEM+A) and incubated at 37°C for 24 h. The graphs show the mean (± SEM; n = 3) OD_{600nm} over time for each of the three *F. prausnitzii* strains.

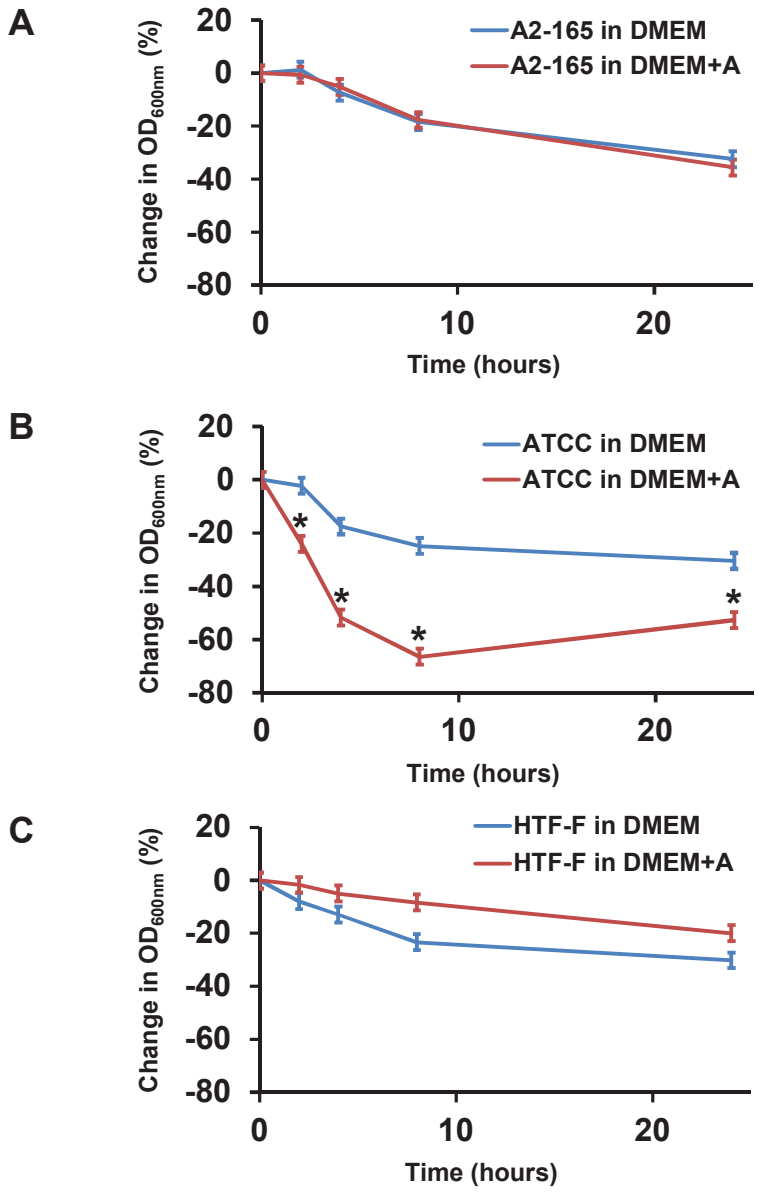

Figure 4.10 Normalised change in OD_{600nm} (%) of the three *F. prausnitzii* strains in anaerobic DMEM with or without acetate supplementation.

Secondary cultures of the three *F. prausnitzii* strains ((A) A2-165, (B) ATCC 27768 and (C) HTF-F) in stationary phase were resuspended in anaerobic DMEM or anaerobic DMEM supplemented with 33 mM acetate (DMEM+A). The bacterial solutions were incubated at 37°C and the OD_{600nm} was measured over 24 h. The mean values (± SEM; n = 3) were obtained after normalising by the OD_{600nm} at 0 h for each strain in each medium. There was a significant interaction between the strain, time and medium (P = 0.01). * Mean OD_{600nm} values for each *F. prausnitzii* strain differ significantly between acetate and control media for this time point at $P < 0.05$.

the apical anaerobic co-culture model. In order to optimise the growth of the *F. prausnitzii* strains with HEK293-TLR-Luc cells, anaerobic DMEM+FBS, the medium used to culture these cells, was therefore also supplemented with 50% of anaerobic BHI, referred to as DMEM+BHI.

Secondary cultures of the three *F. prausnitzii* strains in stationary phase were resuspended in DMEM+BHI at a density of 1.5 x 10^7 bacterial cells/mL. A bacterial solution of this density equals a MOI of 10, as the HEK293-TLR2-Luc cells were seeded at a density of 1.5 x 10^6 cells/mL. In general, the MOI is determined using the cell density at the time of the treatment. However since the HEK293-TLR2-Luc cells were only seeded the day before the assay, the seeding density was used to calculate the MOI. The bacterial cultures were incubated anaerobically at 37°C and the OD_{600nm} was measured over 12 h.

The absolute OD_{600nm} values are shown in Figure 4.11A. The statistical analysis was performed after normalising by the OD_{600nm} at 0 h because of the different starting OD_{600nm}. There was a significant interaction between the strain and time ($P = 0.004$). As shown in the change in the OD_{600nm} (Figure 4.11B), *F. prausnitzii* A2-165 did not grow in this medium over 12 h of incubation. However, the other *F. prausnitzii* strains, ATCC 27768 and HTF-F, both showed a significant increase in the OD_{600nm} after 12 h ($P < 0.05$).

4.4.6. Toll-like receptor activation assay with Transwell inserts

The first step to adapt the TLR activation assay to the apical anaerobic co-culture model was performing the assay with HEK293-TLR2-Luc cells seeded onto the membranes of Transwell inserts because these were used in the co-culture chamber. This was first performed in conventional conditions (5% CO_2 in air atmosphere) in order to change only one factor at a time.

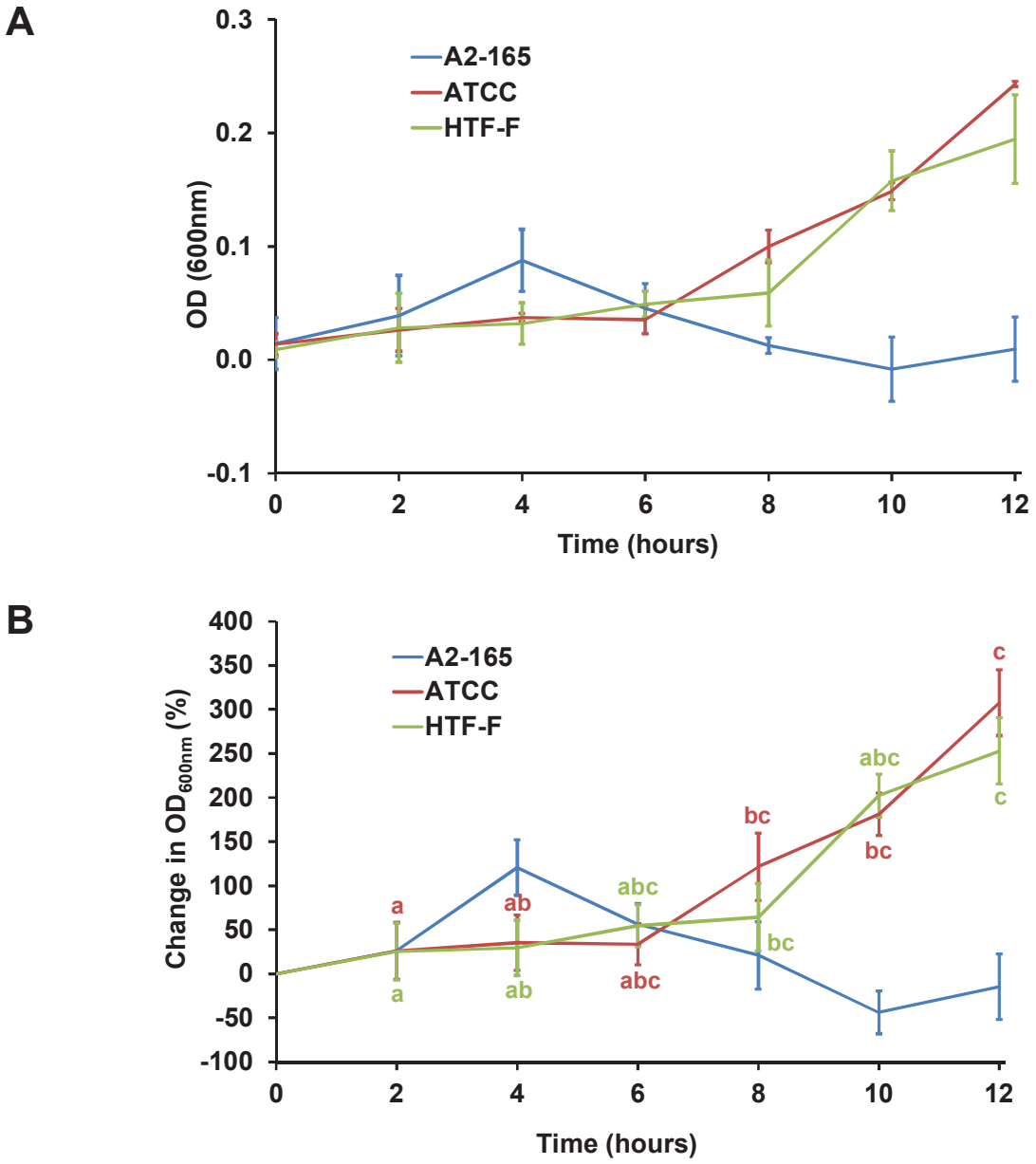

Figure 4.11 Viability of the three *F. prausnitzii* strains in cell culture medium (DMEM+FBS) supplemented with bacterial culture medium (BHI).

The three *F. prausnitzii* strains (A2-165, ATCC 27768 and HTF-F) in stationary phase were resuspended in anaerobic DMEM+FBS supplemented with 50% BHI, incubated anaerobically at 37°C and the OD_{600nm} was measured over 12 h. Graphs show (A) the mean (± SEM; n = 3) OD_{600nm} for each of the three *F. prausnitzii* strains over 12 h and (B) the mean values (± SEM; n = 3) after normalising by the OD_{600nm} at time 0 h. The statistical analysis was performed using the normalised change in OD_{600nm} because of the different starting OD_{600n}. There was a significant interaction between the strain and the time ($P = 0.004$). The time points that do not share the same letters for each curve are significantly different ($P < 0.05$).

HEK293-TLR2-Luc cells seeded in Transwell inserts were stimulated with a positive control (HKLM, 10^8 cells/mL) and a negative control (sterile endotoxin free water). Following 24 h of incubation, the cells were transferred to a 96-well plate for the luminescence quantification using two different methods. For the first technique (referred to as Inserts A), 120 µL of the apical medium was removed from the inserts. The remaining medium was used to remove the cells from the membrane by pipetting the medium up and down. The cell suspension was transferred to a 96-well assay plate and the luminescence signal upon receptor activation was quantified using the Bright-Glo reagent as described in 4.3.4. For the second technique (referred to as Inserts B), 120 µL of the apical medium were removed from the inserts and 100 µL of the Bright-Glo reagent were added. The cell suspension was mixed with the Bright-Glo reagent, which also removed the cells from the membranes. This mixture was transferred into a 96-well assay plate and the luminescence signal upon receptor stimulation was measured using a plate reader as described in 4.3.4. The results were compared to a standard TLR activation assay performed on a 96-well plate. All of the three assay conditions resulted in a significant TLR2 activation by the positive control compared to the negative control as shown in Figure 4.12 ($P < 0.001$).

4.4.7. Approaches to improve the attachment of HEK293-TLR2-Luc cells in the apical anaerobic co-culture model

Various approaches were tested to improve the attachment of HEK293-TLR2-Luc cells in the co-culture model as summarised in Table 4.3. In addition, different apical medium compositions were tested in these experiments in order to improve the growth of *F. prausnitzii* co-cultured with HEK293-TLR2-Luc cells. For all of these experiments a

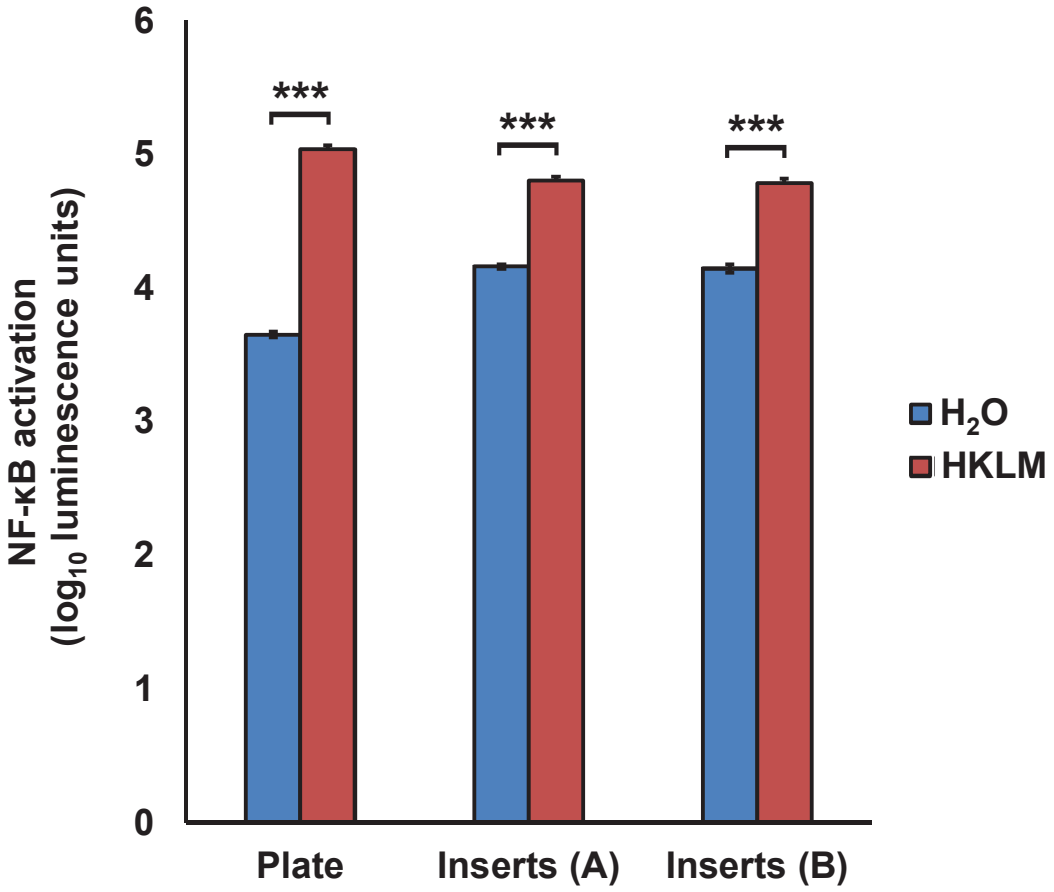

Figure 4.12 TLR activation assay using Transwell inserts.

HEK293-TLR2-Luc cells were seeded in a 96-well plate or in Transwell inserts and stimulated with a positive control (HKLM, 10^8 cells/mL) or a negative control (sterile endotoxin free water). The TLR2 activation was determined after 24 h of incubation with the treatments using two different techniques to transfer the cells from the inserts to a 96-well plate for the luminescence quantification (referred to as Inserts (A) and Inserts (B)). The graph shows the mean (± SEM, n = 3) $\log_{10}$ luminescence units following TLR2 activation. *** TLR2 activation significantly different ($P < 0.001$).

Table 4.3 Summary of experiments to improve the attachment of HEK293-TLR2-Luc cells in the co-culture model.

Approach	Apical medium (anaerobic)	Incubation time	Seeding density (cells/mL)	TrypLE	Collagen-coating	Detached/disrupted cell layers	Viability compared to conventional conditions
A	DMEM+FBS, M199 TEER, M199 TEER+BHI mixtures	12 h	1.5×10^6	No	No	88%	Not different (P = 0.69)
B	DMEM+FBS	12 h	7.5×10^5	No	No	83%	N/A
C	DMEM+FBS	6 h	1.5×10^6	Yes	No	83%	Not different (P = 0.98)
D	DMEM+FBS	6 h	1.5×10^6	Yes	Yes	0%	Not different (P = 0.07)
E	DMEM+FBS, M199 TEER, M199 TEER+BHI mixtures	6 h	1.5×10^6	Yes	Yes	8%	Not different (P = 0.19)

control with cells treated with aerobic DMEM+FBS and incubated in conventional conditions (5% CO_2 in air atmosphere, 37°C) was included.

In approach A the viability and attachment of HEK293-TLR2-Luc cells on Transwell inserts used in the apical anaerobic co-culture model and exposed to different apical medium compositions (DMEM+FBS, M199 TEER, and M199 TEER supplemented with 25, 50, 75 and 100% BHI) was determined (n = 4 per treatment). Following 12 h of incubation in the apical anaerobic co-culture model the majority (88%) of the cell layers were disrupted or detached from the membranes of the inserts.

For the approaches B to D anaerobic DMEM+FBS was used as apical medium, because the attachment had to be enhanced first before testing different apical medium compositions again. In approach B a lower seeding density (7.5 x 10^5 cells/mL) compared to the one used in approach A (1.5 x 10^6 cells/mL) was tested (n = 6). In this approach the cells were used three days after seeding instead of one day. The rationale was that by using a lower seeding density and a longer incubation period before performing the assay, the cells will form a monolayer rather than a multilayer which was observed when using the high seeding density. When Transwell inserts containing multilayers of cells are inserted into the co-culture chamber, the pressure due to the tightness of the cell layers may be too high, even when using pressure relief valves. This may cause the detachment or disruption of the cell layers. Hence, it was hypothesised that using cells forming a monolayer on the Transwell inserts prevents this technical difficulty. Additionally, a monolayer would also represent the natural growth and morphology of HEK293 cells. However, this attempt was not successful, following 12 h of incubation in apical anaerobic conditions 83% of the cell layers detached or were disrupted, whereas in conventional conditions all cell layers were still intact.

In approach C a shorter incubation time (6 instead of 12 h) and the use of the dissociation reagent TrypLE when harvesting the cells were tested to enhance the cell attachment in the apical anaerobic co-culture model. During the initial culture of the HEK293-TLR cells and the stable transfection, the passaging of the cells was performed without the use of trypsin, a proteolytic enzyme commonly used in cell culture for detaching adherent cells from the surface of the cell culture flask. Instead, the cells were removed from the bottom of the flask by flushing them down with cell culture medium. The cell suspension was then centrifuged, the supernatant discarded and the pellet was resuspended in fresh culture medium. This method was preferred instead of using trypsin, as the supplier's protocol (Invivogen, San Diego, USA) states that the response of HEK293-TLR cells may be altered by the action of trypsin. However, when passaging the cells without trypsin, cell clumps remained in the solution even after thorough resuspension of the cell pellet. This led to difficulties in the accurate determination of the cell density and in the formation of multi-layered cell structures when seeding the cells in Transwell inserts. It was anticipated that by using trypsin, in this case TrypLE (Life Technologies, Auckland, New Zealand), a recombinant cell dissociation enzyme, the cells would be dissociated into a single cell suspension which would result in the formation of a monolayer rather than a multilayer when the cells are seeded in inserts. It was necessary to first test if the use of TrypLE affected the response of the HEK293-TLR2-Luc cell line. The luminescence signal in response to the stimulation of HEK293-TLR2-Luc cells with a positive control and a negative control (HKLM, 10^8 cells/mL and sterile endotoxin free water, respectively) was compared using cells harvested with and without TrypLE ($n = 6$).

As shown in Figure 4.13 there was a significant TLR2 activation by the positive control compared to the negative control when using cells harvested with and without using TrypLE ($P < 0.001$). For approach C HEK293-TLR2-Luc cells harvested with TrypLE and

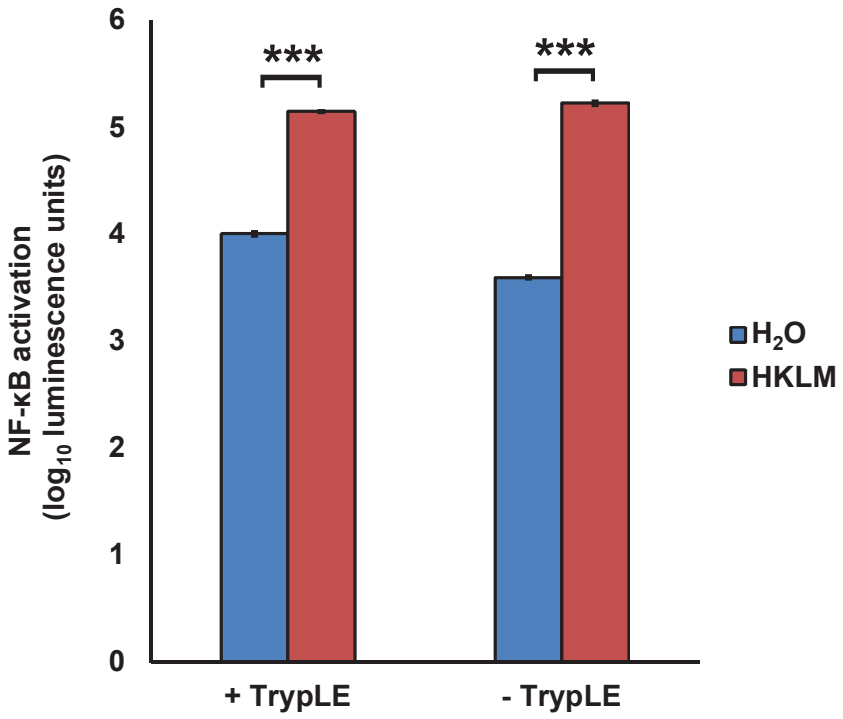

Figure 4.13 TLR activation assay using cells harvested with or without TrypLE.

HEK293-TLR2-Luc cells were harvested with and without the use of the dissociation reagent TrypLE, seeded into a 96-well plate and stimulated with a positive control (HKLM, 10^8 cells/mL) and a negative control (sterile endotoxin free water). Following 24 h of incubation the luminescence signal upon TLR2 activation was determined. The graph shows the mean (± SEM, n = 6) $\log_{10}$ luminescence units following TLR2 activation. *** TLR2 activation significantly different ($P < 0.001$).

seeded in inserts were then tested in the apical anaerobic co-culture model for 6 h of incubation (n = 6). It was anticipated that with an incubation time of 12 h the HEK293-TLR2-Luc cell layers detach because they are overgrown and start to peel off from the border of the inserts, which does not occur when incubating for 6 h. However, this approach did not enhance cell attachment, 83% of the cell layers detached or were disrupted after 6 h.

The next approach to enhance the cell attachment (approach D) was to use HEK-TLR2-Luc cells harvested with TrypLE and seeded in Transwell inserts coated with collagen I, an extracellular matrix protein often used in cell culture to enhance cell attachment and proliferation [303,304] (n = 6). This approach was successful as all cell layers were still attached after 6 h of incubation in apical anaerobic conditions using anaerobic DMEM+FBS on the apical side.

After achieving improved cell attachment using DMEM+FBS as apical medium, the effect of different apical medium compositions on the cell attachment and viability was tested again using the adapted conditions (harvesting the cells using TrypLE, 6 h incubation and collagen-coated inserts, approach E). The apical medium compositions were DMEM+FBS, M199 TEER, 75% M199 TEER+25% BHI, 50% M199 TEER+50% BHI, 25% M199 TEER+75% BHI and BHI as in approach A. This experiment was performed three times using four replicates per treatment (total n = 12). Following 6 h of incubation only 8% of the cell layers detached. However, when visualising the cell layers under a light microscope, the cell layers treated with 25% M199 TEER+75% BHI and 100% BHI had a porous structure. Figure 4.14A shows a typical light micrographic image of HEK293-TLR2-Luc cells exposed to 100% BHI in the apical anaerobic co-culture model for 6 h showing several intermittent voids within the cell layer. This problem was not observed

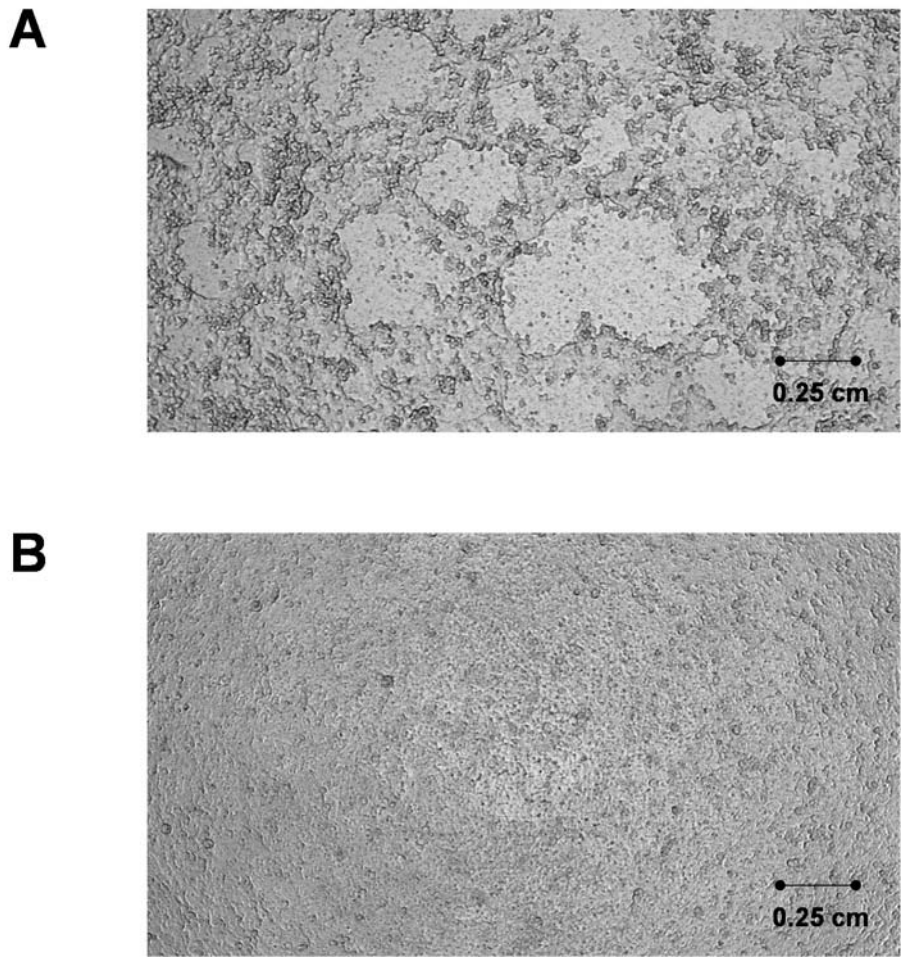

Figure 4.14 HEK293-TLR2-Luc cells exposed to bacterial culture medium and a mixture of cell and bacterial culture media in the apical anaerobic co-culture model.

Typical light micrographic images of HEK293-TLR2-Luc cells grown on collagen-coated Transwell inserts and incubated for 6 h in the apical anaerobic co-culture model with (A) 100% BHI and (B) 50% M199 TEER+50% BHI as apical culture medium.

when 50% M199 TEER+50% BHI was used as apical medium as shown in Figure 4.14B.

In general, there was no difference between the viability of HEK293-TLR2-Luc cells incubated in apical anaerobic conditions compared to conventional conditions for all of the above described experiments as summarised in Table 4.3. In addition, when using the adapted conditions there was no difference between the viability of cells treated with different apical medium compositions (DMEM+FBS, M199 TEER, 75% M199 TEER+25% BHI, 50% M199 TEER+50% BHI, 25% M199 TEER+75% BHI and BHI in apical anaerobic conditions and DMEM+FBS and M199 TEER in conventional conditions) as shown in Figure 4.15 ($P = 0.19$).

4.4.8. Toll-like receptor activation assay in apical anaerobic conditions

In order to test if the TLR activation assay could be performed in apical anaerobic conditions, HEK-TLR2-Luc cells seeded on collagen-coated Transwell inserts were stimulated with a positive control (HKLM, 10^8 and 10^9 cells/mL) and a negative control (sterile endotoxin free water) using the co-culture model. In addition, the TLR2 stimulation was conducted in conventional conditions using HEK293-TLR2-Luc cells grown on Transwell inserts placed in a 24-well culture plate. Figure 4.16A shows the TLR2 activation after 6 h in both conventional and apical anaerobic conditions. However, because there was no significant interaction between the environment and the treatment, this interaction was removed from the statistical model and only the effects of the main factors (environment and treatment) were analysed. There was a significant treatment effect ($P < 0.001$). Figure 4.16B shows the pooled data from conventional and apical anaerobic conditions. The luminescence signal obtained after treatment with HKLM (10^8 cell/mL) was higher than that obtained after treatment with the negative control, and the

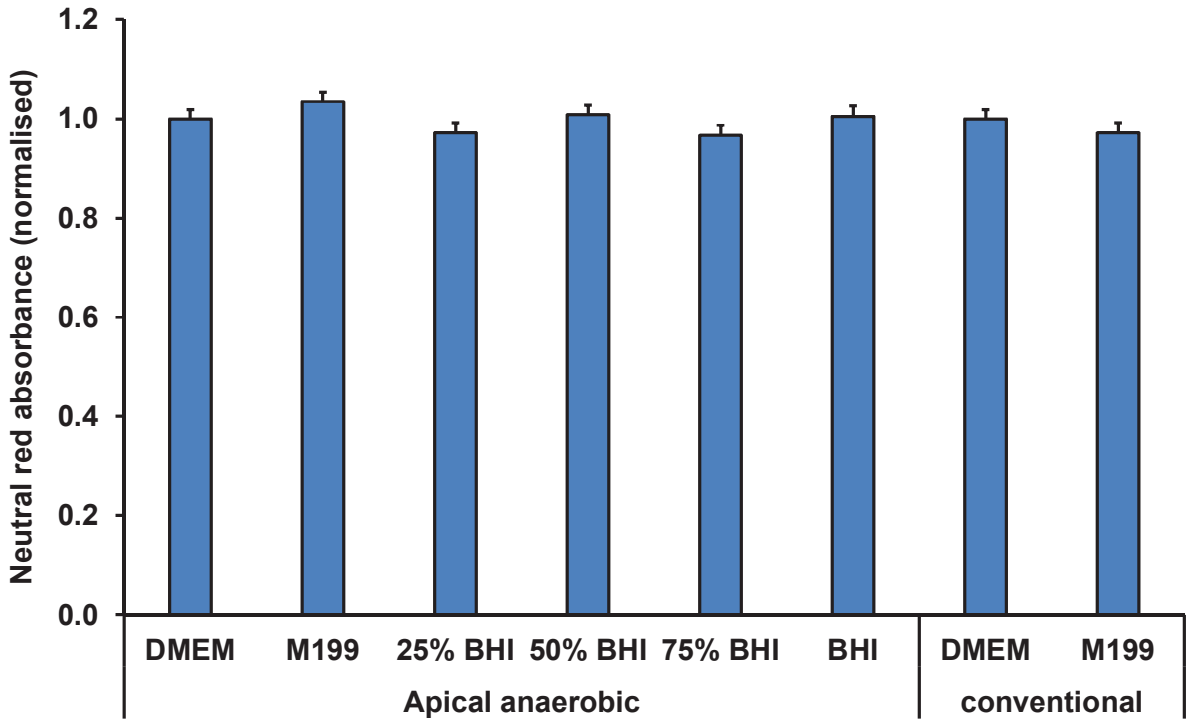

Figure 4.15 Viability of HEK293-TLR2-Luc cells exposed to different apical media in apical anaerobic and conventional conditions.

HEK293-TLR2-Luc cells in the apical anaerobic co-culture model were exposed on the apical side to anaerobic DMEM+FBS, M199 TEER, 75% M199 TEER+25% BHI, 50% M199 TEER+50% BHI, 25% M199 TEER+75% BHI and BHI. In addition, HEK293-TLR2-Luc cells were exposed to DMEM+FBS and M199 TEER in conventional conditions. The graph shows the normalised viability (mean ± SEM; n = 9) of HEK293-TLR2-Luc cells after 6 h of incubation with the treatments. The neutral red absorbance was normalised by adjusting the control cells (treated with DMEM+FBS) to 1 for each environment (apical anaerobic or conventional). There were no differences between the viability of HEK293-TLR2-Luc cells exposed to the different media in different environments ($P = 0.19$).

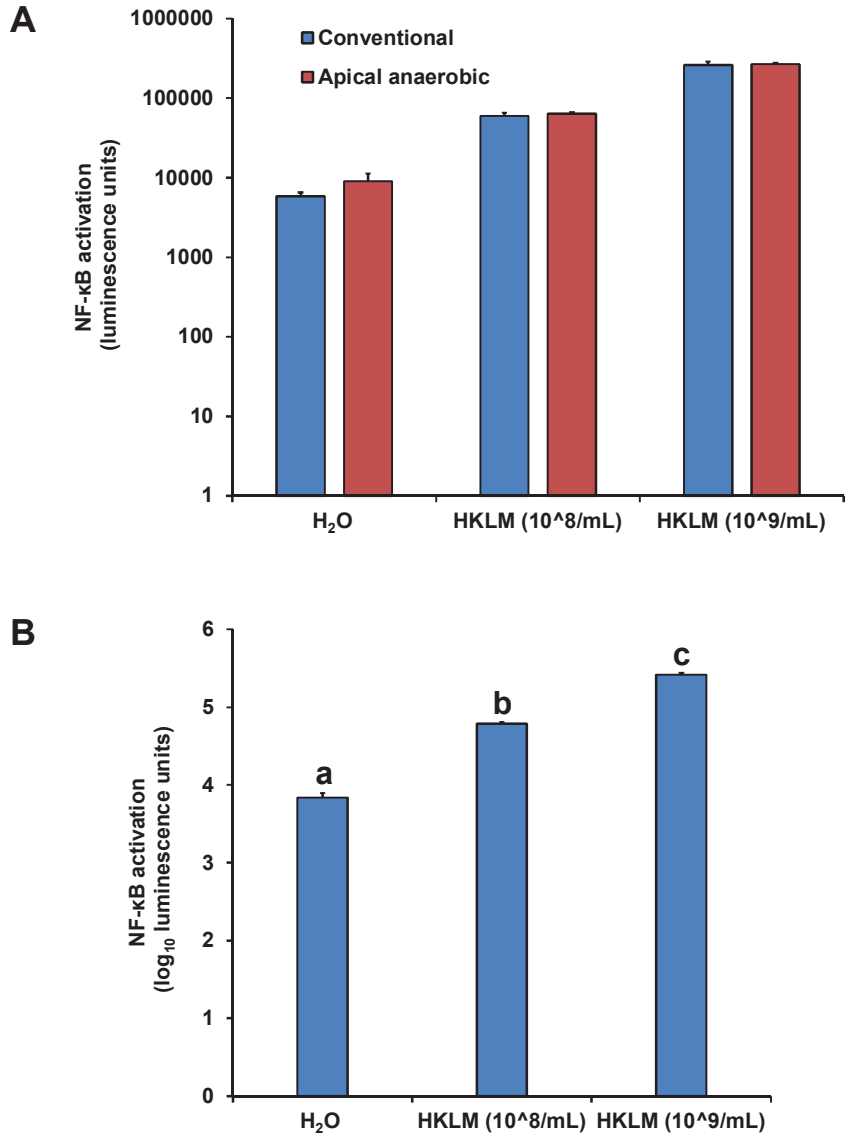

Figure 4.16 TLR activation assay in conventional and apical anaerobic conditions.

HEK293-TLR2-Luc cells were stimulated with a positive control in two different concentrations (HKLM, 10^8 and 10^9 cells/mL) and a negative control (sterile endotoxin free water) in conventional and apical anaerobic conditions. Following 6 h of incubation with the treatments the luminescence was measured. (A) Mean (± SEM; n = 4) luminescence units following TLR2 activation in conventional and apical anaerobic conditions. There was no significant interaction between the environment and the treatment therefore it was removed from the statistical model. (B) This graph shows the mean (± SEM; n = 4) $\log_{10}$ luminescence units from the pooled data from conventional and apical anaerobic conditions. Treatments that do not share the same letters are significantly different ($P < 0.05$).

signal from HKLM (10^9 cells/mL) treated cells was higher than those exposed to the two other treatments ($P < 0.05$). The luminescence signals after stimulation with the positive control in different concentrations therefore represented a dose-dependent response as expected. The effect of the environment was not significant ($P = 0.25$).

4.4.9. Apical and basal dissolved oxygen concentrations

The apical and basal DO concentrations of HEK293-TLR2-Luc cells incubated in the apical anaerobic co-culture model were measured to determine if sufficient oxygen remained in the basal compartment over the 6 h of incubation and if oxygen leaked from the basal to the apical side. The culture media used were aerobic DMEM+FBS in the basal compartment and anaerobic 50% M199 TEER+50% BHI in the apical compartment.

After the 6 h of incubation several HEK293-TLR2-Luc cell layers were disrupted in which case the basal medium passed through to the apical compartment. The apical DO concentrations of the disrupted cell layers were compared to those that remained intact throughout the 6 h of incubation. The obtained DO values were expressed as the percentage of aerobic cell culture medium.

There was a significant interaction between the status (intact or disrupted cell layers) and the time ($P = 0.005$). No oxygen was detected in the apical compartment of intact HEK293-TLR2-Luc cell layers. In contrast, oxygen was detected in the apical compartment of the disrupted HEK293-TLR2-Luc cell layers, however, the concentration was low. The highest DO concentration was observed at the beginning of the experiment ($t = 0$ h) to be $1.1 \pm 0.2\%$. The DO concentrations in the apical compartment of disrupted cell layers were significantly higher than those of intact cell layers at the start of the experiment ($t = 0$ h) and after 1 and 4 h of incubation ($P < 0.05$).

The basal DO levels dropped significantly at every time point of the hourly measurements as shown in Figure 4.17 ($P < 0.05$). In the first 2 h the DO concentration dropped approximately 9% per hour. Subsequently, the DO concentrations dropped less per hour, with 7% after the third and fourth hour of incubation to 6% and 5% after the fifth and sixth hour, respectively. Following the 6 h of incubation of the HEK293-TLR2-Luc cells in the apical anaerobic co-culture model (the duration of the TLR activation assays), 57.9% ± 1.9 of the starting DO concentration remained in the basal compartment.

4.4.10. Viability of *F. prausnitzii* A2-165 in co-culture with HEK293-TLR2-Luc cells with different apical medium compositions

F. prausnitzii A2-165 was co-cultured with HEK293-TLR2-Luc cells in the apical anaerobic co-culture model using DMEM+FBS, M199 TEER, 75% M199 TEER+25% BHI, 50% M199 TEER+50% BHI, 25% M199 TEER+75% BHI and BHI on the apical side. The CFU of the bacteria before and after 6 h of incubation with HEK293-TLR2-Luc cells was determined. No bacteria grew from the cell lysate, therefore it was concluded that *F. prausnitzii* A2-165 did not attach to the cells.

For all six apical medium compositions tested there was a significant drop in the CFU of *F. prausnitzii* A2-165 after 6 h of co-culture with HEK293-TLR2-Luc cells as shown in Figure 4.18 ($P < 0.01$). In order to test if the different apical medium compositions had an influence on the viability of *F. prausnitzii* A2-165, the CFU after 6 h (the duration of the TLR activation assay) were compared (Figure 4.19). There was a significant difference between the CFU of *F. prausnitzii* A2-165 when cell culture medium alone (DMEM+FBS and M199 TEER) was used as apical medium compared to when using bacterial culture medium (BHI) or mixtures of M199 TEER and BHI ($P < 0.001$). The addition of bacterial culture medium to the apical medium (75% M199 TEER+25% BHI, 50% M199

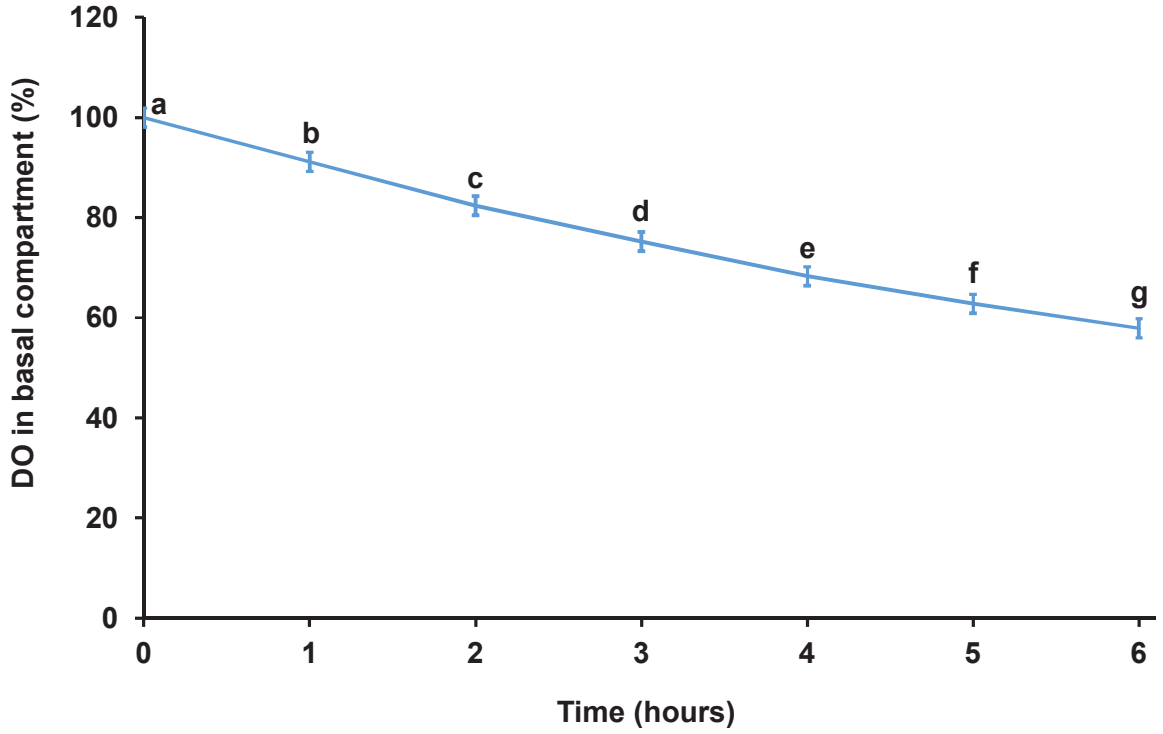

Figure 4.17 Basal DO levels when incubating HEK293-TLR2-Luc cells in the apical anaerobic co-culture model.

HEK293-TLR2-Luc cell layers seeded on Transwell inserts were inserted into the apical anaerobic co-culture model and the apical medium was replaced with anaerobic 50% M199 TEER+50% BHI. Aerobic DMEM+FBS was used as medium on the basal side of the cell layers. The basal DO concentrations were measured hourly over 6 h. The graph shows the mean (± SEM; n = 3) percentage of basal DO compared to the starting values. Time points which do not share the same letters are significantly different ($P < 0.05$).

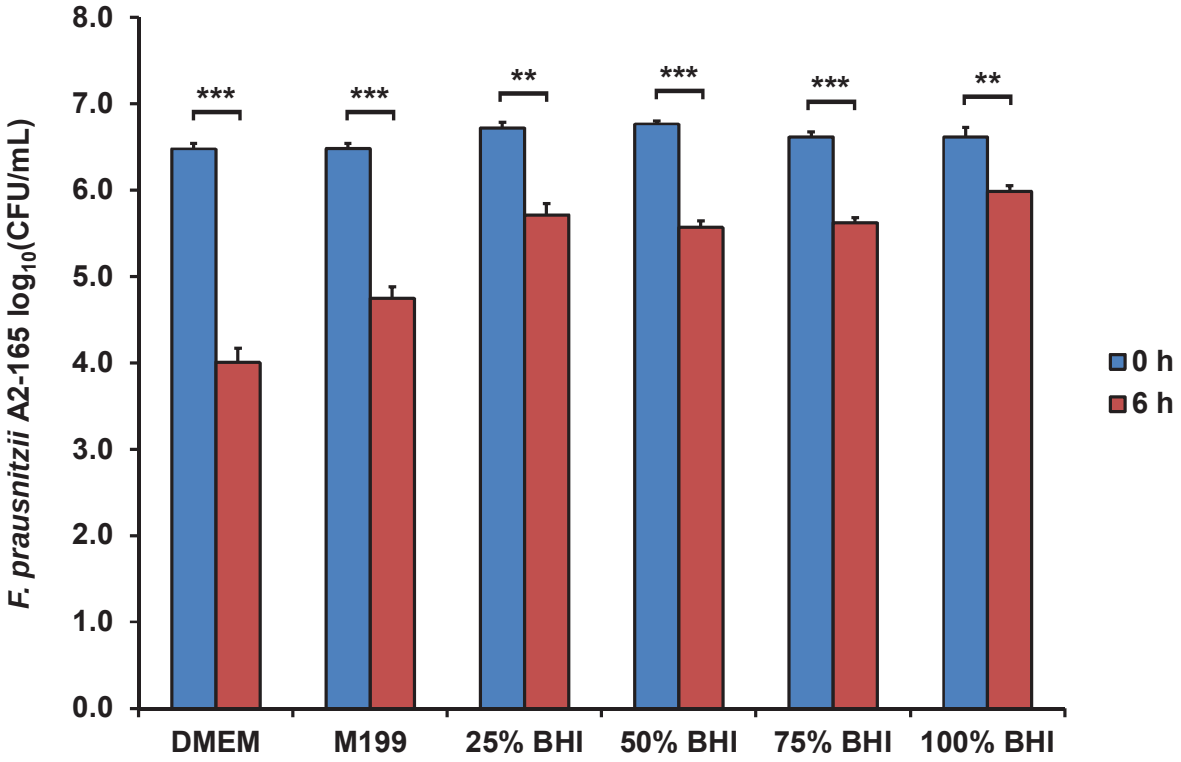

Figure 4.18 Viability of *F. prausnitzii* A2-165 before and after the co-culture with HEK293-TLR2-Luc cells in the apical anaerobic co-culture model.

F. prausnitzii A2-165 was co-cultured for 6 h with HEK293-TLR2-Luc cells using different apical media (DMEM+FBS, M199 TEER, 75% M199 TEER+25% BHI, 50% M199 TEER+50% BHI, 25% M199 TEER+75% BHI and BHI). The graph shows the mean (± SEM; n = 3 and 10 for time 0 and 6 h, respectively) $\log_{10}$(CFU/mL) of the bacteria at 0 and 6 h of incubation with HEK293-TLR2-Luc cells in the co-culture model. Mean $\log_{10}$(CFU/mL) differ between 0 and 6 h at ** $P < 0.01$ and *** $P < 0.001$. The bacterial treatments were added to four inserts with HEK293-TLR2-Luc cells, however, several cell monolayers were disrupted after the 6 h of incubation. For these reasons the number of observations differed between time 0 and 6 h.

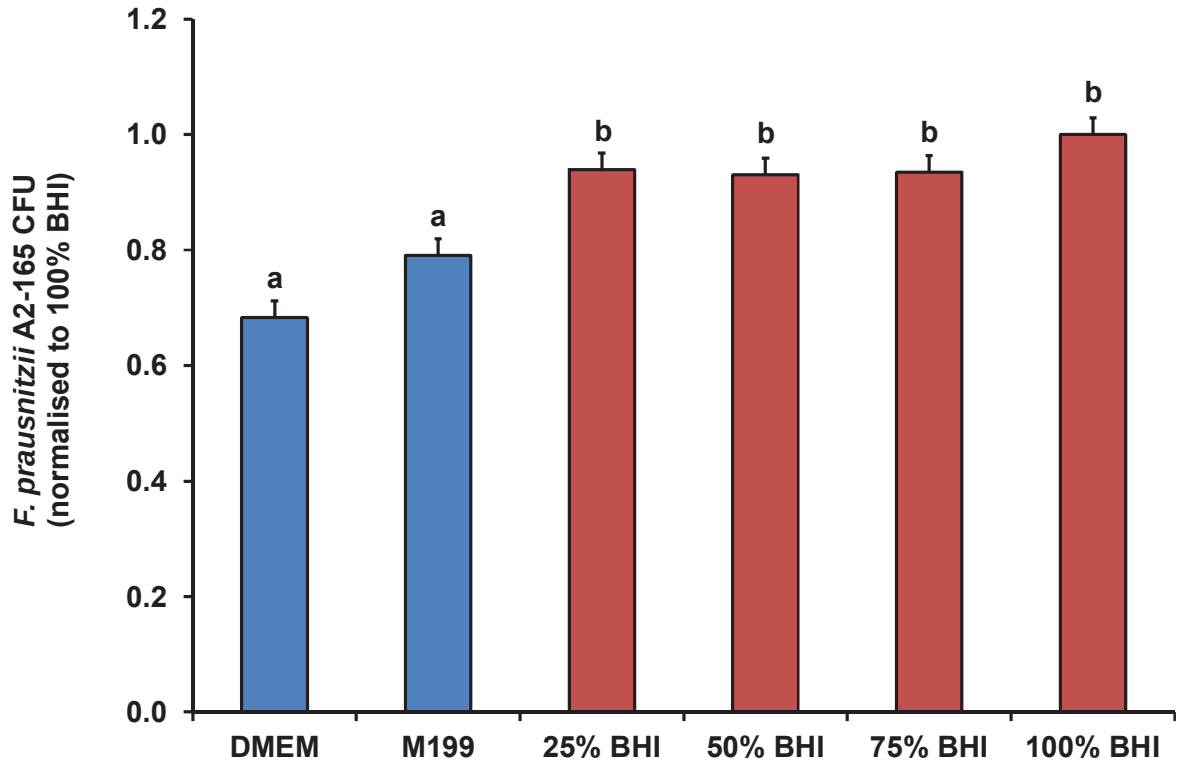

Figure 4.19 Viability of *F. prausnitzii* A2-165 after 6 h of co-culture with HEK293-TLR2-Luc cells in the apical anaerobic co-culture model.

The CFU of *F. prausnitzii* A2-165 after 6 h of co-culture with HEK293-TLR2-Luc cells using different apical media (DMEM+FBS, M199 TEER, 75% M199 TEER + 25% BHI, 50% M199 TEER + 50% BHI, 25% M199 TEER + 75% BHI and BHI) were compared. The graph shows the normalised mean (± SEM; n = 12) $\log_{10}$(CFU/mL) of *F. prausnitzii* A2-165 after 6 h of incubation with HEK293-TLR2-Luc cells in the co-culture model. The $\log_{10}$ transformed CFU/mL were normalised against the values obtained with 100% BHI as this is the medium used to grow *F. prausnitzii* A2-165. Treatments that do not share the same letters are significantly different ($P < 0.05$). Bars in blue colour indicate the use of cell culture media for the co-culture of *F. prausnitzii* A2-165 with HEK293-TLR2-Luc cells and bars in red colour indicate the use of bacterial culture medium or mixtures of cell and bacterial culture media.

TEER+50% BHI, 25% M199 TEER+75% BHI and 100% BHI) increased the *F. prausnitzii* A2-165 viable cell titre on average by approximately one order of magnitude compared to cell culture medium alone (DMEM+FBS and M199 TEER).

4.5. DISCUSSION

In accordance to the hypothesis of this work, the results reported in this thesis chapter showed that it is possible to perform the TLR activation assay in the apical anaerobic co-culture model. Several adaptations were required to conduct this assay in the co-culture model, which included the improvement of the attachment of the HEK293-TLR2-Luc cells by using collagen-coated inserts, a shorter incubation time (6 h instead of 12 h) and the use of TrypLE when harvesting the cells. The viability of the HEK293-TLR2-Luc cells was maintained using the adapted assay conditions. However, the *F. prausnitzii* viable cell titre decreased approximately 100-fold after 6 h of co-culture with HEK293-TLR2-Luc cells when using different cell culture media (DMEM+FBS and M199 TEER) as apical medium. Even though the viability of *F. prausnitzii* was improved when using mixtures of cell culture medium (M199 TEER) and bacterial culture medium (BHI) or 100% BHI as apical medium, there was still an approximate tenfold decrease of *F. prausnitzii* viable cell titre.

As discussed in Chapter 2, *F. prausnitzii* requires complex media to grow. Consistent with this previous chapter, none of the three *F. prausnitzii* strains had the ability to grow in anaerobic cell culture medium, in this case DMEM, and the supplementation with acetate did not improve the growth. When using the Caco-2 cell culture medium, M199 TEER, supplemented with 50% of the bacterial culture medium BHI, all of the three *F. prausnitzii* strains showed an increase in the OD_{600nm} over 12 h of incubation. However, when using the HEK293-TLR-Luc cell culture medium, DMEM+FBS, supplemented with 50% BHI,

only *F. prausnitzii* ATCC 27768 and HTF-F showed an increase in the OD_{600nm} over 12 h, no difference was observed for *F. prausnitzii* A2-165. This was unexpected as *F. prausnitzii* A2-165 had the fastest growth rate compared to the other strains. As the mixture of M199 TEER and BHI allowed better growth of the three *F. prausnitzii* strains than the mixture of DMEM+FBS and BHI, it was decided to use M199 TEER supplemented with BHI as the apical medium for both Caco-2 and HEK293-TLR-Luc cells.

The main technical difficulty of performing the TLR activation assay in the apical anaerobic co-culture model was the pressure on the HEK293-TLR2-Luc cell layer when the inserts were transferred into the co-culture chamber. Every well of the co-culture chamber is equipped with a one-way pressure relief valve and the inserts were carefully transferred into the co-culture chamber using a slow twisting motion to reduce the pressure on the cell layer. Despite these precautions a high percentage of the cell layers, 88% in the first experiment and 83% in the second experiment, detached or were disrupted after 12 h of incubation in the co-culture chamber. This was not observed when HEK293-TLR2-Luc cells on inserts were incubated for 12 h in a 24-well culture plate in conventional conditions (5% CO_2 in air atmosphere), supporting that the pressure in the co-culture model was causing this problem.

The pressure exerted by inserting the inserts into the airtight co-culture model caused the basal aerobic medium to pass through to the apical side of the cell layer and therefore breaching the concept of the dual environment of the apical anaerobic co-culture model. It was observed that this usually happened immediately after the inserts were transferred into the co-culture chamber. Therefore a shorter incubation time did not solve the problem. In addition, approaches to obtain a cell monolayer rather than a multilayer (trying a lower

seeding density or the use of TrypLE when harvesting the cells) did not improve the attachment of the HEK293-TLR2-Luc cells in the co-culture model and the flow of basal medium to the apical side was observed. For all experiments, inserts with basal medium passing through to the apical side were excluded from any subsequent analyses (e.g. neutral red viability assay or luminescence quantification) because the dual environment was not maintained.

The technical issue of basal medium passing through to the apical side was also observed when using Caco-2 cells in the co-culture model, however not as frequent as with HEK293-TLR2-Luc cells. In the case of Caco-2 cells, the inserts where the flow of basal medium to the apical side was observed also had a drop in TEER suggesting a disruption of the TJ. However, Caco-2 cells remained attached to the membranes of the inserts. Caco-2 cells adhere strongly and require the use of dissociation reagents like trypsin for the detachment of culture surfaces. HEK293 cells adhere weakly and easily detach from culture surfaces by pipetting cell culture medium over the cell layer. Therefore HEK293-TLR2-Luc cell layers often detached when exposed to the pressure in the co-culture model, which was improved when using collagen-coated Transwell inserts.

The frequency of detaching of the HEK293-TLR2-Luc cell layers was increased when using BHI or mixtures of M199 TEER and BHI suggesting that BHI disrupted the surface structures of the cells. The cell attachment was improved when using collagen-coated inserts, however, when visualising the cell layers under a light microscope a porous structure of the cell layers treated with 75 and 100% BHI was observed. BHI also disrupted cell structures of Caco-2 cells as shown in thesis chapter 2. Caco-2 cells exposed to high BHI concentrations (75 and 100%) had lower TEER values compared to cells treated with cell culture medium, suggesting that BHI disrupts the TJ integrity. However, this effect

was only observed in apical anaerobic conditions. In contrast, the surface disrupting effect of BHI on HEK293-TLR2-Luc cells was observed in both conventional and apical anaerobic conditions. This suggests that different mechanisms and components of the BHI medium are involved in the surface disrupting effects of BHI on HEK293-TLR2-Luc cells and Caco-2 cells. In a preliminary experiment HEK293-TLR2-Luc cells exposed to 100% BHI detached completely from the culture plate after 12 h of incubation in conventional conditions. The cells had transformed into round-shaped suspension cells similar to what is observed when detaching cells using the dissociation reagent TrypLE. BHI may affect the actin cytoskeleton of the cells, which was shown to be the reason for the morphological differences between adherent and suspended cells [305]. Remarkably, as for Caco-2 cells, the viability of HEK293-TLR2-Luc cells exposed to BHI or mixtures of M199 TEER and BHI was not compromised, suggesting that the viability and the attachment of the cells are independent factors.

The first experiments using HEK293-TLR2-Luc cells in the apical anaerobic co-culture model were performed with an incubation time of 12 h. This time was chosen because the validation and previous applications of this system were performed with 12 h of incubation [19]. Furthermore, assays to determine the TLR activation have been performed using different incubation times with short times such as 4 [306] and 6 h [207] but also longer times such as 16 h [307,308]. However, due to the technical difficulties using HEK293-TLR2-Luc cells in the co-culture model as described above, a shorter incubation time of 6 h was chosen for the method development described in this chapter and the TLR activation assays in chapter 5.

When co-culturing *F. prausnitzii* A2-165 with HEK293-TLR2-Luc cells for 6 h in the co-culture model using cell culture medium (M199 TEER) supplemented with 50% bacterial

culture medium (BHI) on the apical side, a significant decrease in CFU was determined. However, using the same apical medium for the co-culture of Caco-2 cells and *F. prausnitzii* A2-165 resulted in an increase in CFU. One reason for this difference could be the shorter incubation time used for the co-culture of HEK293-TLR2-Luc cells with *F. prausnitzii* compared to the co-culture of Caco-2 cells with *F. prausnitzii* (6 h compared to 12 h). *F. prausnitzii* may also require the mutualistic benefits from IECs to grow in the co-culture model. Mutualism between Caco-2 cells and *F. prausnitzii* has been recently demonstrated using a simple co-culture model [252]. In accordance to the results described in chapter 2 of this thesis, this suggests that the presence of the Caco-2 cells may stimulate the growth of *F. prausnitzii,* for example through Caco-2 secreted mucins [252]. However, the cell lines used for the TLR activation assays are human embryonic kidney cells (HEK293), which were chosen for these experiments as they are known for their high transfection efficiency [309]. In contrast to the co-culture of Caco-2 cells with *F. prausnitzii*, no mutualistic effects between HEK293 cells and *F. prausnitzii* would occur based on the different locations within the human body that the cells and the bacteria originate from.

Another explanation why *F. prausnitzii* A2-165 grew in co-culture with Caco-2 cells but not with HEK293-TLR2-Luc cells, despite using the same apical medium, may be small amounts of oxygen leaking from the basal to the apical side of the cell layer. No oxygen was detected when measuring the apical DO concentrations of intact cell layers. However, the method to determine the DO concentration had the limitation that in the case of oxygen leaking to the apical side it would diffuse quickly due to the anaerobic environment and would therefore not be detected by the DO probe. HEK293-TLR2-Luc cells do not form a tight monolayer compared to a differentiated Caco-2 cell monolayer that are connected by TJ. For this reason it may be possible that small amounts of oxygen could pass from the

basal through to the apical side causing the decreased viability of the obligate anaerobe *F. prausnitzii*. Disrupted HEK293-TLR2-Luc cell layers with basal medium passing through to the apical side were excluded from any further analyses including the determination of the viability of *F. prausnitzii* A2-165 in co-culture with the cells.

Compared to the incubation of Caco-2 cells in the apical anaerobic co-culture model there was a higher drop in the basal DO concentration when incubating HEK293-TLR2-Luc cells in the co-culture model. After 12 h the basal DO concentration was approximately 80% from the starting value when Caco-2 cells were incubated in the co-culture model [19], whereas for HEK293-TLR2-Luc cells a drop to approximately 58% after 6 h was determined. This difference may be due to the higher cell numbers at the time of the experiment when using HEK293-TLR2-Luc cells in the co-culture model compared to the Caco-2 cell numbers (3×10^5 compared to 4×10^4 cells per insert, respectively). The HEK293-TLR2-Luc cells may also have a higher oxygen consumption compared to Caco-2 cells due to their embryonic origin. However, the DO concentration with Caco-2 cells in the apical anaerobic co-culture model was determined using the prototype I of the co-culture chamber and a different DO probe and meter were used, which included a different calibration method. Therefore the DO concentrations obtained when incubating HEK293-TLR2-Luc cells in the co-culture model were not directly comparable to the values obtained when using Caco-2 cells.

In conclusion, the adaptation of the TLR activation assay to the co-culture model included the coating of the membranes of the Transwell inserts with collagen I to improve the attachment of the HEK293-TLR2-Luc cells and using a shorter incubation time (6 h). Furthermore, a mixture of M199 TEER supplemented with 50% BHI was chosen to be used as apical medium in the determination of the effects of the three *F. prausnitzii* strains

on TLR activation in the following chapter. This medium composition was selected because it improved the viability of *F. prausnitzii* A2-165 in co-culture with HEK293-TLR2-Luc cells compared to when using the cell culture media M199 TEER and DMEM+FBS. There was no difference in the CFU of *F. prausnitzii* A2-165 after 6 h of co-culture between M199 TEER supplemented with 50% BHI and other BHI concentrations (25, 75 and 100% BHI). None of the medium compositions tested compromised the viability of the HEK293-TLR2-Luc cells. However, higher BHI concentrations (75 and 100% BHI) disrupted the integrity of the cell layers.

CHAPTER FIVE:
TLR activation by *F. prausnitzii* in conventional and apical anaerobic conditions†

† Selected material from this section combined with sections from Chapter 4 will be submitted for publication to the journal *Cellular Microbiology*.

5.1. INTRODUCTION

Various GI diseases, for example IBD, are linked to an inappropriate activation of mucosal immune responses causing chronic inflammation [310]. Paradoxical to the role of innate immune receptors in triggering inflammation in the defence against pathogens, ample evidence is now accumulating that the recognition of commensal microorganism by innate immune receptors is required for homeostasis in the GI tract [27,148]. TLRs are one example of innate immune receptors that are expressed in immune cells and also IECs and recognise common surface structures of microorganisms, for example LPS [149]. TLR activation has been implicated in maintaining homeostasis between immunity and tolerance in the GI epithelium [27].

The obligate anaerobe *F. prausnitzii*, a prominent member of the commensal microbiota, has been intensely studied for its beneficial effects in the GI tract [311]. Due to its decreased abundance in patients with inflammatory diseases like IBD [10-14], IBS [15] and celiac disease [16], *F. prausnitzii* is considered a protective factor for the large intestinal mucosa and promoter of health. In line with this, several *in vitro* and *in vivo* studies reported anti-inflammatory effects of *F. prausnitzii*. Some of the mechanisms suggested to contribute to its beneficial effects are the stimulation of the secretion of anti-inflammatory IL-10 by DCs [207], the increase of the differentiation of regulatory T cells (Treg) [182], and the inhibition of the production of pro-inflammatory cytokines [179].

The capacity of several strains of *F. prausnitzii* to induce IL-10 secretion in human DCs was shown to correlate with the extent to which the bacteria activated TLRs [207]. Interestingly, in addition to inducing the secretion of anti-inflammatory IL-10, the *F. prausnitzii* strains also induced the secretion of large amounts of pro-inflammatory TNF-α by DCs [207]. This indicates that the balance between pro- and anti-inflammatory

responses induced by commensal bacteria contributes to immune homeostasis in the GI tract. In this respect, the activation of the transcription factor NF-κB, a result of TLR activation, was suggested to play a dual role in the GI tract by triggering pro-inflammatory responses but also contributing to the regulation of immune homeostasis [312,313]. However, whether NF-κB activation results in detrimental pro-inflammatory or beneficial regulatory consequences remains to be elucidated.

A limitation of the above mentioned study was that the TLR activation by strains of *F. prausnitzii* was tested in conventional cell culture conditions (5% CO_2 in air atmosphere) [207]. Consequently, obligate anaerobic *F. prausnitzii* would have been killed in the presence of oxygen and therefore only the effect of non-viable bacteria was determined. Previous research has highlighted the importance of testing the effects of live obligate anaerobic bacteria using physiologically relevant models of the GI tract because live and dead bacteria exerted different effects on host cells [19]. For example, live *F. prausnitzii* A2-165 inhibited the gene expression of the NF-κB transcription factor complex in human IECs [19]. In this thesis chapter the effect of live *F. prausnitzii* on TLR activation was determined using the apical anaerobic co-culture model and compared to the results obtained when testing dead bacteria that were killed in the presence of oxygen or through exposure to UV-light.

5.2. HYPOTHESIS AND AIMS

The hypothesis of this thesis chapter was that live and dead *F. prausnitzii* (strains A2-165, ATCC 27768 and HTF-F) activate TLRs to a different extent, with higher TLR activation induced by live bacteria. The first aim was to determine a suitable ratio between HEK293-TLR-Luc cells and *F. prausnitzii* for the TLR activation assays in apical anaerobic conditions. The second aim was to determine which TLRs recognise the three *F.*

prausnitzii strains and if there are differences between the TLR activation by live and dead bacteria. The activation of TLR2, TLR2/6 and TLR4 by *F. prausnitzii* was determined because these receptors are expressed on the surface of IECs in the GI tract. For this aim the effects of live and UV-killed *F. prausnitzii* in both conventional and apical anaerobic conditions were tested. The third aim was to determine if the luminescence signals obtained in the TLR activation assays were specific to the respective TLRs tested. In order to complete this aim, HEK293 cells that did not express TLRs, but were stably transfected with the luciferase reporter plasmid (HEK293-null-Luc), were exposed to live and UV-killed *F. prausnitzii* in conventional and apical anaerobic conditions.

5.3. METHODS

5.3.1. Culture of *F. prausnitzii*

The three *F. prausnitzii* strains described in Table 2.1 were cultured in anaerobic BHI prepared as described in 2.3.2.2. For the TLR activation assays secondary bacterial cultures in stationary phase were used which were prepared as described in section 2.3.7.

5.3.2. Preparation of aerobic brain-heart infusion broth

In order to compare the effects of the three *F. prausnitzii* strains in conventional and apical anaerobic conditions, aerobic and anaerobic medium was used on the apical side of the HEK293-TLR-Luc cell layers. The apical medium used was anaerobic 50% M199 TEER+50% BHI for apical anaerobic conditions and aerobic 50% M199 TEER+50% BHI for conventional conditions.

Anaerobic BHI broth was prepared as described in section 2.3.2.2 using the ingredients listed in Table 2.3. The same ingredients were used for the preparation of aerobic BHI

broth, however the reducing agent L-cystein was not added to the aerobic medium. After dissolving the ingredients in distilled water, the pH was adjusted and the broth was distributed into Hungate culture tubes and autoclaved.

5.3.3. Preparation of the HEK293-TLR-Luc cells for the TLR activation assays

Three TLR expressing cell lines (HEK293-TLR2-Luc, HEK293-TLR2/6-Luc and HEK293-TLR4-Luc) were used to determine the effect of the three *F. prausnitzii* strains on TLR activation. These cell lines were stably transfected with a reporter plasmid containing the luciferase gene under the control of the human NF-κB promotor (pNiFty2-Luc, Invivogen, San Diego, USA) as described in section 4.3.2.

Based on the manufacturer's information (Invivogen), HEK293-TLR-Luc cells express endogenous levels of TLR1, TLR3, TLR5, and NOD1. In order to ensure the specificity of the NF-κB activation by TLR2, TLR2/6 or TLR4, a control cell line (HEK293-null-Luc) that only carried the luciferase reporter plasmid was included.

5.3.3.1. Maintenance of HEK293-TLR-Luc cells

The three HEK293-TLR-Luc cell lines and the control cell line (HEK293-null-Luc) were recovered from frozen stocks as described in 4.3.1.4. All four cell lines were maintained in unselective DMEM (Table 4.2) for the first two passages after reviving from frozen stocks. As per manufacturer's instructions, from the third passage onwards, the unselective DMEM was supplemented with the selective antibiotics blasticidin and zeocin (both Invivogen) (referred to as DMEM+BZ) for the HEK293-TLR2-Luc, HEK293-TLR2/6-Luc and HEK293-null-Luc cells. For the HEK293-TLR4-Luc cells unselective DMEM was supplemented with blasticidin, hygromycin B gold (Invivogen) and zeocin (referred to as DMEM+BHZ). The cells were maintained in large cell culture flasks (T175) in 25 mL of

the appropriate culture medium. The medium was changed twice a week and the cells were subcultured at a confluence of approximately 80%.

5.3.3.2. Seeding HEK293-TLR-Luc cells on Transwell inserts

On the day before seeding the HEK293-TLR-Luc cell lines and the control cell line (HEK293-null-Luc) on Transwell inserts, the inserts were coated with collagen I as described in 4.3.3.2. The cell lines were used for seeding for the TLR activation assays when the cells in a large cell culture flask were approximately 80% confluent. The cells were removed from the bottom of the cell culture flask using trypsin as described in4.3.3.1. After determining the cell density using an automated cell counter (Countess, Life technologies, Auckland, New Zealand), the cell suspension was diluted with DMEM+FBS to a cell density of 1.5 x 10^6 cells/mL. The diluted cell suspension was seeded in Transwell inserts with 200 µL per insert. The inserts were placed into 24-well culture plates and 810 µL of DMEM+FBS were added per well. The culture plates were incubated at 5% CO_2 in air and 37°C for 24 h before being used for the TLR activation assays.

5.3.4. Preparation of the positive controls

TLR ligands known to stimulate the three TLRs used during these studies were used as positive controls (Table 5.1). For the control cell line (HEK293-null-Luc) which was transfected only with the luciferase reporter plasmid TNF-α was used as positive control to activate NF-κB. All of the positive controls were provided lyophilised and were reconstituted as per the manufacturer's instructions. The reconstituted solutions were mixed by vortexing for 10 sec and either used on the day of the preparation or frozen in aliquots at -20°C to avoid repeated freeze-thaw cycles. For each positive control two working solution were prepared by diluting the stock solutions with aerobic and anaerobic

Table 5.1 Details of the positive controls used for the TLR activation assays including concentrations of stock and working solutions.

Positive control	Cell line	Stock solution	Working solution	Company
Tumor necrosis factor-α (TNF-α), human	HEK293-null-Luc	5 µg/mL	50 ng/mL	Sigma-Aldrich, Auckland, New Zealand
HKLM	HEK293-TLR2-Luc	10^{10} cells/mL	10^{10} cells/mL	Invivogen, San Diego, USA
Pam2CSK4	HEK293-TLR2/6-Luc	1 mg/mL	100 ng/mL	Invivogen, San Diego, USA
LPS, ultrapure, from *E. coli* K12	HEK293-TLR4-Luc	1 mg/mL	100 ng/mL	Invivogen, San Diego, USA

50% M199 TEER+50% BHI. The concentration of the stock and working solutions for the positive controls are shown in Table 5.1.

The TLR activation induced by the three *F. prausnitzii* strains was normalised against the results obtained using the respective positive controls. For each cell line the first TLR activation assay was performed using different concentrations of the positive controls in order to determine the most appropriate concentration.

5.3.5. TLR activation assays with live and UV-killed *F. prausnitzii* in conventional and apical anaerobic conditions

The two co-culture chambers were assembled inside the biosafety cabinet. The solutions used for the TLR activation assays in apical anaerobic conditions were placed inside the anaerobic workstation with opened lids the day before the assays in order to obtain anaerobic solutions.

On the day of the experiment the secondary bacterial cultures of the three *F. prausnitzii* strains prepared as described in 5.3.1 were centrifuged at 2492 x g for 6 min (11180/13190 rotor, Sigma 3-18K centrifuge, Sigma, Osterode am Harz, Germany). Inside the anaerobic workstation the supernatant was discarded and each bacterial pellet was resuspended in 2.5 mL of anaerobic 50% M199 TEER+50% BHI. The bacterial density was determined using a Petroff-Hausser counting chamber as described in 2.3.5.1.

The bacterial solutions of the three *F. prausnitzii* strains were diluted with anaerobic 50% M199 TEER+50% BHI to a density of 1.5 x 10^6 bacterial cells/mL which resulted in a MOI of 1, as the HEK293-TLR-Luc cell lines were seeded with 1.5 x 10^6 cells/mL. For each of the three strains 5 mL of diluted bacterial solutions were prepared. The same dilutions of the three *F. prausnitzii* strains were prepared using aerobic 50% M199

TEER+50% BHI. From each of the six bacterial solutions (three *F. prausnitzii* strains diluted in either anaerobic or aerobic 50% M199 TEER+50% BHI) 2 mL was removed and added to wells of 6-well plates. The 6-well plates were placed on ice with opened lids and exposed to UVC light for 15 min in order to kill the bacteria.

The wells of the two co-culture chambers were filled with 3 mL of DMEM+FBS. The Transwell inserts containing the HEK293-TLR-Luc cells were carefully inserted into the co-culture chambers using a slow twisting motion. The co-culture chambers were closed with the lids and one co-culture chamber was transferred inside the anaerobic workstation using the interlock. Inside the anaerobic workstation the lids were removed and the apical medium was replaced with 200 µL of the anaerobic treatment solutions. The eight anaerobic treatments were the negative control (sterile endotoxin-free water), the positive control for the respective cell line (50 ng/mL TNF-α for HEK293-null-Luc, 10^{10} HKLM cells/mL for HEK293-TLR2-Luc, 100 ng/mL Pam2CSK4 for HEK293-TLR2/6-Luc and 100 ng/mL LPS for HEK293-TLR4-Luc cells) and live and UV-killed bacterial cells of each *F. prausnitzii* A2-165, *F. prausnitzii* ATCC 27768 and *F. prausnitzii* HTF-F. Each treatment was used in triplicate. In order to prevent a prolonged exposure of the HEK293-TLR-Luc cells to the anaerobic environment the apical medium was removed from only three inserts at a time and immediately replaced with the anaerobic treatment solutions. The co-culture chamber was closed with the lids and incubated for 6 h inside the anaerobic workstation. For the HEK293-TLR-Luc cells in the second co-culture chamber the apical medium was removed inside a biosafety cabinet and replaced with 200 µL of the aerobic treatment solutions. The eight aerobic treatments were the same as described above, however all treatments were prepared using aerobic 50% M199 TEER+50% BHI. The second co-culture chamber was incubated for 6 h inside a 5% CO_2-incubator at 37 °C.

After the 6 h of incubation the co-culture chambers were removed from the anaerobic workstation and the CO_2-incubator. The inserts from both co-culture chambers were removed carefully and transferred to 24-well plates filled with 810 µL of DMEM+FBS. From each insert 120 µl of medium was removed. The HEK293-TLR-Luc cells were transferred from the inserts into a 96-well assay plate (Corning Costar 3610) by pipetting the remaining medium up and down carefully and thereby detaching the cell layers from the membrane. Inside a fume hood 100 µL of the Bright-Glo reagent (Promega) was added to each of the wells of the 96-well plate and mixed with the cell suspension. After an incubation at room temperature for at least 2 min in order to allow the complete cell lysis, the luminescence was measured using a plate reader (FlexStation 3, Molecular Devices, Sunnyvale, USA; top read, 750 ms integration time, wavelength nonspecific (all wavelengths between 360 nm and 630 nm)). For each of the HEK293-TLR-Luc cell lines the TLR activation assays were performed at least three times using three replicates per treatment (total n = 9).

5.3.5.1. Determination of the multiplicity of infection for the TLR activation assays

In a preliminary experiment, the TLR activation assay was performed using the HEK293-TLR2-Luc cell line as described in the section above (5.3.5), however, using two different ratios between HEK293-TLR2-Luc cells and *F. prausnitzii* (i.e. MOI). The bacteria were used at a density of 1.5×10^6 and 1.5×10^7 bacterial cells/mL resulting in a MOI of 1 and 10, respectively, as HEK293-TLR2-Luc cells were seeded at a concentration of 1.5×10^6 cells/mL. To be able to test the different MOIs, this TLR activation assay was performed only in apical anaerobic conditions using two co-culture chambers.

5.3.6. Phylogenetic analysis of bacterial cell envelope marker genes

Phylogenetic analyses of bacterial cell envelope marker genes were conducted in order to deduce whether the cell envelope of *F. prausnitzii* contains one membrane (monoderm) or two membranes (diderm). It was hypothesised that *F. prausnitzii* may be one of the rare irregular Gram-staining bacteria in which case the results of the Gram-stain may not correspond to the correct dermis structure. Analysis of genetic marker genes and highly conserved amino acid sequence characteristics is therefore a more reliable way to determine the correct dermis status of *F. prausnitzii*. For this analysis the bacterial homologs of the heat shock proteins Hsp60 and Hsp70 (GroEL and DnaK, respectively) were chosen due to reported conserved inserts in these proteins that make it possible to distinguish between monoderm and diderm bacteria [1,2]. Diderm bacteria are characterised by a highly conserved one amino acid insert in the Hsp60 protein at position 154 and a 21 to 23 amino acid long conserved insert in the Hsp70 protein at position 80. In contrast, these inserts are absent in monoderm bacteria [1,2]. Amino acid sequences of the Hsp60 and Hsp70 protein homologs of *Faecalibacterium,* including *F. prausnitzii* A2-165 used in this PhD project, *Fusobacterium,* species of the clostridial cluster IV, *Bacillus subtilis* as a typical monoderm bacterium, and *E. coli* as a typical diderm bacterium were obtained from the NCBI protein database and aligned using ClustalX version 2.1 [3]. Phylogenetic trees for both marker genes were inferred using the Neighbour-Joining algorithm in the Molecular Evolutionary Genetics Analysis (Mega) version 7.0 software [4]. GeneDoc [5] was used to display the sequence alignment.

5.3.7. Statistical analysis

The statistical analyses were performed using SAS (SAS/STAT version 9.3; SAS Institute Inc., Cary, NC, USA). For the preliminary TLR2 activation assay to determine the MOI an

ANOVA was performed to test the effect of the treatments on the luminescence signals. A 3 x 2 x 2 factorial design was used to test the effect of the three *F. prausnitzii* strains, the two statuses (live and UV-killed) and the two environments (conventional and apical anaerobic) on TLR2 and TLR2/6 activation. In order to be able to include the negative control into the analyses (only one status), a 7 x 2 factorial design was used to test the effect of the seven treatments (negative control and the three *F. prausnitzii* strains live and UV-killed) and the two environments (conventional and apical anaerobic) on TLR4 activation and the activation of the control cell line (HEK293-null-Luc). If an interaction was not significant ($P > 0.05$) it was removed from the model. When the F-values of the analyses were significant ($P < 0.05$), the means were compared using adjusted Tukey tests. For all of the statistical analyses the model assumptions (e.g. normal distribution and the homogeneity of variance) were evaluated using the ODS graphics in SAS. If the response variable did not fulfil these assumptions a $\log_{10}$ transformation was performed in order to reach these assumptions. Due to the reasons stated in section 2.3.16 each HEK293-TLR2-Luc cell monolayer seeded into one Transwell insert was used as an independent replicate for the statistical analysis. A complete randomised block design was firstly performed with the run (or experimental day) as a random effect. There was no effect of the run for any of the tested variables, consequently the random effect was removed from the model.

5.4. RESULTS

The ability of live and UV-killed *F. prausnitzii* (strains A2-165, ATCC 27768 and HTF-F) to activate TLRs (TLR2, TLR2/6 and TLR4) was determined in conventional (5% CO_2 in air atmosphere) and apical anaerobic conditions. For each cell line negative and positive controls were included. The luminescence readings obtained with the negative control were low as expected. The first time performing a TLR activation assay with a new cell line

different concentrations of the positive controls (TLR ligands for the HEK293-TLR-Luc cells and TNF-α for the HEK293-null-Luc cells) were tested in order to obtain luminescence signals within a similar range to the bacterial treatments. The results obtained with the bacterial treatments were normalised to the results obtained with the positive controls for each cell line.

5.4.1. TLR2 activation

5.4.1.1. Determination of the multiplicity of infection

In an initial experiment the most appropriate ratio between HEK293-TLR-Luc cells and *F. prausnitzii* (MOI) to be used in subsequent TLR activation assays was determined. This experiment was performed using the HEK293-TLR2-Luc cell line testing a MOI of 1 and 10 in apical anaerobic conditions. For *F. prausnitzii* A2-165 and HTF-F there was a significant difference for the NF-κB activation between live and dead (UV-killed) bacteria when using a bacteria to cell ratio of 1:1 (MOI 1), with higher NF-κB activation induced by live bacteria ($P < 0.05$; Figure 5.1). When using a bacteria to cell ratio of 10:1 (MOI 10), no significant differences were determined between live and dead bacteria for all of the three *F. prausnitzii* strains tested. For this reason it was decided to use the bacteria to cell ratio of 1:1 for the following TLR activation assays.

5.4.1.2. TLR2 activation in conventional and apical anaerobic conditions

HEK293-TLR2-Luc cells were exposed to live and UV-killed *F. prausnitzii* (strains A2-165, ATCC 27768 and HTF-F) in conventional and apical anaerobic conditions for 6 h. The observed values for the TLR2 activation are shown in Figure 5.2. The interaction between the environment, status and strain and the interaction between the strain and status were not significant and were therefore removed from the statistical analysis. There was a

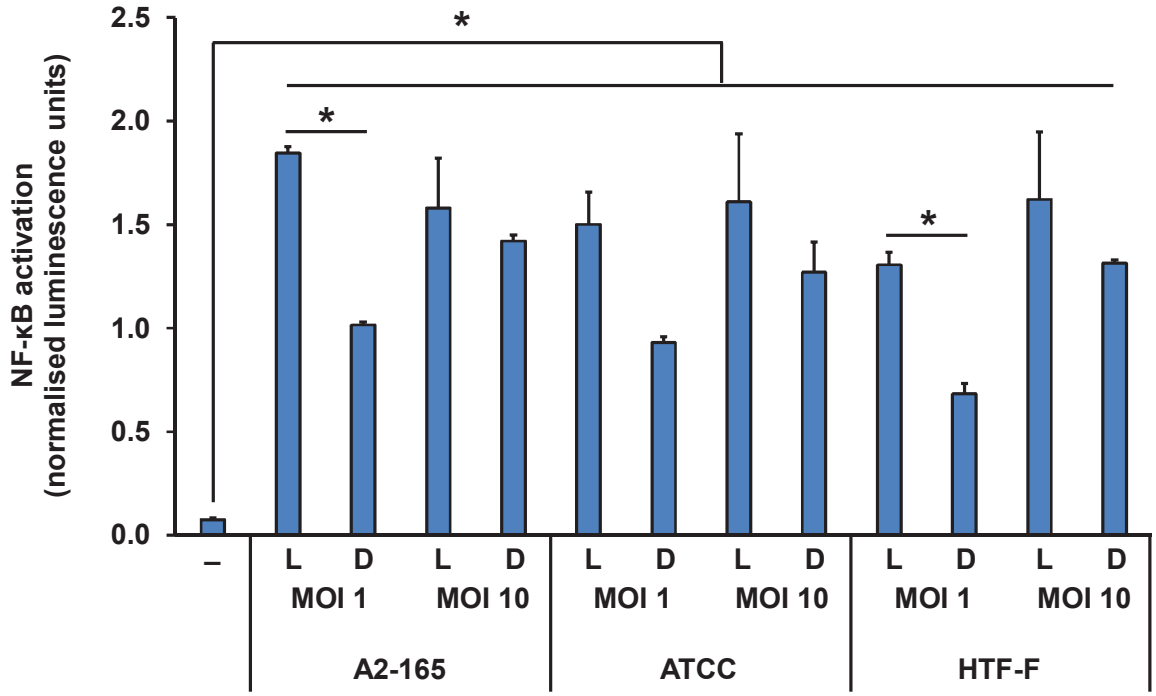

Figure 5.1 Determination of the MOI for the TLR activation assays.

HEK293-TLR2-Luc cells were stimulated for 6 h with live and UV-killed *F. prausnitzii* (strains A2-165, ATCC 27768 and HTF-F) in apical anaerobic conditions using two different ratios between cells and bacteria (MOI 1 and MOI 10). The results were normalised to the luminescence signal obtained when stimulating the cells with a positive control (HKLM, 10^9 cells/mL). The graph shows the normalised mean (± SEM; n = 3) luminescence units after TLR2 stimulation. * TLR2 activation significantly different ($P < 0.05$). L = Live, D = Dead (UV-killed).

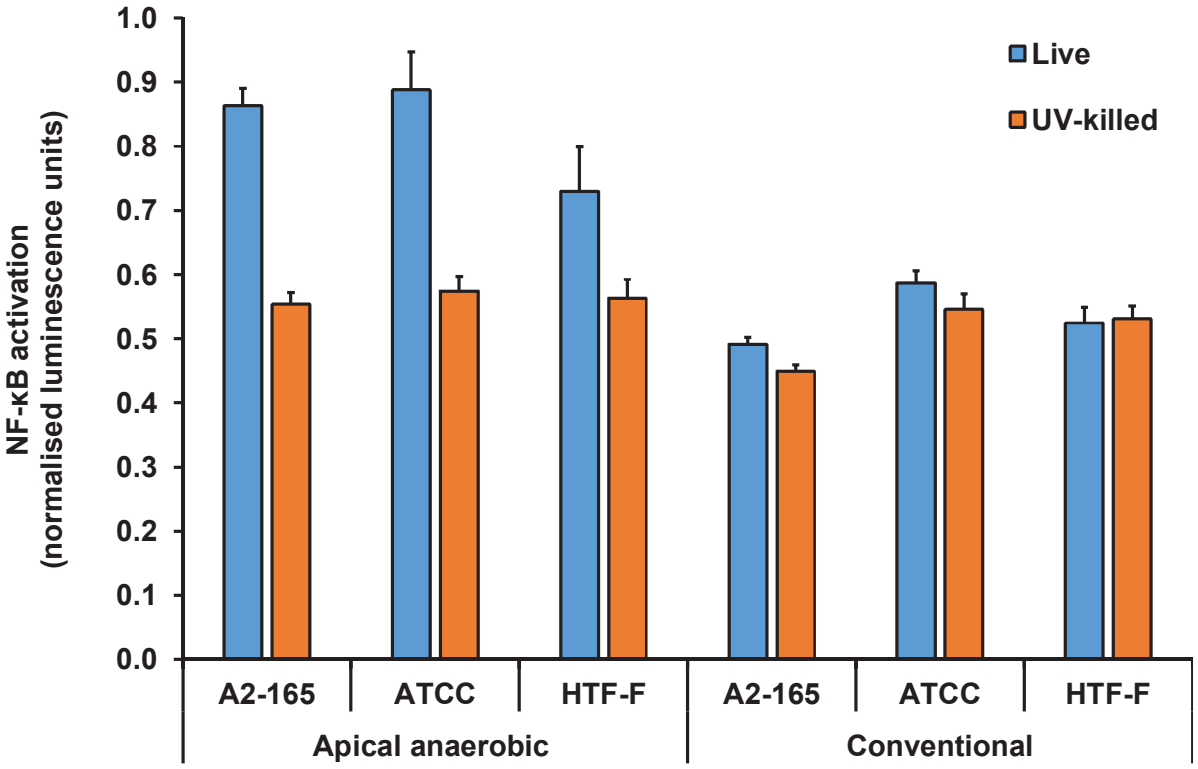

Figure 5.2 TLR2 activation (observed values) by live and UV-killed *F. prausnitzii* in conventional and apical anaerobic conditions.

HEK293-TLR2-Luc cells were exposed to live or UV-killed *F. prausnitzii* (strains A2-165, ATCC 27768 and HTF-F) in conventional and apical anaerobic conditions. After 6 h of incubation the luminescence as a measure of NF-κB activation was determined. The results were normalised to the luminescence signal obtained when stimulating the cells with a positive control (HKLM, 10^{10} cells/mL). The graph shows the normalised observed mean (± SEM; total n between 6 to 9 for each treatment) luminescence units after TLR2 stimulation. The number of observations differed between the treatments because several cell monolayers were disrupted after the 6 h of incubation. The interaction between the environment, status and strain was not significant and was therefore removed from the statistical model. The results of the statistical analyses are shown in Figure 5.3 and Figure 5.4.

significant interaction between the environment and status ($P < 0.001$) as shown in Figure 5.3. The highest NF-κB reporter activity following TLR2 activation was determined when testing live bacteria in apical anaerobic conditions which was on average 1.6-fold higher compared to the other treatments (UV-killed bacteria in apical anaerobic conditions and live and UV-killed bacteria in conventional conditions). There was no difference between UV-killed bacteria in apical anaerobic conditions compared to live bacteria in conventional conditions. Compared to the TLR2 activation in apical anaerobic conditions, where live bacteria induced a 1.5-fold higher response than UV-killed bacteria, the responses induced by live and UV-killed bacteria were less different in conventional conditions. In this environment the TLR2 activation induced by live bacteria was only 1.1-fold higher compared to the response obtained using UV-killed bacteria.

A significant interaction between the strain and environment was determined ($P = 0.02$) as shown in Figure 5.4. No differences were observed between the three *F. prausnitzii* strains in apical anaerobic conditions ($P > 0.05$). However, the TLR2 activation by all three strains was higher in apical anaerobic conditions compared to conventional conditions. In conventional conditions, the *F. prausnitzii* strains ATCC 27768 and HTF-F induced a higher TLR2 response compared to *F. prausnitzii* A2-165 ($P < 0.05$).

5.4.2. TLR2/6 activation in conventional and apical anaerobic conditions

The observed values for the activation of TLR2/6 by live and dead *F. prausnitzii* (strains A2-165, ATCC 27768 and HTF-F) in conventional and apical anaerobic conditions are shown in Figure 5.5. The interaction between the environment, status and strain was not significant and was therefore removed from the statistical model, as were the interactions between the environment and strain and between the strain and status. The interaction between the environment and status was significant as shown in Figure 5.6 ($P < 0.001$). In

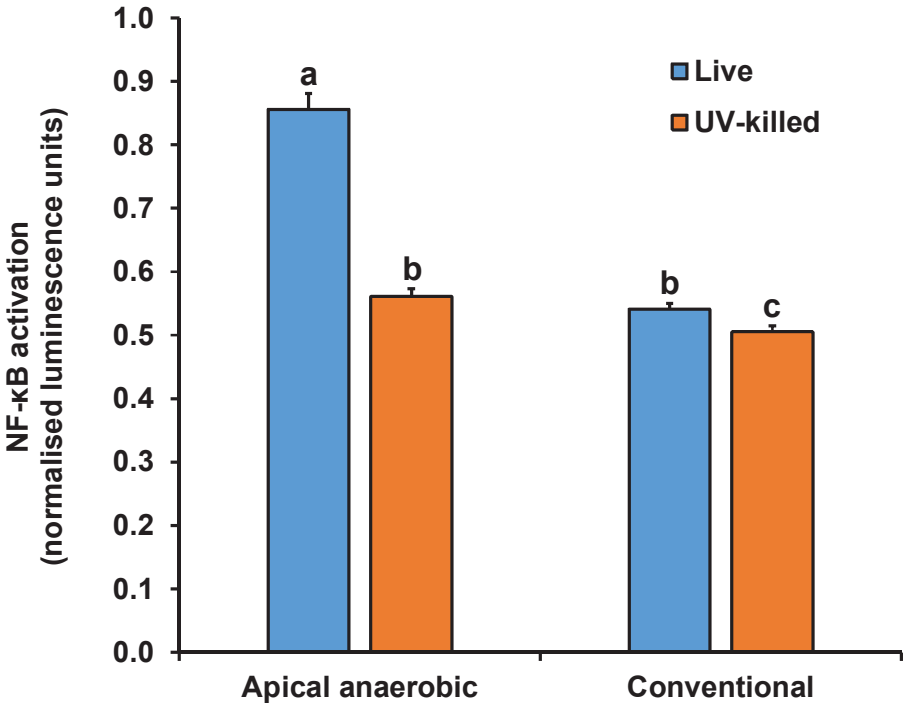

Figure 5.3 TLR2 activation (fitted values) by live and UV-killed *F. prausnitzii* in conventional and apical anaerobic conditions.

HEK293-TLR2-Luc cells were exposed to live or UV-killed *F. prausnitzii* (strains A2-165, ATCC 27768 and HTF-F) and the TLR2 activation after 6 h of incubation was determined by measuring the luminescence upon NF-κB activation. The results were normalised to the results obtained when stimulating TLR2 with a positive control (HKLM, 10^{10} cells/mL) in the respective environment. The interaction between the environment (apical anaerobic and conventional), strain and status (live and UV-killed) was not significant and was therefore removed from the statistical model. There was a significant interaction between the environment and status ($P < 0.001$). The graph shows the normalised fitted mean (± SEM; total n between 6 to 9 for each treatment) luminescence units after TLR2 stimulation. The number of observations differed between the treatments because several cell monolayers were disrupted after the 6 h of incubation. Treatments that do not share the same letters are significantly different ($P < 0.05$).

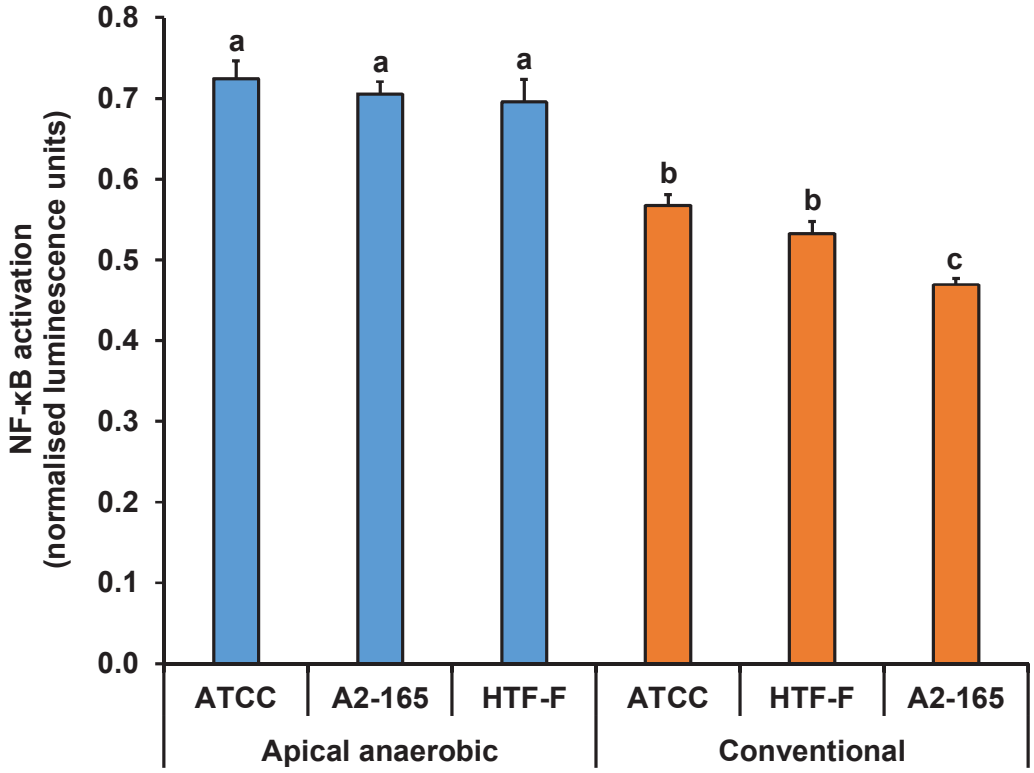

Figure 5.4 TLR2 activation (fitted values) by *F. prausnitzii* in conventional and apical anaerobic conditions.

HEK293-TLR2-Luc cells were exposed to live and UV-killed *F. prausnitzii* (strains A2-165, ATCC 27768 and HTF-F) in conventional and apical anaerobic conditions for 6 h. The TLR2 activation was determined by measuring the luminescence upon NF-κB activation. The results were normalised to the NF-κB activation after TLR2 stimulation with a positive control (HKLM, 10^{10} cells/mL) for each environment. A significant interaction between the strain and environment was determined ($P = 0.02$). The graph shows the normalised fitted mean (± SEM; total n between 6 to 9 for each treatment) luminescence units following TLR2 stimulation. The number of observations differed between the treatments because several cell monolayers were disrupted after the 6 h of incubation. Treatments that do not share the same letters are significantly different ($P < 0.05$).

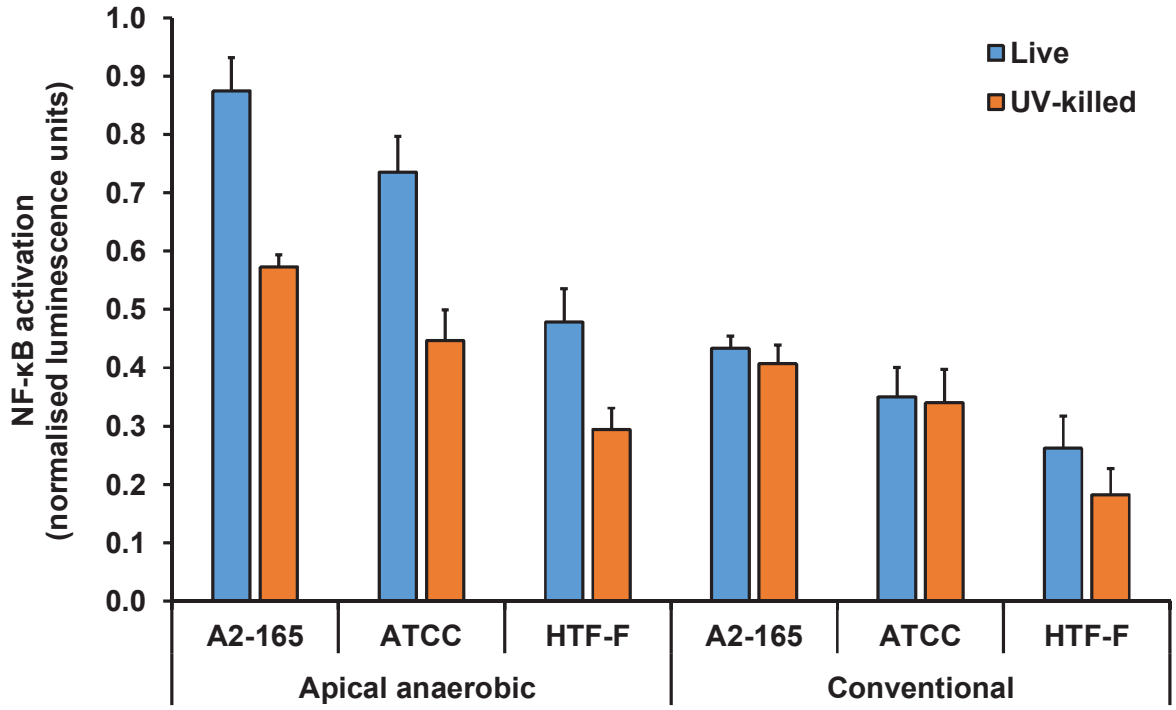

Figure 5.5 TLR2/6 activation (observed values) by live and UV-killed *F. prausnitzii* in conventional and apical anaerobic conditions.

HEK293-TLR2/6-Luc cells were incubated with live or UV-killed *F. prausnitzii* (strains A2-165, ATCC 27768 and HTF-F) in conventional and apical anaerobic conditions and after 6 h the luminescence was measured to determine the TLR2/6 activation. Results were normalised against a positive control (cells stimulated with 100 ng/mL Pam2CSK4). The graph shows the normalised observed mean (± SEM; total n between 8 to 11 for each treatment) luminescence units after TLR2/6 stimulation. The number of observations differed between the treatments because several cell monolayers were disrupted after the 6 h of incubation. The interaction between the environment, status and strain was not significant and was therefore removed from the statistical model. The results of the statistical analyses are shown in Figure 5.6 and Figure 5.7.

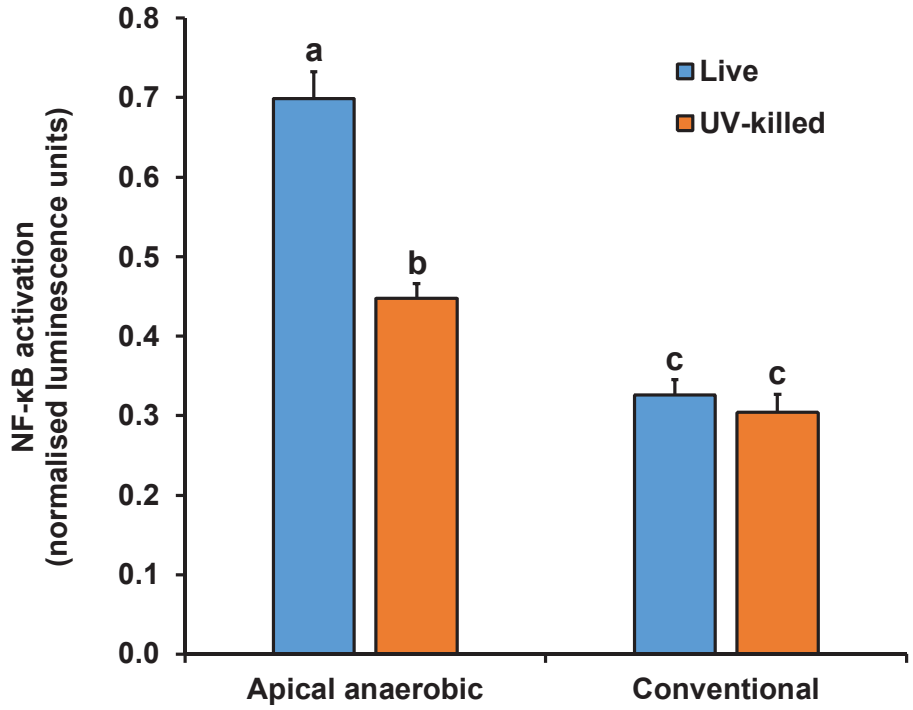

Figure 5.6 TLR2/6 activation (fitted values) by live and UV-killed *F. prausnitzii* in conventional and apical anaerobic conditions.

HEK293-TLR2/6-Luc cells were stimulated with live or UV-killed *F. prausnitzii* (strains A2-165, ATCC 27768 and HTF-F) in conventional and apical anaerobic conditions. The TLR2/6 activation was determined after 6 h of incubation by measuring the luminescence. The results were normalised to the results obtained when using a positive control (Pam2CSK4, 100 ng/mL). The interaction between the environment, status and strain was not significant and was therefore removed from the statistical model. A significant interaction between the environment and status was determined ($P < 0.001$). The graph shows the normalised fitted mean (± SEM; total n between 8 to 11 for each treatment) luminescence units after TLR2/6 stimulation. The number of observations differed between the treatments because several cell monolayers were disrupted after the 6 h of incubation. Treatments that do not share the same letters are significantly different ($P < 0.05$).

apical anaerobic conditions, the TLR2/6 activation by live *F. prausnitzii* was 1.6-fold higher than UV-killed bacteria. Furthermore, the TLR2/6 activation by live *F. prausnitzii* in apical anaerobic conditions was 2.2-fold higher than the TLR2/6 activation by live and UV-killed *F. prausnitzii* in conventional conditions. In conventional conditions there was no difference for the TLR2/6 activation between live and UV-killed bacteria.

There was a significant effect of the strain on the luminescence response as shown in Figure 5.7 ($P < 0.001$). The highest TLR2/6 response was observed for *F. prausnitzii* A2-165, followed by *F. prausnitzii* ATCC 27768 and the lowest TLR2/6 response was determined for *F. prausnitzii* HTF-F ($P < 0.05$).

5.4.3. TLR4 activation in conventional and apical anaerobic conditions

The observed values for the TLR4 activation by live and UV-killed *F. prausnitzii* (strains A2-165, ATCC 27768 and HTF-F) in conventional and apical anaerobic conditions are shown in Figure 5.8. The results from cells treated with the negative control were included in the statistical analysis. There was no significant treatment effect ($P = 0.08$), demonstrating that the luminescence signal obtained with the negative control was not different from the bacterial treatments. This shows that there was no TLR4 activation by either live or UV-killed *F. prausnitzii* in both conventional and apical anaerobic conditions.

The only significant effect observed was the effect of the environment ($P < 0.001$). The TLR4 activation was higher in conventional conditions than in apical anaerobic conditions ($P < 0.05$). The statistical analysis was repeated using the absolute values of the luminescence measurements, which also showed a higher TLR4 activation in conventional conditions ($P < 0.05$; data not shown).

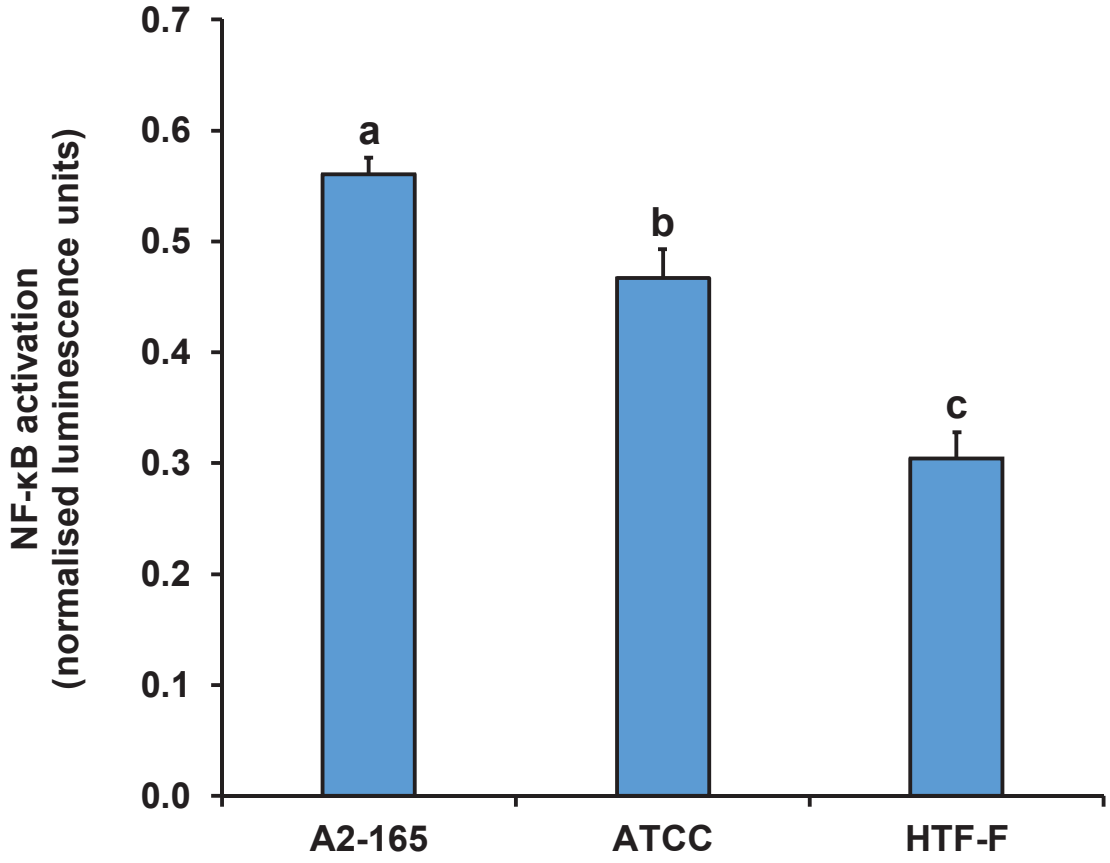

Figure 5.7 TLR2/6 activation (fitted values) by live and UV-killed *F. prausnitzii* in conventional and apical anaerobic conditions.

HEK293-TLR2/6-Luc cells were stimulated with live or UV killed *F. prausnitzii* (strains A2-165, ATCC 27768 and HTF-F) in conventional and apical anaerobic conditions. The luminescence upon TLR2/6 activation was determined. Results were normalised against a positive control (cells stimulated with 100 ng/mL Pam2CSK4). There was a significant effect of the strain on the luminescence response ($P < 0.001$). The graph shows the normalised fitted mean (± SEM; total n between 8 to 11 for each treatment) luminescence units after TLR2/6 stimulation. The number of observations differed between the treatments because several cell monolayers were disrupted after the 6 h of incubation. Treatments that do not share the same letters are significantly different ($P < 0.05$).

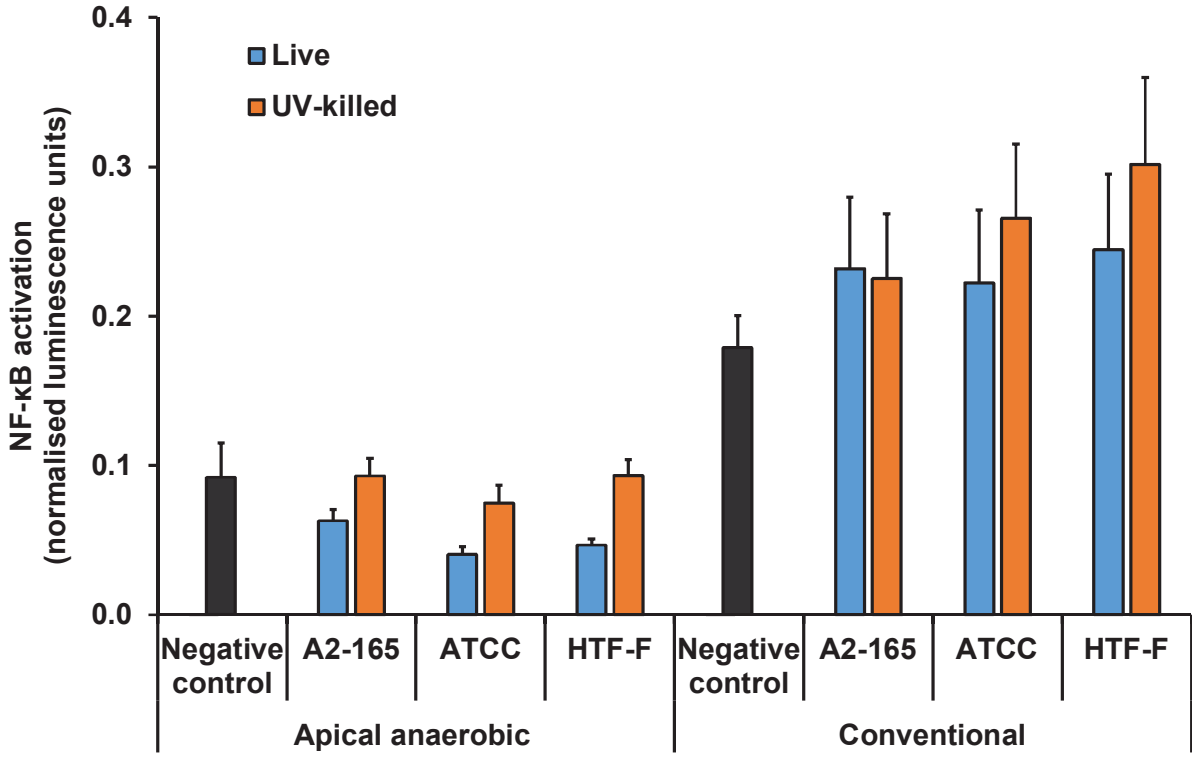

Figure 5.8 TLR4 activation by the controls and by live and UV-killed *F. prausnitzii* in conventional and apical anaerobic conditions.

HEK293-TLR4-Luc cells were exposed to live and UV killed *F. prausnitzii* (strains A2-165, ATCC 27768 and HTF-F) in conventional and apical anaerobic conditions and after 6 h the luminescence upon TLR4 activation was measured. Results were normalised to a positive control (LPS, 100 ng/mL) in the respective environment. The interaction between the treatment and environment was not significant and was therefore removed from the statistical model. There was no significant treatment effect ($P = 0.08$) and therefore no difference between the negative control and the bacterial treatments. However, there was a significant effect of the environment on the luminescence signal ($P < 0.001$). The graph shows the normalised observed mean (± SEM; total n between 6 and 14 for each treatment) luminescence units after TLR4 stimulation. The number of observations differed between the treatments because several cell monolayers were disrupted after the 6 h of incubation.

5.4.4. Activation of the control cell line in conventional and apical anaerobic conditions

The control cells (HEK293-null-Luc), which did not express TLRs but were transfected with the luciferase reporter plasmid, were exposed to the same treatments as the TLR-expressing cell lines (live and UV-killed *F. prausnitzii* (strains A2-165, ATCC 27768 and HTF-F) in conventional and apical anaerobic environment). The observed values for the activation of the HEK293-null-Luc cells are shown in Figure 5.9. The luminescence signals from cells treated with the negative control were included in the statistical analysis. There was no significant treatment effect ($P = 0.08$), which means that there was no difference between the negative control and the bacterial treatments. Since the control cell line was not activated by the bacterial treatments, the NF-κB activation determined for the TLR-expressing cell lines was specific for the respective TLRs tested.

There was a significant effect of the environment on the luminescence signal ($P < 0.001$) with a higher NF-κB activation in apical anaerobic compared to conventional conditions ($P < 0.05$). In addition to the statistical analysis using the normalised data the absolute values of the luminescence measurements were analysed which also showed a higher NF-κB activation in apical anaerobic conditions ($P < 0.05$; data not shown).

5.4.5. Phylogenetic analysis of bacterial cell envelope marker genes

The phylogenetic trees for the bacterial cell envelope marker genes Hsp60 and Hsp70 are shown in Figure 5.10 and Figure 5.11, respectively. These analyses demonstrate that *F. prausnitzii* is closer related with respect to its dermis to Gram-positive bacteria such as species of the clostridial cluster IV and *Bacillus subtilis,* than to traditional Gram-negative bacteria such as *E. coli.* The *F. prausnitzii* Hsp60 and Hsp70 homologs were located on

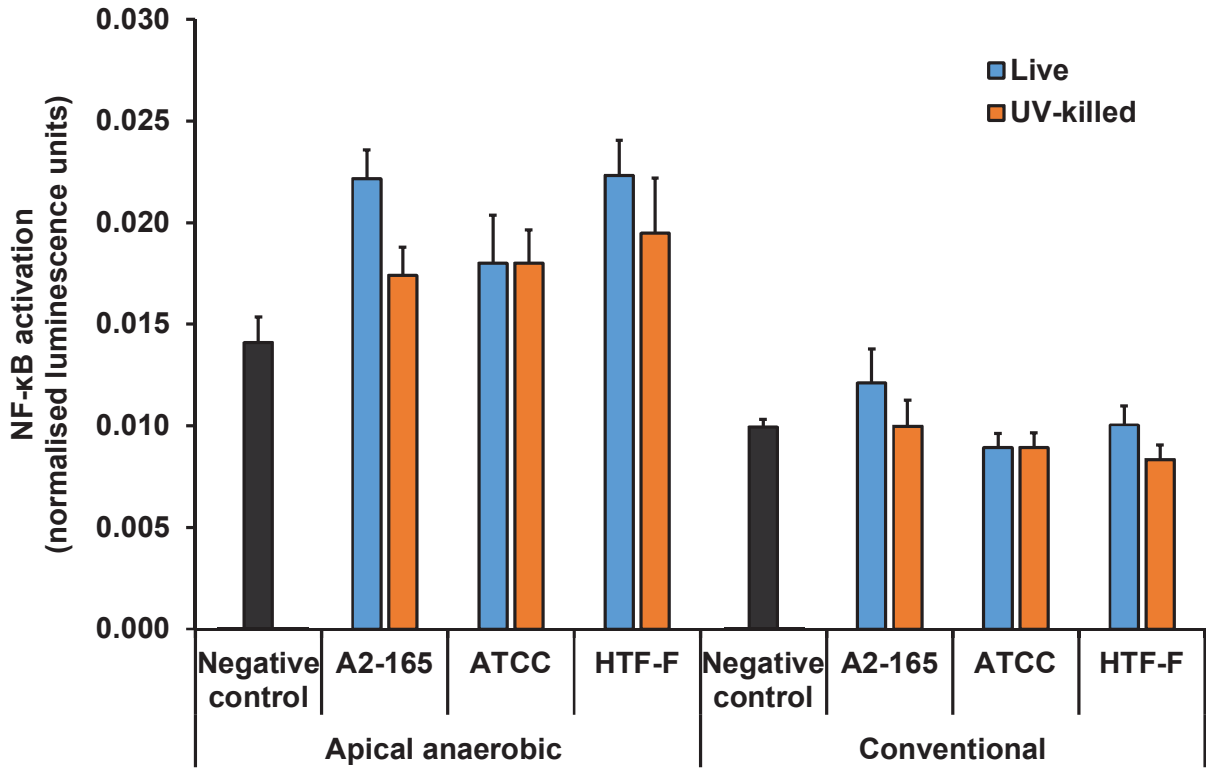

Figure 5.9 Activation of the control cell line (HEK293-null-Luc) by the controls and by live and UV-killed *F. prausnitzii* in conventional and apical anaerobic conditions.

The control cell line (HEK293-null-Luc) was exposed to live and UV-killed *F. prausnitzii* (strains A2-165, ATCC 27768 and HTF-F) in conventional and apical anaerobic conditions. After 6 h of co-culture the NF-κB activation was determined by measuring the luminescence. The results were normalised to a positive control (TNF-α, 50 ng/mL) in the respective environment. The interaction between the treatment and environment was not significant and was therefore removed from the statistical model. There was no significant treatment effect ($P = 0.08$) and therefore no difference between the negative control and the bacterial treatments. However, there was a significant effect of the environment on the luminescence signal ($P < 0.001$). The graph shows the normalised observed mean (± SEM; total n between 5 to 8 for each treatment) luminescence units. The number of observations differed between the treatments because several cell monolayers were disrupted after the 6 h of incubation.

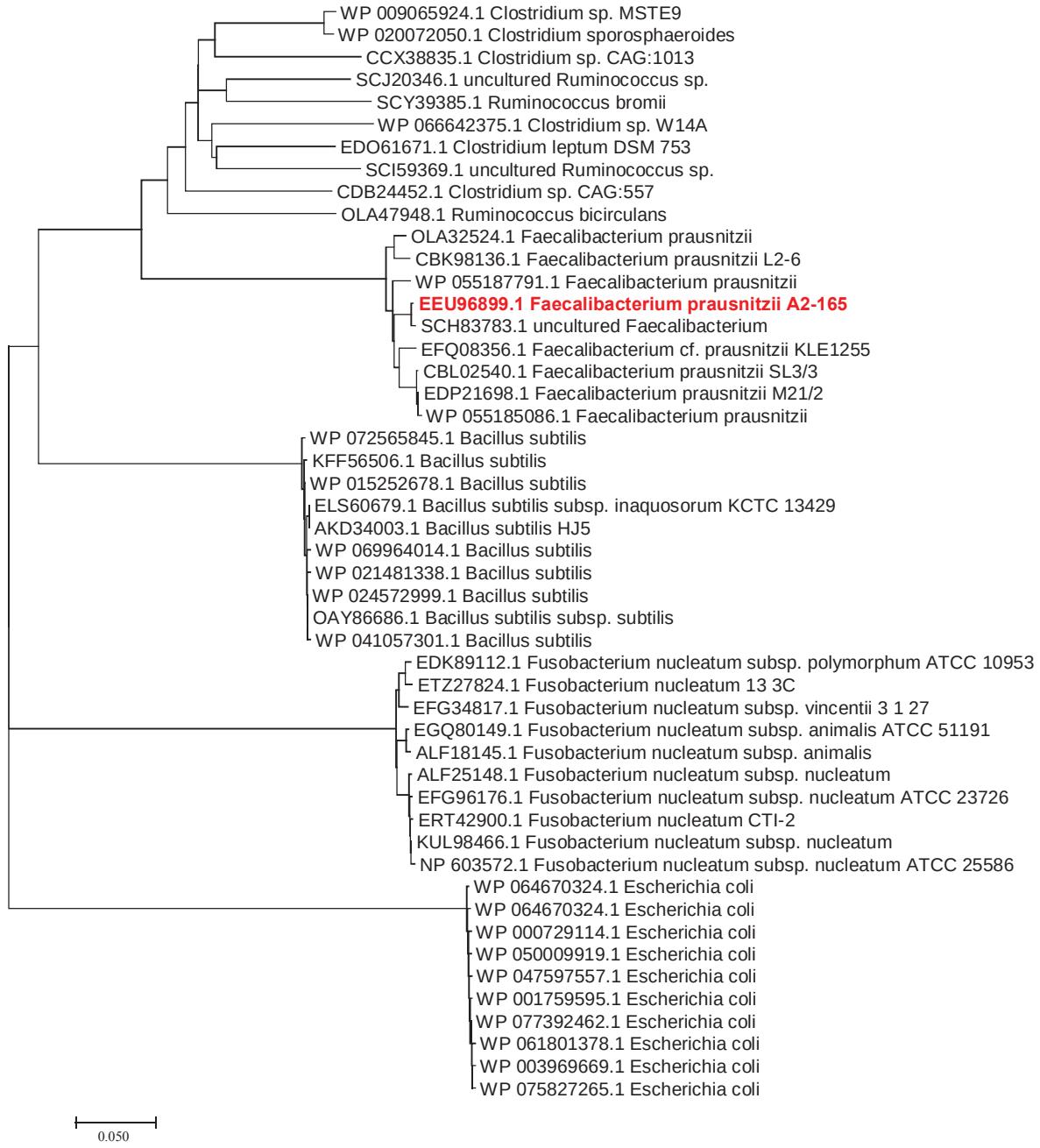

Figure 5.10 Evolutionary relationships of taxa based on the phylogenetic analysis of the bacterial cell envelope marker gene Hsp60.

The evolutionary history was inferred using the Neighbour-Joining method [9]. The optimal tree with the sum of branch length = 1.95327348 is shown. The tree is drawn to scale, with branch lengths in the same units as those of the evolutionary distances used to infer the phylogenetic tree. The evolutionary distances were computed using the Poisson correction method [10] and are in the units of the number of amino acid substitutions per site. The analysis involved 49 amino acid sequences. All positions containing gaps and missing data were eliminated. There were a total of 533 positions in the final dataset. Evolutionary analyses were conducted in MEGA7 [4].

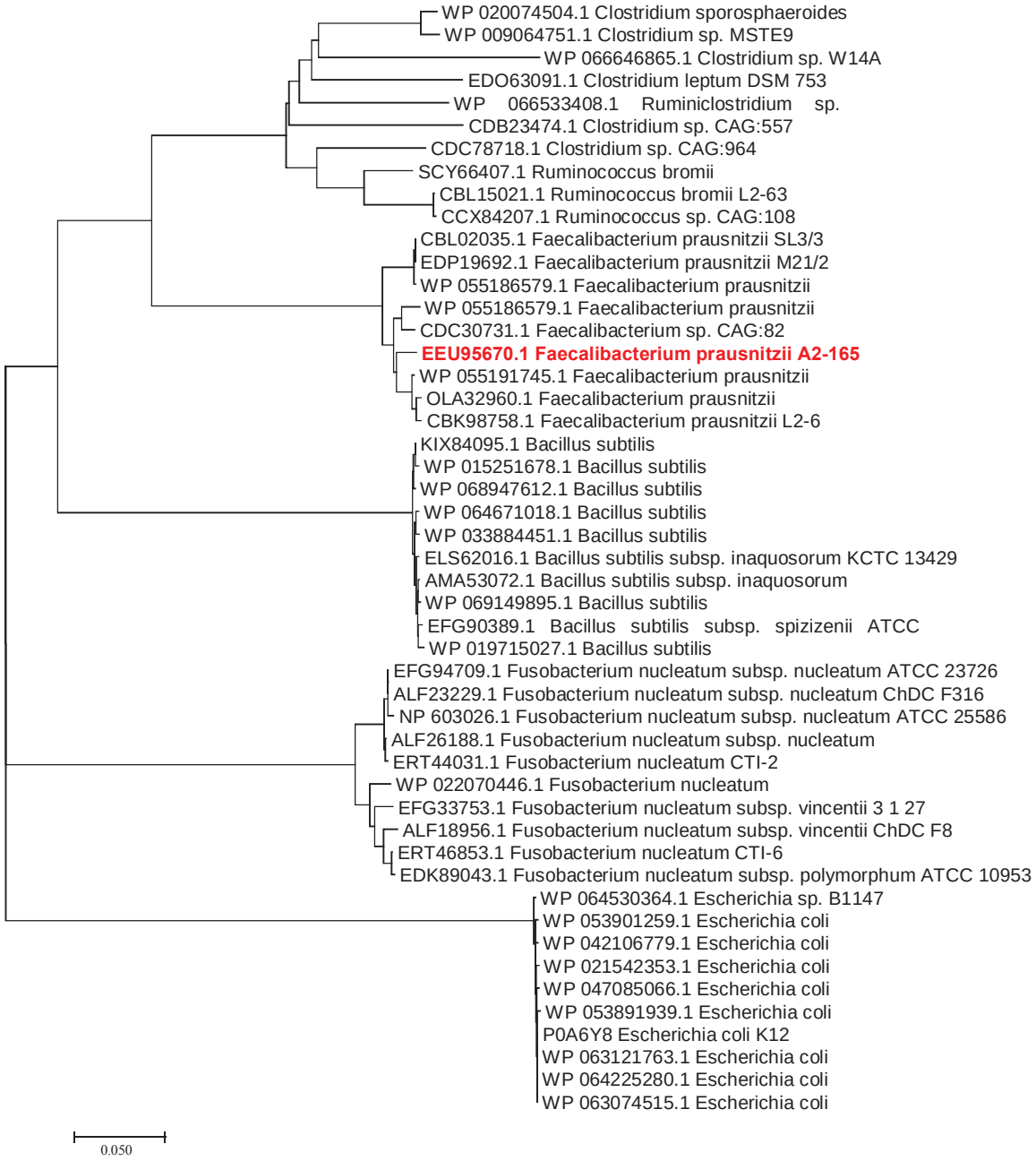

Figure 5.11 Evolutionary relationships of taxa based on the phylogenetic analysis of the bacterial cell envelope marker gene Hsp70.

The evolutionary history was inferred using the Neighbour-Joining method [9]. The optimal tree with the sum of branch length = 1.79497509 is shown. The tree is drawn to scale, with branch lengths in the same units as those of the evolutionary distances used to infer the phylogenetic tree. The evolutionary distances were computed using the Poisson correction method [10] and are in the units of the number of amino acid substitutions per site. The analysis involved 49 amino acid sequences. All positions containing gaps and missing data were eliminated. There were a total of 588 positions in the final dataset. Evolutionary analyses were conducted in MEGA7 [4].

branches deriving from the same tree node as the species of the clostridial cluster IV and the neighbouring node contained the Hsp60 and Hsp70 homologs of *Bacillus subtilis*. In contrast, Hsp60 and Hsp70 homologs of *Fusobacterium* and *E. coli* branched separately from the other bacterial groups. In addition, Figure 5.12 and Figure 5.13 show the partial sequence alignments of the Hsp60 and Hsp70 proteins, respectively. These reveal that the one and the 24 amino acid inserts in conserved regions in Hsp60 and Hsp70 were only present in *E. coli,* but absent in all of the other taxa, including *F. prausnitzii*.

5.5. DISCUSSION

The results reported in this research chapter support the hypothesis that live and dead *F. prausnitzii* (strains A2-165, ATCC 27768 and HTF-F) activate TLRs to a different extent, with higher TLR activation induced by live bacteria. For both TLR2 and TLR2/6 the higher activation was induced by live *F. prausnitzii* compared to dead bacteria (killed by UV-light or in the presence of oxygen). Neither live nor UV-killed bacteria activated TLR4, in both apical anaerobic and conventional conditions. HEK293 cells expressing no TLRs but transfected with the luciferase reporter plasmid (HEK293-null-Luc cells) were not stimulated by *F. prausnitzii*, demonstrating that the NF-κB activation was dependent on the expression of the respective TLRs. The activation of TLRs is known as the first step of triggering inflammatory responses against pathogenic bacteria in the GI tract [316]. However, it is becoming increasingly evident that TLR signalling also contributes to maintaining immune homeostasis through a 'tonic' level of TLR activation by commensal bacteria [148]. The TLR2 and TLR2/6 activation by live *F. prausnitzii* may therefore contribute to its beneficial effects in the GI tract.

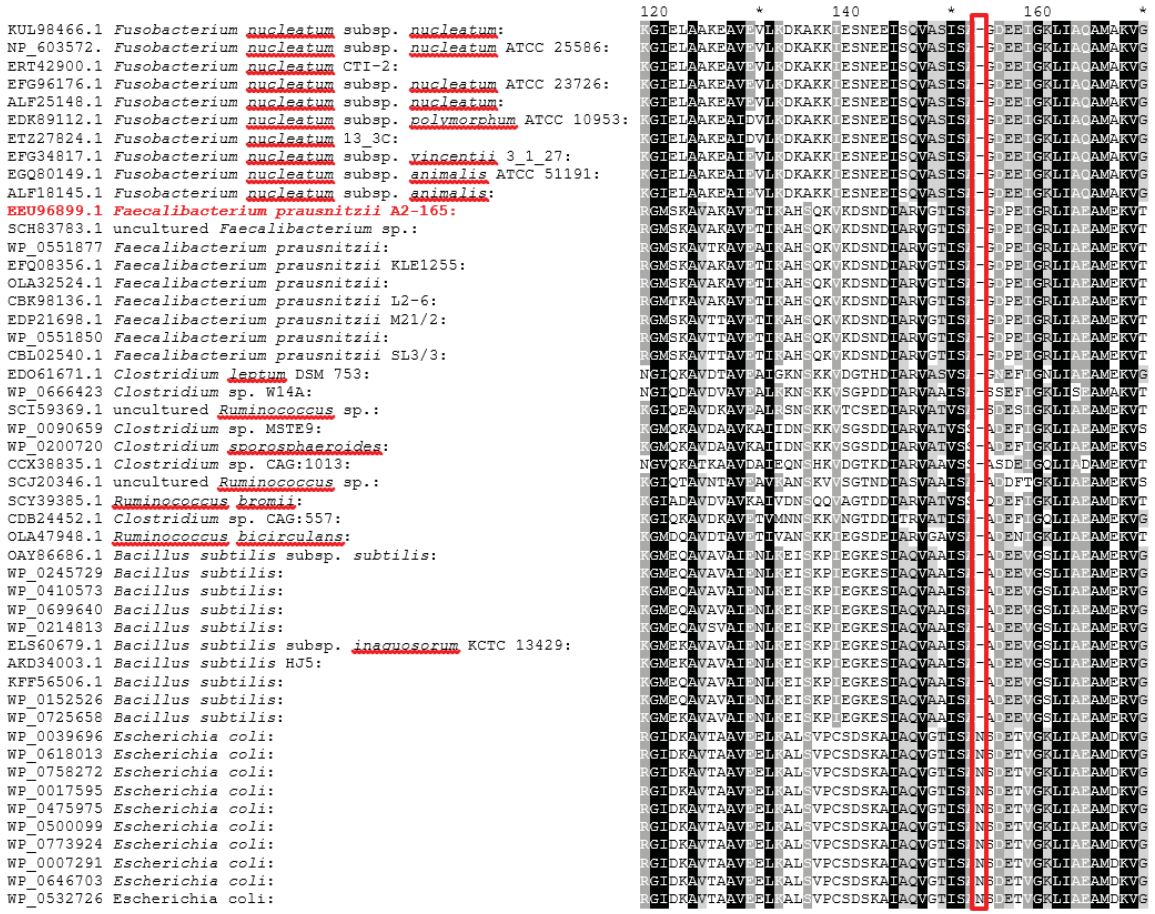

Figure 5.12 Partial sequence alignment of the Hsp60 protein.

Amino acid sequences of the Hsp60 protein of strains of *Faecalibacterium,* including *F. prausnitzii* A2-165, *Fusobacterium,* species of the clostridial cluster IV, *Bacillus subtilis* and *E. coli* were aligned using the software GeneDoc. This partial sequence alignment shows a one amino acid insert (boxed) in a conserved region in the Hsp60 protein that is only present in *E. coli.*

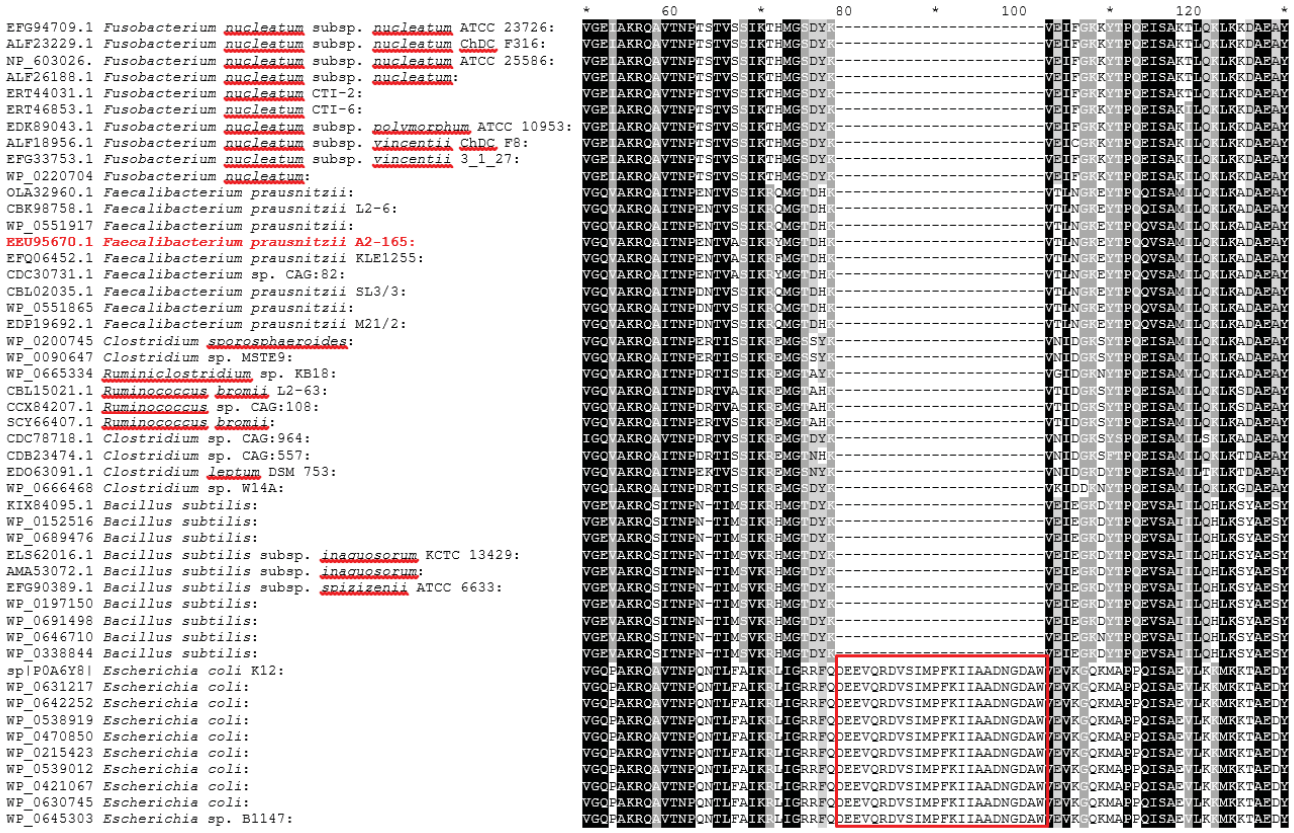

Figure 5.13 Partial sequence alignment of the Hsp70 protein

Amino acid sequences of the Hsp70 protein of strains of *Faecalibacterium,* including *F. prausnitzii* A2-165, *Fusobacterium,* species of the clostridial cluster IV, *Bacillus subtilis* and *E. coli* were aligned using the software GeneDoc. This partial sequence alignment shows a 24 amino acid long insert (boxed) in a conserved region in the Hsp70 protein, which is only present in *E. coli*.

TLRs recognise surface structures of microorganisms, so called PAMPs [27]. Therefore, it could be anticipated that live and dead bacterial cells induce the same level of TLR activation or that dead bacteria induce greater TLR activation because the killing, for example through cell lysis, may increase the availability of PAMPs [317]. In contrast, greater TLR activation by live compared to dead bacteria was shown for both pathogenic and commensal bacteria [318,319]. These findings are supported by the results of this research showing higher TLR2 and TLR2/6 activation when treated with live *F. prausnitzii*.

One explanation for the greater TLR activation by live bacteria could be the ability of viable organisms to replicate resulting in a higher receptor activation through an increased abundance of PAMPs. However, as shown in the previous thesis chapter, *F. prausnitzii* A2-165 did not grow in co-culture with HEK293-TLR2-Luc cells in the apical anaerobic co-culture model. Although the supplementation of the cell culture medium M199 TEER with 50% of the bacterial culture medium BHI improved the bacterial viability compared to M199 TEER alone, the *F. prausnitzii* A2-165 CFU decreased by approximately one log after 6 h of co-culture. The other *F. prausnitzii* strains used in this study (ATCC 27768 and HTF-F) generally grow slower compared to *F. prausnitzii* A2-165. Hence, a higher loss in viability in the co-culture model could be anticipated for these strains. Consequently, it is unlikely that the higher TLR2 and TLR2/6 activation by live *F. prausnitzii* was caused by higher bacterial numbers due to replication.

Since live *F. prausnitzii* induced higher TLR2 and TLR2/6 activation compared to dead bacteria in the absence of bacterial growth, it can be hypothesised that the activation of TLRs is not only induced by bacterial surface structures. Live bacteria may produce metabolites that directly or indirectly influence TLR activation, thereby causing

differential immune responses. This is in agreement with the results of a study showing that the *F. prausnitzii* A2-165 supernatant, and therefore secreted metabolites, but not UV-killed bacteria or bacterial fractions exerted immunomodulatory effects [179].

The higher NF-κB activation due to TLR2 and TLR2/6 signalling induced by live *F. prausnitzii* may be mediated by secreted butyrate. *F. prausnitzii* is one of the major butyrate producers in the GI tract [178,311,320]. This short chain fatty acid is well known for its beneficial functions [166]. Previous research demonstrated that butyrate affected innate immune signalling [321]. For example, butyrate mediated nucleotide-binding and oligomerisation domain (NOD)2-dependent mucosal immune responses against peptidoglycan in IECs [321]. The chemokine secretion induced by peptidoglycan was enhanced in the presence of butyrate. Furthermore, using Caco-2 cells stably transfected with a NF-κB-driven luciferase reporter plasmid, it was shown that butyrate caused a significant increase in NF-κB activation upon peptidoglycan stimulation [321]. In addition, at the concentration present in the supernatant of *F. prausnitzii* A2-165 grown in BHI supplemented with cellobiose and maltose (i.e., 40 mM), butyrate increased NF-κB activation after IL-1β stimulation in Caco-2 reporter cell lines [179]. In this respect, further studies could investigate whether the *F. prausnitzii* strains produce butyrate in co-culture with HEK293-TLR-Luc cells in the apical anaerobic-co-culture model using anaerobic 50% M199 TEER+50% BHI as apical medium.

The different immune-stimulatory potential of live and dead *F. prausnitzii* may also be caused by proteins secreted by live bacteria. Recently, an anti-inflammatory protein isolated from *F. prausnitzii* A2-165 supernatant was identified [213]. It is plausible that this protein influences TLR signalling either directly through receptor stimulation or indirectly by modulating TLR-induced downstream signalling cascades.

Remarkably, it was demonstrated that the mammalian innate immune system is able to directly sense microbial viability through the recognition of so-called viability-associated PAMPs (vita-PAMPs) [322]. Prokaryotic messenger ribonucleic acid (mRNA) released following phagocytosis of live but not dead bacteria was identified as a vita-PAMP. Though first thought as a trait of pathogenic bacteria, viable non-pathogenic bacteria were also shown to induce innate immune responses triggered by viability and prokaryotic mRNA. Similarly, it may be possible that the higher TLR2 and TLR2/6 activation by live *F. prausnitzii* is triggered by not yet identified vita-PAMPs recognised by these innate immune receptors. In case of pathogenic bacteria, vita-PAMPs were suggested as 'danger' signals that allow for scaling of appropriate immune responses depending on the level of microbial threat [322,323]. However, it may be plausible that the recognition of vita-PAMPs expressed or secreted by beneficial commensal bacteria, such as *F. prausnitzii*, play a role in maintaining immune homeostasis in the GI tract. Similar to providing a mechanism to distinguish between live and dead bacteria in case of vita-PAMPs, the innate immune system may also be able to distinguish between pathogenic bacteria and non-pathogenic beneficial commensals by recognising specific commensal-associated molecular patterns.

The different immune-stimulatory potential of live and dead bacteria determined in this study may also be caused by epigenetic mechanisms, which have been recently shown to play a role in host-microbe interaction [324,325]. For example, live and heat-treated probiotics induced distinct IL-10 expression levels, which was reported to be due to differential modulation of mRNA stabilisation and microRNA expression [324]. This finding highlights that depending on their physiological state, bacteria may induce varying effects in host cells caused by mechanisms beyond classical molecular pattern recognition,

which may also explain the different effects of live and dead *F. prausnitzii* observed in this study.

The beneficial effects of *F. prausnitzii* in the human GI tract may be attributed, at least in part, to its activation of TLR2 and TLR2/6 and the following signalling. Paradoxical to its pro-inflammatory role in the defence against pathogens, the recognition of commensal bacteria by TLRs was demonstrated to play a crucial role in limiting inflammation and maintaining homeostasis in the GI tract [27]. This was highlighted in mice deficient of TLRs, including TLR2, which had an increased susceptibility to colitis induced by DSS [148]. In addition, TLR2 activation preserved the TJ-associated epithelial barrier integrity in IECs against stressed-induced damage [150]. This effect was confirmed with mice deficient in TLR2 being predisposed to stress-induced disruption of the TJ-modulated barrier function [150]. Moreover, regulation of epithelial integrity by the probiotic *L. plantarum* WCFS1 were shown to be mediated through TLR2 signalling [116]. Furthermore, the activation of TLR2/6 was shown to exert immune-regulatory effects by driving the differentiation of DCs towards a tolerogenic phenotype, which promoted regulatory IL-10 immune responses [153]. Although in this example used as an immune evasion strategy of the pathogen *Yersinia pestis*, this mechanism may also be used by commensal bacteria such as *F. prausnitzii* to maintain immune homeostasis in the GI tract. In addition, the activation of the transcription factor NF-κB in general was suggested to play a dual role by inducing the expression of pro-inflammatory mediators in response to pathogenic bacteria but also contributing to the regulation of immune homeostasis in the GI tract [312,313]. For example, genetic mouse models with impaired NF-κB activation in IECs developed severe chronic colitis with epithelial ulceration, increased expression of pro-inflammatory mediators and infiltration of immune cells [326]. Collectively, these results demonstrate the beneficial role of TLR activation, so it is therefore plausible that

the TLR2 and TLR2/6 stimulation and the following NF-κB activation by live *F. prausnitzii* may cause its anti-inflammatory effects in the GI tract.

The high abundance of *F. prausnitzii* in the human GI tract, which was reported to account for more than 5% of the total bacterial population [311], may be enabled through TLR signalling. In line with this *Bacteroides fragilis,* another prominent commensal within the human microbiota, used the activation of the TLR pathway as a mechanism to establish host microbial symbiosis [327]. The TLR2 activation induced by polysaccharide A (PSA), a product of *B. fragilis*, actively suppressed immunity and promoted tolerance, thereby enhancing its own colonisation in the GI tract. It is plausible that the colonisation of *F. prausnitzii* in the GI tract and thus its symbiotic host-microbe interactions are enabled through TLR2 signalling induced by symbiotic bacterial molecules.

The results of this research showing that live *F. prausnitzii* induced higher NF-κB activation compared to dead bacteria appears conflicting with the previous research showing inhibitory effects of *F. prausnitzii* on NF-κB activation [19,179,213]. For example, gene expression analyses of Caco-2 cells exposed to live and UV-killed *F. prausnitzii* A2-165 in the apical anaerobic co-culture model showed that live bacteria inhibited the gene expression of the NF-κB transcription factor complex [19]. Also, the recently identified anti-inflammatory protein secreted by *F. prausnitzii* inhibited the NF-κB pathway in several IEC lines [213]. However, the functional consequences of TLR activation were reported to strongly depend on the responding cell type [328]. In contrast to this research, previous studies have mostly used IEC lines to examine the anti-inflammatory effects of *F prausnitzii*. The response of IECs to bacteria is a complex fine-tuning of the signalling of different innate immune receptors expressed on IECs (e.g. TLRs, NOD-like receptors) [132]. Moreover, IECs have evolved to co-exist with the

trillions of microorganisms within the GI tract by inducing tolerant reactions towards the commensal microbiota. Mechanisms include the spatially regulated expression of TLRs within IECs [140,141] and different functional consequences of TLR signalling depending on the site of the IEC where the receptor stimulation with the ligand occurs [142]. Furthermore, IECs express negative regulators of TLR signalling like TOLLIP [141,144]. Therefore, the results obtained with IECs cannot be directly compared to the results reported in this study. The approach applied in this research aimed in deciphering which TLRs recognise the three strains of *F. prausnitzii* and if there are differences in the TLR activation between live and dead bacteria. Based on the manufacturer's information (Invivogen), HEK293-TLR-Luc cells only express endogenous levels of TLR1, TLR3, TLR5, and NOD1. Consequently, in contrast to the immune responses in IECs, the activation of NF-κB in HEK293-TLR-Luc cells was specific for the respective TLRs tested.

The TLR2/6 activation was different between the three *F. prausnitzii* strains tested. *F. prausnitzii* A2-165 induced the highest NF-κB activation through TLR2/6 signalling, which was 1.2-fold higher compared to the activation induced by *F. prausnitzii* ATCC 27768 and 1.8-fold higher compared to *F. prausnitzii* HTF-F. This is in agreement with the results of a previous study comparing the immune-stimulatory potential of different strains of *F. prausnitzii*, including *F. prausnitzii* A2-165 and HTF-F, and other abundant commensals [207]. *F. prausnitzii* A2-165 was distinct from the other strains by inducing high TLR signalling activity which was associated with its ability to induce high levels of cytokines in human DCs. Moreover, principal component analysis demonstrated that the cytokine response to *F. prausnitzii* A2-165 was distinct from the other strains tested due to the high levels of IL-10 induced by this strain. Together with the results reported in this chapter, these findings highlight that bacterial effects can differ between strains of the

same species. Compared to other strains, *F. prausnitzii* A2-165 could be of particular interest as a next-generation probiotic due to its strong immune-stimulatory potential.

In conventional conditions there was a difference in the TLR2 activation between live and UV-killed *F. prausnitzii*. However, the TLR2 activation by live bacteria was only 1.1-fold higher compared to UV-killed bacteria, therefore less different compared to the TLR2 activation by live and UV-killed bacteria in apical anaerobic conditions and possibly not a biologically relevant difference. For TLR2/6 there was no difference between live and dead bacteria in conventional conditions. In conventional conditions the *F. prausnitzii* that were added live were quickly killed in the presence of oxygen. These results indicate that the way the bacteria were killed, either through exposure to UV-light or in the presence of oxygen, did not influence the receptor activation. UV-light may affect bacterial surface structures. However, *F. prausnitzii* killed by UV-light or oxygen induced the same TLR activation, which was in both cases lower compared to live bacteria in apical anaerobic conditions. This observation confirms the hypothesis that TLR activation is not only induced by bacterial surface structures but also influenced by metabolites secreted by live bacteria.

None of three *F. prausnitzii* strains were recognised by TLR4, independent of the status of the bacteria (live or UV-killed) and the environment in which the assay was performed (conventional or apical anaerobic). This is consistent with the results of the study mentioned above [6]. *F. prausnitzii* stains Gram-negative, which is also supported by the Gram staining performed in this research, and would therefore be anticipated to activate TLR4 through its ligand LPS, which is present in the cell wall of traditional Gram-negative bacteria. However, previous analyses of the cell surface structures of *F. prausnitzii* suggested either a lack of LPS or an unusual LPS composition [7]. In addition, even

though characterised as a Gram-negative bacterium, phylogenetic analysis based on 16S rRNA sequences indicated that *F. prausnitzii* is related to Gram-positive bacteria of clostridial cluster IV [8]. Similarly, phylogenetic analyses based on the bacterial cell envelope marker genes Hsp60 and Hsp70 performed in this PhD project, demonstrated that the cell envelope of *F. prausnitzii* resembles more that of Gram-positive bacteria such as *Bacillus subtilis* than of Gram-negative bacteria such as *E. coli.* Furthermore, the sequence alignment showed that the one amino acid insert in Hsp60 and the 24 amino acid insert in Hsp70, which has been shown to be a shared characteristic of traditional Gram-negative bacteria that have an outer membrane containing LPS [1,2], is absent in *F. prausnitzii.* Collectively, based on the *in silico* studies performed in this PhD project and by Gupta *et al.* [1,2], it can be proposed that *F. prausnitzii* is a monoderm bacterium. It therefore lacks LPS which is only present in the outer membrane of diderm bacteria and, consequently, does not activate TLR4. It may be possible that despite being a monoderm bacterium, *F. prausnitzii* stains Gram-negative because it may have a thinner peptidoglycan layer compared to bacteria that stain Gram-positive. Further structural studies investigating the fine structure of the *F. prausnitzii* cell envelope are required to further validate this hypothesis.

In the absence of TLR activation, the luminescence signal was very low in both anaerobic and conventional conditions. There was no difference between the negative control and the bacterial treatments for HEK293-TLR4-Luc and HEK293-null-Luc cells. Consequently, there was no TLR4 dependent or TLR-independent NF-κB activation. For this reason the difference observed between the environments was only a difference between the background luminescence. Based on the manufacturer's information (Promega), the culture medium used for the luciferase assays can contribute to the background luminescence and affect the assay characteristics (e.g. light intensity and signal stability). The apical medium

in conventional conditions was aerobic 50% M199 TEER+50% BHI, whereas in apical anaerobic conditions anaerobic 50% M199 TEER+50% BHI was used. The absence of oxygen and the addition of the reducing agent L-cysteine to anaerobic but not to aerobic BHI may have caused the different background luminescence in the two environments.

In conclusion, the higher TLR2 and TLR2/6 activation by live *F. prausnitzii* may contribute to its immune-regulatory effects and to the maintenance of immune homeostasis in the GI tract. The higher TLR activation by live compared to dead *F. prausnitzii* may possibly be mediated by secreted metabolites or through epigenetic mechanisms. These findings allow insights into the mechanisms of innate signalling, indicating that TLR activation is not only induced by bacterial surface structures. The different effects on TLR activation between live and dead bacteria highlight the importance of using physiologically relevant co-culture models, such as the apical anaerobic co-culture model, to decipher the mechanisms of action of live obligate anaerobes.

CHAPTER SIX:
General Discussion

6.1. BACKGROUND

The prevalence of inflammatory diseases, for example IBD, has increased over the past decades in industrialised countries [7]. Accumulating human data have established a link between an imbalance in the GI microbiota composition, so called dysbiosis, and the development of inflammatory diseases [6]. Probiotics, 'live microorganisms that, when administered in adequate amounts, confer a health benefit on the host' [171,172], have been extensively studied as a potential treatment to alleviate chronic inflammation and improve human health. Traditionally, bacterial species used for probiotic formulations mainly belong to the lactic acid bacteria, such as *Lactobacillus* spp. Whereas lactobacilli are common members of the infant GI microbiota, they comprise only a small percentage in the human adult microbiota, with most *Lactobacillus* spp. colonising the upper GI tract [177]. For this reason classical probiotics have often been associated with a poor ability to stably colonise the human GI tract [330]. Only in recent years, the interest in the development for novel probiotics has shifted towards bacterial species that are naturally abundant within the human microbiota and are associated with beneficial effects [17]. However, it is difficult to study the mechanisms of these species using conventional *in vitro* co-culture models, given that over 99% of the bacteria in the human GI tract are obligate anaerobes [18] and for this reason cannot be readily co-cultured with oxygen-requiring human cells to study their interactions. This difficulty explains the scarcity of knowledge about interactions between the anaerobes and the gut epithelium.

The novel apical anaerobic co-culture model developed at AgResearch overcomes this technical difficulty [19]. Through the separation of anaerobic and aerobic compartments it allows the co-culture and study of the direct interactions between live obligate anaerobes and human cells. This model was used in this PhD dissertation to decipher the mechanisms

of action of *F. prausnitzii*, an abundant obligate anaerobe associated with anti-inflammatory effects in the human GI tract [178,179,213]. The effects of *F. prausnitzii* on intestinal barrier function and immune homeostasis were investigated, both of which are impaired in inflammatory diseases [5]. The main hypotheses addressed in this study were: (i) live and growing *F. prausnitzii* co-cultured with IEC monolayers increase the barrier integrity of these cells, (ii) live *F. prausnitzii* mitigate the TNF-α-induced decrease in barrier integrity of the IEC monolayers, (iii) live *F. prausnitzii* activates innate immune receptors (TLRs) to a greater extent compared to dead bacteria. Method development was required to be able to test these hypotheses. The secondary hypotheses testing this method development were (a) *F. prausnitzii* (strains A2-165, ATCC 27768 and HTF-F) is able to grow in the apical anaerobic co-culture model if the apical medium is supplemented with substrates required for its growth and (b) the viability of both TLR expressing HEK293 cell lines and *F. prausnitzii* is maintained in the TLR activation assay carried out in the apical anaerobic co-culture model.

6.2. SUMMARY OF RESULTS

This dissertation was divided into two method development chapters (Chapters 2 and 4) and two respective results chapters (Chapters 3 and 5) that applied the developed methods. The method development was performed to be able to co-culture two types of human epithelial cells, Caco-2 and HEK293 cells, with strains of *F. prausnitzii* (A2-165, ATCC 27768 and HTF-F) in the apical anaerobic co-culture model to recreate conditions relevant to the GI tract. Using the adapted methods the effects of *F. prausnitzii* on intestinal barrier function and immune homeostasis were investigated.

The method development conducted for the co-culture of Caco-2 cells with *F. prausnitzii* in Chapter 2 comprised optimising the growth of the *F. prausnitzii* strains in the co-culture

model. The existing method for co-culturing Caco-2 cells with *F. prausnitzii* improved the viability of *F. prausnitzii* in the co-culture model compared to when grown under standard atmospheric conditions [19]. However, the bacterial growth was stagnant in the cell culture medium used for the co-culture experiments. It was hypothesised that growing and metabolically active bacteria exert differential effects on host cells compared to dead bacteria. In this research the growth of the *F. prausnitzii* strains in the co-culture model was optimised by supplementing the apical anaerobic cell culture medium (M199 TEER) with 50% bacterial culture medium (BHI). This supplementation resulted in an increase in CFUs of *F. prausnitzii* A2-165 and ATCC 27768 after 12 h of co-culture with Caco-2 cells in the apical anaerobic co-culture model. The viability and barrier integrity of the Caco-2 cells was maintained when using the adapted apical medium.

The optimised co-culture conditions were applied in Chapter 3 to assess the effect of *F. prausnitzii* on intestinal barrier integrity. Contrary to the hypothesis, live and growing strains of *F. prausnitzii* did not alter TEER across healthy Caco-2 monolayers. It was also determined whether the *F. prausnitzii* strains alleviate the decrease in TEER across Caco-2 monolayers induced by the pro-inflammatory cytokine TNF-α. Unexpectedly, the previously used dosage of TNF-α did not decrease TEER. It is plausible that the basal TNF-α concentration was insufficient to disrupt the TJ structure of the Caco-2 cells. The previously used dosage was applied under conventional conditions (5% CO_2 in air atmosphere), however, Caco-2 cells may respond different to the TNF-α treatment under apical anaerobic conditions. Even though the expected TNF-α induced TEER decrease did not occur, the bacterial strains exerted differential effects on TEER across healthy and TNF-α-treated Caco-2 monolayers. Whereas neither live nor dead *F. prausnitzii* strains altered TEER across healthy Caco-2 monolayers, dead *F. prausnitzii* HTF-F decreased TEER of TNF-α treated Caco-2 cells likely due to surface interactions.

The method development in Chapter 4 for the co-culture of HEK293 cells and *F. prausnitzii* was required to be able to test the activation of TLRs by live *F. prausnitzii*. HEK293 cell lines expressing human TLRs (TLR2, TLR2/6 and TLR4) and a control cell line (HEK293-null) were stably transfected with a NF-κB-inducible luciferase plasmid to be able to quantify receptor activation upon stimulation. These cells were referred to as HEK293-TLR-Luc and HEK293-null-Luc cells. The TLR activation assay was successfully adapted to be carried out in the novel model. The adaptations to the apical anaerobic conditions included improving the attachment of the HEK293-TLR-Luc cells in the co-culture model by using collagen-coated inserts and using a shorter incubation time (6 h instead of 12 h). Furthermore, the dissociation reagent TrypLE was used when harvesting the cells in order to obtain a single cell suspension rather than cell aggregates when seeding the cells on Transwell inserts. In the basal aerobic compartment 60% of the starting DO concentration remained after 6 h of incubation providing sufficient oxygen for the HEK293-TLR-Luc cells. Accordingly, the viability of the cells was maintained using the adapted assay conditions. No oxygen was detected in the apical anaerobic compartment at any time point and it could therefore be anticipated that the viability of obligate anaerobic *F. prausnitzii* would be maintained. However, when using cell culture media (DMEM+FBS and M199 TEER) as apical medium, a decrease of *F. prausnitzii* A2-165 viable cell titre by approximately 100-fold was observed when co-cultured with HEK293-TLR2-Luc cells for 6 h. M199 TEER supplemented with 50% BHI was chosen for the TLR activation assays carried out in Chapter 5. This medium was selected because it improved the viability of *F. prausnitzii* co-cultured with HEK293-TLR-Luc cells compared to the viability in the presence of cell culture medium alone (tenfold decrease in viable cell titre over 6 h). Additionally, in contrast to higher BHI concentrations (75 and

100%), M199 TEER supplemented with 50% BHI did not disrupt the integrity of the HEK293-TLR-Luc cell layers.

In Chapter 5 the activation of TLR2, TLR2/6 and TLR4 by live and dead *F. prausnitzii* was determined. Live *F. prausnitzii* activated TLR2 and TLR2/6 to a greater extent compared to dead bacteria (killed by UV-light or in the presence of oxygen). Neither live nor dead *F. prausnitzii* activated TLR4. It was also demonstrated that the NF-κB activation was dependent on the expression of the respective TLRs because the control cell line which contained the luciferase reporter plasmid but did not express TLRs (HEK293-null-Luc cells) was not stimulated by *F. prausnitzii*.

6.3. GENERAL DISCUSSION, LIMITATIONS AND FUTURE PERSPECTIVES

6.3.1. Method development

The main aim of the method development described in Chapters 2 and 4 was the optimisation of the growth of the three *F. prausnitzii* strains in co-culture with Caco-2 cells and HEK293-TLR-Luc cell lines in the apical anaerobic co-culture model. Furthermore, the viability and barrier integrity (Caco-2 cells) and the viability and cell attachment (HEK293-TLR-Luc cells) needed to be maintained under the adapted conditions. Previous studies mostly used mammalian cell culture media for the co-culture of bacteria with human cells [19,274,275]. For some bacteria the viability was not different when grown in mammalian or bacterial culture medium as shown for the examples of *L. fructosus* C2, *S. typhimurium* SL1344 and enterotoxigenic *E. coli* K88 [275]. However, *F. prausnitzii* is a fastidious species that requires complex media to grow and defined media, such as the mammalian cell culture media used in these studies (M199 TEER and DMEM+FBS), do not contain sufficient nutrients to enable its growth.

Using an apical medium consisting of 50% cell culture medium (M199 TEER) and 50% bacterial culture medium (BHI) has proved to be a suitable compromise to improve the viability of *F. prausnitzii* while maintaining the viability of the human cell lines. However, BHI impaired cell surface structures of both Caco-2 and HEK293-TLR-Luc cells as visualised through light microscopy. The addition of BHI to the apical medium caused a greater initial drop in TEER of Caco-2 cells compared to when using M199 TEER alone. Furthermore, using 75 or 100% BHI on the apical side of the HEK293-TLR-Luc cell layers resulted in the disruption and detachment of the cell layers. Although this effect was minimised when using mixtures of 50% M199 TEER and 50% BHI, the model conditions could be further improved. For example, the addition of a mucus layer could protect the human cells from the negative effects of BHI. Furthermore, IECs covered by a mucus layer would represent a more physiologically relevant *in vitro* model. Co-cultures of absorptive enterocytes (Caco-2 cells) and mucus-secreting goblet cells (HT29-MTX cells) have been established to simulate the cell proportions as present in the small (90:10) and large intestine (75:25) [331]. Future experiments could aim to use Caco-2/HT29-MTX co-cultures in the apical anaerobic co-culture model. The addition of a mucus layer to protect the human cells may allow the use of undiluted BHI as apical medium in the co-culture model, which may enable growth of all three *F. prausnitzii* strains with both of the cell lines.

The apical medium could be further supplemented with fermentable substrates, e.g. cellobiose, to stimulate the butyrate production by *F. prausnitzii*. Increased bacterial butyrate production may exert additional effects on barrier integrity of Caco-2 cells and on TLR activation in the apical anaerobic co-culture model.

A further limitation of the apical anaerobic co-culture model experienced during the method development studies was the pressure build up when inserting the Transwell inserts containing the cell layers into the airtight system. This pressure caused the basal aerobic medium to pass through to the apical side both when using Caco-2 and HEK293-TLR-Luc cells in the co-culture model. Using different one-way pressure relief valves in the co-culture chamber could prevent this technical difficulty. Pressure relief valves can be customised for the intended use to obtain the ideal opening pressure.

6.3.2. Effect of *F. prausnitzii* on intestinal barrier function and immune homeostasis

Specific probiotic and commensal bacteria enhance the integrity of the intestinal barrier [112,113,116]. However, in this research live and growing strains of *F. prausnitzii* did not enhance the barrier integrity of healthy IECs because the bacteria did not alter TEER across healthy Caco-2 monolayers. In contrast to the hypothesis, the growth phase of *F. prausnitzii* and potential metabolites secreted by growing bacteria did therefore not affect TEER across healthy Caco-2 monolayers.

However, under TNF-α-mediated inflammatory conditions dead *F. prausnitzii* HTF-F decreased TEER whereas live bacteria maintained it. It may be possible that surface structures of *F. prausnitzii* HTF-F disrupted the TJs of TNF-α-treated Caco-2 cells. *F. prausnitzii* HTF-F surface structures may have increased the expression levels of genes and the abundance of proteins involved in TJ disassembly which was shown to cause the barrier disrupting effects of the human oral isolate *L. fermentum* AGR1487 [274]. It is plausible that the barrier disrupting effect occurred only using dead *F. prausnitzii* HTF-F because live *F. prausnitzii* may compensate for the detrimental effect on TJ structure potentially through secreted metabolites. These have previously been shown to exert barrier protecting effects in TNF-α-treated IECs [120]. It is plausible that live *F.*

prausnitzii in the human GI tract also contributes to maintaining barrier integrity under inflammatory conditions.

Previous studies demonstrated a direct link between the activation of innate signalling and maintaining intestinal barrier function through the regulation of TJ integrity and expression. For example, the activation of TLR2 and following signalling has been implicated in enhancing barrier integrity [116,150,151]. Through the regulation of TJ integrity in IECs, TLR2 signalling influences susceptibility to intestinal injury and inflammation as demonstrated in TLR2 knockout mice [150]. TLR2 signalling was also indicated to contribute to the regulation of barrier integrity by the probiotic *Lactobacillus plantarum* WCFS1 [116]. One mechanism behind the barrier enhancing effect of TLR2 signalling is the activation of specific isoforms of protein kinase C in IECs which causes the translocation of the TJ protein ZO-1 [151]. The results reported here also suggest a link between the activation of innate signalling and barrier integrity because barrier maintaining properties of live *F. prausnitzii* were associated with a greater activation of TLR2 and TLR2/6. However, the barrier maintaining properties of live *F. prausnitzii* were only observed under TNF-α-mediated inflammatory conditions. This indicates that unstimulated Caco-2 cells remain hypo-responsive to bacterial challenge, which is in accordance with previous studies [295]. For example, no responses were observed when exposing Caco-2 cells to non-pathogenic bacteria; however, the treatment of Caco-2/PBMC co-cultures with the same bacteria resulted in the production of pro-inflammatory cytokines by the Caco-2 cells [295]. It was therefore hypothesised that IEC responses to bacteria depend on the cross-talk with immune cells and TNF-α was identified as a key mediator in these interactions [295]. This may also explain the different effects of *F. prausnitzii* on healthy and TNF-α-treated Caco-2 cells in this research.

However, a major limitation of the studies assessing the effect of *F. prausnitzii* on intestinal barrier function was that the positive control, i.e. TNF-α, failed. The expected decrease in TEER by TNF-α did not occur. This limitation has to be considered when interpreting the effects of the bacteria on TNF-α treated Caco-2 cells and future studies are required to validate the apical anaerobic co-culture model using TNF-α. Dose-response studies with increasing basal TNF-α concentrations or preincubation of Caco-2 cells with TNF-α prior to adding the treatments may solve this problem. However, the preincubation would involve an extended treatment time in the apical anaerobic co-culture model. In the current prototype of the co-culture chamber the Caco-2 cells remain viable for 12 h. An extended treatment time would therefore require further modifications on the co-culture chamber as discussed below.

Whereas TLRs have first been identified to be important in triggering inflammation in the defence against pathogens in the GI tract [316], evidence is now accumulating that TLR signalling is also crucial in maintaining homeostasis [148]. This study showed that live *F. prausnitzii* activated TLR2 and TLR2/6 to a greater extent compared to dead bacteria, which is in accordance with previous studies comparing the effects of live and dead pathogenic and commensal bacteria on TLR activation [318,319]. The higher TLR2 and TLR2/6 activation by live *F. prausnitzii* may contribute to the maintenance of immune homeostasis in the GI tract because several studies indicate a role for TLR2 and TLR2/6 activation in inducing anti-inflammatory responses. For example, mice deficient of TLRs, including TLR2, showed an increased susceptibility to experimental colitis [148]. Moreover, several studies indicate a role for anti-inflammatory TLR2 signalling in response to potential probiotic species in the protection of TLR4 mediated pro-inflammatory signalling induced by enteropathogens or protection from experimental colitis [156-158]. The anti-inflammatory effects of PSA, a symbiosis factor produced by

the abundant human commensal *B. fragilis*, is also mediated through TLR2 activation [159,160]. Additionally, NF-κB activation in general, although critical in the defence against pathogens through the initiation of pro-inflammatory responses, has been linked to maintaining immune homeostasis in the GI tract [312,313,332]. Taken together, it can be hypothesised that the greater TLR2 and TLR2/6 activation by live *F. prausnitzii* contributes to its anti-inflammatory effects in the human GI tract, for example through maintaining barrier integrity.

The activation of TLR2/1 by the *F. prausnitzii* strains could not be investigated in this study because the company that supplied the TLR expressing cell lines (Invivogen) only produces HEK293 cells transfected with TLR2/1 of mouse but not human origin. Further studies are required to determine whether *F. prausnitzii* activates TLR2/1 and whether there are differences in TLR2/1 activation between live and dead bacteria. This is of particular interest because in contrast to TLR2/6, TLR2/1 has been reported to trigger pro-inflammatory responses [153]. Results obtained from studies testing the activation of both TLR2/1 and TLR2/6 would therefore provide important insights into the immunoregulatory mechanisms of *F. prausnitzii.*

In accordance to the results presented in this study, *F. prausnitzii* exerted immunoregulatory effects when co-cultured with Caco-2 cells in a simple dual-environment co-culture model (Figure 1.6D, [252]). Caco-2 cells co-cultured with *F. prausnitzii* had reduced mRNA levels of the pro-inflammatory cytokine Il-1β compared to Caco-2 cell mono-cultures. Moreover, comparably to the results reported here, the barrier function of the Caco-2 cells was maintained when co-cultured with *F. prausnitzii* in the simple co-culture model because mRNA levels of the TJ protein claudin-1 were not altered

in the absence or presence of *F. prausnitzii* [252]. These findings therefore support the validity of the results obtained here.

The differences in TLR2 and TLR2/6 activation by live and dead *F. prausnitzii* indicate that TLR activation may be induced by mechanisms beyond the recognition of bacterial surface structures. The greater TLR2 and TLR2/6 activation induced by live *F. prausnitzii* may be mediated through secreted metabolites, for example butyrate, which enhances innate immune signalling [321]. To test this hypothesis, further experiments could test the effects of cell-free *F. prausnitzii* culture supernatants on TLR activation. Another explanation for the different immunostimulatory potential between live and dead *F. prausnitzii* could be epigenetic mechanisms, which has recently been demonstrated to cause the differing effects of live and dead bacteria [324]. For example, the differential modulation of IL-10 mRNA stabilisation and microRNA (MiR-27a) expression by live and heat-treated probiotics induced distinct IL-10 expression levels [324].

Since live *F. prausnitzii* induced greater activation of innate signalling it could be further investigated whether this effect correlates with the induction of higher cytokine secretion. *F. prausnitzii* induces the production of large amounts of anti-inflammatory IL-10 by DCs [207], however, these results were obtained using conventional co-culture models and effects were therefore only relevant to dead *F. prausnitzii*. In order to test the effect of live *F. prausnitzii* on activation of immune cells, the apical anaerobic co-culture model could be further developed to include this cell type. For example, the maturation and phenotype of immature DCs upon exposure to *F. prausnitzii* could be determined. In addition, the co-culture model could be used to study interactions between IECs, immune cells and *F. prausnitzii.* In this respect DCs could be included in the basal compartment of the co-culture chamber beneath the Caco-2 monolayer to mimic the situation *in vivo*. Following

exposure of the Caco-2 cells to *F. prausnitzii*, the crosstalk between Caco-2 cells, DCs and *F. prausnitzii* could be investigated. Whereas co-cultures of IECs, DCs and bacteria are established in conventional cell culture conditions (5% CO_2 in air atmosphere) [333], it would be new in the apical anaerobic co-culture model and would therefore require further method development.

A major limitation of the apical anaerobic co-culture model is the limited timeframe for co-culture experiments due to the consumption of the basal oxygen by the human cell lines. Due to this reason the initial validation studies for the co-culture model were performed using 12 h of incubation. However, bacterial effects on host cell function may only occur after a longer incubation. For example, effects of *F. prausnitzii* secreted metabolites on TJ integrity may require an extended treatment time which has been shown for butyrate, in which case the barrier enhancing properties occurred only after 24 h of incubation [293]. The design of a third prototype of the co-culture chamber could include the replenishment of the oxygen levels in the basal compartment thereby maintaining the viability of the human cell lines over a longer time. This alteration could allow an extended duration of co-culture experiments to test the interactions between *F. prausnitzii* and human cells.

The design of a third prototype co-culture chamber allowing the replenishment of the basal oxygen levels would also confer advantages for methods determining the cytokine secretion by DCs exposed to *F. prausnitzii.* The current co-culture chamber prototype has a large basal volume (3 mL) to provide sufficient oxygen for the human cell lines. The dilution with the large volume of basal cell culture medium would most likely lead to technical difficulties in detecting secreted cytokine levels. Due to the basal oxygen replenishment, the volume of the basal compartment of the new co-culture chamber could be decreased and therefore improve the cytokine measurements.

A further limitation of this study was that the effects of one species in isolation were tested. However, under physiological conditions, bacterial effects on host cells are the consequence of the complex interplay between the up to 1000 different bacterial species. For example, commensals can adapt their metabolism to the presence of other species [46] and the balance between major commensal species, *F. prausnitzii* and *B. thetaiotaomicron*, was demonstrated to play an important role in maintaining homoeostasis in the GI tract [221]. Future investigations could therefore aim to test the effects of *F. prausnitzii* on host function in combination with other species or in addition to a complex microbiota using the apical anaerobic co-culture model.

6.4. CONCLUDING REMARKS

This study investigated the effects of *F. prausnitzii* on intestinal barrier function and immune homeostasis using a novel dual-environment *in vitro* model, the apical anaerobic co-culture model. This model is more physiologically relevant compared to conventional co-culture models because it contains both anaerobic and aerobic compartments to allow the survival of both obligate anaerobic bacteria and oxygen-requiring human cells.

The results presented in this study have demonstrated greater TLR2 and TLR2/6 activation by live *F. prausnitzii* compared to dead bacteria. Live and growing strains of *F. prausnitzii* did not alter barrier integrity of healthy IECs. However, under TNF-α-mediated inflammatory conditions, dead *F. prausnitzii* decreased barrier integrity of TNF-α treated IEC monolayers whereas live bacteria maintained it. Previous studies demonstrated a direct link between TLR2 activation and the maintenance of intestinal barrier function [116,150,151]. It could therefore be hypothesised that the greater TLR2 activation by live *F. prausnitzii* contributes to its barrier maintaining effects.

The differing effects of live and dead *F. prausnitzii* observed in this research show the importance of using dual-environment *in vitro* co-culture models, such as the apical anaerobic co-culture model, to study the effects of live obligate anaerobic bacteria on human cells. The method development performed in this study successfully adapted and improved assay protocols to be performed in the novel co-culture model. Future research aiming to advance the apical anaerobic co-culture model, for example through the inclusion of other cell types, such as immune cells or mucus-secreting goblet cells, could further unravel the mechanisms underlying the beneficial effects of *F. prausnitzii* in the GI tract. In addition, these methods could be applied in future experiments to test the effects of additional species or combinations of species of the mostly anaerobic GI microbiota to study their mechanisms of action.

Prior to this research it was known that *F. prausnitzii* induced anti-inflammatory host responses in the GI tract but the mechanisms by which this occurs were unknown. The research presented in this dissertation provided some insights on how this bacterium might exert its effects. Live *F. prausnitzii* had differing effects on epithelial barrier integrity and activation of innate signalling compared to those obtained with its dead form. Compared to dead *F. prausnitzii*, live *F. prausnitzii* induced greater immunostimulatory effects, via TLR2 activation, and this effect is potentially linked to its barrier maintaining properties, because previous research showed enhancement of barrier integrity induced by TLR2 signalling. This new knowledge contributes to the understanding of how *F. prausnitzii* may maintain immune homeostasis in the GI tract. Unravelling the biological mechanisms used by prevalent species of the human microbiota, such as *F. prausnitzii*, will ultimately allow a better comprehension of microbial regulation of the GI function.

References

1 Hollister, E. B., Gao, C. & Versalovic, J. Compositional and functional features of the gastrointestinal microbiome and their effects on human health. *Gastroenterology* **146**, 1449-1458, (2014).

2 Mowat, A. M. & Agace, W. W. Regional specialization within the intestinal immune system. *Nat. Rev. Immunol.* **14**, 667-685, (2014).

3 Cahenzli, J., Balmer, M. L. & McCoy, K. D. Microbial-immune cross-talk and regulation of the immune system. *Immunology* **138**, 12-22, (2013).

4 Turner, J. R. Intestinal mucosal barrier function in health and disease. *Nat. Rev. Immunol.* **9**, 799-809, (2009).

5 Vindigni, S. M., Zisman, T. L., Suskind, D. L. & Damman, C. J. The intestinal microbiome, barrier function, and immune system in inflammatory bowel disease: A tripartite pathophysiological circuit with implications for new therapeutic directions. *Therap. Adv. Gastroenterol.* **9**, 606-625, (2016).

6 Carding, S., Verbeke, K., Vipond, D. T., Corfe, B. M. & Owen, L. J. Dysbiosis of the gut microbiota in disease. *Microb. Ecol. Health Dis.* **26**, 10.3402/mehd.v3426.26191, (2015).

7 Molodecky, N. A. et al. Increasing incidence and prevalence of the inflammatory bowel diseases with time, based on systematic review. *Gastroenterology* **142**, 46-54.e42, (2012).

8 Walsh, C. J., Guinane, C. M., O'Toole, P. W. & Cotter, P. D. Beneficial modulation of the gut microbiota. *FEBS Lett.* **588**, 4120-4130, (2014).

9 Sánchez, B. et al. Probiotics, gut microbiota and their influence on host health and disease. *Mol. Nutr. Food Res.*, Article in press, (2016).

10 Swidsinski, A., Loening-Baucke, V., Vaneechoutte, M. & Doerffel, Y. Active Crohn's disease and ulcerative colitis can be specifically diagnosed and monitored based on the biostructure of the fecal flora. *Inflamm. Bowel Dis.* **14**, 147-161, (2008).

11 Sokol, H. et al. Low counts of *Faecalibacterium prausnitzii* in colitis microbiota. *Inflamm. Bowel Dis.* **15**, 1183-1189, (2009).

12 Mondot, S. et al. Highlighting new phylogenetic specificities of Crohn's disease microbiota. *Inflamm. Bowel Dis.* **17**, 185-192, (2011).

13 Kabeerdoss, J., Sankaran, V., Pugazhendhi, S. & Ramakrishna, B. S. *Clostridium leptum* group bacteria abundance and diversity in the fecal microbiota of patients with inflammatory bowel disease: A case-control study in India. *BMC Gastroenterol.* **13**, 20, (2013).

14 Fujimoto, T. et al. Decreased abundance of *Faecalibacterium prausnitzii* in the gut microbiota of Crohn's disease. *J. Gastroenterol. Hepatol.* **28**, 613-619, (2013).

15 Rajilic-Stojanovic, M. et al. Global and deep molecular analysis of microbiota signatures in fecal samples from patients with irritable bowel syndrome. *Gastroenterology* **141**, 1792-1801, (2011).

16 De Palma, G. et al. Intestinal dysbiosis and reduced immunoglobulin-coated bacteria associated with coeliac disease in children. *BMC Microbiol.* **10**, 63, (2010).

17 Neef, A. & Sanz, Y. Future for probiotic science in functional food and dietary supplement development. *Curr. Opin. Clin. Nutr. Metab. Care* **16**, 679-687, (2013).
18 Eckburg, P. B. et al. Microbiology: Diversity of the human intestinal microbial flora. *Science* **308**, 1635-1638, (2005).
19 Ulluwishewa, D. et al. Live *Faecalibacterium prausnitzii* in an apical anaerobic model of the intestinal epithelial barrier. *Cell. Microbiol.* **17**, 226-240, (2015).
20 Marzorati, M. et al. The HMI™ module: A new tool to study the Host-Microbiota Interaction in the human gastrointestinal tract *in vitro*. *BMC Microbiol.* **14**, 133, (2014).
21 Shah, P. et al. A microfluidics-based *in vitro* model of the gastrointestinal human-microbe interface. *Nat. Commun.* **7**, (2016).
22 Luckey, T. D. Introduction to intestinal microecology. *Am. J. Clin. Nutr.* **25**, 1292-1294, (1972).
23 Sender, R., Fuchs, S. & Milo, R. Revised estimates for the number of human and bacteria cells in the body. *bioRxiv*, (2016).
24 Qin, J. et al. A human gut microbial gene catalogue established by metagenomic sequencing. *Nature* **464**, 59-65, (2010).
25 Claesson, M. J. et al. Comparative analysis of pyrosequencing and a phylogenetic microarray for exploring microbial community structures in the human distal intestine. *PLoS ONE* **4**, e6669, (2009).
26 Artis, D. Epithelial-cell recognition of commensal bacteria and maintenance of immune homeostasis in the gut. *Nat. Rev. Immunol.* **8**, 411-420, (2008).
27 Wells, J. M., Loonen, L. M. & Karczewski, J. M. The role of innate signaling in the homeostasis of tolerance and immunity in the intestine. *Int. J. Med. Microbiol.* **300**, 41-48, (2010).
28 Brown, E. M., Sadarangani, M. & Finlay, B. B. The role of the immune system in governing host-microbe interactions in the intestine. *Nat. Immunol.* **14**, 660-667, (2013).
29 Arumugam, M. et al. Enterotypes of the human gut microbiome. *Nature* **473**, 174-180, (2011).
30 Wu, G. D. et al. Linking long-term dietary patterns with gut microbial enterotypes. *Science* **334**, 105-108, (2011).
31 Ding, T. & Schloss, P. D. Dynamics and associations of microbial community types across the human body. *Nature* **509**, 357-360, (2014).
32 Jeffery, I. B., Claesson, M. J., O'Toole, P. W. & Shanahan, F. Categorization of the gut microbiota: Enterotypes or gradients? *Nat. Rev. Micro.* **10**, 591-592, (2012).
33 Huse, S. M., Ye, Y., Zhou, Y. & Fodor, A. A. A core human microbiome as viewed through 16S rRNA sequence clusters. *PLoS ONE* **7**, e34242, (2012).
34 Koren, O. et al. A guide to enterotypes across the human body: Meta-analysis of microbial community structures in human microbiome datasets. *PLoS Comp. Biol.* **9**, e1002863, (2013).
35 Gorvitovskaia, A., Holmes, S. P. & Huse, S. M. Interpreting *Prevotella* and *Bacteroides* as biomarkers of diet and lifestyle. *Microbiome* **4**, 1-12, (2016).
36 Zoetendal, E. G. et al. Mucosa-associated bacteria in the human gastrointestinal tract are uniformly distributed along the colon and differ from the community recovered from feces. *Appl. Environ. Microbiol.* **68**, 3401-3407, (2002).

37 Ouwerkerk, J. P., de Vos, W. M. & Belzer, C. Glycobiome: Bacteria and mucus at the epithelial interface. *Best Pract. Res. Clin. Gastroenterol.* **27**, 25-38, (2013).

38 Hong, P. Y., Croix, J. A., Greenberg, E., Gaskins, H. R. & Mackie, R. I. Pyrosequencing-based analysis of the mucosal microbiota in healthy individuals reveals ubiquitous bacterial groups and micro-heterogeneity. *PLoS ONE* **6**, e25042, (2011).

39 Png, C. W. et al. Mucolytic bacteria with increased prevalence in IBD mucosa augment *in vitro* utilization of mucin by other bacteria. *Am. J. Gastroenterol.* **105**, 2420-2428, (2010).

40 Martens, E. C., Chiang, H. C. & Gordon, J. I. Mucosal glycan foraging enhances fitness and transmission of a saccharolytic human gut bacterial symbiont. *Cell Host Microbe* **4**, 447-457, (2008).

41 Derrien, M., Vaughan, E. E., Plugge, C. M. & de Vos, W. M. *Akkermansia muciniphila* gen. nov., sp. nov., a human intestinal mucin-degrading bacterium. *Int. J. Syst. Evol. Microbiol.* **54**, 1469-1476, (2004).

42 Kelly, D. et al. Commensal anaerobic gut bacteria attenuate inflammation by regulating nuclear-cytoplasmic shuttling of PPAR-γ and RelA. *Nat. Immunol.* **5**, 104-112, (2004).

43 Hooper, L. V., Stappenbeck, T. S., Hong, C. V. & Gordon, J. I. Angiogenins: A new class of microbicidal proteins involved in innate immunity. *Nat. Immunol.* **4**, 269-273, (2003).

44 Kang, C. S. et al. Extracellular vesicles derived from gut microbiota, especially *Akkermansia muciniphila*, protect the progression of dextran sulfate sodium-induced colitis. *PLoS ONE* **8**, e76520, (2013).

45 Everard, A. et al. Cross-talk between *Akkermansia muciniphila* and intestinal epithelium controls diet-induced obesity. *Proc. Natl. Acad. Sci. U. S. A.* **110**, 9066-9071, (2013).

46 Mahowald, M. A. et al. Characterizing a model human gut microbiota composed of members of its two dominant bacterial phyla. *Proc. Natl. Acad. Sci. U. S. A.* **106**, 5859-5864, (2009).

47 Stewart, J. A., Chadwick, V. S. & Murray, A. Investigations into the influence of host genetics on the predominant eubacteria in the faecal microflora of children. *J. Med. Microbiol.* **54**, 1239-1242, (2005).

48 Claesson, M. J. et al. Gut microbiota composition correlates with diet and health in the elderly. *Nature* **488**, 178-184, (2012).

49 Gibson, G. R., Probert, H. M., Loo, J. V., Rastall, R. A. & Roberfroid, M. B. Dietary modulation of the human colonic microbiota: Updating the concept of prebiotics. *Nutr. Res. Rev.* **17**, 259-275, (2004).

50 Ramirez-Farias, C. et al. Effect of inulin on the human gut microbiota: Stimulation of *Bifidobacterium adolescentis* and *Faecalibacterium prausnitzii*. *Br. J. Nutr.* **101**, 541-550, (2009).

51 Martin, R. et al. Early-life events, including mode of delivery and type of feeding, siblings and gender, shape the developing gut microbiota. *PLoS ONE* **11**, e0158498, (2016).

52 Collado, M. C., Rautava, S., Aakko, J., Isolauri, E. & Salminen, S. Human gut colonisation may be initiated *in utero* by distinct microbial communities in the placenta and amniotic fluid. *Sci. Rep.* **6**, (2016).

53 Ardissone, A. N. et al. Meconium microbiome analysis identifies bacteria correlated with premature birth. *PLoS ONE* **9**, e90784, (2014).

54 Jiménez, E. et al. Is meconium from healthy newborns actually sterile? *Res. Microbiol.* **159**, 187-193, (2008).
55 Dominguez-Bello, M. G. et al. Delivery mode shapes the acquisition and structure of the initial microbiota across multiple body habitats in newborns. *Proc. Natl. Acad. Sci. U. S. A.* **107**, 11971-11975, (2010).
56 Bezirtzoglou, E., Tsiotsias, A. & Welling, G. W. Microbiota profile in feces of breast- and formula-fed newborns by using fluorescence *in situ* hybridization (FISH). *Anaerobe* **17**, 478-482, (2011).
57 Yatsunenko, T. et al. Human gut microbiome viewed across age and geography. *Nature* **486**, 222-227, (2012).
58 Claesson, M. J. et al. Composition, variability, and temporal stability of the intestinal microbiota of the elderly. *Proc. Natl. Acad. Sci. U. S. A.* **108**, 4586-4591, (2011).
59 Franceschi, C. et al. Inflamm-aging: An evolutionary perspective on immunosenescence. *Ann. N. Y. Acad. Sci.* **908**, 244-254, (2000).
60 Guigoz, Y., Doré, J. & Schiffrin, E. J. The inflammatory status of old age can be nurtured from the intestinal environment. *Curr. Opin. Clin. Nutr. Metab. Care* **11**, 13-20, (2008).
61 Lawley, T. D. & Walker, A. W. Intestinal colonization resistance. *Immunology* **138**, 1-11, (2013).
62 Lee, Y. K., Puong, K. Y., Ouwehand, A. C. & Salminen, S. Displacement of bacterial pathogens from mucus and Caco-2 cell surface by lactobacilli. *J. Med. Microbiol.* **52**, 925-930, (2003).
63 Kim, Y., Kim, S. H., Whang, K. Y., Kim, Y. J. & Oh, S. Inhibition of *Escherichia coli* O157:H7 attachment by interactions between lactic acid bacteria and intestinal epithelial cells. *J. Microbiol. Biotechnol.* **18**, 1278-1285, (2008).
64 Crost, E. H. et al. Ruminococcin C, a new anti-*Clostridium perfringens* bacteriocin produced in the gut by the commensal bacterium *Ruminococcus gnavus* E1. *Biochimie* **93**, 1487-1494, (2011).
65 Hooper, L. V., Xu, J., Falk, P. G., Midtvedt, T. & Gordon, J. I. A molecular sensor that allows a gut commensal to control its nutrient foundation in a competitive ecosystem. *Proc. Natl. Acad. Sci. U. S. A.* **96**, 9833-9838, (1999).
66 Resta, S. C. Effects of probiotics and commensals on intestinal epithelial physiology: Implications for nutrient handling. *J. Physiol. (Lond).* **587**, 4169-4174, (2009).
67 Russell, W. R., Hoyles, L., Flint, H. J. & Dumas, M. E. Colonic bacterial metabolites and human health. *Curr. Opin. Microbiol.* **16**, 246-254, (2013).
68 Segain, J.-P. et al. Butyrate inhibits inflammatory responses through NFκB inhibition: Implications for Crohn's disease. *Gut* **47**, 397-403, (2000).
69 Macpherson, A. J. & Harris, N. L. Interactions between commensal intestinal bacteria and the immune system. *Nat. Rev. Immunol.* **4**, 478-485, (2004).
70 Smith, K., McCoy, K. D. & Macpherson, A. J. Use of axenic animals in studying the adaptation of mammals to their commensal intestinal microbiota. *Semin. Immunol.* **19**, 59-69, (2007).
71 Gordon, H. A. & Bruckner-Kardoss, E. Effect of normal microbial flora on intestinal surface area. *Am. J. Physiol.* **201**, 175-178, (1961).
72 Savage, D. C., Siegel, J. E., Snellen, J. E. & Whitt, D. D. Transit time of epithelial cells in the small intestines of germfree mice and ex-germfree mice associated

with indigenous microorganisms. *Appl. Environ. Microbiol.* **42**, 996-1001, (1981).
73 Alam, M., Midtvedt, T. & Uribe, A. Differential cell kinetics in the ileum and colon of germfree rats. *Scand. J. Gastroenterol.* **29**, 445-451, (1994).
74 Sharma, R., Schumacher, U., Ronaasen, V. & Coates, M. Rat intestinal mucosal responses to a microbial flora and different diets. *Gut* **36**, 209-214, (1995).
75 Stappenbeck, T. S., Hooper, L. V. & Gordon, J. I. Developmental regulation of intestinal angiogenesis by indigenous microbes via Paneth cells. *Proc. Natl. Acad. Sci. U. S. A.* **99**, 15451-15455, (2002).
76 Jones, R. M. et al. Symbiotic lactobacilli stimulate gut epithelial proliferation via Nox-mediated generation of reactive oxygen species. *EMBO J.* **32**, 3017-3028, (2013).
77 Groschwitz, K. R. & Hogan, S. P. Intestinal barrier function: Molecular regulation and disease pathogenesis. *J. Allergy Clin. Immunol.* **124**, 3-20, (2009).
78 McGuckin, M. A., Eri, R., Simms, L. A., Florin, T. H. J. & Radford-Smith, G. Intestinal barrier dysfunction in inflammatory bowel diseases. *Inflamm. Bowel Dis.* **15**, 100-113, (2009).
79 Martínez, C., González-Castro, A., Vicario, M. & Santos, J. Cellular and molecular basis of intestinal barrier dysfunction in the irritable bowel syndrome. *Gut and Liver* **6**, 305-315, (2012).
80 Fasano, A. & Schulzke, J. D. Vol. 12 89-98 (2008).
81 de Kort, S., Keszthelyi, D. & Masclee, A. A. M. Leaky gut and diabetes mellitus: What is the link? *Obesity Reviews* **12**, 449-458, (2011).
82 Hijazi, Z., Molla, A. M., Al-Habashi, H., Muawad, W. M. R. A. & Sharma, P. N. Intestinal permeability is increased in bronchial asthma. *Arch. Dis. Child.* **89**, 227-229, (2004).
83 Yacyshyn, B., Meddings, J., Sadowski, D. & Bowen-Yacyshyn, M. Multiple sclerosis patients have peripheral blood CD45RO+ B cells and increased intestinal permeability. *Dig. Dis. Sci.* **41**, 2493-2498, (1996).
84 Ren, W.-y. et al. Age-related changes in small intestinal mucosa epithelium architecture and epithelial tight junction in rat models. *Aging-Clin. Exp. Res.* **26**, 183-191, (2014).
85 Kelly, J. et al. Breaking down the barriers: The gut microbiome, intestinal permeability and stress-related psychiatric disorders. *Front. Cell. Neurosci.* **9**, (2015).
86 Anderson RC, D. J., Gopal PK, Bassett S, Ellis A & Roy NC. in *Fukata M (Ed)* (Colitis 3-30, 2011).
87 Ulluwishewa, D. et al. Regulation of tight junction permeability by intestinal bacteria and dietary components. *J. Nutr.* **141**, 769-776, (2011).
88 Johansson, M. E. V., Larsson, J. M. H. & Hansson, G. C. The two mucus layers of colon are organized by the MUC2 mucin, whereas the outer layer is a legislator of host–microbial interactions. *Proc. Natl. Acad. Sci. U. S. A.* **108**, 4659-4665, (2011).
89 Bevins, C. L. & Salzman, N. H. Paneth cells, antimicrobial peptides and maintenance of intestinal homeostasis. *Nat. Rev. Micro.* **9**, 356-368, (2011).
90 Zanetti, M. The role of cathelicidins in the innate host defenses of mammals. *Curr. Issues Mol. Biol.* **7**, 179-196, (2005).

91 Acheson, D. W. K. & Luccioli, S. Mucosal immune responses. *Best Pract. Res. Clin. Gastroenterol.* **18**, 387-404, (2004).
92 Natividad, J. M. M. & Verdu, E. F. Modulation of intestinal barrier by intestinal microbiota: Pathological and therapeutic implications. *Pharmacol. Res.* **69**, 42-51, (2013).
93 Farquhar, M. G. & Palade, G. E. Junctional complexes in various epithelia. *J. Cell Biol.* **17**, 375-412, (1963).
94 Furuse, M. et al. Occludin: a novel integral membrane protein localizing at tight junctions. *J. Cell Biol.* **123**, 1777-1788, (1993).
95 Furuse, M., Fujita, K., Hiiragi, T., Fujimoto, K. & Tsukita, S. Claudin-1 and -2: novel integral membrane proteins localizing at tight junctions with no sequence similarity to occludin. *J. Cell Biol.* **141**, 1539-1550, (1998).
96 Ikenouchi, J. et al. Tricellulin constitutes a novel barrier at tricellular contacts of epithelial cells. *J. Cell Biol.* **171**, 939-945, (2005).
97 Martìn-Padura, I. et al. Junctional adhesion molecule, a novel member of the immunoglobulin superfamily that distributes at intercellular junctions and modulates monocyte transmigration. *J. Cell Biol.* **142**, 117-127, (1998).
98 Stevenson, B. R., Siliciano, J. D., Mooseker, M. S. & Goodenough, D. A. Identification of ZO-1: A high molecular weight polypeptide associated with the tight junction (zonula occludens) in a variety of epithelia. *J. Cell Biol.* **103**, 755-766, (1986).
99 Jesaitis, L. & Goodenough, D. Molecular characterization and tissue distribution of ZO-2, a tight junction protein homologous to ZO-1 and the Drosophila discs-large tumor suppressor protein. *J. Cell Biol.* **124**, 949-961, (1994).
100 Balda, M. S., Gonzalez-Mariscal, L., Matter, K., Cereijido, M. & Anderson, J. M. Assembly of the tight junction: The role of diacylglycerol. *J. Cell Biol.* **123**, 293-302, (1993).
101 Fanning, A. S., Jameson, B. J., Jesaitis, L. A. & Anderson, J. M. The tight junction protein ZO-1 establishes a link between the transmembrane protein occludin and the actin cytoskeleton. *J. Biol. Chem.* **273**, 29745-29753, (1998).
102 Furuse, M. et al. Direct association of occludin with ZO-1 and its possible involvement in the localization of occludin at tight junctions. *J. Cell Biol.* **127**, 1617-1626, (1994).
103 Itoh, M. et al. Direct binding of three tight junction-associated Maguks, ZO-1, ZO-2, and ZO-3, with the Cooh termini of claudins. *J. Cell Biol.* **147**, 1351-1363, (1999).
104 Stuart, R. O. & Nigam, S. K. Regulated assembly of tight junctions by protein kinase C. *Proc. Natl. Acad. Sci. U. S. A.* **92**, 6072-6076, (1995).
105 Turner, J. R. et al. Physiological regulation of epithelial tight junctions is associated with myosin light-chain phosphorylation. *Am. J. Physiol. Cell Physiol.* **273**, C1378-C1385, (1997).
106 Jou, T.-S., Schneeberger, E. E. & James Nelson, W. Structural and functional regulation of tight junctions by RhoA and Rac1 small GTPases. *J. Cell Biol.* **142**, 101-115, (1998).
107 Sakakibara, A., Furuse, M., Saitou, M., Ando-Akatsuka, Y. & Tsukita, S. Possible involvement of phosphorylation of occludin in tight junction formation. *J. Cell Biol.* **137**, 1393-1401, (1997).

108 Caballero-Franco, C., Keller, K., De Simone, C. & Chadee, K. The VSL#3 probiotic formula induces mucin gene expression and secretion in colonic epithelial cells. *Am. J. Physiol. Gastrointest. Liver Physiol.* **292**, G315-G322, (2007).

109 Schlee, M. et al. Probiotic lactobacilli and VSL#3 induce enterocyte β-defensin 2. *Clin. Exp. Immunol.* **151**, 528-535, (2008).

110 Campeotto, F. et al. A fermented formula in pre-term infants: Clinical tolerance, gut microbiota, down-regulation of faecal calprotectin and up-regulation of faecal secretory IgA. *Br. J. Nutr.* **105**, 1843-1851, (2011).

111 Fogh, J., Fogh, J. M. & Orfeo, T. One hundred and twenty seven cultured human tumor cell lines producing tumors in nude mice. *J. Natl. Cancer Inst.* **59**, 221-226, (1977).

112 Anderson, R. et al. *Lactobacillus plantarum* MB452 enhances the function of the intestinal barrier by increasing the expression levels of genes involved in tight junction formation. *BMC Microbiol.* **10**, 316, (2010).

113 Anderson, R. C., Cookson, A. L., McNabb, W. C., Kelly, W. J. & Roy, N. C. *Lactobacillus plantarum* DSM 2648 is a potential probiotic that enhances intestinal barrier function. *FEMS Microbiol. Lett.* **309**, 184-192, (2010).

114 Madsen, K. et al. Probiotic bacteria enhance murine and human intestinal epithelial barrier function. *Gastroenterology* **121**, 580-591, (2001).

115 Mennigen, R. et al. Probiotic mixture VSL#3 protects the epithelial barrier by maintaining tight junction protein expression and preventing apoptosis in a murine model of colitis. *Am. J. Physiol. Gastrointest. Liver Physiol.* **296**, G1140-G1149, (2009).

116 Karczewski, J. et al. Regulation of human epithelial tight junction proteins by *Lactobacillus plantarum in vivo* and protective effects on the epithelial barrier. *Am. J. Physiol. Gastrointest. Liver Physiol.* **298**, G851-G859, (2010).

117 Johnson-Henry, K. C., Donato, K. A., Shen-Tu, G., Gordanpour, M. & Sherman, P. M. *Lactobacillus rhamnosus* strain GG prevents enterohemorrhagic *Escherichia coli* O157:H7-induced changes in epithelial barrier function. *Infect. Immun.* **76**, 1340-1348, (2008).

118 Resta-Lenert, S. & Barrett, K. E. Live probiotics protect intestinal epithelial cells from the effects of infection with enteroinvasive *Escherichia coli* (EIEC). *Gut* **52**, 988-997, (2003).

119 Resta–Lenert, S. & Barrett, K. E. Probiotics and commensals reverse TNF-α– and IFN-γ–induced dysfunction in human intestinal epithelial cells. *Gastroenterology* **130**, 731-746, (2006).

120 Ewaschuk, J. B. et al. Secreted bioactive factors from *Bifidobacterium infantis* enhance epithelial cell barrier function. *Am. J. Physiol. Gastrointest. Liver Physiol.* **295**, G1025-G1034, (2008).

121 Donato, K. A., Gareau, M. G., Wang, Y. J. J. & Sherman, P. M. *Lactobacillus rhamnosus* GG attenuates interferon-γ and tumour necrosis factor-α-induced barrier dysfunction and pro-inflammatory signalling. *Microbiology* **156**, 3288-3297, (2010).

122 Hooper, L. V., Littman, D. R. & Macpherson, A. J. Interactions between the microbiota and the immune system. *Science* **336**, 1268-1273, (2012).

123 Helgeland, L., Vaage, J. T., Rolstad, B., Midtvedt, T. & Brandtzaeg, P. Microbial colonization influences composition and T-cell receptor V beta repertoire of intraepithelial lymphocytes in rat intestine. *Immunology* **89**, 494-501, (1996).

124 Macpherson, A. J., Hunziker, L., McCoy, K. & Lamarre, A. IgA responses in the intestinal mucosa against pathogenic and non-pathogenic microorganisms. *Microb. Infect.* **3**, 1021-1035, (2001).
125 Bauer, H., Horowitz, R. E., Levenson, S. M. & Popper, H. The response of the lymphatic tissue to the microbial flora. Studies on germfree mice. *Am. J. Pathol.* **42**, 471-483, (1963).
126 Frank, D. N. et al. Molecular-phylogenetic characterization of microbial community imbalances in human inflammatory bowel diseases. *Proc. Natl. Acad. Sci. U. S. A.* **104**, 13780-13785, (2007).
127 Manichanh, C. et al. Reduced diversity of faecal microbiota in Crohn's disease revealed by a metagenomic approach. *Gut* **55**, 205-211, (2006).
128 Walker, A. et al. High-throughput clone library analysis of the mucosa-associated microbiota reveals dysbiosis and differences between inflamed and non-inflamed regions of the intestine in inflammatory bowel disease. *BMC Microbiol.* **11**, 7, (2011).
129 Li, Q., Wang, C., Tang, C., Li, N. & Li, J. Molecular-phylogenetic characterization of the microbiota in ulcerated and non-ulcerated regions in the patients with Crohn's disease. *PLoS ONE* **7**, e34939, (2012).
130 Frank, D. N., Zhu, W., Sartor, R. B. & Li, E. Investigating the biological and clinical significance of human dysbioses. *Trends Microbiol.* **19**, 427-434, (2011).
131 Garrett, W. S. et al. Communicable ulcerative colitis induced by T-bet deficiency in the innate immune system. *Cell* **131**, 33-45, (2007).
132 Peterson, L. W. & Artis, D. Intestinal epithelial cells: Regulators of barrier function and immune homeostasis. *Nat. Rev. Immunol.* **14**, 141-153, (2014).
133 Cao, X. Self-regulation and cross-regulation of pattern-recognition receptor signalling in health and disease. *Nat. Rev. Immunol.* **16**, 35-50, (2016).
134 Chen, G. Y. & Nuñez, G. Sterile inflammation: Sensing and reacting to damage. *Nat. Rev. Immunol.* **10**, 826-837, (2010).
135 Liu, Q. & Ding, J. L. The molecular mechanisms of TLR-signaling cooperation in cytokine regulation. *Immunol. Cell Biol.* **94**, 538-542, (2016).
136 De Nardo, D. Toll-like receptors: Activation, signalling and transcriptional modulation. *Cytokine* **74**, 181-189, (2015).
137 Jiménez-Dalmaroni, M. J., Gerswhin, M. E. & Adamopoulos, I. E. The critical role of Toll-like receptors — From microbial recognition to autoimmunity: A comprehensive review. *Autoimmun. Rev.* **15**, 1-8, (2016).
138 Thaiss, C. A., Levy, M., Itav, S. & Elinav, E. Integration of innate immune signaling. *Trends Immunol.* **37**, 84-101.
139 Wells, J. M., Rossia, O., Meijerink, M. & Van Baarlen, P. Epithelial crosstalk at the microbiota-mucosal interface. *Proc. Natl. Acad. Sci. U. S. A.* **108**, 4607-4614, (2011).
140 Abreu, M. T. et al. Decreased expression of Toll-like receptor-4 and MD-2 correlates with intestinal epithelial cell protection against dysregulated proinflammatory gene expression in response to bacterial lipopolysaccharide. *J. Immunol.* **167**, 1609-1616, (2001).
141 Melmed, G. et al. Human intestinal epithelial cells are broadly unresponsive to Toll-like receptor 2-dependent bacterial ligands: Implications for host-microbial interactions in the gut. *J. Immunol.* **170**, 1406-1415, (2003).

142 Gewirtz, A. T., Navas, T. A., Lyons, S., Godowski, P. J. & Madara, J. L. Cutting edge: Bacterial flagellin activates basolaterally expressed TLR5 to induce epithelial proinflammatory gene expression. *J. Immunol.* **167**, 1882-1885, (2001).

143 Lee, J. et al. Maintenance of colonic homeostasis by distinctive apical TLR9 signalling in intestinal epithelial cells. *Nat. Cell Biol.* **8**, 1327-1336, (2006).

144 Burns, K. et al. Tollip, a new component of the IL-1RI pathway, links IRAK to the IL-1 receptor. *Nat. Cell Biol.* **2**, 346-351, (2000).

145 Zhang, G. & Ghosh, S. Negative regulation of Toll-like receptor-mediated signaling by Tollip. *J. Biol. Chem.* **277**, 7059-7065, (2002).

146 Wald, D. et al. SIGIRR, a negative regulator of Toll-like receptor-interleukin 1 receptor signaling. *Nat. Immunol.* **4**, 920-927, (2003).

147 Xiao, H. et al. The Toll–interleukin-1 receptor member SIGIRR regulates colonic epithelial homeostasis, inflammation, and tumorigenesis. *Immunity* **26**, 461-475, (2007).

148 Rakoff-Nahoum, S., Paglino, J., Eslami-Varzaneh, F., Edberg, S. & Medzhitov, R. Recognition of commensal microflora by Toll-like receptors is required for intestinal homeostasis. *Cell* **118**, 229-241, (2004).

149 Abreu, M. T. Toll-like receptor signalling in the intestinal epithelium: How bacterial recognition shapes intestinal function. *Nat. Rev. Immunol.* **10**, 131-144, (2010).

150 Cario, E., Gerken, G. & Podolsky, D. K. Toll-like receptor 2 controls mucosal inflammation by regulating epithelial barrier function. *Gastroenterology* **132**, 1359-1374, (2007).

151 Cario, E., Gerken, G. & Podolsky, D. K. Toll-like receptor 2 enhances ZO-1-associated intestinal epithelial barrier integrity via protein kinase C. *Gastroenterology* **127**, 224-238, (2004).

152 Kamdar, K., Nguyen, V. & DePaolo, R. W. Toll-like receptor signaling and regulation of intestinal immunity. *Virulence* **4**, 207-212, (2013).

153 Depaolo, R. W. et al. Toll-like receptor 6 drives differentiation of tolerogenic dendritic cells and contributes to LcrV-mediated plague pathogenesis. *Cell Host Microbe* **4**, 350-361, (2008).

154 Peres, A. G. et al. Uncoupling of pro- and anti-Inflammatory properties of *Staphylococcus aureus*. *Infect. Immun.* **83**, 1587-1597, (2015).

155 Parveen, N. et al. Endocytosis of *Mycobacterium tuberculosis* heat shock protein 60 is required to induce interleukin-10 production in macrophages. *J. Biol. Chem.* **288**, 24956-24971, (2013).

156 Finamore, A. et al. *Lactobacillus amylovorus* inhibits the TLR4 inflammatory signaling triggered by enterotoxigenic *Escherichia coli* via modulation of the negative regulators and involvement of TLR2 in intestinal Caco-2 cells and pig explants. *PLoS ONE* **9**, e94891, (2014).

157 Tomosada, Y. et al. Immunoregulatory effect of bifidobacteria strains in porcine intestinal epithelial cells through modulation of ubiquitin-editing enzyme A20 expression. *PLoS ONE* **8**, e59259, (2013).

158 Hayashi, A. et al. A single strain of *Clostridium butyricum* induces intestinal IL-10-producing macrophages to suppress acute experimental colitis in mice. *Cell Host Microbe* **13**, 711-722, (2013).

159 Round, J. L. & Mazmanian, S. K. Inducible Foxp3+ regulatory T-cell development by a commensal bacterium of the intestinal microbiota. *Proc. Natl. Acad. Sci. U. S. A.* **107**, 12204-12209, (2010).
160 Shen, Y. et al. Outer membrane vesicles of a human commensal mediate immune regulation and disease protection. *Cell Host Microbe* **12**, 509-520, (2012).
161 Assas, B. M., Miyan, J. A. & Pennock, J. L. Cross-talk between neural and immune receptors provides a potential mechanism of homeostatic regulation in the gut mucosa. *Mucosal Immunol.* **7**, 1283-1289, (2014).
162 Ghadimi, D., De Vrese, M., Heller, K. J. & Schrezenmeir, J. Effect of natural commensal-origin DNA on Toll-like receptor 9 (TLR9) signaling cascade, chemokine IL-8 expression, and barrier integritiy of polarized intestinal epithelial cells. *Inflamm. Bowel Dis.* **16**, 410-427, (2010).
163 Hiramatsu, Y. et al. Differences in TLR9-dependent inhibitory effects of H_2O_2-induced IL-8 secretion and NF-kappa B/I kappa B-alpha system activation by genomic DNA from five *Lactobacillus* species. *Microb. Infect.* **15**, 96-104, (2013).
164 Neish, A. S. et al. Prokaryotic regulation of epithelial responses by inhibition of IκB-α ubiquitination. *Science* **289**, 1560-1563, (2000).
165 Tripathi, P. & Aggarwal, A. NF-κB transcription factor: A key player in the generation of immune response. *Curr. Sci.* **90**, 519-531, (2006).
166 Hamer, H. M. et al. Review article: The role of butyrate on colonic function. *Aliment. Pharmacol. Ther.* **27**, 104-119, (2008).
167 Place, R. F., Noonan, E. J. & Giardina, C. HDAC inhibition prevents NF-κB activation by suppressing proteasome activity: Down-regulation of proteasome subunit expression stabilizes IκBα. *Biochem. Pharmacol.* **70**, 394-406, (2005).
168 Rimoldi, M. et al. Intestinal immune homeostasis is regulated by the crosstalk between epithelial cells and dendritic cells. *Nat. Immunol.* **6**, 507-514, (2005).
169 Zeuthen, L. H., Fink, L. N. & Frokiaer, H. Epithelial cells prime the immune response to an array of gut-derived commensals towards a tolerogenic phenotype through distinct actions of thymic stromal lymphopoietin and transforming growth factor-β. *Immunology* **123**, 197-208, (2008).
170 Metchnikoff, E. The prolongation of life. Optimistic Studies. *Putnam's Sons: New York*, 161 – 183, (1908).
171 FAO/WHO: Health and nutritional properties of Probiotics in food including powder milk with live lactic acid bacteria. Report of a Joint FAO WHO Expert Consultation, Córdoba, Argentina, 1 - 4 October 2001. *Food and Agriculture Organization of the United Nations, and World Health Organization*, (2001).
172 Hill, C. et al. Expert consensus document: The International Scientific Association for Probiotics and Prebiotics consensus statement on the scope and appropriate use of the term probiotic. *Nat. Rev. Gastroenterol. Hepatol.* **11**, 506-514, (2014).
173 Mattia, A. & Merker, R. Regulation of probiotic substances as ingredients in foods: Premarket approval or "generally recognized as safe" notification. *Clin. Infect. Dis.* **46**, S115-S118, (2008).
174 Saxelin, M. *Lactobacillus* GG - A human probiotic strain with thorough clinical documentation. *Food Rev. Int.* **13**, 293-313, (1997).

175 Ringel, Y., Quigley, E. M. M. & Lin, H. C. Using probiotics in gastrointestinal disorders. *Am. J. Gastroenterol. Suppl.* **1**, 34-40, (2012).
176 Rijkers, G. T. et al. Guidance for substantiating the evidence for beneficial effects of probiotics: Current status and recommendations for future research. *J. Nutr.* **140**, 671S-676S, (2010).
177 Walter, J. Ecological role of lactobacilli in the gastrointestinal tract: Implications for fundamental and biomedical research. *Appl. Environ. Microbiol.* **74**, 4985-4996, (2008).
178 Duncan, S. H., Hold, G. L., Harmsen, H. J. M., Stewart, C. S. & Flint, H. J. Growth requirements and fermentation products of *Fusobacterium prausnitzii*, and a proposal to reclassify it as *Faecalibacterium prausnitzii* gen. nov., comb. nov. *Int. J. Syst. Evol. Microbiol.* **52**, 2141-2146, (2002).
179 Sokol, H. et al. *Faecalibacterium prausnitzii* is an anti-inflammatory commensal bacterium identified by gut microbiota analysis of Crohn disease patients. *Proc. Natl. Acad. Sci. U. S. A.* **105**, 16731-16736, (2008).
180 Hold, G. L., Schwiertz, A., Aminov, R. I., Blaut, M. & Flint, H. J. Oligonucleotide probes that detect quantitatively significant groups of butyrate-producing bacteria in human feces. *Appl. Environ. Microbiol.* **69**, 4320-4324, (2003).
181 Cato, E. P., Salmon, C. W. & Moore, W. E. C. *Fusobacterium prausnitzii* (Hauduroy *et al*.) Moore and Holdeman: Emended description and designation of neotype strain. *Int. J. Syst. Bacteriol.* **24**, 225-229, (1974).
182 Qiu, X., Zhang, M., Yang, X., Hong, N. & Yu, C. *Faecalibacterium prausnitzii* upregulates regulatory T cells and anti-inflammatory cytokines in treating TNBS-induced colitis. *J. Crohns Colitis* **7**, e558-568, (2013).
183 Mazmanian, S. K., Round, J. L. & Kasper, D. L. A microbial symbiosis factor prevents intestinal inflammatory disease. *Nature* **453**, 620-625, (2008).
184 Lopez-Siles, M. et al. Cultured representatives of two major phylogroups of human colonic *Faecalibacterium prausnitzii* can utilize pectin, uronic acids, and host-derived substrates for growth. *Appl. Environ. Microbiol.* **78**, 420-428, (2012).
185 Nielsen, T. S. et al. Diets high in resistant starch and arabinoxylan modulate digestion processes and SCFA pool size in the large intestine and faecal microbial composition in pigs. *Br. J. Nutr.* **112**, 1837-1849, (2014).
186 Scott, K. P., Martin, J. C., Duncan, S. H. & Flint, H. J. Prebiotic stimulation of human colonic butyrate-producing bacteria and bifidobacteria, *in vitro*. *FEMS Microbiol. Ecol.* **87**, 30-40, (2014).
187 Khan, M. T., Browne, W. R., Van Dijl, J. M. & Harmsen, H. J. M. How can *Faecalibacterium prausnitzii* employ riboflavin for extracellular electron transfer? *Antioxid. Redox Signal.* **17**, 1433-1440, (2012).
188 Khan, M. T. et al. The gut anaerobe *Faecalibacterium prausnitzii* uses an extracellular electron shuttle to grow at oxic-anoxic interphases. *ISME J*, (2012).
189 Matijašić, B. B. et al. Association of dietary type with fecal microbiota in vegetarians and omnivores in Slovenia. *Eur. J. Nutr.* **53**, 1051-1064, (2014).
190 Mu, C., Yang, Y., Luo, Z., Guan, L. & Zhu, W. The colonic microbiome and epithelial transcriptome are altered in rats fed a high-protein diet compared with a normal-protein diet. *J. Nutr.* **146**, 474-483, (2016).
191 Liu, X. et al. High-protein diet modifies colonic microbiota and luminal environment but not colonocyte metabolism in the rat model: The increased

luminal bulk connection. *Am. J. Physiol. Gastrointest. Liver Physiol.* **307**, G459-G470, (2014).
192 Hedin, C. R. et al. Altered intestinal microbiota and blood T cell phenotype are shared by patients with Crohn's disease and their unaffected siblings. *Gut* **63**, 1578-1586, (2014).
193 Hedin, C. et al. Siblings of patients with Crohn's disease exhibit a biologically relevant dysbiosis in mucosal microbial metacommunities. *Gut* **65**, 944-953, (2016).
194 Balamurugan, R., Rajendiran, E., George, S., Samuel, G. V. & Ramakrishna, B. S. Real-time polymerase chain reaction quantification of specific butyrate-producing bacteria, *Desulfovibrio* and *Enterococcus faecalis* in the feces of patients with colorectal cancer. *J. Gastroenterol. Hepatol.* **23**, 1298-1303, (2008).
195 Bruzzese, E. et al. Disrupted intestinal microbiota and intestinal inflammation in children with cystic fibrosis and its restoration with *Lactobacillus* GG: A randomised clinical trial. *PLoS ONE* **9**, e87796, (2014).
196 Debyser, G. et al. Faecal proteomics: A tool to investigate dysbiosis and inflammation in patients with cystic fibrosis. *J. Cyst. Fibros.* **15**, 242-250, (2016).
197 Jackson, M. A. et al. Signatures of early frailty in the gut microbiota. *Genome Med.* **8**, 1-11, (2016).
198 Jiang, H. et al. Altered fecal microbiota composition in patients with major depressive disorder. *Brain, Behav., Immun.* **48**, 186-194, (2015).
199 Andoh, A. et al. Comparison of the gut microbial community between obese and lean peoples using 16S gene sequencing in a Japanese population. *J. Clin. Biochem. Nutr.* **59**, 65-70, (2016).
200 Haro, C. et al. The gut microbial community in metabolic syndrome patients is modified by diet. *J. Nutr. Biochem.* **27**, 27-31, (2016).
201 Remely, M. et al. Gut microbiota composition correlates with changes in body fat content due to weight loss. *Benef. Microbes* **6**, 431-439, (2015).
202 Remely, M. et al. Effects of short chain fatty acid producing bacteria on epigenetic regulation of FFAR3 in type 2 diabetes and obesity. *Gene* **537**, 85-92, (2014).
203 Van Immerseel, F. et al. Butyric acid-producing anaerobic bacteria as a novel probiotic treatment approach for inflammatory bowel disease. *J. Med. Microbiol.* **59**, 141-143, (2010).
204 Rossi, O. et al. *Faecalibacterium prausnitzii* strain HTF-F and its extracellular polymeric matrix attenuate clinical parameters in DSS-induced colitis. *PLoS ONE* **10**, (2015).
205 Martín, R. et al. The commensal bacterium *Faecalibacterium prausnitzii* is protective in DNBS-induced chronic moderate and severe colitis models. *Inflamm. Bowel Dis.* **20**, 417-430, (2014).
206 Martín, R. et al. *Faecalibacterium prausnitzii* prevents physiological damages in a chronic low-grade inflammation murine model. *BMC Microbiol.* **15**, 1-12, (2015).
207 Rossi, O. et al. *Faecalibacterium prausnitzii* A2-165 has a high capacity to induce IL-10 in human and murine dendritic cells and modulates T cell responses. *Sci. Rep.* **6**, (2016).

208 Zhang, M. et al. *Faecalibacterium prausnitzii* inhibits interleukin-17 to ameliorate colorectal colitis in rats. *PLoS ONE* **9**, (2014).
209 Khan, M. T., Van Dijl, J. M. & Harmsen, H. J. M. Antioxidants keep the potentially probiotic but highly oxygen-sensitive human gut bacterium *Faecalibacterium prausnitzii* alive at ambient air. *PLoS ONE* **9**, (2014).
210 Hansen, R. et al. Microbiota of *de-novo* pediatric IBD: Increased *Faecalibacterium prausnitzii* and reduced bacterial diversity in Crohn's but not in ulcerative colitis. *Am. J. Gastroenterol.* **107**, 1913-1922, (2012).
211 Assa, A. et al. Mucosa-associated ileal microbiota in new-onset pediatric crohn's disease. *Inflamm. Bowel Dis.* **22**, 1533-1539, (2016).
212 Gerasimidis, K. et al. Decline in presumptively protective gut bacterial species and metabolites are paradoxically associated with disease improvement in pediatric Crohn's disease during enteral nutrition. *Inflamm. Bowel Dis.* **20**, 861-871, (2014).
213 Quévrain, E. et al. Identification of an anti-inflammatory protein from *Faecalibacterium prausnitzii*, a commensal bacterium deficient in Crohn's disease. *Gut* **65**, 415-425, (2016).
214 Carlsson, A. H. et al. *Faecalibacterium prausnitzii* supernatant improves intestinal barrier function in mice DSS colitis. *Scand. J. Gastroenterol.* **48**, 1136-1144, (2013).
215 Comstock, L. E. & Coyne, M. J. *Bacteroides thetaiotaomicron*: a dynamic, niche-adapted human symbiont. *Bioessays* **25**, 926-929, (2003).
216 Xu, J. et al. A genomic view of the human-*Bacteroides thetaiotaomicron* symbiosis. *Science* **299**, 2074-2076, (2003).
217 Conte, M. P. et al. Gut-associated bacterial microbiota in paediatric patients with inflammatory bowel disease. *Gut* **55**, 1760-1767, (2006).
218 Takaishi, H. et al. Imbalance in intestinal microflora constitution could be involved in the pathogenesis of inflammatory bowel disease. *Int. J. Med. Microbiol.* **298**, 463-472, (2008).
219 Hooper, L. V. et al. Molecular analysis of commensal host-microbial relationships in the intestine. *Science* **291**, 881-884, (2001).
220 Varyukhina, S. et al. Glycan-modifying bacteria-derived soluble factors from *Bacteroides thetaiotaomicron* and *Lactobacillus casei* inhibit rotavirus infection in human intestinal cells. *Microb. Infect.* **14**, 273-278, (2012).
221 Wrzosek, L. et al. *Bacteroides thetaiotaomicron* and *Faecalibacterium prausnitzii* influence the production of mucus glycans and the development of goblet cells in the colonic epithelium of a gnotobiotic model rodent. *BMC Biol.* **11**, 61, (2013).
222 Cato, E. P. & Johnson, J. L. Reinstatement of species rank for *Bacteroides fragilis*, *B. ovatus*, *B. distasonis*, *B. thetaiotaomicron*, and *B. vulgatus*: Designation of neotype strains for *Bacteroides fragilis* (Veillon and Zuber) Castellani and Chalmers and *Bacteroides thetaiotaomicron* (Distaso) Castellani and Chalmers. *Int. J. Syst. Bacteriol.* **26**, 230-237, (1976).
223 Moore, W. E. C. & Holdeman, L. V. Human fecal flora: The normal flora of 20 Japanese-Hawaiians. *Appl. Microbiol.* **27**, 961-979, (1974).
224 Polk, B. F. & Kasper, D. L. *Bacteroides fragilis* subspecies in clinical isolates. *Ann. Intern. Med.* **86**, 569-571, (1977).
225 Dasgupta, S., Erturk-Hasdemir, D., Ochoa-Reparaz, J., Reinecker, H. C. & Kasper, D. L. Plasmacytoid dendritic cells mediate anti-inflammatory responses to a

gut commensal molecule via both innate and adaptive mechanisms. *Cell Host Microbe* **15**, 413-423, (2014).

226 Wang, Y. et al. An intestinal commensal symbiosis factor controls neuroinflammation via TLR2-mediated CD39 signalling. *Nat. Commun.* **5**, (2014).

227 Derrien, M., Collado, M. C., Ben-Amor, K., Salminen, S. & de Vos, W. M. The mucin degrader *Akkermansia muciniphila* is an abundant resident of the human intestinal tract. *Appl. Environ. Microbiol.* **74**, 1646-1648, (2008).

228 Karlsson, C. L. J. et al. The microbiota of the gut in preschool children with normal and excessive body weight. *Obesity* **20**, 2257-2261, (2012).

229 Santacruz, A. et al. Gut microbiota composition is associated with body weight, weight gain and biochemical parameters in pregnant women. *Br. J. Nutr.* **104**, 83-92, (2010).

230 Candela, M. et al. Unbalance of intestinal microbiota in atopic children. *BMC Microbiol.* **12**, 95, (2012).

231 Belzer, C. & de Vos, W. M. Microbes inside-from diversity to function: The case of *Akkermansia*. *ISME J.* **6**, 1449-1458, (2012).

232 Shen, J. et al. Low-density lipoprotein receptor signaling mediates the triglyceride-lowering action of *Akkermansia muciniphila* in genetic-induced hyperlipidemia. *Atertio. Thromb. Vasc. Biol.* **36**, 1448-1456, (2016).

233 Shin, N.-R. et al. An increase in the *Akkermansia* spp. population induced by metformin treatment improves glucose homeostasis in diet-induced obese mice. *Gut* **63**, 727-735, (2014).

234 Reunanen, J. et al. *Akkermansia muciniphila* adheres to enterocytes and strengthens the integrity of the epithelial cell layer. *Appl. Environ. Microbiol.* **81**, 3655-3662, (2015).

235 Dao, M. C. et al. *Akkermansia muciniphila* and improved metabolic health during a dietary intervention in obesity: relationship with gut microbiome richness and ecology. *Gut* **65**, 426-436, (2016).

236 Devkota, S. et al. Dietary-fat-induced taurocholic acid promotes pathobiont expansion and colitis in Il10-/- mice. *Nature* **487**, 104-108, (2012).

237 Rey, F. E. et al. Metabolic niche of a prominent sulfate-reducing human gut bacterium. *Proc. Natl. Acad. Sci. U. S. A.* **110**, 13582-13587, (2013).

238 Sanz, Y., Rastmanesh, R. & Agostonic, C. Understanding the role of gut microbes and probiotics in obesity: How far are we? *Pharmacol. Res.* **69**, 144-155, (2013).

239 Cano, P. G., Santacruz, A., Moya, A. & Sanz, Y. *Bacteroides uniformis* CECT 7771 ameliorates metabolic and immunological dysfunction in mice with high-fat-diet induced obesity. *PLoS ONE* **7**, e41079, (2012).

240 Davis, C. P. & Savage, D. C. Habitat, succession, attachment, and morphology of segmented, filamentous microbes indigenous to the murine gastrointestinal tract. *Infect. Immun.* **10**, 948-956, (1974).

241 Klaasen, H. L. B. M. et al. Intestinal, segmented, filamentous bacteria in a wide range of vertebrate species. *Lab. Anim.* **27**, 141-150, (1993).

242 Sczesnak, A. et al. The genome of Th17 cell-inducing segmented filamentous bacteria reveals extensive auxotrophy and adaptations to the intestinal environment. *Cell Host Microbe* **10**, 260-272, (2011).

243 Ericsson, A. C. et al. Isolation of segmented filamentous bacteria from complex gut microbiota. *BioTechniques* **59**, 94-98, (2015).

244 Schnupf, P. et al. Growth and host interaction of mouse segmented filamentous bacteria *in vitro*. *Nature* **520**, 99-103, (2015).

245 Klaasen, H. L. B. M., Koopman, J. P., Van den Brink, M. E., Van Wezel, H. P. N. & Beynen, A. C. Mono-association of mice with non-cultivable, intestinal, segmented, filamentous bacteria. *Arch. Microbiol.* **156**, 148-151, (1991).

246 Klaasen, H. L. et al. Apathogenic, intestinal, segmented, filamentous bacteria stimulate the mucosal immune system of mice. *Infect. Immun.* **61**, 303-306, (1993).

247 Ivanov, I. I. et al. Induction of intestinal Th17 cells by segmented filamentous bacteria. *Cell* **139**, 485-498, (2009).

248 Gaboriau-Routhiau, V. et al. The key role of segmented filamentous bacteria in the coordinated maturation of gut helper T cell responses. *Immunity* **31**, 677-689, (2009).

249 Adams, C. A. The probiotic paradox: Live and dead cells are biological response modifiers. *Nutr. Res. Rev.* **23**, 37-46, (2010).

250 Ma, D., Forsythe, P. & Bienenstock, J. Live *Lactobacillus reuteri* is essential for the inhibitory effect on tumor necrosis factor alpha-induced interleukin-8 expression. *Infect. Immun.* **72**, 5308-5314, (2004).

251 Marzorati, M., Pinheiro, I., Van den Abbeele, P., Van de Wiele, T. & Possemiers, S. An *in vitro* technology platform to assess host-microbiota interactions in the gastrointestinal tract. *Agro Food Ind. Hi. Tec.* **23**, 8-11 (2012).

252 Sadaghian Sadabad, M. et al. A simple coculture system shows mutualism between anaerobic faecalibacteria and epithelial Caco-2 cells. *Sci. Rep.* **5**, 17906, (2015).

253 McCormick, B. A. The use of transepithelial models to examine host–pathogen interactions. *Curr. Opin. Microbiol.* **6**, 77-81, (2003).

254 Travis, S. & Menzies, I. Intestinal permeability: Functional assessment and significance. *Clin. Sci.* **82**, 471-488, (1992).

255 Jung, P. et al. Isolation and *in vitro* expansion of human colonic stem cells. *Nat. Med.* **17**, 1225-1227, (2011).

256 Sato, T. et al. Long-term expansion of epithelial organoids from human colon, adenoma, adenocarcinoma, and Barrett's epithelium. *Gastroenterology* **141**, 1762-1772, (2011).

257 Jabaji, Z. et al. Use of collagen gel as an alternative extracellular matrix for the *in vitro* and *in vivo* growth of murine small intestinal epithelium. *Tissue Eng. Part C Methods* **19**, 961-969, (2013).

258 Foulke-Abel, J. et al. Human enteroids as an *ex-vivo* model of host–pathogen interactions in the gastrointestinal tract. *Exp. Biol. Med.* **239**, 1124-1134, (2014).

259 Sobhani, I. et al. Microbial dysbiosis in colorectal cancer (CRC) patients. *PLoS ONE* **6**, e16393, (2011).

260 Scanlan, P. D. et al. Culture-independent analysis of the gut microbiota in colorectal cancer and polyposis. *Environ. Microbiol.* **10**, 789-798, (2008).

261 Ley, R. E. et al. Obesity alters gut microbial ecology. *Proc. Natl. Acad. Sci. U. S. A.* **102**, 11070-11075, (2005).

262 Clemente, Jose C., Ursell, Luke K., Parfrey, Laura W. & Knight, R. The impact of the gut microbiota on human health: An integrative view. *Cell* **148**, 1258-1270, (2012).

263 Ulluwishewa, D. Interactions between commensal obligate anaerobes and human intestinal cells. *PhD thesis, Massey University, Manawatu, New Zealand*, (2013).
264 Harmsen, H. J. M. et al. Use of *Faecalibacterium prausnitzii* HTF-F (DSM 26943) to suppress inflammation. *US patent US20160000838A1* (2016).
265 Miquel, S. et al. Identification of metabolic signatures linked to anti-inflammatory effects of *Faecalibacterium prausnitzii*. *mBio* **6**, (2015).
266 Nyström, T. Stationary-phase physiology. *Annu. Rev. Microbiol.* **58**, 161-181, (2004).
267 Grajek, W. o. & Olejnik, A. Epithelial cell cultures *in vitro* as a model to study functional properties of food. *Pol. J. Food. Nutr. Sci.* **13**, 5-24, (2004).
268 Pinto, M., Robine Leon, S. & Appay, M. D. Enterocyte-like differentiation and polarization of the human colon carcinoma cell line Caco-2 in culture. *Biol. Cell* **47**, 323-330, (1983).
269 Sambuy, Y. et al. The Caco-2 cell line as a model of the intestinal barrier: Influence of cell and culture-related factors on Caco-2 cell functional characteristics. *Cell Biol. Toxicol.* **21**, 1-26, (2005).
270 Pinto, M., Appay, M. D. & Simon-Assmann, P. Enterocytic differentiation of cultured human colon cancer cells by replacement of glucose by galactose in the medium. *Biol. Cell* **44**, 193-196, (1982).
271 Dharmsathaphorn, K., McRoberts, J., Mandel, K., Tisdale, L. & Masui, H. A human colonic tumor cell line that maintains vectorial electrolyte transport. *Am. J. Physiol. Gastrointest. Liver Physiol.* **246**, G204-G208, (1984).
272 Cox, M. E. & Mangels, J. I. Improved chamber for the isolation of anaerobic microorganisms. *J. Clin. Microbiol.* **4**, 40-45, (1976).
273 De Man, J. C., Rogosa, M. & Sharpe, M. E. A medium for the cultivation of lactobacilli. *J. Appl. Bacteriol.* **23**, 130-135, (1960).
274 Anderson, R. C. et al. Human oral isolate *Lactobacillus fermentum* AGR1487 reduces intestinal barrier integrity by increasing the turnover of microtubules in Caco-2 cells. *PLoS ONE* **8**, (2013).
275 Yu, Q., Yuan, L., Deng, J. & Yang, Q. *Lactobacillus* protects the integrity of intestinal epithelial barrier damaged by pathogenic bacteria. *Front. Cell. Infect. Microbiol.* **5**, 26, (2015).
276 Messenger, A. J. & Barclay, R. Bacteria, iron and pathogenicity. *Biochem. Educ.* **11**, 54-63, (1983).
277 Wilkins, T. D. & Chalgren, S. Medium for use in antibiotic susceptibility testing of anaerobic bacteria. *Antimicrob. Agents Chemother.* **10**, 926-928, (1976).
278 Wandersman, C. & Delepelaire, P. Bacterial iron sources: From siderophores to hemophores. *Annu. Rev. Microbiol.* **58**, 611-647, (2004).
279 Bentley, R. & Meganathan, R. Biosynthesis of vitamin K (menaquinone) in bacteria. *Microbiol. Rev.* **46**, 241-280, (1982).
280 Kurosu, M. & Begari, E. Vitamin K2 in electron transport system: Are enzymes involved in vitamin K2 biosynthesis promising drug targets? *Molecules* **15**, 1531, (2010).
281 Nakagawa, K. et al. Identification of UBIAD1 as a novel human menaquinone-4 biosynthetic enzyme. *Nature* **468**, 117-121, (2010).
282 Heinken, A. et al. Functional metabolic map of *Faecalibacterium prausnitzii*, a beneficial human gut microbe. *J. Bacteriol.* **196**, 3289-3302, (2014).

283 Miyakawa, M. F., Creydt, V. P., Uzal, F., McClane, B. & Ibarra, C. *Clostridium perfringens* enterotoxin damages the human intestine *in vitro*. *Infect. Immun.* **73**, 8407-8410, (2005).

284 Soler, A. P. et al. Increased tight junctional permeability is associated with the development of colon cancer. *Carcinogenesis* **20**, 1425-1432, (1999).

285 Schroeder, B. O. et al. Reduction of disulphide bonds unmasks potent antimicrobial activity of human beta-defensin 1. *Nature* **469**, 419-423, (2011).

286 Anderson, R. C., Maier, E., Ulluwishewa, D. & Roy, N. C. A dual-environment co-culture system to better evaluate effects of host-microbe-food interactions on intestinal barrier function in physiologically relevant conditions. *The Fifth Beneficial Microbes Conference, 10th-12th October 2016, Amsterdam, the Netherlands*, Article in press, (2016).

287 Shekels, L. L., Lyftogt, C. T. & Ho, S. B. Bile acid-induced alterations of mucin production in differentiated human colon cancer cell lines. *Int. J. Biochem. Cell Biol.* **28**, 193-201, (1996).

288 Klinken, B. J.-W. et al. The human intestinal cell lines Caco-2 and LS174T as models to study cell-type specific mucin expression. *Glycoconj. J.* **13**, 757-768.

289 Kaur, N., Chen, C. C., Luther, J. & Kao, J. Y. Intestinal dysbiosis in inflammatory bowel disease. *Gut Microbes* **2**, 211-216, (2011).

290 Haller, D., Bode, C. & Hammes, W. P. Cytokine secretion by stimulated monocytes depends on the growth phase and heat treatment of bacteria: A comparative study between lactic acid bacteria and invasive pathogens. *Microbiol. Immunol.* **43**, 925-935, (1999).

291 Otte, J.-M. & Podolsky, D. K. Functional modulation of enterocytes by gram-positive and gram-negative microorganisms. *Am. J. Physiol. Gastrointest. Liver Physiol.* **286**, G613-G626, (2004).

292 Segawa, S. et al. Probiotic-derived polyphosphate enhances the epithelial barrier function and maintains intestinal homeostasis through integrin–p38 MAPK pathway. *PLoS ONE* **6**, e23278, (2011).

293 Peng, L., Li, Z.-R., Green, R. S., Holzman, I. R. & Lin, J. Butyrate enhances the intestinal barrier by facilitating tight junction assembly via activation of AMP-activated protein kinase in Caco-2 cell monolayers. *J. Nutr.* **139**, 1619-1625, (2009).

294 Li, Q. et al. Interferon-γ and tumor necrosis factor-α disrupt epithelial barrier function by altering lipid composition in membrane microdomains of tight junction. *Clin. Immunol.* **126**, 67-80, (2008).

295 Haller, D. et al. Non-pathogenic bacteria elicit a differential cytokine response by intestinal epithelial cell/leucocyte co-cultures. *Gut* **47**, 79-87, (2000).

296 Cario, E. Bacterial interactions with cells of the intestinal mucosa: Toll-like receptors and NOD2. *Gut* **54**, 1182-1193, (2005).

297 Cheigh, C.-I., Park, M.-H., Chung, M.-S., Shin, J.-K. & Park, Y.-S. Comparison of intense pulsed light- and ultraviolet (UVC)-induced cell damage in *Listeria monocytogenes* and *Escherichia coli* O157:H7. *Food Control* **25**, 654-659, (2012).

298 Gascón, J., Oubiña, A., Pérez-Lezaun, A. & Urmeneta, J. Sensitivity of selected bacterial species to UV radiation. *Curr. Microbiol.* **30**, 177-182, (1995).

299 Lavelle, E. C., Murphy, C., O'Neill, L. A. J. & Creagh, E. M. The role of TLRs, NLRs, and RLRs in mucosal innate immunity and homeostasis. *Mucosal Immunol.* **3**, 17-28, (2010).

300 Anderson, R. C. et al. Human oral isolate *Lactobacillus fermentum* AGR1487 induces a pro-inflammatory response in germ-free rat colons. *Sci. Rep.* **6**, 20318, (2016).
301 Huang, L.-Y. et al. Use of Toll-like receptor assays to detect and identify microbial contaminants in biological products. *J. Clin. Microbiol.* **47**, 3427-3434, (2009).
302 Graham, F. L., Smiley, J., Russell, W. C. & Nairn, R. Characteristics of a human cell line transformed by DNA from human adenovirus type 5. *J. Gen. Virol.* **36**, 59-72, (1977).
303 Cooke, M. J. et al. Enhanced cell attachment using a novel cell culture surface presenting functional domains from extracellular matrix proteins. *Cytotechnology* **56**, 71-79, (2008).
304 Kleinman, H. K., Klebe, R. J. & Martin, G. R. Role of collagenous matrices in the adhesion and growth of cells. *J. Cell Biol.* **88**, 473-485, (1981).
305 Haghparast, S. M. A., Kihara, T. & Miyake, J. Distinct mechanical behavior of HEK293 cells in adherent and suspended states. *PeerJ* **3**, e1131, (2015).
306 Anderson, R. C. et al. Human oral isolate Lactobacillus fermentum AGR1487 induces a pro-inflammatory response in germ-free rat colons. *Scientific Reports* **6**, (2016).
307 van Bergenhenegouwen, J. et al. Extracellular vesicles modulate host-microbe responses by altering TLR2 activity and phagocytosis. *PLoS ONE* **9**, e89121, (2014).
308 Fedele, G. et al. *Bordetella pertussis* commits human dendritic cells to promote a Th1/Th17 response through the activity of adenylate cyclase toxin and MAPK pathways. *PLoS ONE* **5**, e8734, (2010).
309 Thomas, P. & Smart, T. G. HEK293 cell line: A vehicle for the expression of recombinant proteins. *J. Pharmacol. Toxicol. Methods* **51**, 187-200, (2005).
310 Sartor, R. B. & Mazmanian, S. K. Intestinal microbes in inflammatory bowel diseases. *Am. J. Gastroenterol. Suppl.* **1**, 15-21, (2012).
311 Miquel, S. et al. *Faecalibacterium prausnitzii* and human intestinal health. *Curr. Opin. Microbiol.* **16**, 255-261, (2013).
312 Wullaert, A., Bonnet, M. C. & Pasparakis, M. NF-[kappa]B in the regulation of epithelial homeostasis and inflammation. *Cell Res.* **21**, 146-158, (2011).
313 Pasparakis, M. Regulation of tissue homeostasis by NF-[kappa]B signalling: Implications for inflammatory diseases. *Nat. Rev. Immunol.* **9**, 778-788, (2009).
314 Gupta, R. S. & Singh, B. Phylogenetic analysis of 70 kD heat shock protein sequences suggests a chimeric origin for the eukaryotic cell nucleus. *Curr. Biol.* **4**, 1104-1114, (1994).
315 Gupta, R. S. Origin of diderm (Gram-negative) bacteria: antibiotic selection pressure rather than endosymbiosis likely led to the evolution of bacterial cells with two membranes. *Antonie Van Leeuwenhoek* **100**, 171-182, (2011).
316 Perez-Lopez, A., Behnsen, J., Nuccio, S.-P. & Raffatellu, M. Mucosal immunity to pathogenic intestinal bacteria. *Nat. Rev. Immunol.* **16**, 135-148, (2016).
317 de Zoete, M. R., Keestra, A. M., Roszczenko, P. & van Putten, J. P. M. Activation of human and chicken Toll-like receptors by *Campylobacter* spp. *Infect. Immun.* **78**, 1229-1238, (2010).
318 Mogensen, T. H., Paludan, S. R., Kilian, M. & Østergaard, L. Live *Streptococcus pneumoniae*, *Haemophilus influenzae*, and *Neisseria meningitidis* activate the

inflammatory response through Toll-like receptors 2, 4, and 9 in species-specific patterns. *J. Leukocyte Biol.* **80**, 267-277, (2006).

319 Stoeker, L. et al. Assessment of *Lactobacillus gasseri* as a candidate oral vaccine vector. *Clin. Vaccine Immunol.* **18**, 1834-1844, (2011).

320 Miquel, S. et al. Ecology and metabolism of the beneficial intestinal commensal bacterium *Faecalibacterium prausnitzii*. *Gut Microbes* **5**, 146-151, (2014).

321 Leung, C.-H., Lam, W., Ma, D.-L., Gullen, E. A. & Cheng, Y.-C. Butyrate mediates nucleotide-binding and oligomerisation domain (NOD) 2-dependent mucosal immune responses against peptidoglycan. *Eur. J. Immunol.* **39**, 3529-3537, (2009).

322 Sander, L. E. et al. Detection of prokaryotic mRNA signifies microbial viability and promotes immunity. *Nature* **474**, 385-389, (2011).

323 Blander, J. M. & Sander, L. E. Beyond pattern recognition: Five immune checkpoints for scaling the microbial threat. *Nat. Rev. Immunol.* **12**, 215-225, (2012).

324 Demont, A. et al. Live and heat-treated probiotics differently modulate IL10 mRNA stabilization and microRNA expression. *J. Allergy Clin. Immunol.* **137**, 1264-1267.e1210, (2016).

325 Ghadimi, D., Helwig, U., Schrezenmeir, J., Heller, K. J. & de Vrese, M. Epigenetic imprinting by commensal probiotics inhibits the IL-23/IL-17 axis in an *in vitro* model of the intestinal mucosal immune system. *J. Leukocyte Biol.* **92**, 895-911, (2012).

326 Nenci, A. Epithelial NEMO links innate immunity to chronic intestinal inflammation. *Nature* **446**, 557-561, (2007).

327 Round, J. L. et al. The Toll-like receptor 2 pathway establishes colonization by a commensal of the human microbiota. *Science* **332**, 974-977, (2011).

328 Kubinak, J. L. & Round, J. L. Toll-like receptors promote mutually beneficial commensal-host interactions. *PLoS Path.* **8**, e1002785, (2012).

329 Jantzen, E. & Hofstad, T. Fatty acids of *Fusobacterium* species: Taxonomic implications. *J. Gen. Microbiol.* **123**, 163-171, (1981).

330 Bezkorovainy, A. Probiotics: Determinants of survival and growth in the gut. *Am. J. Clin. Nutr.* **73**, 399s-405s, (2001).

331 Barnett, A. M., Roy, N. C., McNabb, W. C. & Cookson, A. L. Effect of a semi-purified oligosaccharide-enriched fraction from caprine milk on barrier integrity and mucin production of co-culture models of the small and large intestinal epithelium. *Nutrients* **8**, (2016).

332 Nenci, A. et al. Epithelial NEMO links innate immunity to chronic intestinal inflammation. *Nature* **446**, 557-561, (2007).

333 Zoumpopoulou, G., Tsakalidou, E., Dewulf, J., Pot, B. & Grangette, C. Differential crosstalk between epithelial cells, dendritic cells and bacteria in a co-culture model. *Int. J. Food Microbiol.* **131**, 40-51, (2009).